ACTA PHYSICA

ACADEMIAE SCIENTIARUM HUNGARICAE

TOMUS XLI FASCICULUS 1

AKADÉMIAI KIADÓ, BUDAPEST
1976

ACTA PHYS. HUNG. APAHAQ 41 (1) 1–70 (1976)

ACTA PHYSICA

ACADEMIAE SCIENTIARUM HUNGARICAE

SZERKESZTI

KOVÁCS ISTVÁN

Az *Acta Physica* angol, német, francia vagy orosz nyelven közöl értekezéseket. Évente két kötetben, kötetenként 4—4 füzetben jelenik meg. Kéziratok a szerkesztőség címére (1521 Budapest XI., Budafoki út 8.) küldendők.

Megrendelhető a belföld számára az Akadémiai Kiadónál (1363 Budapest Pf. 24. Bankszámla 215-11488), a külföld számára pedig a „Kultúra" Könyv- és Hírlap Külkereskedelmi Vállalatnál (1389 Budapest 62, P. O. B. 149. Bankszámla 217-10990 sz.), vagy annak külföldi képviseleteinél és bizományosainál.

The *Acta Physica* publish papers on physics in English, German, French or Russian, in issues making up two volumes per year. Subscription price: $32.00 per volume. Distributor: KULTURA Hungarian Trading Co. for Books and Newspapers (1389 Budapest 62, P. O. Box 149) or its representatives abroad.

Die *Acta Physica* veröffentlichen Abhandlungen aus dem Bereich der Physik in deutscher, englischer, französischer oder russischer Sprache, in Heften die jährlich zwei Bände bilden.

Abonnementspreis pro Band $32.00. Bestellbar bei: KULTURA Buch- und Zeitungs-Außenhandelsunternehmen (1389 Budapest 62, Postfach 149) oder bei seinen Auslandsvertretungen.

Les *Acta Physica* publient des travaux du domaine de la physique, en français, anglais, allemand ou russe, en fascicules qui forment deux volumes par an.

Prix de l'abonnement: $32.00 par volume. On peut s'abonner à l'Entreprise du Commerce Extérieur de Livres et Journaux KULTURA (1389 Budapest 62, P. O. B. 149) ou chez ses représentants à l'étranger.

«*Acta Physica*» публикуют трактаты из области физических наук на русском, немецком, английском и французском языках.

«*Acta Physica*» выходят отдельными выпусками, составляющими два тома в год.

Подписная цена — $32.00 за том. Заказы принимает предприятие по внешней отрговле книг и газет KULTURA (1389 Budapest 62, P. O. B. 149) или его заграничные представительства и уполномоченные.

ACTA PHYSICA

ACADEMIAE SCIENTIARUM HUNGARICAE

TOMUS XLI

AKADÉMIAI KIADÓ, BUDAPEST

1976

ACTA PHYS. HUNG.

INDEX

Tomus 41

ACTA PHYSICA

ACADEMIAE SCIENTIARUM HUNGARICAE

TOMUS XLI FASCICULUS 1

AKADÉMIAI KIADÓ, BUDAPEST

1976

ACTA PHYS. HUNG.

INDEX

Acta Physica Academiae Scientiarum Hungaricae, Tomus 41(1), pp. 3—17 (1976)

О ВОЗВУЖДЕНИИ ЛОКАЛЬНЫХ КОЛЕБАНИЙ ЗАРЯЖЕННЫМИ ЧАСТИЦАМИ И СТУПЕНЬКАМИ ДВИЖУЩИХСЯ ДИСЛОКАЦИЙ В ЩЕЛОЧНОГАЛОИДНЫХ КРИСТАЛЛАХ

Ю. Я. ЮШИН

ИНСТИТУТ КРИСТАЛЛОГРАФИИ им. А. В. ШУБНИКОВА АКАДЕМИИ НАУК СССР, МОСКВА, СССР

и

Й. ЯНСКИ

ИССЛЕДОВАТЕЛЬСКАЯ ГРУППА ПО КРИСТАЛЛОФИЗИКЕ ВЕНГЕРСКОЙ АКАДЕМИИ НАУК БУДАПЕШТ

(Поступило 22. I. 1976)

Решена задача о возбуждении оптически активных локальных колебаний в щелочногалоидных кристаллах движущейся заряженной частицей. Вычислены величина поглощаемой локальными колебаниями энергии и интенсивность их инфракрасного излучения в случаях, когда движущимися зарядами являются ионы и заряженные ступеньки движущихся дислокаций. Предлагается использовать детектирование этого излучения для определения количества нерелятивистских ионов в каскадах, создаваемых в кристаллах частицами высоких энергий, и для диагностики плазмы при разрушении кристалла интенсивным световым импульсом.

1) Существование локальных колебаний в кристаллах с примесями проявляется в различных физических свойствах этих кристаллов [1—3]. В щелочно-галоидных кристаллах (щ. г. к.) с примесями замещения наличие оптически активных локальных колебательных мод приводит к инфракрасному поглощению на частотах, превышающих частоты поперечных оптических колебаний совершенного кристалла [2—3].

В настоящей работе рассматривается задача о воздействии заряженной частицы, движущейся внутри кристалла, на локальное оптическое колебание в щ. г. к. со структурой NaCl. Предполагается, что температура кристалла произвольна. Поэтому до прохождения заряженной частицы локальная мода находится в тепловом равновесии с остальными колебательными модами кристалла, а её возбуждение описывается планковской функцией распределения. Учитывая что это обстоятельство, мы провели исследование в рамках квантовой теории.

В п. 2, 3 изложено решение указанной задачи в гармоническом приближении, полученное с помощью методов нерелятивистской квантовой теории поля. Возбуждение локальной моды значительно, если эффективное время пролета заряженной частицы порядка периода колебания и много меньше его времени жизни, что и оправдывает применение гармонического приближения.

Полученные результаты мы используем в п. 4, 5 для тех случаев, когда движущимися зарядами являются ионы и заряженные ступеньки краевых дислокаций. В частности, в этих случаях может быть обнаружено инфракрасное излучение из кристалла на частоте локальных колебаний ω_0. Следует подчеркнуть, что это излучение, в отличие от излучения основной решетки, не будет поглощено внутри кристалла, что облегчает его детектирование.

Наши результаты, записанные в общем виде, справедливы для любых центров в щ. г. к. Однако наиболее изучены, как экспериментально, так и теоретически, U-центры в щ. г. к. [2, 3], когда примесью замещения является водород или дейтерий. Поэтому в дальнейшем мы будем конкретизировать наше рассмотрение, используя теоретические модели U-центров.

2) Если на ионы кристаллической решетки действуют силы, зависящие от времени, и $F_\alpha(l, k, t)$ — декартова компонента ($\alpha = 1, 2, 3$) силы, действующей на k-ый атом в l-ой ячейке в момент времени t, то в гармоническом приближении поведение системы ионов будет описываться гамильтонианом

$$H = H_0 + H_1, \qquad H_1 = -\sum_{l,R,\alpha} u_a(l, k)\, F_\alpha(l, k, t), \tag{1}$$

$$H_0 = \sum_{l,k,\alpha} \frac{p_\alpha^2(l,k)}{2\, M_{ek}} + \frac{1}{2} \sum_{l,k,\alpha} \sum_{l',k',\beta} \varphi_{\alpha\beta}(lk; l'k')\, U_\alpha(l, k)\, U_\beta(l', k'). \tag{2}$$

Здесь M_{lk}, $p_\alpha(l, k)$, $u_\alpha(l, k)$ — соответственно масса и компоненты импульса и отклонений k-го иона в l-ой ячейке кристалла, $\varphi_{\alpha\beta}(lk; l'k')$ — динамическая матрица кристалла [2]. Отклонения и импульсы отдельных ионов можно выразить через нормальные координаты $A = a_s + a_s^+$ и канонически сопряженные им импульсы

$$P_s = \frac{\hbar}{2i}(a_s - a_s^+),$$

$$u_\alpha(lk) = \left(\frac{\hbar}{2M_{lk}}\right)^{1/2} \sum_n \omega_s^{-1/2}\, B_\alpha^{(s)}(lk)\, A_s, \tag{3}$$

$$p_\alpha(lk) = \left(\frac{2M_{lk}}{\hbar}\right)^{1/2} \sum_s \omega_s^{1/2}\, B_\alpha^s(lk)\, P_s. \tag{4}$$

Здесь $\hbar$ — постоянная Планка, ω_s — частоты нормальных колебаний. Операторы рождения и уничтожения фононов s-ой моды колебаний a_s^+, a_s удовлетворяют перестановочным соотношениям $[a_\alpha^s, a_{s'}^R] = \delta_{ss'}$, а коэффициенты $B_\alpha^s(lk)$ — условиям ортонормированности и замкнутости

$$\sum_{lk\alpha} B_\alpha^s(lk)\, B_\alpha^{(s')}(lk) = \delta_{ss'}, \qquad \sum_n B_\alpha^{(s)}(lk)\, B_\beta^{(s)}(l'\, k') = \delta_{ll'}\, \delta_{kk'}\, \delta_{\alpha\beta}. \tag{5}$$

Используя (3), преобразуем $H_1(t)$ к виду

$$H_1 = -\sum_k f_s(t) A_s\,, \quad f_s(t) = \sum_{l,k,\alpha} \left(\frac{\hbar}{2M_{lk}\omega_s}\right)^{1/2} B_\alpha^{(s)}(l,k)\, F_\alpha(l+k,t)\,. \tag{6}$$

Гейзенберговские уравнения движения для операторов $A_s(t)$, $P_s(t)$, вытекающие из (1)—(6), имеют вид

$$\dot{A}_s(t) = 2\frac{\omega_s}{\hbar} P_s(t)\,, \quad \dot{P}(t) = -\frac{\hbar\omega_s}{2} A_s(t) + f_s(t), \tag{7}$$

или

$$\ddot{A}_s(t) + \omega_s^2 A_s(t) = \frac{2\omega_s}{\hbar} f_s(t)\,. \tag{8}$$

Используя запаздывающую функцию Грина ур. (8), получаем его решение

$$A_s(t) = A_s^{(in)}(t) + \frac{2}{\hbar}\int_{-\infty}^{t} dt' f_s(t') \sin\omega_s(t-t')\,. \tag{9}$$

Здесь предполагается, что при $t \to -\infty$ силы $F_\alpha(l,k,t) \to 0$, $A_s^{(in)}(t)$ — операторное решение соответствующего однородного уравнения, удовлетворяющее некоторому начальному условию при $t \to -\infty$.

Рассматривая задачу о возбуждении заряженной частицей локальных колебаний оптического типа, предположим, что частица с зарядом Ze движется прямолинейно со скоростью $\vec{\mathbf{v}}$ в плоскости, образованной кристаллографическими осями x, y, траектория совпадает с кристаллографической осью x, а примесный атом находится в той же плоскости на оси y на расстоянии b от начала координат.

При вычислении $f_s(t)$ по ф. (6) учтем, что $F_\alpha(l,k,t) = \mathbf{e}_{lk} E_\alpha(l,k,t)$, $\mathbf{E}(l,k,t)$ — напряженность электрического поля, создаваемая заряженной частицей в точке, совпадающей с положением равновесия иона (lk), $\mathbf{e}_{lk}$ — электрический заряд этого иона.

Кроме примесного атома, в локальном колебании участвует лишь небольшое число его соседей, для которых $B_\alpha^{(s)}(l,k)$ существенно отличны от нуля. Так в модели примеси замещения [3], в которой учтено отличие массы примесного атома от массы замещенного им атома основной решетки и изменение силы взаимодействия между атомом примеси и его ближайшими соседями, лишь для этих последних $B_\alpha^{(s)}(l,k) \neq 0$.

Как следует из модели междуузельного дефекта, рассмотренной в [4] (U_1 центр в KI), в локальном колебании, ответственном за инфракрасное поглощение, практически участвует лишь ион водорода.

Предполагая, что прицельное расстояние $b > a$ (a — расстояние между ближайшими соседями в решетке), запишем $E_\alpha(l,k,t) \approx E_\alpha(0,t) +$

$+ (\mathbf{R}_{lk} - \mathbf{R}_0) \nabla E_\alpha$, пренебрегая высшими членами разложения по $\mathbf{R}_{lk} - \mathbf{R}_0$, где $\mathbf{R}$ — радиус-векторы иона примеси (0) и его соседей (lk), а градиент $\nabla E_\alpha(t)$ вычислен в точке нахождения примеси. Для дефектов замещения в щ. г. к. примесный атом является центром симметрии. Поэтому второй член разложения дает нулевой вклад в $f_s(t)$, так как для двух одноименных ионов, расположенных симметрично относительно примесного атома, все множители в (6) одинаковы, за исключением $\mathbf{R}_{lk} - \mathbf{R}_0$, которые отличаются знаком. Учитывая это в (6), получаем

$$f_s(t) = \sum_\alpha E_\alpha(0, t)\, g_\alpha^{(s)},\ g_\alpha^{(s)} = \sum_{l,k} \mathbf{e}_{lk} \left(\frac{\hbar}{2M_{lk}\omega_s}\right)^{1/2} B_\alpha^{(s)}(lk)\ . \tag{10}$$

Заметим, что оператор дипольного момента, связанного с отклонением ионов от равновесных положений, равен

$$\hat{d}_\alpha = \sum_{l,k} \mathbf{e}_{tk}\ u_\alpha(_{lk}) = \sum_s g_\alpha^{(s)} A_s\,. \tag{11}$$

Таким образом, возбуждение локального колебания происходит за счёт взаимодействия его дипольного момента $\mathbf{g}^{(s)} A_s$ с кулоновским полем движущейся заряженной частицы.

Локальные оптические колебания, связанные с дефектами замещения в щ. г. к. с кубической решеткой, трехкратно вырождены. Векторы $\mathbf{g}^{(s)}$ для трех вырожденных ветвей $s = 1, 2, 3$ ортогональны, поскольку при поворотах на углы $\pi/2$ они должны переходить друг в друга. Произведя линейное преобразование для нормальных координат A_1, A_2, A_3, мы можем добиться того, что векторы $\mathbf{g}^{(s)}$ будут направлены по кристаллографическим осям. Поэтому запишем $g_\alpha^{(s)} = g\delta_{\alpha s}$, $s = 1, 2, 3$. Мы вычислили величину g для упомянутой выше модели [3] и получили

$$|g| = \frac{\mathbf{e}_0 \hbar}{\omega_0 (M_1 M_2)^{1/2}}\ \frac{M_1 + M_2}{M_1 + 2M_2}\ . \tag{12}$$

Здесь M_1 — масса одновалентного примесного иона, M_2 — масса ближайшего соседнего иона основной решетки, $e_0 = |\, e_{lk}\,|$, ω_0 — частота локального колебания. С другой стороны, величина g может быть найдена из результатов экспериментов по инфракрасному поглощению на частоте ω_0.

Предположим, что в момент времени $t = 0$ заряженная частица находится в начале координат на расстоянии b от примесного иона. Тогда компоненты напряженности её собственного кулоновского поля в точке расположения примеси в момент времени t равны ($v_x = v > 0$)

$$\tilde{E}_y(0, t) = \frac{Zeb}{(v^2t^0 + b^2)^{3/2}}\ ,\quad \tilde{E}_x(0, t) = -\frac{Zevt}{(v^2t^2 + b^2)^{2/2}}\ ,\quad \tilde{E}_z(0, t) = 0\,. \tag{13}$$

Разложим $\tilde{E}_{x,y}(t)$ в интеграл Фурье и вычислим компоненты Фурье

$$\tilde{E}_{x,y}(\omega) = \frac{1}{2\pi}\int_{-\infty}^{\infty} \tilde{E}_{x,y}(t)\, e^{i\omega t}\, dt.$$

Получаем [5]

$$\tilde{E}_y(\omega) = \frac{Zeb}{2\pi v}\int_{-\infty}^{\infty} dx(x^2+b^2)^{-1/3}\cos\frac{\omega x}{v} = \frac{Ze\omega}{\pi v^2} K_1\left(\frac{\omega b}{v}\right), \tag{14}$$

$$\tilde{E}_x(\omega) = -i\frac{Ze}{2\pi v}\int_{-\infty}^{\infty} dx(x^2+b^2)^{-3/2}\, x\sin\frac{\omega x}{v} = -i\frac{Ze\omega}{\pi v^2} K_0\left(\frac{\omega b}{v}\right), \tag{15}$$

где $K_{0,1}\left(\frac{\omega b}{v}\right)$ — модифицированные функции Бесселя третьего рода.

Учтем теперь поляризацию кристаллической среды электрическим полем заряженной частицы. Для этого мы воспользуемся результатом, полученным в теории многих тел в рамках диэлектрического формализма [6, 7], и запишем

$$U(\omega, \mathbf{q}) = \frac{V(\omega, \mathbf{q})}{\varepsilon(\omega, \mathbf{q})},$$

где $V(\omega, \mathbf{q})$ — компонента 4-мерного преобразования Фурье кулоновского потенциала заряженной частицы в вакууме, равная

$$\frac{Ze}{2\pi^2 q^2}\,\delta(\omega - \mathbf{qv}) \qquad [8],$$

$\varepsilon(\omega, q)$ — продольная диэлектрическая проницаемость кристалла, q — волновой вектор. $U(\omega, \mathbf{q}) = V(\omega, \mathbf{q}) + V_p(\omega, \mathbf{q})$ есть суммарный (эффективный) потенциал, создаваемый «сторонней» заряженной частицей в среде, а $V_p(\omega, \mathbf{q})$ — потенциал индуцированных зарядов. Разложим $\varepsilon^{-1}(\omega, \mathbf{q})$ в ряд по $\mathbf{q}^2 = q^2$ (из соображений симметрии нечётные по q члены в разложении отсутствуют)

$$\varepsilon^{-1}(\omega, \mathbf{q}) = \varepsilon^{-1}(\omega, 0) + q^2\frac{\partial\varepsilon^{-1}}{\partial(q^2)} + \ldots . \tag{16}$$

Эффективным безразмерным параметром разложения в (16) является $(qa)^2$ [9], a — расстояние между ближайшими соседями в решетке. В то же время в кулоновский потенциал на расстояниях $\gtrsim b$ от заряженной частицы основной вклад дают компоненты Фурье $V(\omega, \mathbf{q})$ с $q \lesssim 1/b$.

При вычислении напряженности $\mathbf{E}(0, t)$ мы ограничимся в разложении (16) его первым членом $\varepsilon^{-1}(\omega, 0) = \varepsilon^{-1}(\omega)$ (в кубических кристаллах тензор $\varepsilon_{ik}(\omega) = \delta_{ik}\varepsilon(\omega)$). Это приближение является точным при $b \gg a$, а при $b \lesssim a$

соответствует учёту главной части поляризации среды, ввиду частичной взаимной компенсации неучитываемых вкладов от наведенных поляризаций ионов в напряженность $\mathbf{E}(0, t)$. В частности, нетрудно видеть, что второй член разложения (16) дает нулевой вклад в $\mathbf{E}(0, t)$. Мы получаем в результате, что компоненты Фурье напряженности электрического поля $E_\alpha(0, t)$ равны $E_{x,y}(\omega) = \tilde{E}_{x,y}(\omega)/\varepsilon(\omega)$.

3) Попытаемся выяснить, в каком состоянии будут находиться осцилляторы локальных мод после прохождения заряженной частицы, если до этого они находились в состоянии теплового равновесия с остальными колебательными модами кристалла. Поскольку при $t \to \pm\infty$ $f_s(t) \to 0$ мы можем использовать формализм in, out — операторов квантовой теории поля [10]. Получаем из (9)

$$A_s^{(\mathrm{out})}(t) = A_s^{(\mathrm{in})}(t) + u_s^* \, \mathrm{e}^{i\omega_s t} + u_s \, \mathrm{e}^{-i\omega_s t}, \quad u_s = \frac{i}{\hbar}\int_{-\infty}^{\infty} dt' \, f_s(t') \, \mathrm{e}^{i\omega_s t'}. \tag{17}$$

Интервал времени T, когда $f_s(t)$ практически отлична от нуля $T \sim C\dfrac{b}{v}$, где число $C \sim 10$. Поэтому гейзенберговский оператор $A_s(t)$, даваемый (9), совпадает с $A_s^{(\mathrm{out})}(t)$ при $t > T$. Используя (10)—(15), мы получаем величины u_1, u_2 для мод, дипольный момент которых поляризован соответственно по осям x, y

$$u_1 = K_0\left(\frac{\omega_0 b}{v}\right), \quad u_2 = i\gamma K_1\left(\frac{\omega_0 b}{v}\right), \quad \gamma = \frac{2Ze g\omega_0}{\hbar v^2 \varepsilon(\omega_0)}. \tag{18}$$

Для вычисления средних значений динамических величин, относящихся к колебанию данной моды, перейдем к представлению взаимодействия и найдем матрицу плотности локального колебания после прохождения заряженной частицы $\hat{\varrho}^{(\mathrm{out})} = \hat{\varrho}_1$, предполагая, что до этого

$$\hat{\varrho}_0 = \hat{\varrho}^{(\mathrm{in})} = \exp\{-\hbar\omega_0 (a_s^+ a_s + 1)/kT\}\, n^{-1}(T).$$

Здесь k — постоянная Больцмана, T — температура кристалла.

Для нахождения $\hat{\varrho}_1$ удобно использовать представление когерентных состояний осцилляторов $|\alpha\rangle$, обладающих свойством $a_s|\alpha\rangle = \alpha|\alpha\rangle$ [11]. В α-представлении для матрицы плотности

$$\hat{\varrho}_0 = \int d^2\alpha \, P_0(\alpha) |\alpha\rangle\langle\alpha|, \quad P_0(\alpha) = \frac{1}{\pi n(T)} \exp\left(-\frac{|\alpha|^2}{n(T)}\right) \tag{19}$$

и $n(T) = \left[\exp\left(\dfrac{\hbar\omega_0}{kT}\right) - 1\right]^{-1}$. Когерентное состояние $|\alpha\rangle$ получается из основного состояния осциллятора $|0\rangle$ действием унитарного оператора сдвига

$|\alpha\rangle = D(\alpha)\,|0\rangle, D(\alpha) = \exp(\alpha a_s^+ - \alpha^* a_s)$ [11]. Учитывая соотношения $A_s^{(\mathrm{out})} = S^+ A_s^{(\mathrm{in})} S$, находим, что матрицы рассеяния S, соответствующие (17), (18), равны $D(u_s)$ для $s = 1, 2$. Поэтому оператор $\hat{\varphi}_1 = S\hat{\varphi}_0 S^+$ можно представить в виде

$$\hat{\varrho}_1 = \int d^2\alpha\, P_0(\alpha)\, D(u_s)\, D(\alpha)\,|0\rangle\langle 0|\, D^+(\alpha)\, D^+(u_s)\,. \tag{20}$$

Используя закон умножения операторов сдвига [11]

$$D(\alpha_2)\, D(\alpha_1) = D(\alpha_1+\alpha_2)\exp\left(\frac{\alpha_2\,\alpha_1^* - \alpha_2^*\,\alpha_1}{2}\right),$$

получаем

$$\hat{\varrho}_1(\alpha) = \int d^2\alpha\, P_0(\alpha)\, D(\alpha)\, D(\alpha+u_s)\,|0\rangle\langle 0|\, D^+(\alpha+u_s)\,. \tag{21}$$

Соответствующая (21) весовая функция

$$P_1(\alpha) = \int \delta^2(\alpha-\alpha_1-u_s)\, P_0(\alpha_1)\, d^2\alpha_1 \equiv \frac{1}{\pi n(T)}\exp\left\{-\frac{|\alpha-u_s|^2}{n(T)}\right\}. \tag{22}$$

Для вычисления средних значений различных величин с помощью (21), (22), запишем выражение для соответствующего оператора в виде суммы нормальных произведений от операторов $a_s^+(t)$, $a_s(t)$. Учитывая определение когерентных состояний и ф. (19), (22), получим

$$Sp\{\hat{\varrho}_1 (a_s^+(t))^n\,(a^m(t)\} = \frac{e^{i(n-m)\omega_0 t}}{\pi n(T)}\int (\alpha^*+u^*)^n\,(\alpha+u)^m \exp\left[-\frac{|\alpha|^2}{n(T)}\right] d^2\alpha. \tag{23}$$

Переходя к полярным координатам в комплексной плоскости α, находим

$$[\pi n(T)]^{-1}\int (\alpha^*)^m\,\alpha^n \exp\left[-\frac{|\alpha|^2}{n(T)}\right] d^2\alpha = [n(T)]^m\, m!\,\delta_{mn}. \tag{24}$$

Формулы (23), (24) позволяют найти среднее значение произвольного оператора, зависящего от a_s^+, a_s. Из них следует, что средние от операторов, линейных по a_s^+, a_s, получаются из соответствующего выражения для этих операторов заменой $a_s \to u_s$, $a_s^+ \to u_s^*$. Средние от операторов, квадратичных по a_s^+, a_s, находятся с помощью соотношения $\langle a_s^+ a_s\rangle = n(T) + |u_s|^2$. В частности, под действием заряженной частицы локальная мода приобретает энергию $\hbar\omega_0 |u_s|^2$. Для энергии, приобретаемой тремя вырожденными модами одного примесного центра, получаем

$$\mathscr{E}_1(b) = \frac{4g^2 Z_2\, e\omega_0^3}{\hbar v^4\,\varepsilon^2(\omega_0)}\left[K_0^2\left(\frac{\omega_0 b}{v}\right) + K_1^2\left(\frac{\omega_0 b}{v}\right)\right]. \tag{25}$$

Вычислим теперь с помощью матрицы плотности $\hat{\varphi}_1$ интенсивность инфракрасного излучения на частоте ω_0 для одного локального центра, возбужденного заряженной частицей. Используя формулу для интенсивности дипольного излучения в среде [12], получаем

$$I_0 = 2\mathscr{E}_1(b)\,\Gamma_r\,,\quad \Gamma_r = \frac{2g^2\,\omega_0^3\,\varepsilon^{1/2}\,(\omega_0)}{3\,\hbar\,c^3}\,. \tag{26}$$

В этой формуле и в дальнейшем не учитывается всегда существующее тепловое излучение оптического колебания $\sim n(T)$.

После прохождения заряженной частицы амплитуды локальных колебаний будут затухать в соответствии с формулой $u(t) = ue^{-\Gamma t}$ из-за взаимодействия с остальными колебательными модами кристалла вследствие ангармонизма, Γ — полуширина линии инфракрасного поглощения [2]. Будет затухать и интенсивность инфракрасного излучения $\sim e^{-2\Gamma t}$. Полная энергия, излученная одним центром после прохождения заряженной частицы, равна ($\Gamma_r \ll \Gamma$)

$$\mathscr{E}_r = I_0\int_0^\infty \mathrm{e}^{-2\Gamma t}\,dt = \frac{I_0}{2\Gamma} = \mathscr{E}_1(b)\,\frac{\Gamma_r}{\Gamma}\,. \tag{27}$$

Обобщим полученные результаты на случай произвольного направления движенной частицы по отношению к кристаллографическим осям. С этой целью проведем плоскость, проходящую через траекторию частицы и примесной атом и введем в этой плоскости декартову систему координат x', y' таким образом, что траектория частицы совпадает с осью x', а примесный атом лежит на оси y' на расстоянии b от начала координат. Величины $\tilde{E}_{y'}(t)$, $\tilde{E}_{x'}(t)$ и их компоненты Фурье даются ф. (13)—(15), а результирующие сдвиги координаты s-го локального колебания равны $u_s = u_1\cos(\widehat{y'\,g_s}) + u_2\cos(\widehat{y'\,g_s})$. В эту формулу входят косинусы углов между осями x', y' и вектором $\mathbf{g}^{(s)}$, направленным по соответствующей кристаллографической оси, u_1, u_2 даются ф. (18). Нетрудно убедиться, что ф. (25)—(27) будут попрежнему справедливы.

Вычислим энергию $\mathscr{E}$, теряемую заряженной частицей на единице пути на возбуждение локальных колебаний. Предполагая, что примесные атомы расположены в кристалле равномерно с плотностью N_c, находим

$$\begin{aligned}\mathscr{E} &= N_c\int_{b_0}^\infty 2\pi b\,\mathscr{E}_1(b)\,db = Dv^{-3}\,K_0\left(\frac{\omega_0\,b_0}{v}\right)K_1\left(\frac{\omega_1\,b_0}{v}\right),\\ D &= \frac{8\,\pi b_0\,Z^2\,\mathrm{e}^2\,g^2\,\omega_0^2\,N_1}{\hbar\varepsilon^2\,(\omega_0)}\,,\end{aligned} \tag{28}$$

где b_0 — минимальное значение прицельного параметра. Физическим основанием для производимого при интегрировании по прицельному параметру

усреднения по расстояниям между примесным атомом и траекторией заряженной частицы является процесс многократного рассеяния заряженной частицы на малые углы. Энергия, теряемая заряженной частицей в единицу времени, $W = \mathcal{E}v$. При определении интенсивности инфракрасного излучения на частоте ω_0 из кристалла, в котором N заряженных частиц движутся со скоростью v, учтём, что возбужденное частицей локальное колебание затухает за время $\sim \Gamma^{-1}$, а в эксперименте измеряется усредненная по времени интенсивность, которая равна

$$I = N\mathcal{E}v\frac{\Gamma_r}{\Gamma}. \tag{29}$$

Величина указанных выше эффектов существенно зависит от численного значения $z = b_0\omega_0/v$ и быстро убывает при $z \gg 1$, что связано с асимптотическим поведением функций

$$K_{0,1}(z) \approx \sqrt{\frac{\pi}{2z}}\,\mathrm{e}^{-z}.$$

Полученные результаты можно использовать и при рассмотрении взаимодействия движущихся зарядов с оптически активными резонансными колебаниями, для которых $\Gamma \ll \omega_0$, поскольку для промежутков времени $\sim \omega_0^{-1}$ резонансное колебание можно приближенно описать как локальное движение оптического типа [2, 3]. В заключение данного раздела остановимся на конкретной причине, из-за которой можно использовать гармоническое приближение при решении нашей задачи. С учётом ангармонизма второй член в ур. (9) принимает вид

$$\frac{2}{\hbar}\int_{-\infty}^{t} dt'\, f_0(t')\,\sin\left[\omega_0(t-t')\right]\,\mathrm{e}^{-\Gamma(t-t')}.$$

Как следует из проведенного нами анализа, локальное колебание возбуждается пролетающей частицей значительным образом лишь в том случае, если возбуждающая сила $f_0(t')$ существенно отлична от нуля для величин $|t'| \gtrsim \tau$, а время пролета $\tau \sim \omega_0^{-1}$. Будем рассматривать времена t такие, что $|t| \gtrsim \tau$. Соответственно, $|t - t'| \gtrsim \tau \sim \omega_0^{-1}$. Так как величина затухания $\Gamma \ll \omega_0$, то $\Gamma(t - t') \ll 1$. Поэтому величину $\exp[-\Gamma(t - t')]$ можно заменить единицей для указанных значений t.

4) В случае, когда движущимся зарядом является ион с массой M_j, рассмотрение п. 2, 3 применимо при условии $\frac{M_j v^2}{2} \gg \mathcal{E}_1(b)$. В случае $\varepsilon_0 = \frac{M_j v_0^2}{2} > \mathcal{E}_1(b)$ его можно использовать для приближенного самосогласованного решения задачи, полагая $v = \sqrt{\frac{\varepsilon_0}{2M_d}} + \sqrt{\frac{\varepsilon_0 - \mathcal{E}_1(b)}{2M_j}}$. Для электронов указанное неравенство для скоростей $v \sim a\omega_0$ не выполняется.

При облучении твердых тел потоками релятивистских частиц (протонов, нейтронов и т. д.) в кристаллах образуются различного рода радиационные нарушения в результате смещений атомов из их равновесных положений. Если падающая на кристалл частица обладает достаточно высокой энергией, то она может вызвать каскад нарушений, поскольку выбиваемые ею «первичные» атомы могут, в свою очередь, образовать на длине своего пробега несколько «вторичных» смещенных атомов и т. д. [13, 14]. Так по оценке Зейтца [13] нейтрон с энергией 2 Мэв при замедлении до тепловых энергий производит в твердых телах $\sim 10^3$ смещений.

Выбиваемые ионы в результате сильного взаимодействия с атомами кристалла могут потерять часть электронов своих внешних оболочек. В анализе этого процесса, проведенном Н. Бором и Д. Лидхардом [15], учитывались результаты экспериментов Н. Лассена [15]. Измеряя отклонения ионов в магнитном поле, Лассен определял величину их заряда после прохождения через газы и твердые тела. В последнем случае были обнаружены большие флуктуации зарядов ионов относительно среднего заряда, определяемого балансом между процессами потери и захвата электронов. Рассматривая движение ионов в щ. г. к., следует учитывать большую ширину запрещенной зоны, что затрудняет процессы захвата электронов ионами.

Детектирование инфракрасного излучения локальных мод может дать сведения о числе ионов с нерелятивистскими скоростями, имеющихся в кристалле в результате каскадного процесса, и величинах их зарядов.

Предположим, что на щ. г. к. падает стационарный по времени поток релятивистских частиц и вследствие каскадного процесса в кристалле имеется N_j ионов, обладающих зарядом Z_j e, и $f_j(\mathbf{v})$ — функция распределения этих ионов по скоростям, $\int f(\mathbf{v}) d^3 v = 1$. В этом случае интенсивность инфракрасного излучения на частоте ω_0 есть

$$I = \Gamma_r \Gamma^{-1} \sum_j N_j \int f_j(\mathbf{v}) \, \mathscr{E}_j(v) \, d^3 v \,, \tag{30}$$

а $\mathscr{E}_j(v)$ дается ф. (28) при замене $Z \to Z_j$. В качестве минимального прицельного расстояния b_0 можно выбрать сумму радиусов примесного и пролетающего ионов. Сделаем следующее замечание относительно такого выбора. В классической теории рассеяния имеется однозначное соответствие между углом рассеяния и значением прицельного параметра [17]. Поэтому, ограничивая интегрирование по прицельному параметру, мы фактически не учитываем процессов рассеяния заряженной частицы на примесном ионе на углы, большие некоторого угла Θ_0, зависящего от b_0. Следует иметь в виду, что из-за известной угловой зависимости амплитуды [18, 19] рассеяния и резерфордовского сечения рассеяние, обязанное кулоновскому взаимодействию, происходит, в основном, на малые углы. С другой стороны, для рассматри-

ваемых нами энергий движущихся ионов большим углам рассеяния отвечает такая величина переданной примесному иону кинетической энергии, которая может превзойти энергию $E_d \sim 25$ эв, достаточную для его смещение в междуузельное положение [13]. Этот процесс следует учитывать при вычислении энергии, теряемой движущимся ионом [13], но он не дает вклад в интенсивность инфракрасного излучения на частоте ω_0. При рассмотрении рассеяния на большие углы необходимо, наряду с кулоновским взаимодействием, учитывать отталкивательный потенциал взаимодействия между ионами [20], обязанный перекрытию их электронных оболочек, имеющий малый радиус действия и препятствующий сближению ионов. Тот факт, что при столкновении между ионами, которое сопровождается передачей энергии, большей E_d, в момент наибольшего сближения движущегося и примесного ионов имеет место заметное взаимное проникновение их электронных оболочек [13] и определяет выбор нижнего передела интегрирования по b порядка суммы ионных радиусов.

Оценим величину интенсивности излучения U-центров в кристалле KCl(H). При этом $\omega_0 = 10^{14}$ сек$^{-1}$, $g^2\omega_0\hbar^{-1} \approx 7{,}5 \cdot 10^4$ см^3 сек$^{-2}$, $b_0 \approx 3 \cdot 10^{-9}$ см. Положим $N_c \approx 10^{19}$ см$^{-3}$, $Z = 3$, $\omega_0\Gamma^{-1} = 10^2$.

Для скоростей v от $1{,}5 \cdot 10^6$ до $3 \cdot 10^6$ см/сек, которым соответствуют кинетические энергии ионов K 45 и 180 эв, интенсивность $I \sim N(v)10^{-18}$ вт, где $N(v)$ — число ионов в указанном интервале скоростей.

Предположим, что производится бомбардировка кристалла нейтронами, при которой используется нейтронный генератор, преобразующий пучок ускоренных дейтронов в нейтроны посредством реакции типа $Be^9(d, n)B^{10}$ [14]. Этот метод обеспечивает поток нейтронов j до 10^{11} см$^{-2}$ сек$^{-1}$ и обладает тем преимуществом, что энергии нейтронов сосредоточены в узком интервале. Оценим $N(v)$ по формуле $N(v) \sim jSK\alpha$, где S — поперечное сечение кристалла, K — число ионов, смещенных одним нейтроном, а коэффициент $\alpha = \Delta T/T$. Здесь T — среднее время пробега выбитого иона, ΔT — время, когда скорость иона находится в указанном выше интервале скоростей. Полагая $K \sim 10^3$, $\alpha \sim 10^{-2}$, $S = 10^2$ см^2, получаем $I \sim 10^{-4}$ вт.

Если на диэлектрик падает лазерный световой пучок, энергия фотонов в котором меньше ширины запрещенной зоны, то при достаточно высокой интенсивности света происходит разрушение кристалла, физический механизм которого детально не известен [21]. После воздействия лазерного импульса в исследуемых образлах имеются полости, свободные от основного вещества кристалла [21—24]. Поэтому можно предположить, что на одной из стадии процесса разрушения в кристалле образуется электронно-ионная плазма, которая «выплескивается» в близлежащие области кристалла. Одной из трудностей экспериментального изучения разрушения является то, что процесс имеет характер «взрыва». Можно ли использовать измерение интенсивности инфракрасного излучения возбужденных ионами локальных колеба-

ний для диагностики плазмы-определения степени ионизации ионов, их распределения по энергии, эффективной температуры плазмы?

Чтобы ответить на этот вопрос, вычислим интенсивность излучения на частоте ω_0, предполагая, что ионы «внедряются» в область кристалла с концентрацией примесных центров N_c и имеют максвелловское распределение по скоростям, соответствующее температуре T. Тогда интенсивность излучения I_j ионов с зарядом $Z_j e$ и массой M_j и полная интенсивность I равны

$$I_j = R_j \int_0^\infty dv\, e^{-\lambda_j v^2} K_0\left(\frac{\omega_0 b_0}{v}\right), \quad I = \sum_j I_j, \tag{31}$$

где $R_j = 4\pi N_j \left(\frac{M_j}{2\pi kT}\right)^{3/2} D\Gamma_r \Gamma^{-1}$, D дается ф. (28), N_j — число ионов данного типа, $\lambda_j = M_j/2kT$. Интеграл (31) можно вычислить численно для различных температур T.

Чтобы получить оценку для T_j, поступим следующим образом: заменим бесселевы функции их асимптотиками $K_\nu(z) \approx \sqrt{\frac{\pi}{2z}}\, e^{-z}$, а v^2 в показателе экспоненты разложим около среднеквадратичной скорости максвелловского распределения $\tilde{v}_j = \sqrt{\frac{3kT}{M_j}}$ и оставим два первых члена этого разложения. Получаем

$$I_j \approx R_j e^{\lambda_j \tilde{v}_j^2} \frac{\pi}{2\omega_0 b_0} \int_0^\infty dv\, v\, \exp\left(-2\lambda_j \tilde{v}\, v - \frac{2\omega_0 b_0}{v}\right). \tag{32}$$

Такая оценка правильно учитывает вклад в интенсивность максимума максвелловского распределения и несколько завышает вклад его высокоэнергетического «хвоста». Вычисление (32) дает [5]

$$I_j \approx 2\sqrt{6\pi} \exp\left(\frac{3}{2}\right) D N_j \frac{\Gamma_r}{\Gamma} \tilde{v}_j^{-2} K_2\left(4\sqrt{\frac{3\omega_0 b_0}{2\tilde{v}_j}}\right). \tag{33}$$

При определении температуры плазмы T с помощью измерения интенсивности I следует учитывать, что величина (33) резко уменьшается с ростом отношения $\omega_0 b_0/\tilde{v}_j$. Мы провели оценки интенсивности для кристалла KCl(H), полагая объем полости $\sim 10^{-8}$ см^3, чему соответствует полное число ионов $N \sim 10^{14}$, $\omega_0 \Gamma^{-1} = 5$, $N_c = 10^{20}$ см$^{-3}$, $Z = 1$. Численные значения других величин указаны выше в этом разделе. Для температур T, равных $2 \cdot 10^4$, $2{,}5 \cdot 10^9$, градусов K мы получили соответственно $I \sim 2{,}4 \cdot 10^{-9}$; 10^{-6}; $2{,}3 \cdot 10^{-6}$ вт.

Следует иметь в виду возможность сравнения результатов измерений, проведенных на образцах, содержащих разные примеси (при одинаковом

кристалле — матрице), чему осответствуют различные частоты ω_0. В частности, в кристаллах с U-центрами водород может быть заменен дейтерием. Инфракрасное излучение основной решетки может быть эффективно отфильтровано, если использовать фильтры из порошков того же кристалла без примесей [25].

5) Известно [26], что краевые дислокации в щ. г. к. при своем движении переносят электрический заряд, а взаимодействие заряженных ступенек дислокаций с дефектами весьма существенно для механических свойств ионных кристаллов [27]. В работе [28] экспериментально выявлено значительное влияние заряженных ступенек на электронную подсистему дефекта (F — центра).

Используя полученные нами результаты, можно оценить степень возбуждения локальных оптических колебаний заряженными ступеньками быстро движущихся дислокаций, а также соответствующие этому взаимодействию силу торможения дислокации и интенсивность инфракрасного излучения.

Считается [29, 30], что элементарные ступеньки на краевой дислокации в щ.г.к. имеют эффективный заряд $\pm$ e/2. Пусть краевая дислокация единичной длины имеет n_j заряженных ступенек и движется со скоростью v в своей плоскости скольжения. Энергия, теряемая ею на единице пути на возбуждение локальных оптических колебаний, совпадает с соответствующей силой торможения F и равна $F = \mathcal{E} n_j$ ($\mathcal{E}$ дается ф. (28) с $b_0 = a$). Она сильно зависит от скорости дислокации и имеет резкий максимум при $\omega_0 a/v \sim 1$.

Если плотность дислокаций, движущихся со скоростью v есть N_d, то энергия, теряемая ими в единицу времени в объеме V, и соответствующая интенсивность инфракрасного излучения равны

$$\mathcal{E}_d = n_j v \mathcal{E} N_d V, \quad I = \mathcal{E}_d \frac{\Gamma_v}{\Gamma}, \tag{34}$$

Оценим силу F в кристалле KBr(Li), где частота квазилокального колебания $\omega_0 = 4 \cdot 10^{12}$ сек$^{-1}$ [3], для следующих значений величин: $n_j = 4 \cdot 10^6$см$^{-1}$ [28], $N_d = 10^8$ см$^{-2}$, $N_c = 10^{20}$ см$^{-3}$, $v = 6 \cdot 10^4$ см/сек. Получаем $F \sim 2{,}8$ дн/см и соответствующее ему напряжение сдвига $\sigma = Fb^{-1} \sim 560$ гмм$^{-2}$, b — длина вектора Бюргерса. Для сравнения отметим, что используя формулу для силы торможения дислокации $F = Bv$, где определенный из эксперимента коэффициент торможения $B \approx 2 \cdot 10^{-3}$ дн сек. см$^{-2}$ для кристалла KBr [29], мы получим при $v = 6 \cdot 10^4$ см/сек. величину $F \sim 120$ дн/см.

Для указанных выше значений величин и $\omega_0 \Gamma \approx 30$ [3] интенсивность $I \sim (2 \cdot 10^{-7})$ вт/см$^3 \cdot V$. Поскольку причиной этого излучения является взаимодействие заряженной ступеньки с отдельными примесными центрами на расстояниях порядка нескольких постоянных решетки, то его детектиро-

вание позволило бы подтвердить концепцию заряда, связанного со ступенькой, в «микромасштабе» при скоростях дислокаций, близких к предельным.

Для высокочастотных локальных колебаний с $\omega_0 \sim 10^{14}$ сек$^{-1}$ (например, U-центр) величины F, I малы из-за ограниченности скорости краевых дислокаций скоростью поперечных звуковых волн в кристаллах.

В заключение укажем на возможность безызлучательных электронных переходов в примесных центрах, связанную с возбуждением локальных колебаний, а также на возможность выхода примесного иона в междоузлие. Оба эти процесса приводят к разрушению примесного центра. Возбуждение локальных колебаний может быть зафиксировано также, если одновременно измерять сечение неупругого рассеяния нейтронов на локальных колебаниях. Это сечение пропорционально среднему числу квантов $\bar{n}$ для процесса поглощения и $\bar{n} + 1$ для процесса испускания фонона.

*

Авторы благодарны Л. М. Беляеву, В. В. Набатову, Н. М. Плакиде, И. Тарьяну и Г. Турчани за полезные обсуждения.

ЛИТЕРАТУРА

1. И. М. Лифшиц, ЖЭТФ, **12**, 156, 1942.
2. A. Марадулин, Solid State Physics, **18**, 273, 1966; **19**, 1, 1967.
3. M. V. Klein, in "Physics of Colour Centers", ed W. B. Fowler, Academic Press, New York—London, 1968, p. 430.
4. G. Benedek, в книге «Физика примесных центров в кристаллах», г. Таллин, 1972, стр. 181.
5. Г. Бейтмен и А. Эрдейи, Таблицы интегральных преобразований, т. 1, изд-во «Наука», 1969.
6. C. Kittel, Quantum Theory of Solids, John Wiley and Sons Inc., New York—London, 1963.
7. J. M. Ziman, Principles of the Theory of Solids, Cambridge University Press, 1972.
8. Л. Д. Ландау и Е. М. Лифшиц, Теория поля, Физматгиз, 1960.
9. В. М. Агранович, В. Л. Гинзбург, Кристаллооптика с учетом пространственной дисперсии и теория экситонов, изд-во «Наука», 1965.
10. E. M. Henley and W. Thirring, Elementary Quantum Field Theory, McGraw-Hill Book Company, Inc., New York—London, 1962.
11. R. J. Glauber, Phys. Rev., **131**, 2766, 1963.
12. Л. Д. Ландау и Е. М. Лифшиц, Электродинамика сплошных сред, § 69, Гостехиздат, 1957.
13. F. Seitz, Discuss. Farad. Soc., **5**, 271, 1949.
14. M. W. Thompson, Defects and Radiation Damage in Metals, Cambridge University Press, 1969.
15. N. Bohr, J. Linhard, Dan. Math.-Fys. Medd., **28**, 3, 1954.
16. N. O. Lassen, Phys. Rev., **79**, 1016, 1950.
17. J. O. Hirschfelder, Ch. F. Curtiss, R. B. Bird, Molecular Theory of Gases and Liquids, John Wiley and Sons, Inc., New York, Chapman and Hall, Lim., London, 1954.
18. S. S. Schweber, An Introduction to Relativistic Quantum Field Theory, Row, Peterson and Co., New York, 1961.
19. Л. Д. Соловьев, Ю. Я. Юшин, ЖЭТФ, **45**, 1202, 1963.
20. M. Born, Huang Kun, Dynamical Theory of Crystal Lattices, Oxford University Press, 1954.

21. Действие лазерного излучения, Изд-во «Мир», М., 1968.
22. C. R. Giuliano, Appl. Phys. Lett., **5,** 137, 1964.
23. Л. М. Беляев, В. В. Набатов, Ю. В. Писаревский, Ю. В. Шалдин, Кристаллография, **10,** 767, 1965.
24. Л. М. Беляев, А. Н. Головистиков, В. В. Набатов, ФТТ, **10,** 3733, 1968.
25. Длинноволновая инфракрасная спектроскопия, изд-во «Мир», М., 1966.
26. А. А. Урусовская, УФН, **96,** 39, 1968.
27. J. D. Eshelby, C. W. Newly, P. L. Pratt, A. B. Lidiard, Phil. Mag., **3,** 75, 1958.
28. G. Turchányi, J. Janszky, M. Mátrai, I. Tarján, Phys. Stat. Sol., **38,** K 35, 1970.
29. F. Seitz, Phys. Rev., **80,** 239, 1950.
30. J. P. Hirth, J. Lothe, Theory of Dislocations, Academic Press, New York, 1968.
31. R. Strumane, R. De Batist, Phys. Stat. Sol., **3,** 1387, 1963.
32. В. Б. Парийский, А. И. Третьяк, ФТТ, **9,** 2457, 1967.

Acta Physica Academiae Scientiarum Hungaricae, Tomus 41 (1), pp. 19—27 (1976)

ELASTIC SHEAR WAVES IN THE PRESENCE OF COUPLE STRESSES

By

V. B. NYAYADHISH

UNIVERSITY DEPARTMENT OF CHEMICAL TECHNOLOGY, BOMBAY, INDIA

(Received 18. III. 1976)

In this paper the effect of the presence of couple stresses in an elastic medium on the propagation of shear waves is discussed. Two different analytical representations for the solution are obtained. Diffusion is seen to dominate near the source. Far down the source two wave fronts appear. One is associated with damping, the other, corresponding to the classical one, is associated with dispersion and its variation for large time is obtained in terms of *Airy function*. By using the Fourier-Laplace transforms, the displacement is expressed in terms of integrands of the modified Bessel function. The integrals are numerically calculated for all time and the results are presented by suitable graphs.

1. Introduction

Continuum mechanics is the study of the response of a medium to deformation. The conservation laws for mass, momentum and energy have to be supplemented by a constitutive law to characterise the medium. The statement of a constitutive law is based on the *Hypothesis* of the existence of a *Stress Vector*. As the body deforms it is assumed that contiguous parts exert a mutual action across bounding surfaces. It is *further assumed* that these surface forces reduce, in the limit of vanishing area, to a *single force* inclined, in general, to the common normal. Symmetry of the stress tensor follows from this *further assumption*. It is important to realise that this symmetry is an assumption. There is nothing in the derivation of basic laws to prove it. Once it is recognised as an assumption, it is natural to inquire into the consequence of rejecting it. The mutual action has then to be assumed to reduce to a force and a couple, without loss of any generality.

Several attempts have been made to construct a new theory of elasticity based on this broader assumption. Recently the subject has attracted attention again. The different authors have, sometimes, varied attitudes to the development. TOUPIN [1] has given a general review of earlier work and the formulation of this general theory. MINDLIN and TIERSTEN [2] have rederived the general and linearised equations. They give solutions to a number of new problems. They conclude that the existence of couple stresses may be of microscopic character and may not show up in ordinary problems of engineering interest. KOITER [3] reviews earlier work by himself and others. His original enquiry

was to seek an explanation of fatigue by use of this theory. He also gives solutions to a number of simple problems where the new theory can be tested. KRÖNER [4] gives a quite novel explanation. He traces the difficulty to the limiting procedure involved. In the reduction of mutual action to a resultant, one proceeds to the limit of vanishing areas. But there exists a lower bound dictated by the interatomic distances beyond which one cannot shrink areas. This lower bound below which the dimensions of an element cannot shrink, gives rise to couple stresses of various orders in macroscopic phenomena. HUNTINGTON [5] gives an interesting discussion of the physical circumstances under which couple stresses are possible. It is possible that the best indication of the existence of couple stresses is given by moving dislocations, since it is one of the bridges connecting the microscopic and the macroscopic states of a body.

Wave propagation is one of the important experimental methods of evaluating elastic constants. So in the following we attempt to study the propagation of shear waves. The dilational wave propagated is unaffected by the existence of couple stresses. The theory of singular surfaces gives a sharp wave front for this irrotational wave while it does not lead to any discontinuous variation of rotation. So it is only the shear wave that is affected by the new theory, therefore we study the simplest shear wave generated by a source. The existence of couple stresses drastically modifies these 'waves'. The governing equation is no more hyperbolic. We first give an exact integral representation of the solution. Using the interesting technique followed by STEKETEE [6] in the study of magnetohydrodynamic waves in the presence of viscosity and electrical conductivity, we obtain the solution as a superposition of solutions of 'elliptic' equations. We then give the Laplace transform solution. We obtain now 'two' 'wave-fronts'. One is exponentially damped while the other, corresponding to the classical wavefront, decays in amplitude as the cube root of the inverse distance for large distances, near to the wave front, while everywhere else it appears to fall off exponentially.

2. Statement and solution of the problem

Referred to a Cartesian System (x, y, z) let the displacement vector be $(0, v(x, t), 0)$. We then seek the solution of the problem [2]:

$$\left(1 - l^2 \frac{\partial^2}{\partial x^2}\right) \frac{\partial^2 v}{\partial x^2} = \frac{1}{c^2} \frac{\partial^2 v}{\partial t^2} + \frac{A}{c^2} \delta'(x)\delta(t). \tag{2.1}$$

Here the right-hand member consisting of delta functions, gives the 'source' term; A may-be taken as the strength of this source; $c = (\mu/\varrho)^{1/2}$ gives

the shearwave velocity in absence of couple stresses; l is a new parameter, of the dimension of the length, and, is the square root of the ratio of the new elastic constant to shear modulus. We choose $ct \to t$ so that the new wave velocity is unity and the new time has the dimension of length. We further set $x \to lx$, $t \to lt$, $v \to vl$ and take the coefficient of the source term as unity. We then have

$$\left(1 - \frac{\partial^2}{\partial x^2}\right) \frac{\partial^2 v}{\partial x^2} = \frac{\partial^2 v}{\partial t^2} + \delta'(x)\,\delta(t). \tag{2.1a}$$

In the absence of couple stresses $l = 0$ and we have the simple wave equation. Since the new parameter multiplies the highest derivatives it should exhibit boundary layer behaviour. But in addition it changes the basic character of the equation, which is no more hyperbolic. This change in the character of the equation is brought out very clearly by the following solution. We also feel that this procedure offers an additional novel way of treating transform problems.

The fourth order differential operator in (2.1a) does not formally separate into two second order ones. We are able to effect this 'factorisation' by the following technique.

Taking the Laplace transform of (2.1a), we obtain

$$(1 - D^2)D^2\,\bar{v} = p^2\,\bar{v} + \delta'(x)\,, \tag{2.2}$$

where a bar denotes Laplace transform, p the transform variable, and D denotes differentiation with respect to x. This can be rewritten as

$$(D^4 - D^2 + p^2)\,\bar{v} = -\,\delta'(x)\,. \tag{2.3}$$

Formal 'factorisation' leads to

$$(D^2 - \sqrt{2}\,\sqrt{p+1/2}\,D + p)\,(D^2 + \sqrt{2}\,\sqrt{p+1/2}\,D + p)\,v = -\,\delta'(x)\,. \tag{2.4}$$

If $v = \exp(-t/2)u$, then $v(x, p) = u(x, p + 1/2)$ [7]. Replacing p by $(p - 1/2)$ and v by u, we get,

$$(D^2 - \sqrt{2p}\,D + p - 1/2)\,(D^2 + \sqrt{2p}\,D + p - 1/2)\,\bar{u} = -\,\delta'(x)\,. \tag{2.5}$$

Further if

$$u(x, t) = \int_0^\infty \frac{T}{2\sqrt{\pi t^3}} \exp\left(-\frac{T^2}{4t}\right) w(x, T)\,dT\,, \tag{2.6a}$$

then we have [7],

$$\bar{u}(x, p) = \bar{w}(x, \sqrt{p})\,. \tag{2.6b}$$

So replacing $\sqrt{p}$ by p and $\bar{u}$ by $\bar{w}$ we obtain

$$(D^2 - \sqrt{2}pD + p^2 - 1/2)(D^2 + \sqrt{2}pD + p^2 - 1/2)\,\bar{w} = -\delta'(x)\,. \quad (2.7)$$

The equation has now formally 'factored' out. The above is equivalent to

$$\left(\frac{\partial^2}{\partial x^2} - \sqrt{2}\frac{\partial^2}{\partial x \partial t} + \frac{\partial^2}{\partial t^2} - \frac{1}{2}\right)\left(\frac{\partial^2}{\partial x^2} + \sqrt{2}\frac{\partial^2}{\partial x\,\partial t} + \frac{\partial^2}{\partial t^2}\frac{1}{2}\right) w = $$

$$= -\delta'(x)\delta(t)\,. \quad (2.8)$$

To solve this we exploit the factorisation and introduce

$$L_1 w_1 = \frac{\partial^2 w_1}{\partial x^2} - \sqrt{2}\frac{\partial^2 w_1}{\partial x\,\partial t} + \frac{\partial^2 w_1}{\partial t^2} - \frac{1}{2}w_1 = -\delta(x)H(t)\,, \quad (2.9a)$$

$$L_2 w_2 = \frac{\partial^2 w_2}{\partial x^2} - \sqrt{2}\frac{\partial^2 w_2}{\partial x\,\partial t} + \frac{\partial^2 w_2}{\partial t^2} - \frac{1}{2}w_2 = -\delta(x)H(t)\,. \quad (2.9b)$$

Note that $L_1 w_1 = L_2 w_2$. Also L_1, L_2 are linear differential operators and so commute. Using this property we get

$$L_1 L_2(w_1 - w_2) = L_2(L_1 w_1) - L_1(L_2 w_2) = (L_2 - L_1)\left(-\delta(x)H(t)\right)$$

$$= 2\sqrt{2}\frac{\partial^2}{\partial x\,\partial t} - \left(\delta(x)H(t)\right) = -2\sqrt{2}\,\delta'(x)\delta(t)\,. \quad (2.10)$$

Comparing (2.8) and (2.10) we obtain

$$w = \frac{1}{2\sqrt{2}}(w_1 - w_2). \quad (2.11)$$

We further note that (2.6a) can be integrated by parts to give

$$u(x,t) = \frac{1}{\sqrt{\pi t}}\left\{\left[-\exp\left(-\frac{T^2}{4t}\right)w(x,T)\right]_{T=0}^{\infty} + \int_0^{\infty}\exp\left(-\frac{T^2}{4t}\right)\frac{\partial\omega}{\partial t}(x,T)\,dT\right\} =$$

$$= \frac{1}{\sqrt{\pi t}}\int_0^{\infty}\exp\left(-\frac{T^2}{4t}\right)\frac{\partial w}{\partial t}(x,t)\,dT. \quad (2.12)$$

Since we thus need $(\partial w/\partial t)$, we need only $z_1 = (\partial w_1/\partial t)$ and $z_2 = (\partial w_2/\partial t)$ satisfying the differential equations

$$\frac{\partial^2 z_1}{\partial t^2} - \sqrt{2}\frac{\partial^2 z_1}{\partial x \partial t} + \frac{\partial^2 z_1}{\partial t^2} - \frac{1}{2} z_1 = -\delta(x)\delta(t)\,, \tag{2.13a}$$

$$\frac{\partial^2 z_2}{\partial t^2} + \sqrt{2}\frac{\partial^2 z_2}{\partial x \partial t} + \frac{\partial^2 z_2}{\partial t^2} - \frac{1}{2} z_2 = -\delta(x)\delta(t)\,. \tag{2.13b}$$

To obtain z_1 we change it to the canonical form by the following transformation of variables. Let

$$\xi = x + \frac{1}{\sqrt{2}} t,\ \eta = \frac{1}{\sqrt{2}} t\,. \tag{2.14}$$

Using this we obtain the equation for z_1 as

$$\frac{\partial^2 z_1}{\partial \xi^2} + \frac{\partial^2 z_1}{\partial \eta^2} - z_1 = -2\,\delta(\xi)\,\delta(\eta)\frac{\partial(\xi, \eta)}{\partial(x, t)} = -\sqrt{2}\,\delta(\xi)\delta(\eta)\,. \tag{2.15}$$

The last Jacobian transforms the delta functions to the new variables. But the Eq. (2.15) is an elliptic equation. Thus the solution of the basic problem of 'wave propagation' is obtained by superposing solutions of 'elliptic equation'. The new variables are of course different. In view of the transformation (2.12) corresponds to $\sqrt{t}$ and not to t. So the solution may be said to be a superposition of the solutions of a parabolic equation. However strict parabolicity would have been there only if the term in l^2 in (2.1) were positive. The above method is a novel approach to deal with problems and also provides an interesting revelation of the change in the character of the basic equation which does not belong to any standard type.

It is now straightforward to write solutions for z_1 and z_2.

We have,

$$\begin{aligned} z_1 &= \sqrt{2}\,K_0\left(\sqrt{x^2 + t^2 + \sqrt{2}\,xt}\right), \\ z_2 &= \sqrt{2}\,K_0\left(\sqrt{(x^2 + t^2 - \sqrt{2}\,xt}\right). \end{aligned} \tag{2.16}$$

Using these we finally obtain u as

$$\begin{aligned} u(x, t) = &-\frac{1}{2\sqrt{\pi t}}\int_0^\infty \exp\left(-\frac{T^2}{4t}\right)\left[K_0\left(\sqrt{x^2 + t^2 + \sqrt{2}\,xt}\right) - \right. \\ &\left. - K_0\left(\sqrt{x^2 + t^2 + \sqrt{2}\,xt}\right)\right] dT = \\ = &-\frac{1}{\sqrt{\pi}}\int_0^\infty \exp(-u^2)\left[K_0\left(\sqrt{x^2 + 4tu^2 + 2\sqrt{2t}\,xu}\right) - \right. \\ &\left. - K_0\left(\sqrt{x^2 + 4tu^2 - 2\sqrt{2t}\,xu}\right)\right] du\,. \end{aligned} \tag{2.17}$$

The original variable v is easily obtained as $v = \exp(-1/2\, t)u$. The solution clearly exhibits $v(0, t) = v(x, 0) = 0$. The form of representation indicates $(x/\sqrt{t})$ as a similarity variable.

It was not possible to convert it into simpler representations. We could represent the modified second type of Bessel function by use of addition theorem and convert it into a series of integrals involving confluent hypergeometric functions. But that does not help to reveal the nature of propagation any more clearly than (2.17). For large x, K_0 can be replaced by exponentials by use of their asymptotic forms. The contribution to the integral is then seen to be provided by the vicinity of the origin. This indicates the dominant behaviour near $x \sim t$. To see these things clearly we obtain below the Laplace transform solution by a straightforward process.

3. Asymptotic forms

We take the Fourier and Laplace transform of (2.1a) and perform the Fourier inversion. We then obtain for, $x > 0$ the Laplace transform of v as

$$\bar{v} = \frac{1}{2\sqrt{p^2 - \frac{1}{4}}} \exp\left(-\sqrt{p + \frac{1}{2}}\,\frac{x}{\sqrt{2}}\right) \sin\left(\sqrt{p - \frac{1}{2}}\,\frac{x}{\sqrt{2}}\right) \tag{3.1}$$

$$= \frac{1}{\sqrt{1-4p^2}} \exp\left(-\sqrt{p + \frac{1}{2}}\,\frac{x}{\sqrt{2}}\right) \sinh\left(\sqrt{\frac{1}{2} - p}\,\frac{x}{\sqrt{2}}\right). \tag{3.1a}$$

If we replace the original dimensional variables x and t, we can in fact pass the limit $l \to 0$ of the two exponentials in (3.1a),

$$m_{1,2} = \exp\left[-\frac{x}{2}\left(\sqrt{1 + 2\,lp} \pm \sqrt{1 - 2lp}\right)\right], \tag{3.1b}$$

$$m_1 \to \exp(-x/l), \quad m_2 \to (-px).$$

This solution corresponding to m_1 thus tends to zero as $l = 0$, while that corresponding to m_2 leads to the solution

$$v_c = -\frac{1}{2}\,\delta(t - x). \tag{3.2}$$

This solution (3.2) is the solution of the original problem (2.1) in absence of couple stresses viz. $l = 0$. We then have a wave front travelling without change of form.

It is important to note that the Laplace transform is defined as a single valued function on the Browmwhich contour which is any line parallel to the imaginary axis in the complex p-plane, such that all the singularities lie to its left. Any line now such that Re $p > 1/2$ satisfied the requirement. However, it must be noted that $p = 1/2$ is not a singularity of the integrand, while $p = -1/2$ is the only singularity, being a branch point.

For $u \ll 1$, and small x, we expand the sine function and perform the inversion to obtain

$$v = \frac{x}{2\sqrt{2}} \exp\left(\frac{1}{2}t\right) \sum_0 \frac{(-1)^n}{(2n+1)!} \left(\frac{x^2}{2}\right)^n \frac{d^n}{dx^n}\left[\frac{1}{\sqrt{\pi t}} \exp\left(-\frac{x^2}{8t} - t\right)\right]. \quad (3.3)$$

The series (3.3), exhibits the diffusive nature of the solution near the boundary. Again since $p = 1/2$ is not a branch point the imaginary axis is an admissible contour. Taking this we get

$$v = \frac{1}{\pi}\int_0^\infty \frac{\cos\left(ut - x\sqrt{\sqrt{u^2+\frac{1}{4}} - \frac{1}{2}}\right)}{\sqrt{u^2+\frac{1}{4}}}\,du - \quad (3.4)$$

$$- \frac{1}{\pi}\int_0^\infty \frac{\cos(ut)\exp\left(-x\sqrt{\sqrt{u^2+\frac{1}{4}} - \frac{1}{2}}\right)}{u}\,du\,.$$

The second integral is everywhere exponentially small for large x and so it may be disregarded. The first integral is, however, of the known form discussed in the literature [8]. We obtain

$$v \sim \left(\frac{2}{3x}\right)^{1/3} Ai\left[\left(\frac{2}{3x}\right)^{1/3}(t-x)\right], \quad (3.5)$$

where Ai denotes the Airy function.

The variation of the amplitude as inverse cube root of distance near the wave front $t \sim x$ is clear from above. The same conclusions can be seen from the method of *steepest descent* in greater detail. The exponentials in the inversion of (3.1a) can be written as

$$\exp[-x\{m(p) - \delta p\}], \quad (3.6)$$

where $\delta(t/x) = 1/k$.

For each fixed δ or k, for large x, the major contribution to the integral comes from the neighbourhood of the stationary points, given by $m'(p) = \delta$ as

$$p_{1,2} = \mp\frac{1}{8}\left([8 - 4k^2 - k^4 + 8\sqrt{1-k^2}]^{1/2} \pm [8 - 4k^2 - k^4 - 8\sqrt{1-k^2}]^{1/2}\right). \quad (3.7)$$

Of the above two roots it can be verified $p_{1,2}$ belong to $m_{1,2}$ respectively. However, p_1 gives an exponentially small contribution. Limiting attention to the neighbourhood of the wave-front, $t \sim x$ with $k^2 = 1 + \varepsilon$, we obtain

$$p_2 = \frac{2}{\sqrt{3}} \sqrt{\varepsilon} \,. \tag{3.8}$$

Thus for $t = x$, origin is a saddle point. The path of steepest descent is such that

$$\mathrm{Im}[m(p) - p] = 0, \quad \mathrm{Re}[m(p) - p] > 0 \,. \tag{3.9}$$

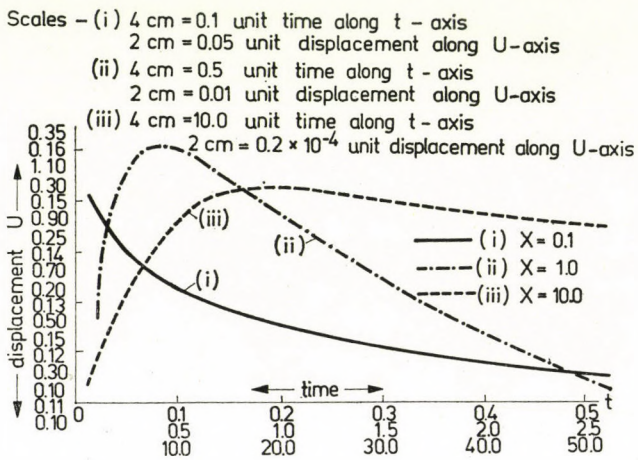

Fig. 1. The curve of displacement against time for $x = 0.1$, $x = 1.0$ and $x = 10.0$

It can be verified that the path starts from the origin, at angles $\pm(2\pi/3)$ and at infinity, is asymptotic to $\sqrt{2\varrho} \sin(\theta/2) = \pm 1$. The analytical expression for the path is not easy to obtain. However, $[m(p) - p]$ behaves, near the origin as p^3 and so, with an exponential error, we can take the path of definition of Airy integral [8]. Then we are led essentially to the same conclusions as in (3.8). For $\varepsilon > 0$, $t < x$, p_2 is real, giving an exponentially small contribution. This shows that there is a sharp fall in the amplitude just in front of $t = x$ i.e. ahead of the classical wave. However, just behind the front it has an oscillatory behaviour since p_2 gives two points on the imaginary axis.

The Figure shows the solution as calculated from (2.17). For different values of x the ranges of the values of t and u are taken as follows.

$x = 0.1,$	$t\,(0.01, \ 3.0),$	$u\,(0.0, \ 11.10).$
$x = 1.0,$	$t\,(0.10, \ 6.0),$	$u\,(0.0, \ 11.10).$
$x = 10.0,$	$t\,(1.0, \ 60.0),$	$u\,(0.0, \ 11.10).$

4. Conclusion

The existence of couple stresses changes the character of the propagation basically. A wave unchanged in form in their absence is modified drastically. Near the source it is highly oscillatory and diffusive, whereas far from the source, the amplitude decays as the inverse cube root of distance, falling off exponentially ahead and in an oscillatory manner behind the classical shear-wave front.

Acknowledgement

The author wishes to thank the Manager, Electronic Data Processing Centre, Bombay University, Bombay 1, for giving free facilities to make use of IBM 1620 Model II computer in order to complete the numerical work of this paper.

REFERENCES

1. R. A. TOUPING, Arch. Rat. Mech. Anal., **5**, 385, 1962.
2. R. D. MINDLING and H. F. TIERSTEN, Arch. Rat. Mech. Anal., II, **5**, 415, 1962.
3. W. T. KOITER, I and II Koninkl. Neder. Akad. Waten. 1964, LXVII No. 1, 17—29 and 30—44, Ser. B.
4. E. KRONER, Inter. Jour. Engg. Sci., **1**, 261, 1963.
5. H. B. HUNTINGTON, Solid State Physics, **7**, 214, 1958.
6. J. A. STEKETEE, IA and IB, Koninkl. Neder. Akad. Western. Sec. B. Bol. LXVI, 216—226 and 227—235, 1963.
7. H. S. CARSLAW and J. C. JAEGER, "Operational Methods in Applied Mathematics", Dover Publ. 259, 1963.
8. H. JEFFREYS and B. JEFFREYS, Methods of Mathematical Physics, Camb., III, 508 and 517.

Acta Physica Academiae Scientiarum Hungaricae, Tomus 41(1), pp. 29—30 (1976)

SELF CONFINEMENT IN HIGHLY IONIZED PLASMAS

By

A. E. POZWOLSKI

75020 PARIS, FRANCE*

(Received 4. V. 1976)

Although the pressure of a plasma usually grows as its density it is shown that for a sufficiently high degree of ionization Z the pressure can decrease even to zero.

The total pressure p of a plasma is the sum of the ionic pressure and the electronic pressure and except for very dilute plasmas such sum is smaller than the value predicted from the perfect gas theory, because of the mutual attraction between particles of opposite charge.

The pressure is then conveniently obtained from:

$$p = -(\partial F/\partial V)_T\,, \tag{1}$$

where F is the free energy and V and T are the volume and the temperature, respectively. The free energy of a plasma is easy to compute for plasmas where a Debye sphere contains a large number of particles; analytically this means:

$$e^2 n^{1/3}/kT \ll 1 \tag{2}$$

or

$$kT/n_i^{1/3}\ e^2 \gg Z^{1/3}\,, \tag{3}$$

where $n = Zn_i$ is the electronic density and e is the electronic charge in e.s.u. Now, if only one kind of ion Z times ionized is present, the pressure has according B. D. FRIED [1] the value:

$$p = nkT\left\{(1 + 1/Z) - \pi^{1/2}/3\left[\frac{n^{1/3}\,(1+Z)\,e^2}{kT}\right]^{3/2}\right\}. \tag{4}$$

Eq. (4) can be rearranged as follows:

$$p = n_i\,kT(Z + 1)[1 - aZ^{3/2}(Z + 1)^{1/2}]\,, \tag{5}$$

where $a = \pi^{1/2}/3(n_i^{1/3}e^2/kT)^{3/2}$.

* 3A3 Résidence Lorraine, 4 — 6 rue de la Plaine, 75020 Paris, France.

The problem to be solved, for fixed density n_i is the effect of an increase of the ion charge number.

Obviously, from (5) the pressure shows a maximum when Z increases and this maximum occurs for a value Z_0 solution of the equation $dp/dZ = 0$:

$$4Z^4 + 8Z^3 + 5Z^2 + Z - 4/9a^2 = 0 .$$

Taking $kT/n_i^{1/3}e^2 = 20$ corresponding to $a = 6.61 \times 10^{-3}$ it is found that the pressure is maximum for $6 < Z < 7$ ($Z_0 = 6.62$).

If Z grows larger than Z_0 the pressure will decrease and becomes equal to zero for a value Z_{00} solution of:

$$Z^4 + Z^3 - 1/a^2 = 0 .$$

For the same example as above it is found that $Z_{00} = 12$. In these conditions the plasma is self confined by the internal electrostatic forces.

The present derivation is restricted to low density and high temperature plasmas, in order to check conditions (2) or (3). For dense plasmas the inequalities (2) and (3) are reversed; however the ionic pressure is still obtainable from (1) [2, 3]. At extremely large densities the ion-electron interaction could lead to an imperfect lattice structure [4]; M. A. Cook expects such conditions in some stars if $Z \geqslant 16$.

REFERENCES

1. Wulf B. Kunkel, Plasma Physics in Theory and in Applications, Chap. III, p. 54—55, McGraw-Hill, 1966.
2. A. E. Pozwolski, Phys. Lett. A **44A**, 196, 1973.
3. A. E. Pozwolski, The Ionic Pressure in Dense Plasmas, International Conference on Statistical Physics, Budapest, August 25—29, 1975.
4. M. A. Cook, The Science of High Explosives, Reinhold, p. 420—426, 1968.

Acta Physica Academiae Scientiarum Hungaricae, Tomus 41 (1), pp. 31—40 (1976)

AN ANGULAR FORCE MODEL FOR LATTICE DYNAMICS OF BODY CENTERED CUBIC METALS

By

M. M. SHUKLA

INSTITUTO DE FISICA "GLEB WATAGHIN", UNIVERSIDADE ESTADUAL DE CAMPINAS
CP 1170 — CAMPINAS — SP. BRASIL

and

H. TEJIMA*

DEPARTAMENTO DE FISICA DA FACULDADE DE FILOSOFIA, CIENCIAS E LETRAS DE RIO CLARO, SP., BRASIL

(Received in revised form 10. V. 1976)

A phenomenological model for lattice dynamics of b.c.c. metals is proposed by combining central ion-ion interaction on BVK scheme, angular ion-ion interaction on CLARK—GAZIS—WALLIS scheme and electron-ion interaction on KREBS's scheme with an essential modification of the dielectric screening function. Calculated phonon dispersion curves of sodium along all the five principal symmetry directions as well as $(\Theta - T)$ curve of it show a good agreement with the experimental findings.

1. Introduction

In the recent past experimental phonon dispersion relations along the principal symmetry directions in almost all cubic metals have been determined by means of cold neutron scattering techniques. The interpretation of the experimental results in terms of the existing theoretical models have demonstrated the fact that none of the models is complete in the sense that it explains satisfactorily well lattice dynamics of all the metals of the same crystallographic structure with equal success. In spite of the boundless efforts of theoreticians to refine the theories on first principles (see for example TOYA [1], HARRISON [2], VOSKO et al. [3] and PRICE et al. [4] and references therein) as well as on phenomenological basis (see for example KREBS [5], CHEVEAU [6] and SHUKLA et al. [7] and references therein), still today a scope exists for new models.

In the present paper a phenomenological model for lattice dynamics of b.c.c. metals is developed in which total interatomic interactions present in b.c.c. metals are divided into three parts, central ion-ion interaction, angular ion-ion interaction and the electron-ion interaction. The ion-ion interactions

* Also at Departamento de Fisica, Instituto de Fisica "Gleb Wataghin", Universidade Estadual de Campinas.

are considered effective between first two neighbours, the central interaction being taken from Born-Von-Karman scheme and the angular one from the work of CLARK et al. [8]. The electron-ion interaction has been considered on the formalism of KREBS [5] with an essential modification in his scheme as far as the dielectric screening in metals is considered. While KREBS [5] has used the Lindhard's form for the dielectric screening function, we have used several existing ones. The present formalism is tested first to sodium for which experimental data on phonon frequencies and elastic and thermal properties exist.

2. Theory

The phonon frequencies are obtained from the solution of the secular determinant

$$| D_{ij}(q) - m\omega^2 I\delta_{ij} | = 0 , \tag{1}$$

where m is ionic mass, δ_{ij} is Kronecker's delta and I is a 3×3 unitary matrix.

Each element of the dynamical matrix D_{ij} is split up into three parts, central ion-ion interaction part $D_{ij}^{ic}(q)$, angular ion-ion interaction part, $D_{ij}^{ia}(q)$ and the electron-ion interaction part, $D_{ij}^{ie}(q)$, written mathematically,

$$D_{ij}(q) = D_{ij}^{ic}(q) + D_{ij}^{ia}(q) + D_{ij}^{ie}(q) . \tag{2}$$

By considering the ion-ion and electron-ion interactions in the way as stated in the introduction, the typical diagonal and non-diagonal parts of the dynamical matrices are given by

$$D_{ii}^{ic}(q) = 8\alpha_1(1 - C_iC_jC_k) + 4\alpha_2 S_i^2 , \tag{3}$$

$$D_{ii}^{ia}(q) = (16\gamma_1 + 24\gamma_2)[(1 - C_iC_jC_k) - 2\gamma_1(4\cos aq_i - \cos aq_j - \cos aq_k - 2)] + \\ + 3\gamma_2(2 - \cos aq_j - \cos aq_k) , \tag{4}$$

$$D_{ii}^{ie}(q) = \frac{a^3\lambda^2}{4} K_e \left[\sum_h \frac{(q_i + h_i)^2}{|\vec{q}+\vec{h}|^2 + \frac{a^2\lambda^2}{4\pi^2} f(t_1)} q^2(u_1) - \frac{h_i^2}{h^2 + \frac{a^2\lambda^2}{4\pi^2} f(t_2)} g^2(u_2) \right], \tag{5}$$

$$D_{ij}^{ic}(q) = 8\alpha_1 S_i S_j C_k , \qquad i \neq j \tag{6}$$

$$D_{ij}^{ia}(q) = 8\,(3/2\ \gamma_2 - \gamma_1)\, S_i S_j C_k ,$$

$$D_{ij}^{ie} = \frac{a^3\lambda^2}{4} K_e \sum_h \frac{(q_i+h_i)(q_j+h_j)}{|\vec{q}+\vec{h}|^2 + \frac{a^2\lambda^2}{4\pi^2} f(t_1)} g^2(u_1) - \frac{h_i h_j}{h^2 + \frac{a^2\lambda^2}{4\pi^2} f(t_2)} g^2(u_2) \Bigg], \tag{7}$$

where α_i, γ_i are respectively the central and angular force constants for the i^{th} neighbour. S_i, C_i and C_{2i} are respectively $\sin(1/2\, aq_i)$, $\cos(1/2\, aq_i)$ and $(\cos q_i a)$. a is the lattice parameter, (k_i, h_i) are respectively i^{th} component of the direct and reciprocal lattice vector. q_i is i^{th} component of the phonon wave vector i.e. $q_i = 2\pi/a\, k_i$. The function $g(u)$ is the same as given in KREBS' paper [4]. Function $f(t)$ has been chosen in the following forms:

$$f(t) = \frac{1}{2} + \frac{4 - t^2}{8t} \ln \frac{2 + t}{2 - t} \quad \text{Lindhard's form} \tag{8}$$

$$f(t_1) = \frac{f(t)}{1 - f(t)\, f(\lambda)} \quad \text{Modified Hubbard's expression (see FALICOV and HEINE [9]),} \tag{9}$$

where

$$f(q) = 1/2\; q^2/(q^2 + k_F + k_{T_F}^2) \tag{10}$$

GELDART and VOSKO's [10] form is obtained by replacing $f(q)$ in Eq. (3.8) by

$$f(q) = \frac{1}{2} \frac{q^2}{q^2 + \xi k_F^2}, \tag{11}$$

where

$$\xi = \frac{2}{1 + 0.026\, \gamma_s^x}, \tag{12}$$

$$\gamma_s^x = \frac{m^x}{m} \gamma_s, \tag{13}$$

where m, m^x are mass and effective mass of electron, k_{T_F} = Thomas—Fermi screening constant.

SINGWI et al's [11] form

$$f(q) = A\; [1 - e^{-B(q/K_F)^2}], \tag{14}$$

where $A = 0.995$, $B = 0.2625$.

By expanding the secular determinant in the long wavelength limit $(q \to 0)$, the following relations are obtained between the elastic constants and force constants:

$$aC_{11} = 2\alpha_1 + 2\alpha_2 + 12\gamma_1 + 6\gamma_2 + aKe, \tag{15}$$

$$aC_{12} = 2\alpha_1 - 6\gamma_1 + 3\gamma_2 + aKe, \tag{16}$$

$$aC_{44} = 2\alpha_1 + 2\gamma_1 + 9\gamma_2. \tag{17}$$

3. Numerical computations

To determine the five disposable parameters in the model, use has been made of five equations i.e. Eqs. (15) to (17) relating the force constants and elastic constants together with two more equations relating the force constants with phonon frequencies. While the experimental values of the elastic constants were taken from the measurements of MARTINSON [12], the experimental phonon frequencies, longitudinal frequency from $|\, 00\xi \,|$ direction and transversal frequency from $|\, \xi\xi\xi \,|$ direction, corresponding to the measurements of WOODS et al. [13]. While the input data to calculate the force constants are given in Table I, the output values of force constants are reported in Table II. The calculated phonon dispersion curves of sodium along all the

Table I

Input data to calculate force constants

Lattice parameter (a) in Å = 4.24

Elastic constants in 10^{11} dyn cm^{-2}

$C_{11} = 0.854$
$C_{12} = 0.709$
$C_{44} = 0.582$

Atomic mass (M) in 10^{-23} gm

$M = 3.8163$

Phonon frequencies in 10^{12} c/s

$\nu L\ \zeta 00 = 3.58$
$\nu L\ \zeta\zeta\zeta = 2.88$

Table II

Calculated values of atomic force constants of sodium in units of 10^3 dyn cm^{-1}

$\alpha_1 = 1.412$
$\alpha_2 = 0.924$
$\gamma_1 = 0.056$
$\gamma_2 = 0.025$
$aKe = 0.420$

five symmetry directions are shown in Figs. 1 to 5. In these Figures the experimental results of WOOD et al. [13] are also shown for comparison purpose, as well as their theoretical predictions of the dispersion curves on point ion model studies. While the present theoretical curve is represented by continuous lines, broken curves correspond to the theoretical predictions of WOODS et al. [13]. The experimental points are shown by the different symbols given in the captions for the Figures. By dividing the first Brillouin zone into 8000 equivalent points, the complete vibration spectrum of sodium was also calculated. The resulting spectrum was utilised to plot the $g(\nu)$ versus ν curve.

Blackman' sampling technique was used to calculate the lattice heat capacities at various temperatures. The corresponding C_v versus temperature curve is shown in Fig. 6 together with the experimental C_v for comparison purpose.

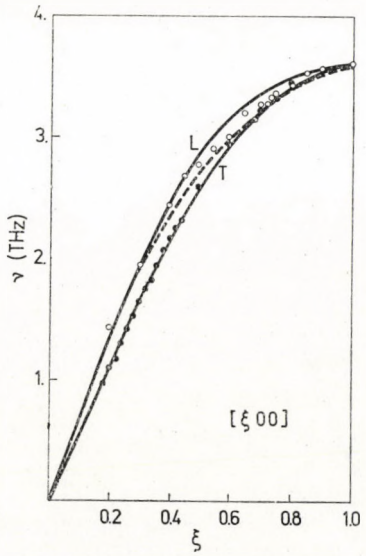

Fig. 1. Phonon dispersion curves of sodium along [ξ00] direction. Present results are shown by solid lines. Broken curves correspond to the theoretical predictions of WOODS et al. Experimental points are shown by ○

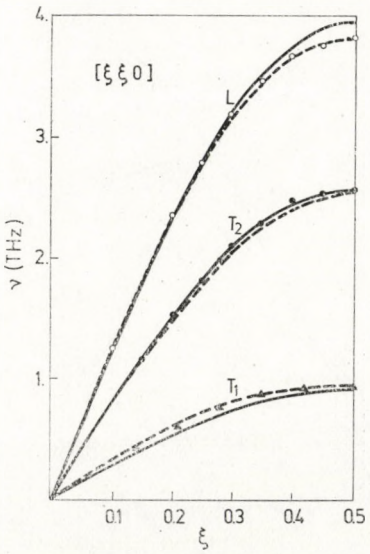

Fig. 2. Phonon dispersion curves of sodium alon [ξξ0] g direction. Broken curves correspond to the theoretical predictions of WOODS et al. Experimental points are shown by ▲

The experimental C_v was taken from the work of SIMON and ZEIDLER [14]. To estimate the heat capacities of sodium metal, the coefficient of the electronic heat capacity, γ, was subtracted from the experimental C_v data. The value

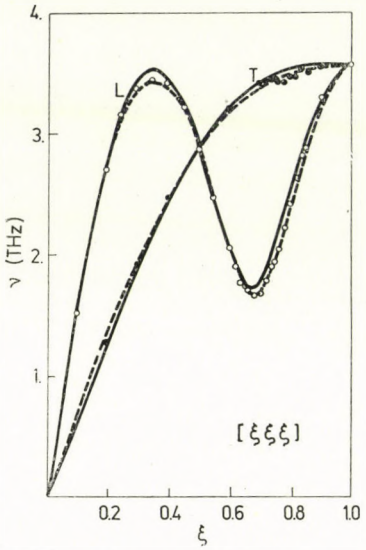

Fig. 3. Phonon dispersion curves of sodium along [ξξξ] direction. Broken curves correspond to the theoretical predictions of WOODS et al. Experimental points are shown by ○

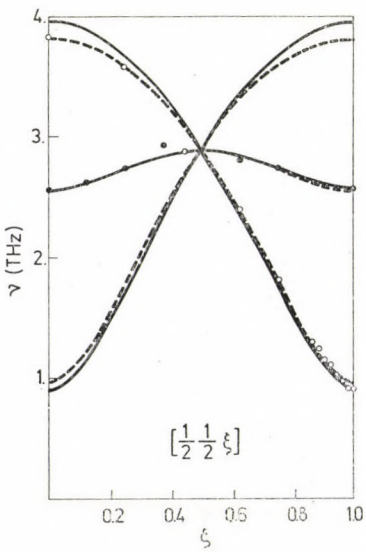

Fig. 4. Phonon dispersion curves of sodium along [1/2 1/2 ξ] direction. Broken curves correspond to the theoretical predictions of WOODS et al. Experimental points are shown by ○

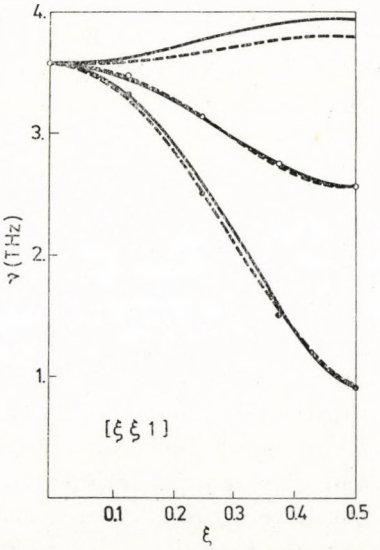

Fig. 5. Phonon dispersion curves of sodium along [ξξ1] direction. Broken curves correspond to the theoretical predictions of WOODS et al. Experimental points are shown by ○

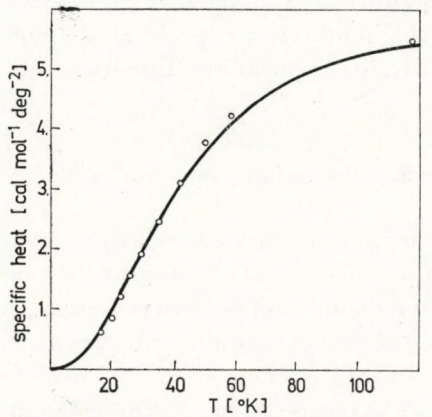

Fig. 6. (C_v — T) curves of sodium. Experimental points are shown by ○

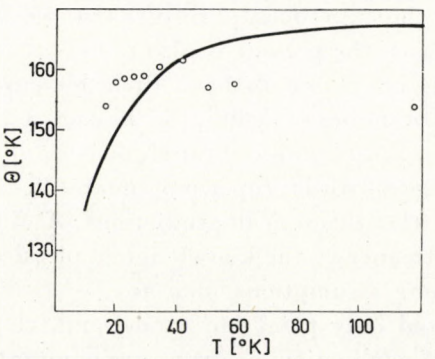

Fig. 7. (Θ — T) curves of sodium. Experimental points are shown by ○

of γ was taken to be $\gamma = 300$ cal deg^{-2} mol^{-1} from the measurements of MARTIN [15]. A knowledge of heat capacities at various temperatures made it possible to compute Debye characteristic temperature of sodium. The resulting ($\theta - T$) curve is shown in Fig. 7.

4. Comparison with the experimental results

A study of Figs 1 to 5 reveals the fact that the theoretical phonon dispersion curves of sodium are in very good agreement with the experimental results. Except at few wave vectors in the high frequency ends of some of the selected branches, the theoretical curves have reproduced the experimental ones within the limits of the experimental errors. The maximum deviations between the calculated and experimental frequencies are found to be about 8%. The study of Fig. 6 shows that the calculated heat capacities are in good agreement with the experimental results. The maximum deviation between the two sets of results is found to be of the order of 5%. Fig. 7 shows that the calculated ($\theta - T$) curve of sodium has reproduced the entire course of the experimental curve. While the experimental curve drops after 40 °K, the theoretical curve attains saturation. The two sets of results differ by about 4%.

5. Discussion and conclusion

The theoretical phonon dispersion relations along all five symmetry directions as well as C_v and θ versus temperature curves of sodium on the basis of a five parameter model proposed here has given a very good account of the experimental results. Such kinds of results are superior to those published so far for this metal by other phenomenological model calculations.

As the theoretical interpretation of the phonon dispersion curves of sodium along all the five symmetry directions by WOODS et al. [13] have been found so close to the experimental results that we deemed it necessary to compare their results with the present study. A close study of Figs. 1 to 5 may reveal that our results are found to be a little bit superior to their results along the longitudinal branches of $|\ \xi 00\ |$, $|\ \xi\xi 0\ |$ and $|\ 1/2\ 1/2\xi\ |$ and transverse branches of $|\ 1/2\ 1/2\xi\ |$, $|\ \xi 00\ |$ and T_2 branch of $|\ \xi\xi 0\ |$. The results of WOODS et al. [13] are found to be a little bit superior to our results in rest of the branches. The comparison with the theoretical predictions of WOODS et al. [13] does not attach much significance to the knowledge of physics as their calculations are based on some wrong assumptions such as:

1. They have used only point ion model and, that too, central forces. Whereas, the effects of conduction electrons are dominating in the determina-

tion of the phonon frequencies. The use of central force is also objectionable because the elastic constant C_{12} differs greatly from C_{44}.

2. They have used a huge number of parameters, 13. A large number of parameters loose the physics behind a model and only reproduce the mathematical fitting.

3. In order to evaluate model parameters they have used an arbitrary weight to the individual phonon frequencies in the least square fit. Also the values of the elastic constants employed by them at that time are found to be quite different from the experimental values of MARTINSON [12]. The experimental values of elastic constants are C_{11}, C_{12} and C_{44}, respectively. 0.808, 0.664 and 0.584, all in units of 10^{11} dyn cm^{-2}. On the other hand, WOODS et al. [13] have used the values of C_{11}, C_{12} and C_{44}, respectively 0.953, 0.745 and 0.584, all in the units of 10^{11} dyn cm^{-2}.

One can say, thus, confidently that the results given by the present five parameter model have been found to be superior to those predicted by the 13 parameter model of WOODS et al. [13]. We also made a comparison of the present results with those of VOSKO et al. [3] (M. O. et al. [16]) and found that our results are quite superior to their results in the high and low wave vector regions in all the three prominent symmetry directions, $|\,\xi 00\,|$, $|\,\xi\xi 0\,|$ and $|\,\xi\xi\xi\,|$.

The present study also shows a clear importance of the angular forces in the study of metals. The ignorance of the angular forces makes the value of bulk modulus Ke to be positive, thus deviating the theoretical predictions from the experimental results.

The present model has also considered the effect of different forms of the dielectric screening functions in calculating the phonon frequencies of sodium. It was found that all screening functions gave almost similar results for sodium. But the best result was obtained by GELDART and VOSKO's forms.

Acknowledgements

The authors thank Dr. R. C. C. LEITE, Director of the Institute, for the necessary research facilities. Computational facilities from UNICAMP Computer Centre is also acknowledged. This work was partially supported by FAPESP, CNPq, BNDE, BID and BADESP.

REFERENCES

1. T. Toya, Journ. Res. Inst. Catalysis, Hokkaido University, **6**, 161, 1958.
2. W. A. Harrison, Pseudopotential in the theory of metals, Benjamin Inc. New York, 1966.
3. S. H. Vosko, R. Taylor and G. H. Keech, Can. J. Phys., **43**, 1187, 1963.
4. D. L. Price, K. S. Singwi and M. P. Tosi, Phys. Rev. B2, 2983, 1970.
5. K. Krebs, Phys. Rev., **138**, 143, 1965.
6. L. Cheveau, Phys. Rev., **169**, 496, 1968.
7. M. M. Shukla, I. C. da Cunha Lima and L. M. Brescansin, Solid State Commun., **11**, 1431, 1972.
8. B. C. Clark, D. C. Gazis and R. F. Wallis, Phys. Rev., **134A**, 1486, 1964.
9. L. M. Falicov and V. Heine, Adv. Phys., **10**, 97, 1961.
10. D. J. W. Geldart and S. H. Vosko, Can. J. Phys., **44**, 2137, 1966.
11. K. S. Singwi, A. Sjolader, M. P. Tosi and R. H. Land, Phys. Rev., **B1**, 1944, 1970.
12. A. B. D. Woods, B. N. Brockhouse, R. H. March and A. T. Stewart, Phys. Rev., **128**, 1112, 1962.
13. F. Simon and W. Z. Zeidler, Z. Phys. Chem., **123**, 383, 1926.
14. D. L. Martin, Proc. Roy. Soc. A, **254**, 433, 1960.
15. M. C. Oliveros, H. Tejima and M. M. Shukla (to be published).

Acta Physica Academiae Scientiarum Hungaricae, Tomus 41 (1), pp. 41—54 (1976)

CLASSICAL AND WAVE MECHANICAL THEORY OF RAYLEIGH SCATTERING

By

L. JÁNOSSY

CENTRAL RESEARCH INSTITUTE OF PHYSICS, BUDAPEST

(Received 26. V. 1976)

The theory of the incoherent scattering of light by a volume of gas is discussed. It is shown that the wave mechanical treatment contains difficulties; the scattering process cannot be accounted for alone by the density fluctuation of an ensemble of atoms described by a collective wave function.

Introduction

The passage of an electromagnetic wave through a gas can be treated satisfactorily by classical theory. The atoms of the gas are forced to oscillate under the influence of the electromagnetic field acting upon them. The superposition of the radiation emitted by the atoms upon the primary radiation field gives rise to the optical effects of refraction, also incoherent radiation is produced, which may be called the Rayleigh scattering.

The effect of refraction is obtained by averaging the effects of the atoms; a satisfactory treatment of these effects is obtained if one replaces the atoms by smoothed out polarizable material.

The incoherent scattering is caused by the microscopic fluctuations of the density which is obtained considering the atoms to be concentrated packets distributed at random.

While the wave mechanical treatment of refraction is quite straightforward (see e.g. [1]) — in connection with the incoherent scattering a peculiar problem arises. The scattered intensity is produced by isolated scattering centres distributed at random. In the wave mechanical description the atoms — even if they were concentrated at an initial moment into packets — are expected to diffuse rapidly. In fact the atoms of a gas enclosed into a box are expected, in the course of short time, to diffuse and ultimately to spread out with nearly uniform density over the whole of the volume of the container.

The question thus arises — is it possible at all to account for the incoherent scattering by pure wave mechanics — or is it necessary to add to wave mechanics other features (e.g. second quantisation) so as to account for phenomena which seem to arise from the action of atoms concentrated into small packets?

The question is certainly not trivial. Presently we show that the wave mechanical treatment of an ensemble of atoms leads to expect density fluctuations, which give rise to incoherent scattered radiation. However, the wave mechanical fluctuations differ from the classical fluctuations and they give rise to much smaller scattered intensity than the observed intensity (which agrees with the intensity calculated by the classical theory).

We show thus in this paper that the wave mechanical theory of incoherent scattering is not caused simply by the wave mechanically expected density fluctuation of a gas. This negative result in itself seems to be of interest. We hope to come back to the full wave mechanical treatment of the process in a later publication.

Part I

The classical theory of incoherent scattering

A wave incident on an ensemble of atoms produces harmonic oscillations of the atoms. The oscillations are in phase with the incident radiation, therefore there are strict phase relations between the dipole fields the individual atoms give rise to.

The phase relations between the fields of the oscillating atoms give rise to beams of intensities comparable with that of the incident radiation. These coherent beams together with the primary radiation give rise to the refracted beam.

In most directions, however, the fields of the dipoles have random phases. Indeed, consider the radiation field in a point P far outside the volume of the gas and also outside the region of the optical beam. The distances of the individual atoms from P have random values and thus in spite of the existing phase relations the fields arrive with random phases in P. Thus the individual fields are incoherent and the total intensity in P fluctuates rapidly around a value

$$J_S \sim NJ_A \,, \tag{1}$$

where N is the number of atoms in the gas and J_A the intensity of secondary radiation emitted by one atom.

Further from electromagnetic theory it follows that

$$J_A \sim \alpha^2 J_0 \,, \tag{2}$$

where J_0 is the intensity of the primary beam and α the dynamical polarisability of one atom.

The refractive index of the gas is obtained considering the coherent part of the radiation fields of the atoms. The well-known theory of this phenomenon leads to

$$n^2 - 1 = 4\pi\alpha N/V \,. \tag{3}$$

From (1) and (2) we have

$$J_S = \beta N \alpha^2 J_0 \,, \tag{4}$$

where β is a geometrical factor the value of which is obtained from the detailed calculation. Thus measuring the refractive index n and the intensity J_S of the incoherently scattered radiation, the number N of scattering centres can be determined from (3) and (4).

A remark on the light of the sky

We note that the determination of J_S supposes the individual atoms to be sources of secondary radiation which radiate independently into the vicinity of the gas. The theory of Rayleigh considered the scattered radiation emitted by small dust particles — and this theory was applied to explain the light intensity of the sky. It was realized later that the sky light is not produced by dust particles but is a scattering on the spatial fluctuations of the density of air. According to (1) this fact can also be formulated by saying that the sky light is due to the scattering on the individual gas atoms themselves, which play the role of the dust particles of the original concept.

The method of virtual lattices

The simple classical consideration giving the intensity J_S of incoherently scattered radiation can be carried out by a method different from that given above. The latter method is mathematically identical with the former, therefore it leads necessarily to the same result. This method is useful in connection with the wave mechanical aspects of the problem.

The radiation induced by an outer field on an ensemble of N atoms can be treated by supposing the atoms to be scattering centres of linear dimensions small compared with λ the wave length of the incident light. The ensemble of atoms can alternatively be replaced by a medium of dynamical polarizability

$$\varkappa(\mathbf{r}) = \varkappa \varrho(\mathbf{r}) \,,$$

where $\varrho(\mathbf{r})$ is the relative density of the medium, thus

$$\int \varrho(\mathbf{r}) \mathrm{d}^3\mathbf{r} = N \,. \tag{5}$$

Supposing the atoms to be points with position vectors $\mathbf{r}^{(n)}$ we have

$$\varrho(\mathbf{r}) = \sum_n \delta(\mathbf{r} - \mathbf{r}^{(n)}) \,, \tag{6}$$

where $\delta(\mathbf{r})$ is the three-dimensional Dirac δ-function. More generally we may suppose

$$\varrho(\mathbf{r}) = \sum_n \delta^*(\mathbf{r} - \mathbf{r}^{(n)}) , \tag{7}$$

where $\delta^*(\mathbf{r})$ is a function with large positive values in the vicinity of $\mathbf{r} = 0$, vanishing outside. Thus (6) describes the density of an ensemble of atoms each spread into a small vicinity of a point $\mathbf{r}^{(n)}$.

The polarization density produced by a field can be taken as

$$\mathbf{P} = \alpha\varrho(\mathbf{r})\,\mathbf{E} .$$

The current density induced by the field is thus

$$\mathbf{i} = \frac{1}{c}\dot{\mathbf{P}} = -\frac{1}{c^2}\alpha\varrho\,\ddot{\mathbf{A}} ,$$

where $\mathbf{A}$ is the vector potential of the total field acting on the medium. Thus in case of a periodic field

$$\mathbf{i} = -\frac{\alpha\varrho}{\lambda^2}\mathbf{A} \quad \text{with } \lambda = c/\Omega \tag{8}$$

(here Ω is the circular frequency of the radiation). The field emitted by the oscillating medium can be derived from a vector potential

$$\mathbf{A}_S(\mathbf{r}, t) = -\frac{\alpha}{\lambda^2}\int \frac{\varrho(\mathbf{r}')\,\mathbf{A}(\mathbf{r}', t')}{|\mathbf{r} - \mathbf{r}'|}\, d^3\mathbf{r}' ; \tag{9}$$

here $t' = t - |\mathbf{r} - \mathbf{r}'|/c$. If the density $\varrho(\mathbf{r})$ is of the form (6), then (9) leads to the same intensity of the scattered field as is obtained from the classical consideration given further above. Instead of splitting $\varrho(\mathbf{r})$ into the densities

$$\varrho^{(n)}(\mathbf{r}) = \delta^*(\mathbf{r} - \mathbf{r}^{(n)}) \tag{10}$$

of the individual atoms, we express the densities by Fourier series. For this purpose we consider the gas to be enclosed into a cubic box with sides L, thus we have

$$\varrho(\mathbf{r}) = \sum_\nu \varrho_\nu e^{i\mathbf{k}_\nu\mathbf{r}} , \tag{11}$$

$$\varrho_\nu = \frac{1}{L^3}\int \varrho(\mathbf{r}) \exp\{-i\mathbf{k}_\nu\mathbf{r}\}\, d^3\mathbf{r},$$

where the $\mathbf{k}_\nu$ are vectors with components

$$\mathbf{k}_\nu = \frac{2\pi}{L}\nu_1, \quad \frac{2\pi}{L}\nu_2, \quad \frac{2\pi}{L}\nu_3; \tag{12}$$

here ν_1, ν_2, ν_3 are integers.

Considering the densities of the individual atoms we have also

$$\begin{aligned} \varrho^{(n)}(\mathbf{r}) &= \sum_\nu \varrho_\nu^{(n)} e^{i\mathbf{k}_\nu \mathbf{r}}, \\ \varrho_\nu^{(n)} &= \frac{1}{L^3}\int \delta^*(\mathbf{r} - \mathbf{r}^{(n)}) e^{-i\mathbf{k}_\nu \mathbf{r}} \mathrm{d}^3\mathbf{r}. \end{aligned} \tag{13}$$

In case of δ-functions in place of δ^* we have

$$\left.\begin{aligned} \varrho_\nu^{(n)} &= \frac{1}{L^3} e^{i\varphi_\nu^{(n)}}, \\ \varphi_\nu^{(n)} &= \mathbf{k}_\nu \mathbf{r}^{(n)}. \end{aligned}\right\} \tag{14}$$

where

Thus

$$\left.\begin{aligned} \varrho_0 &= N/L^3, \\ \varrho_\nu &= \frac{1}{L^3}\sum_n e^{i\varphi_\nu^{(n)}} \approx \frac{\sqrt{N}}{L^3} e^{i\varphi_\nu} \quad \text{if} \quad \nu \neq 0. \end{aligned}\right\} \tag{15}$$

The right hand expression is obtained supposing the $\varphi_\nu^{(n)}$ to have random values for $n = 1, 2, \ldots, N$, in that case the sum of the N complex units $\exp(i\varphi_\nu^{(n)})$ has an absolute value of the order of $\sqrt{N}$ and has random phase.

Relation (15) can be made more precise taking the $\varphi_\nu^{(n)}$ to be random variables and thus we can form expected values with respect to these variables; we have

$$\left.\begin{aligned} \langle \varrho_\nu \rangle &= 0 \\ \langle |\varrho_\nu|^2 \rangle &= N/L^6 \end{aligned}\right\} \quad \text{if} \quad \nu \neq 0. \tag{16}$$

The concept of taking the $\varphi_\nu^{(n)}$ as stochastic variables needs explanation.

Indeed, at a fixed time t and a fixed configuration $\varrho(\mathbf{r})$ each Fourier coefficient has a definite numerical value. When we introduce nevertheless "expected" values this can be done for two reasons:

1) If the atoms are moving with thermal velocities, then the motions are slow as compared with the frequency of the incident radiation — however, in accord with (14) the thermal motion leads to rapid and independent changes of the $\varphi_\nu^{(n)}$. Thus the expected values of ϱ_ν can be taken to be expected values

in short intervals of time which nevertheless are long as compared with the time of oscillation of the primary wave.

2) The phases $\varphi_\nu^{(n)}$ vary strongly with ν. Thus the expected values of ϱ_ν can also be considered as the average values of the ϱ_ν inside a small region of Fourier coefficients δ_ν around ν.

Reflexion on virtual lattices

The field of the scattered radiation can be decomposed to the contributions of the Fourier components

$$\varrho_\nu(\mathbf{r}) = \varrho_\nu e^{i\mathbf{k}_\nu \mathbf{r}} \tag{17}$$

of $\varrho(\mathbf{r})$. We may thus write

$$\mathbf{A}_S(\mathbf{r}, t) = \sum_\nu \mathbf{A}_\nu(\mathbf{r}, t) . \tag{18}$$

Taking the field acting on the atoms to have a vector potential

$$\mathbf{A}(\mathbf{r}, t) = \mathbf{A}_0 \exp \{i(\mathbf{K}\mathbf{r} - \Omega t)\} . \tag{19}$$

The vector potential of the scattered radiation field is thus, making use of (9) and inserting $\varrho_\nu(\mathbf{r})$ in place of $\varrho(\mathbf{r})$:

$$\mathbf{A}_\nu(\mathbf{r}, t) = -\frac{\alpha \varrho_\nu \mathbf{A}_0}{\lambda^2} \int \exp \{i [(\mathbf{k}_\nu + \mathbf{K})\mathbf{r}' - \Omega(t - |\mathbf{r} - \mathbf{r}'|/c)]\} \frac{d^3 \mathbf{r}'}{|\mathbf{r} - \mathbf{r}'|} . \tag{20}$$

The integral is to be extended over the volume of the gas. For points $\mathbf{r}$ far outside the gas and also outside the optical beam the following approximations can be used: in the factor $1/|\mathbf{r} - \mathbf{r}'|$

$$|\mathbf{r} - \mathbf{r}'| \sim r ,$$

in the exponent

$$|\mathbf{r} - \mathbf{r}'| \sim r - \mathbf{r}'\mathbf{r}/r .$$

We find thus

$$\text{exponent} \approx i[(\mathbf{k}_\nu + \mathbf{K} - \mathbf{K}_0)\mathbf{r}' + K_0 r - \Omega t] , \tag{21}$$

where

$$\mathbf{K}_0 = \frac{\Omega}{c} \frac{\mathbf{r}}{r} .$$

Inserting (21) into (20) and carrying out the integration over a cubic box with edges $\mathbf{L}_1$, $\mathbf{L}_2$, $\mathbf{L}_3$; we find thus in a good approximation

$$\mathbf{A}_\nu(\mathbf{r}, t) = \frac{\alpha \varrho_\nu \mathbf{A}_0 L^3}{\lambda^2 r} D_\nu(\mathbf{a}) \, e^{i(K_0 r - \Omega t)} ,$$

where

$$D_\nu(\mathbf{a}) = \frac{8 \sin\left(\frac{1}{2}\mathbf{aL}_1\right) \sin\left(\frac{1}{2}\mathbf{aL}_2\right) \sin\left(\frac{1}{2}\mathbf{aL}_3\right)}{(\mathbf{aL}_1)(\mathbf{aL}_2)(\mathbf{aL}_3)} \tag{22}$$

with

$$\mathbf{a} = \mathbf{k}_\nu + \mathbf{K} - \mathbf{K}_0 .$$

The expected value of the intensity of the radiation in the direction of the vector $\mathbf{K}$ is thus proportional to

$$\langle |A_\nu(\mathbf{r}, t)|^2 \rangle = \frac{\alpha^2 \langle \varrho_r^2 \rangle L^6}{\lambda^4 r^2} |D_\nu(\mathbf{a})|^2 |A_0|^2 . \tag{23}$$

We find with the help of (16) if we take $| A_0 |^2$ to be proportional to the primary intensity

$$J_\nu / J_0 = N \cdot \frac{\alpha^2}{\lambda^4 r^2} |D_\nu|^2 . \tag{24}$$

Rayleigh scattering as Bragg scattering

So as to see the significance of the above considerations, we note tha $D_\nu(0) = 1$ and $D_\nu(\mathbf{a})$ has a pronounced maximum in the vicinity of $\mathbf{a} = 0$ [see (22)]. Appreciable intensities are thus obtained in directions $\mathbf{K}$ so that $\mathbf{a} \sim 0$, i.e.

$$\mathbf{K} \sim \mathbf{K}_0 - \mathbf{k}_\nu . \tag{25}$$

The above relation has the form of the Bragg condition known in X-ray spectroscopy. The densities $\varrho_\nu(\mathbf{r})$ correspond to virtual lattices with lattice vectors $\mathbf{k}_\nu$. Only those lattices contribute appreciably to the scattered radiation for which (25) is satisfied. These lattices give reflexions into narrow cones pointing into definite directions.

The incoherently scattered radiation consists thus of the very numerous Bragg reflexions on the virtual lattices. The phases of the various reflexions are randomly distributed, therefore the reflected rays are incoherent and the intensities J_ν arising from the reflexions can be added so as to obtain the total intensity. Thus the expected value $\langle | A_\nu |^2 \rangle$ [see (23)] gives the intensity of radiation in a direction which depends on ν.

We note further that the lattice corresponding to one particular ν-value gives appreciable reflexion only if

$$| \mathbf{K}_0 - \mathbf{k}_\nu | \approx K = \Omega / c . \tag{26}$$

For $\mathbf{k}_\nu$-values for which (25) is not satisfied practically no reflexion takes place.

The $\mathbf{k}_\nu$-values satisfying (25) give radiation inside a cone with opening angle of the order of $\sqrt{\lambda/L}$. On the other hand lattices with neighbouring vectors $\mathbf{k}_\nu$ give the maximum intensities in directions $\mathbf{K}$ with angles of the order of λ/L between them. From this qualitative consideration we see that the Bragg reflexions overlap to a considerable extent.

Scaterring on diffused atoms

We see that the scattered intensity on the medium with density $\varrho(\mathbf{r})$ depends only on the expected values of the absolute squares of the Fourier coefficients ϱ_ν. Thus any density distribution $\varrho(\mathbf{r})$ for which (16) holds will give the correct intensity distribution for the scattered radiation. We may therefore replace the $\varrho^{(n)}(\mathbf{r})$ by $\bar{\varrho}^{(n)}(\mathbf{r})$ so that

$$\bar{\varrho}^{(n)}(\mathbf{r}) = \sum \bar{\varrho}_\nu^{(n)} e^{i\mathbf{k}_\nu \mathbf{r}}, \tag{27}$$

with

$$\bar{\varrho}_\nu^{(n)} = \frac{1}{L^3} e^{i\bar{\varphi}_\nu^{(n)}}, \tag{28}$$

where the $\bar{\varphi}^{(n)}$ have random values which may however differ arbitrarily from the $\varphi_\nu^{(n)} = \mathbf{k}_\nu \mathbf{r}^{(n)}$.

The $\bar{\varrho}^{(n)}(\mathbf{r})$ thus obtained correspond to the densities of "diffused particles". The $\bar{\varrho}^{(n)}(\mathbf{r})$ because the original phase relations of the Fourier coefficients have been destroyed does, in general, not possess a pronounced maximum. Nevertheless the Fourier coefficients of

$$\bar{\varrho}(\mathbf{r}) = \sum \bar{\varrho}^{(n)}(\mathbf{r})$$

have the form (15), i.e.

$$\begin{aligned} \bar{\varrho}_0 &= N/L^3 , \\ \bar{\varrho}_\nu &= \frac{1}{L^3} \sum e^{i\bar{\varphi}_\nu^{(n)}} \approx \frac{\sqrt{N}}{L^3} e^{i\bar{\varphi}_\nu}, \quad \nu \neq 0 \end{aligned} \tag{29}$$

where the $\bar{\varphi}_\nu$ differ from the φ_ν, but the modified phases have still random values.

From the above considerations it follows that

$$\begin{aligned} \langle \bar{\varrho}_\nu \rangle &= \langle \varrho_\nu \rangle = 0 , \\ \langle | \bar{\varrho}_\nu |^2 \rangle &= \langle | \varrho_\nu |^2 \rangle = N/L^6 , \qquad \nu \neq 0 . \end{aligned} \tag{30}$$

We see thus that the particles if they "diffuse", they produce a change of distribution in accord with

$$\varrho(\mathbf{r}) \to \bar{\varrho}(\mathbf{r}) \tag{31}$$

and the distribution of the scattered radiation is not affected. More precisely, the expected values of the scattered intensities in various directions remain unaffected by the change (31).

The diffusion process (31) has some similarity to the wave mechanical diffusion of a packet — one might suspect therefore that the scattered intensity of radiation which is not affected by the "classical diffusion" (31) might also remain unaffected by wave mechanical diffusion. This is, however, in general not the case, as will be seen in Part II.

Part II

Wave mechanical determination of the incoherent scattering intensity

Using results of former publications [1] we can suppose, that the intensity scattered by an ensemble of atoms with dynamical polarizibility α is the same as the intensity scattered according to classical theory by a medium of polarizibility

$$\varkappa(\mathbf{r}) = N\alpha\varrho(\mathbf{r}) , \tag{32}$$

where $\varrho(\mathbf{r})$ is the density of the quantum mechanical ensemble of atoms. More precisely, considering an ensemble of N H-atoms supposing the state of the ensemble to be described by a wave function $\Psi(\boldsymbol{r}_1, \boldsymbol{r}_2; t)$ where

$$\boldsymbol{r}_n = \mathbf{r}_n^{(1)}, \mathbf{r}_n^{(2)}, \ldots, \mathbf{r}_n^{(N)} \qquad n = 1, 2$$

the suffix $n = 1$ referring to proton, $n = 2$ to electron coordinate vector; the upper indices refer to the various atoms. The density of the k-th electron can thus be written

$$\varrho^{(k)}(\mathbf{r}) = \int | \Psi(\boldsymbol{r}_1, \boldsymbol{r}_2; t) |^2 \delta(\mathbf{r}_2^{(k)} - \mathbf{r}) \mathrm{d}^{3N} \boldsymbol{r}_1 \, \mathrm{d}^{3N} \boldsymbol{r}_2 , \tag{33}$$

where the δ-function is used to express in a concise manner that integration is to be carried out over $6N$-3 variables, i.e. all the variables except the components of the coordinate vectors of the k-th electron. (The proton densities can be worked out in a similar fashion; however, we may neglect the contribution of the protons to the radiation.)

Because of symmetry we have

$$\varrho_2^{(1)}(\mathbf{r}) = \varrho_2^{(k)}(\mathbf{r}) , \qquad k = 2, 3, \ldots, N$$

thus the density appearing in (32) can be taken as

$$\varrho(r) = N\varrho_2^{(1)}(\mathbf{r}) . \tag{34}$$

There exist a large number of wave functions Ψ which satisfy the wave equation representing the ensemble of N H-atoms. We have dealt with the difficulty of choice of the wave function elsewhere [2].

Particular wave functions

In a former paper [3] we have dealt with the emission of photons by the ensemble of N atoms corresponding to a volume of gas enclosed in a cubic box with sides L. Two types of wave functions were found both describing an ensemble of atoms with momenta $\mathbf{p}_1, \mathbf{p}_2, \ldots, \mathbf{p}_N$ of translational motion. These wave functions were built each of two body H-wave functions. Both types of wave functions thus constructed lead to the emission of photons of the same manner as it was found in the case of a single atom enclosed in a box (see [3]). Thus both wave functions lead to a process which appears to be the independent emission of photons by individual atoms.

The first of the two wave functions thus considered corresponds to a constant electron density. In the latter state (if realized in nature) the ensemble would behave as a perfect crystal and no incoherently scattered radiation was to be expected. This type of wave function (as was pointed out in [3]) must be expected to describe a rather unstable configuration in which the energy is concentrated into kinetic energy and energy of excitation without radiation energy. The latter configuration does not seem therefore to represent the state which is realized in nature; this conclusion is further confirmed by the fact that the state produces no incoherent scattered intensity.

The second type of wave function which appears to be more suitable to represent the emission of photons by independent atoms is of the following type.

Consider

$$\overset{(2)}{\Psi}{}^{(\nu)}(\mathbf{r}^{(1)}, \mathbf{r}^{(2)}; t) = F_\nu(\mathbf{R})\, \varphi_\nu(\mathbf{s})\, e^{-i\omega_\nu t}, \tag{35}$$

a normalized solution of the two body wave equation giving a stationary state of an H-atom enclosed into a box such that $\mathbf{R}$ is the coordinate vector of the centre of gravity and $\mathbf{s}$ the coordinate vector pointing from the proton to the electron.

The wave function (35) thus represents an H-atom with some translational momentum $\mathbf{p}_\nu$ in the ground state or in an excited state with energy E_ν.

We form the linear combination of N wave functions of the form (35), i.e.

$$\overset{(2)}{\Psi} = \sum_{\nu=1}^{N} c_\nu \overset{(2)}{\Psi}{}^{(\nu)}, \quad |c_\nu| = 1/\sqrt{N}\,. \tag{36}$$

Further write

$$\Psi_{KL} = \Psi_{KL}(\mathbf{r}^{(1)}, \mathbf{r}^{(2)}; t) = \overset{(2)}{\Psi}{}_{KL}(\mathbf{r}_K^{(1)}, \mathbf{r}_L^{(2)}, t)\,. \tag{37}$$

Thus Ψ_{KL} is the $2N$-body wave function which happens to depend only on one proton coordinate $\mathbf{r}_K^{(1)}$ and one electron coordinate $\mathbf{r}_L^{(2)}$.

The wave function used in [3] is thus

$$\Psi = \frac{1}{\sqrt{N!}} \det \Psi_{KL} . \tag{38}$$

The electron density obtained from (38) with the help of (33) and (34) is found in a good approximation to be

$$\varrho(\mathbf{r}) = N \mid F(\mathbf{r}) \mid^2 / L^3 ,$$

where

$$F(\mathbf{r}) = \sum_{(N)} c_\nu F_\nu(\mathbf{r}) , \tag{39}$$

the sum is to be extended over the amplitudes of the N states occurring in the ensemble. So as to calculate the scattered intensity we have to determine the Fourier coefficients of the density $\varrho(\mathbf{r})$.

When calculating the Fourier coefficients of the density it is important whether or not the states k_ν ($\nu = 1, 2, \ldots, N$) occupy all the states in a compact region of momentum space. Supposing this to be the case we take the ν to take all the values where $k_\nu^2 \leqslant k_{\max}^2$; $k_{\max}^2$ has to be chosen so that the above condition should be satisfied by N $\mathbf{k}_\nu$ vectors. In the latter case we have with the help of (34) and (36)

$$\varrho_\nu = N \sum_\mu c_{\mu+\nu} c_\mu^* / L^3 ,$$

$$\langle \varrho_\nu^2 \rangle = N^2 \sum_{\mu\mu'} \langle c_{\mu+\nu} c_\mu^* c_{\mu'+\nu}^* c_{\mu'} \rangle / L^6 .$$

In the above sums the expected values of the terms with $\mu \neq \mu'$ vanish. If the value of ν is not too large, there remain about N non vanishing terms thus each equal to $1/N^2$ so

$$\langle \varrho_\nu^2 \rangle = N / L^6 .$$

Thus the Fourier coefficients of the wave mechanical density are equal to those obtained from the classical model. The wave function thus obtained gives therefore the correct intensity for the incoherent scattering.

Some criticism of the above result

In spite of the fact that the wave function given by (38) and (39) gives the correct intensity of incoherent scattering, we do not think that the above function is likely to be realized in nature. It seems very unlikely that the real

state of the gas is composed of all states $\mathbf{k}_\nu$ so that *all states* $k_\nu < k_{\max}$ should occur with about equal amplitudes. It is more reasonable to consider a wave function of the form (39) so that the coefficients $c_1, c_2, \ldots, c_N$ correspond to wave numbers $\mathbf{k}_1, \mathbf{k}_2, \ldots \mathbf{k}_N$ each of them giving a harmonic contribution to the density but the values $\mathbf{k}_\nu$ do by no means contain all the possible stationary states. We can thus write

$$c_\mu = \begin{cases} \gamma_\mu & \text{if } \mu \text{ represents one of the } N \text{ states} \\ & \text{occurring in the ensemble} \\ 0 & \text{otherwise.} \end{cases} \tag{40}$$

We have thus

$$\sum_{(N)} c_\nu F_\nu(\mathbf{r}) = \sum_\mu \gamma_\mu F_\mu(\mathbf{r}) ,$$

where on the right hand side a large fraction of the terms vanish.

We obtain e.g. something like a thermal distribution if we suppose that*

$$\gamma_\mu = \begin{cases} 0 & \text{with a probability} \quad 1 - p(\mu) \\ e^{i\varphi\mu}/\sqrt{N} & \text{with a probability} \quad p(\mu) \end{cases} \tag{41}$$

$$p(\mu) = \frac{1}{2} N(2\alpha/\pi)^{3/2} e^{-\alpha\mu^2} ,$$

where $\mu^2 = \mu_1^2 + \mu_2^2 + \mu_3^2$; μ_1, μ_2, μ_3 the components of μ.

The Fourier expansion of the density is thus

$$\varrho(\mathbf{r}) = \sum_\lambda \varrho_\lambda e^{ik_\lambda \mathbf{r}} ,$$

$$\varrho_\lambda = \sum_\mu \gamma_\mu \gamma^*_{\mu-\lambda} .$$

The expected value is

$$\langle \varrho_\lambda \rangle = 0 , \qquad \lambda = 0$$

because of the random phase factors of the γ_μ. For the squares of the Fourier coefficients we find

$$\langle | \varrho_\lambda |^2 \rangle = \sum_{\mu, \mu'} \langle \gamma_\mu \gamma^*_{\mu-\lambda} \gamma^*_{\mu'} \gamma_{\mu'-\lambda} \rangle .$$

For $\lambda \neq 0$ on the right only terms with $\mu = \mu'$ are different from zero.

* The kinetic energy of the system is thus found to be proportional to $1/\alpha$, thus α is a parameter proportional to the reciprocal absolute temperature.

We find

$$\langle | \varrho_\lambda |^2 \rangle = \sum_\mu \langle | \gamma_\mu |^2 | \gamma^2_{\lambda-\mu} | \rangle$$

and with the help of (41)

$$\langle | \varrho_\lambda |^2 \rangle = \frac{1}{2} (\alpha\pi)^{3/2} e^{-1/2\,\alpha\lambda^2} N/L^6 .$$

Comparing the above value with the classical value we find the classical value N/L^6 to be multiplied by a small factor, which gives the incorrect intensity of incoherent scattering — therefore we find a strong discrepancy with the classical result.

The density fluctuation thus calculated has a maximum in the region when

$$\alpha\lambda^2 \sim 1 .$$

In case of visible light $\lambda \gg 1$ thus the maximum is found for $\alpha \gg 1$; we see thus that even the maximum value of $\langle | \varrho_\nu |^2 \rangle$ is much below the value N/L^6 obtained from the classical theory. We see thus that the scattered light obtained from the consideration of the wave mechanical density fluctuation of the ensemble has an intensity proportional to N the number of atoms; however, the intensity has a strong temperature dependence and the calculated intensity is much smaller than the observed one at the temperature where the scattering is maximal.

The above result appears to be surprising at first sight. Indeed, we may consider a wave function which in the initial state $t = 0$ leads to a density distribution $\varrho(\mathbf{r})$ as given by (11) or $\overline{\varrho}(\mathbf{r})$ given by (28). From the general considerations given in (1) we must expect that this distribution leads to the same Rayleigh scattering as is expected from classical theory. Therefore at least for a short time the configuration thus obtained leads indeed to the correct scattered intensity. However, the detailed calculation shows that the wave mechanical diffusion leads to changes, in the course of which the Fourier coefficients of the density $\varrho(\mathbf{r})$ or $\overline{\varrho}(\mathbf{r})$ change rapidly so that the amplitudes show a strong decreasing tendency. Therefore the initial configuration in which the density is of the form $\varrho(\mathbf{r})$ or $\overline{\varrho}(\mathbf{r})$ is according to wave mechanics an exceptional one which in the course of the diffusion shows a tendency of smoothing out until a state with very much smaller fluctuations is reached.

Concluding remarks

The failure of the procedure might be attributed to the incorrect choice of the wave function of the ensemble. We do not think this very likely, because linear combinations of the wave functions we have chosen should in general

give fluctuations which are even more smoothed out than that of the wave function considered here.

The discrepancy pointed out here is one encountered (although not pointed out) in the original treatment of the Compton scattering by KLEIN and NISHINA [4]. In that work the correct Compton intensity of the scattered radiation is obtained by using wave functions of the free electrons which contain all possible momentum values with equal amplitudes. If the original configuration of the free electron were to be replaced in the treatment of KLEIN and NISHINA by a wave packet which contains a reasonable spectrum of frequencies, then a cross section much smaller than the observed one would be obtained.

It seems therefore that initial states with a constant spectrum of momenta have some physical significance the nature of which is, however, not obvious.

We think that the correct scattered intensity might be obtained by extending the consideration we have given here. A correct description might be obtained considering not simply the average fluctuation of the ensemble — but considering the avalanches which develop in an ensemble as the result of suitable thermal disturbances. We think of a process very alike the one considered for the emission of single photons in our previous papers. We hope to come back to this problem later.

REFERENCES

1. L. JÁNOSSY, Acta Phys. Hung., **37**, 355, 1974.
2. L. JÁNOSSY, Acta Phys. Hung., **27**, 35, 1969.
   L. JÁNOSSY, Found Phys. (in the press).
3. L. JÁNOSSY, Acta Phys. Hung. (to be published in Vol. **41** No 2.)
4. O. KLEIN and Y. NISHINA, Zeits. f. Phys., **52**, 853, 1929.

Acta Physica Academiae Scientiarum Hungaricae, Tomus 41 (1), pp. 55—61 (1976)

SCATTERING OF PHOTONS AT THE 15.11 MeV ENERGY LEVEL IN ^{12}C*

By

D. MEHLIG

SGB-IABG, BONN, GERMANY

and

K. H. CZOCK**

INTERNATIONAL ATOMIC ENERGY AGENCY, VIENNA, AUSTRIA

(Received 14. VI. 1976)

The 15.11 MeV energy level in ^{12}C was excited by bremsstrahlung. The scattered photons were detected with a total γ absorption NaI(TI) spectrometer set at 135° to the bremsstrahlung beam. The following level parameters were obtained: $\sigma_a^0 = (17.9 \pm 0.6)$ barn, $\Gamma_{tot} = (69 \pm 4)$ eV and $\sigma_{int} = (1.86 \pm 0.12)$ mb MeV. The branching ratio to the first excited state and the ground state is $\Gamma_{\gamma 1}/\Gamma_{\gamma 0} = (3.6 \pm 1.0)\%$.

Introduction

Scattered photons from the 15.11 MeV energy level in ^{12}C have been studied using high energy bremsstrahlung (end point energy 108 MeV). Although subsequent fluorescence experiments were performed [1—6], considerable uncertainty remained about the level parameters.

The first $T = 1,1^+$ energy level in ^{12}C at 15.11 MeV is of particular interest because it is an isobaric analogous state of several low-lying states in the neighbouring odd-odd nuclei. Scattered photons are easily observed since the integrated scattering cross section is rather large (1.86 mb MeV), the level is narrow (69 eV) and situated in an energy region which is free of other scattering processes. It is, therefore, desirable to have available an accurate determination of the parameters of this level for calibration purposes.

This level disintegrates to the 0^+ ground state of ^{12}C and to the first 2^+ state at 4.43 MeV. ALMQUIST et al. [7] measured a branching ratio of $\Gamma_{\gamma 1}/\Gamma_{\gamma 0} = 3\%$. An α-disintegration to the 0^+-ground state of ^8Be is strongly momentum and parity forbidden and α-particle emission to the 2^+ state at 2.9 MeV of ^8Be does not occur if the 15.11 MeV level is a pure $T = 1$ state. REISMAN et al. [8] reported that the Γ_α width of that state amounts to 2% of the total width Γ_{tot}. Because the experimental errors described in this paper are of the same order, this contribution can be neglected, and

$$\Gamma_{tot} = \Gamma_\gamma + \Gamma_\alpha \approx \Gamma_\gamma = \Gamma_{\gamma 0} + \Gamma_{\gamma 1} .$$

* The experiment was performed at the 300 MeV electron linear accelerator at Mainz.
** On leave from the Fachhochschule Dortmund, Dortmund, Germany.

The level parameters σ_α^0 and Γ_{tot} were determined through a resonant absorption experiment. This experiment consists of two independent measurements:

in the first — the production experiment — the yield of scattered photons from a target of thickness T is measured;

in the second — the self-absorption experiment — an absorber is placed into the incident beam to attenuate the 15 MeV photons.

Experimental arrangement

The experiment was performed using the bremsstrahlung beam from the 300 MeV electron linear accelerator at Mainz.

The experimental set-up is shown below:

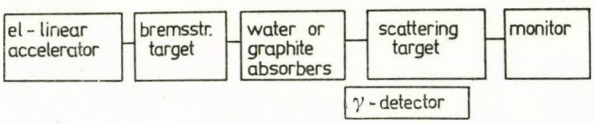

The bremsstrahlung beam is produced by electron bombardment of a 0.1 mm thick tantalum target. A narrow beam of 2.4 mrad is defined by conical lead collimators. At the scattering target, situated 12.5 m from the bremsstrahlung target, the beam was 5 cm in diameter. A sweep magnet and vacuum pipe maintain an electronfree beam up to the target. As target a 2 cm thick (3.31 g/cm^2) disc of reactor graphite was used.

For the "self-absorption" experiment, a 7 cm thick (11.6 g/cm^2) graphite absorber was placed in the primary beam. The absorber and scatterer thicknesses were measured along the direction of the photon beam, thus eliminating cosine factors from the formulae given below.

The scattered photons are detected at 135° and analysed in a total γ-absorption NaI(Tl) spectrometer (9'' diameter $\times$15.5'' length). The detector was placed 1.20 m from the scatterer. The resolution of the spectrometer for 15 MeV was 5.5%. The number of scattered photons $N(T)$ was obtained by summation over the peak shown in Fig. 1. All runs were monitored in terms of the charge collected from a calibrated thick aluminium ionization chamber of the NBS type P2—4 [9]. A detailed description of the bremsstrahlung beam production, the total γ-absorption spectrometer, the electronics and the neutron background subtraction is given elsewhere [10—13].

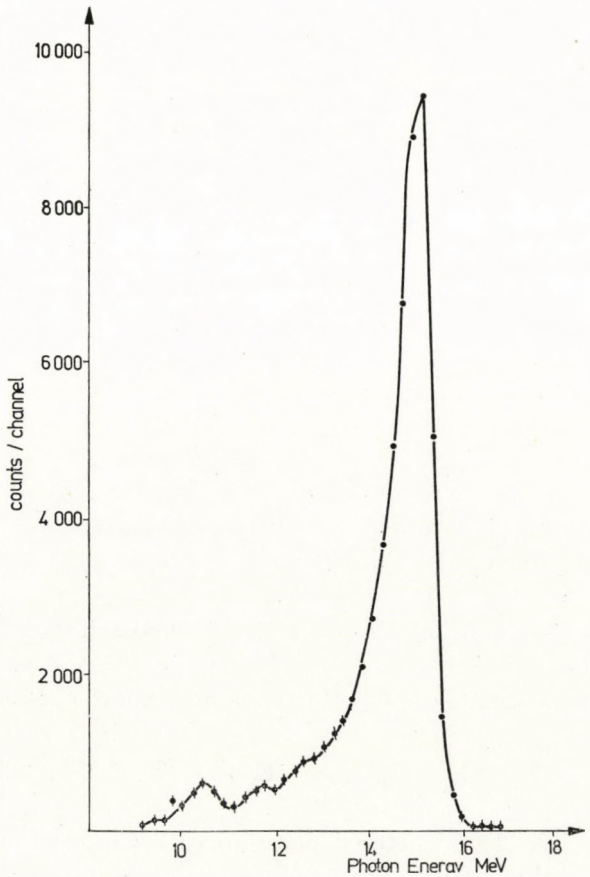

Fig. 1. The pulse-height distribution produced in the NaI(TI) crystal at 135° to the bremsstrahlung beam

Procedure and results

For a target of thickness T the yield of photons scattered by a single level is given:

$$N(T) = C \cdot I_g(T) = C \cdot \frac{I_s(T)}{S(T)} = C \cdot \int_{\text{res}} \sigma^*(E, T)\, dE\,, \tag{1}$$

$$\sigma^*(E, T) = \frac{\sigma_s}{nT\left(\sigma_a(E) + b\sigma_e(E)\right)} \left(1 - e^{-nT(\sigma_a(E)+b\sigma_e(E))}\right).$$

$N(T)$ — yield of scattered photons;

C — includes scattering and solid angle, dipole-distribution of the scattered photons, detector efficiency, number of incident 15 MeV photons, and absorbers in the scattered beam;

T — target thickness;
$S(T)$ — target self-absorption factor;
$I_g(T)$ — measured integral scattering cross section;
$I_s(T)$ — integral scattering cross section;
$\sigma_s(E) = \sigma_a(E) \frac{\Gamma_\gamma}{\Gamma_{\text{tot}}}$ — resonant scattering cross section;
$\sigma_a(E)$ — resonant absorption cross section;
$\sigma_e(E)$ — absorption cross section due to pair production and Compton scattering;
b — mean path of photons in the target.

It is assumed that the bremsstrahlung spectrum is constant in the energy interval where σ_s and σ_a are not zero and, therefore, the number of incident 15 MeV photons could be placed before the integral. It is clear that for such a narrow level photon selfabsorption occurs and the number of scattered photons is no more proportional to the target thickness.

Here we obtained

$$I_g(T = 3.31 \text{ mg/cm}^2) = (1.16 \pm 0.068) \text{ mb MeV} .$$

With an absorber of thickness Δ in the incident beam the attenuated scattered yield is

$$N(T, \Delta) = C_1 \int_{\text{res}} \sigma^*(E, T)\, e^{-\sigma_a(E) n \Delta}\, \mathrm{d}E . \tag{2}$$

$N(T, \Delta)$ — yield of scattered photons with absorber of thickness Δ in the incident beam.

In the production experiment a water absorber was placed in the incident beam of equivalent thickness to the graphite absorber.

This absorber modifies the bremsstrahlung spectrum in the same way as does the graphite absorber, except for the filter effect at 15 MeV.

Therefore C is identical with C_1.

From these two independent measurements the ratio V was experimentally determined

$$V = \frac{N(T)}{N(T, \Delta)} = 3.75 \pm 0.1 . \tag{3}$$

However, V can be also determined by numerical calculation with σ_a^0 and Γ_{tot} as variables:

$$V = \frac{\int_{\text{res}} \sigma^*(E)\, dE}{\int_{\text{res}} \sigma^*(E)\; e^{-\sigma_a(E) n \cdot \Delta}} . \tag{4}$$

For the calculation of (4) the nuclear absorption cross section $\sigma_a(E)$ is given by folding a Gaussian distribution for thermal motions of the scattered nuclei with the Breit—Wigner one-level formula:

$$\sigma_a(E) = \sigma_a^0 \frac{1}{2\sqrt{\pi t}} \int \frac{\exp\left[-(x-y)^2/4t\right]}{1+y^2}\, dy\,,$$

where $x = 2\dfrac{E-E_0}{\Gamma}$, $t = \left(\dfrac{\delta}{\Gamma}\right)^2$,

σ_a^0 — peak absorption cross section at the resonance energy;
E_0 — the resonance energy;
E — the actual energy;
Γ — the full level width at half maximum;
δ — the "Doppler width".

For photons of energy E incident on a nucleus of mass M, the Doppler width may be given by

$$\delta = E\left[\frac{2kT'}{Mc^2}\right]^{1/2},$$

where k — the Boltzmann constant;
c — the velocity of light;
T' — the effective temperature which takes into account the vibration of the scatterer atoms due to their binding in a chemical lattice.

As a lower level for δ SCHMIDT [4] suggested 31.6 eV (for carbon gas at room temperature) and as an upper level 40 eV (for diamant crystals). In our calculation a value of 33 eV was used.

Calculations for various values of $t = (\delta/\Gamma_{\text{tot}})^2$ and σ_a^0 were carried out on a computer at the University of Mainz.

The best fit with the experimental data was obtained for the values

$$\Gamma_{\text{tot}} = (69 \pm 4)\ \text{eV}\,,$$
$$\sigma_a^0 = (17.9 \pm 0.6)\ \text{b}.$$

The obtained data are summarized in the following Table together with the results of other authors.

The integrated cross section I_s was obtained from these values to be:

$$I_s = \int_{\text{res}} \sigma_s(E)\, \mathrm{d}E = \frac{\pi}{2}\sigma_\alpha^0 \Gamma_\gamma = (1.86 \pm 0.12)\ \text{mb. MeV}.$$

Table I

Parameters of the 15.11 MeV level

Reference	I_S [mb. MeV]	σ_a^0 barn	Γ_{tot} [eV]	$\frac{\delta}{\Gamma_{tot}}$	$\frac{\Gamma_{4.43\,MeV}}{\Gamma_{tot}}$ %
FULLER [1]	1.90±0.27	22.2±2.2	79±16	1	7
GARWIN [2]	2.33±0.19	29.7±1.1	64±10	0.62±0.1	5±4
BUSSIERE [3]	2.45±0.5	32	60±8	0	11±5
SCHMID [4]*	1.82±0.12	32	45±10	1	—
GUDDEN [5]*	1.79	32	35.5	—	—
KÜHNE [6]*	1.8±0.2	32	39±5	0.9±0.3	—
present work	1.86±0.12	17.9±0.6	69±4	0.48±0.1	3.6±1.0

Discussion

The authors marked by an asterisk used for σ_a^0 the value obtained from perturbation theory for a single level formula $6\pi\lambda\!\!\!^{-2} = 32$b. In this case the level width is no longer a free parameter, it follows directly from formula (1).

The influence of the following systematic errors on the ratio V should be considered:

- after bremsstrahlung beam reduction by a factor of 4 the ratio does not change. This means that errors due to detector dead-time are negligible;
- the bremsstrahlung spectrum was modified by a 1.3 cm thick lead absorber, and no change in the ratio was observed. It follows that the 15.11 MeV level is not populated by inelastic scattering from levels above the giant resonance;
- the 15.11 MeV level could be reached by the $^{13}C(\gamma, n)^{12}C^*$ reaction. The isotopic abundance of ^{13}C is about 1%, but the (γ, n) cross section is rather high [14].

If all ^{12}C nuclei populate the 15.11 MeV state, the ratio would change so that $\sigma_a^0 = 6\pi\lambda\!\!\!^{-2}$. This is extremely unlikely. But if σ_a^0 is smaller than $6\pi\lambda\!\!\!^{-2}$, the extrapolation made in the perturbation theory is not valid for this level. It is also possible that there are two levels very close to each other and the level broadening could be explained. The resolution of our apparatus was not enough to check this possibility. In Fig. 1 at 10.68 MeV the small peak represents the transition from the 15.11 MeV level into the 2^+ level at 4.43 MeV. The obtained branching ratio $\Gamma_{\gamma 1}/\Gamma_{\gamma 0} = (3.6\pm1)\%$ is in good agreement with reported data [7].

*

We gratefully acknowledge the discussions with Prof. ZIEGLER as well as the financial support given by the Bundesministerium für Wissenschaft und Forschung.

REFERENCES

1. E. G. Fuller and E. Hayward, NBS-Report, 6255, 1959.
2. E. L. Garwin, Phys. Rev., **114,** 143, 1959.
3. A. Bussiere de Nercy, Annales de Physique, **6,** 1961.
4. H. Schmid and W. Scholz, Zeitschr. f. Physik, **175,** 430, 1963.
5. F. Gudden, Thesis, Darmstadt 1964 — unpublished.
6. H. W. Kühne, P. Axel and D. C. Sutton, Phys. Rev., **163,** 1278, 1967.
7. E. Almquist, D. A. Bromley, A. J. Ferguson, H. E. Gove and A. E. Litherland, Phys. Rev., **114,** 1040, 1959.
8. F. D. Reisman, P. I. Connors and J. B. Marion, Bull. Am. Phys. Soc. II., **14,** 507, 1969.
9. J. E. Leiss, NBS-Report, 6149, 1958.
10. D. Mehlig, Thesis, Mainz, 1969.
11. K. H. Czock, Thesis, Mainz, 1969.
12. D. Mehlig, K. H. Czock, J. Ahrens, H. Borchert and B. Ziegler, Zeitschr. f. Physik, **241,** 166, 1971.
13. J. Ahrens, K. H. Czock, D. Mehlig and B. Ziegler, Nucl. Instr. and Meth., **95,** 195, 1971.
14. B. C. Cook, Phys. Rev., **106,** 300, 1957.

Acta Physica Academiae Scientiarum Hungaricae, Tomus 41 (1), pp. 63—66 (1976)

COMMUNICATIO BREVIS

AN EXACT SOLUTION OF THE PROBLEM OF MHD UNSTEADY VISCOUS FLOW THROUGH A POROUS STRAIGHT CHANNEL

By

L. M. SRIVASTAVA

DEPARTMENT OF MATHEMATICS, INDIAN INSTITUTE OF TECHNOLOGY, KANPUR, INDIA

(Received 14. IV. 1976)

The exact solution of the problem of unsteady incompressible viscous flow under a time-varying pressure gradient in a straight channel with two parallel porous walls with uniform suction and injection at the walls has been obtained by PRAKASH [1]. MATHUR [2] dealt with the unsteady flow of an electrically conducting, viscous and incompressible fluid between two parallel uniform porous walls in the presence of transverse magnetic field when there is a constant injection on the lower wall and an equal suction at the upper wall. The present note is concerned with the study of unsteady flow of an electrically conducting, viscous fluid through a straight channel with two parallel porous flat plates under a time varying pressure gradient when there is equal and uniform suction and injection on the walls. The exact solution of the problem has been obtained when pressure gradient is constant and then the case of steady flow under a constant pressure gradient has been deduced taking the time since the start of motion to be infinite. The flow takes place in the presence of a uniform vertical magnetic field.

Consider an unsteady electrically conducting two-dimensional incompressible flow through a straight channel with two parallel porous flat plates situated at a distance h apart. We take x and y values along and transverse to the parallel plates and assume a uniform magnetic field H_0 acting along y-axes. The fluid is being injected into the channel through the wall at $y = 0$ and is being sucked through the wall at $y = h$ with a uniform velocity V_0. Elastic field E is assumed to be zero. The induced magnetic field due to electrical current flow in the fluid is assumed to be very small and the electric conductivity σ of the fluid is sufficiently large.

At a sufficiently large distance from the origin the flow is fully developed and the physical quantities depend on y and t only. Then the governing equations of the problem are

$$\frac{\partial u}{\partial t} + V_0 \frac{\partial u}{\partial y} = -\frac{1}{\varrho}\frac{\partial p}{\partial x} + \nu \frac{\partial^2 u}{\partial y^2} - \frac{\sigma}{\varrho} B^2 u, \tag{1}$$

$$0 = \frac{\partial p}{\partial y}, \tag{2}$$

with the initial and boundary conditions

$$\left.\begin{aligned} 0 \leq y \leq h : u = 0, \quad v = 0 \\ y = 0 : u = 0, \quad v = V_0 \\ y = h : u = 0, \quad v = V \end{aligned}\right] \quad \begin{aligned} &\text{for} \quad t \leq 0, \\ &\text{for} \quad t > 0. \end{aligned} \tag{3}$$

Analysis

Introducing non-dimensional quantities as

$$u_1 = \frac{u}{V_0}, \quad x_1 = \frac{x}{h}, \quad y_1 = \frac{p}{\varrho V_0^2}, \quad p_1 = \frac{t}{h/V_0}, \tag{4}$$

into Eq. (1)—(2), which reduce to

$$\frac{\partial u_1}{\partial t_1} + \frac{\partial u_1}{\partial y_1} = -\frac{\partial p_1}{\partial x_1} + \frac{1}{R_s}\frac{\partial^2 u_1}{\partial y_1^2} - m_1 u_1, \tag{5}$$

$$0 = \frac{\partial p_1}{\partial y_1}, \tag{6}$$

$$\begin{aligned} &0 \leq y_1 \leq 1 : u_1 = 0 \text{ for } t_1 \leq 0, \\ &y_1 = 0, 1 : u_1 = 0 \text{ for } t_1 > 0, \end{aligned} \tag{7}$$

where $R_s = V_0 h/\nu$ = suction and injection Reynolds number,

$$m_1^{1/2} = \left(\frac{h}{V_0} \cdot \frac{\sigma}{\varrho} \mu_e^2 H_0^2\right)^{1/2} = R_M = \text{magnetic parameter},$$

$$m_1 = \frac{M_2}{R_s}, \quad M = \left[\frac{\sigma}{\mu} \mu_e^2 H_0^2 h^2\right] = \text{Hartmann number}.$$

Now assuming $\partial p_1/\partial x_1 = -f(t_1)$, thus (5) reduces to

$$\frac{\partial u_1}{\partial t_1} + \frac{\partial u_1}{\partial y_1} = f(t_1) + \frac{1}{R_s}\frac{\partial^2 u_1}{\partial y_2^2} - m_1 m_1. \tag{8}$$

To obtain the solution of (8), we will apply here Laplace transformation which is defined for velocity u, as

$$\bar{u}_1 = \int_0^\infty u_1 e^{-\varphi t_1} dt_1. \tag{9}$$

Thus (8) and (7) transform to

$$\frac{d^2 \bar{u}_1}{dy_1^2} - R_s \frac{d\bar{u}_1}{dy_1} - R_s(\lambda + m_1) = -R_s \bar{f}(\lambda) \tag{10}$$

$$\bar{u}_1 = 0 \text{ at } y_1 = 0,1, \tag{11}$$

where
$$\bar{f}(\lambda) = \int_0^\infty f(t_1)\, e^{-\lambda_1}\, dt_1 \,. \tag{12}$$

The solution of (10) subject to the boundary condition (11) is

$$\bar{u}_1 = \frac{\bar{f}(\lambda)}{(\lambda+m)\sinh\sqrt{B}}\left[-\exp\left\{(y_1-1)\frac{R_s}{2}\right\}\sinh\left(\sqrt{B}y_1\right) - \right.$$
$$\left. - \exp\left\{y_1\frac{R_s}{2}\right\}\sinh\left\{(1-y_1)\sqrt{B}\right\}\right] + \frac{\bar{f}(\lambda)}{\lambda+m}\,, \tag{13}$$

where
$$B = \frac{R_s^2 + 4R_s(\lambda+m)}{4}\,,$$

thus

$$u_1 = \frac{1}{2\pi i}\int_{\gamma-i\infty}^{\gamma+i\infty}\frac{\bar{f}(\lambda)}{(\lambda+m_1)\sinh\sqrt{B}}\left[-\exp\left\{(y_1-1)\frac{R_s}{2}\right\}\sinh\left(\sqrt{B}y_1\right) - \right.$$
$$\left. - \exp\left\{y_1\frac{R_s}{2}\right\}\sinh\left\{(1-y_1)\sqrt{B}\right\} + \frac{\bar{f}(\lambda)}{(\lambda+m)}\right] e^{\lambda t_1}\, d\lambda\,. \tag{14}$$

After assuming pressure gradient constant (i.e., $\partial p_1/\partial x_1 = -f(t_1) = P$, P is positive constant), (14) becomes

$$u_1 = \frac{1}{B\pi i}\int_{\gamma-i\infty}^{\gamma+i\infty}\left[\frac{P}{[-\lambda(\lambda+m_1)\sinh\sqrt{B}} - e^{(y_1-1)\frac{R_1}{2}}\sinh\left(\sqrt{B}y_1\right) - \right.$$
$$\left. - e^{y\frac{R_1}{2}}\sinh\left\{(1-y_1)\sqrt{B}\right\}\right] + \frac{P}{\lambda(\lambda+m_1)}\right] e^{\lambda t_1}\, d\lambda\,. \tag{15}$$

Therefore solution for constant pressure gradient with the help of poles and residue method is given by

$$u_1 = \frac{P}{m}\left[1 - \frac{e^{(y_1-1)\frac{R_s}{2}}\sinh\left\{\sqrt{\frac{R_s^2+4R_s m_1}{4}}\,y_1\right\} + e^{y_1\frac{R_s}{2}}\sinh\left\{\sqrt{\frac{R_s^2+4R_s m_1}{4}}\,(1-y_1)\right\}}{\sinh\sqrt{\frac{R_s^2+4R_s m_1}{4}}}\right] +$$
$$+ \frac{p}{m}\,e^{-m_1 t_1}\left[1 + \frac{e^{(y_1-1)\frac{R_s}{2}}\sinh\left\{\frac{R_s}{2}\,y_1\right\} - e^{y_1\frac{R_s}{2}}\sinh\left\{\frac{R_s}{2}\,(1-y_1)\right\}}{\sinh\frac{R_s}{2}}\right] + \tag{16}$$
$$+ 32PR_s\pi\sum_{n=0}^{\infty}\left[\frac{nc^{\frac{R_s}{2}y_1}\sinh(n\pi y_1)\left\{e^{-\frac{R_s}{2}}(1)^n - 1\right\}e^{-\left(\frac{R_s^2+4\pi n^2}{z}+m_1\right)t_1}}{(R_s^2+4\pi^2n^2)^2+4R_s m_1(R_s^2+4\pi^2n^2)}\right]$$
$$(n = 0, 1, 2, 3, \ldots)\,.$$

Solution for steady state

Solution for steady state from (16) can be obtained by taking its limit $t \to W$,

$$u_1 = \frac{P}{m}\left[1 - \frac{e^{(y_1-1)\frac{R_s}{2}} \sinh\left\{\sqrt{\frac{R_s^2+4R_s m_1}{4}}\, y_1\right\} + e^{y_1 \frac{R_1}{2}} \sinh\left\{\sqrt{\frac{R_s^2+4R_s m_1}{4}}\,(1-y_1)\right\}}{\sinh\sqrt{\frac{R_\beta^2+4R_s m_1}{4}}}\right]. \tag{17}$$

Now we shall obtain the steady state solution directly from the equation of motion (8) which, after substituting P for $f(t_1)$, reduces to

$$\frac{d^2 u_1}{dy_1^2} - R_s \frac{du_1}{dy_1} - m_1 R_s u_1 = -pR_s \tag{18}$$

with boundary conditions

$$u_1 = 0, \quad y_1 = 0.1\,. \tag{19}$$

It may be easily seen that solution of (18) subject to the boundary conditions (19) is (17).

*

I wish to express my sincere thanks to Professor JAGDISH LAL, D. Sc., Director, Indian Institute of Technology, Kanpur, for his help and guidance in the preparation of this paper.

REFERENCES

1. S. PRAKASH, Proc. Nat. Inst. Sci. India, **35**(A), 123, 1969.
2. A. K. MATHUR, Indian J. Phys., **46**, 165, 1972.

RECENSIONES

BECKER—SAUTER: Theorie der Elektrizität

Band 1. Einführung in die Maxwellsche Theorie. Elektronentheorie. Relativitätstheorie
21. völlig neubearbeitete Auflage, B. G. Teubner, Stuttgart, 1973

Es ist schon fast ein Jahrhundert vergangen, seit die erste Fassung des Buches durch AUGUST FÖPPL erschien. In den Händen der würdigen und kompetenten Nachfolger — es seien nur ABRAHAM, und BECKER erwähnt — sind der Inhalt und die Methode immer auf neuesten Stand gebracht. Bewahrung der Traditionen — Berücksichtigung der Ergebnisse der neuesten Forschung: diese sind die kennzeichnenden Merkmale des Buches, die es zu einem Begriff machten.

Die vorliegende Auflage ist die 21-ste: allein diese Zahl spricht für sich. Sie ist gründlich überarbeitet, zum grössten Teil neu geschrieben. Alle Veränderungen sind nach meiner Meinung zu begrüssen — vielleicht mit der einzigen Ausnahme der "*i*-freien" Behandlung der speziellen Relativitätstheorie. Besonders halte ich die ausführlichere Darstellung der Energieverhältnisse, den Zusammenhang mit der Thermodynamik für nützlich, die trotz ihrer Wichtigkeit oft vernachlässigt wird. Methodisch möchte ich die Berücksichtigung der Vertiefung der mathematischen Kenntnisse der Leser als gelungen hervorheben.

Dieser erste Band behandelt auf 310 Seiten in 12 Kapiteln die Gesetze der Elektrostatik, des elektrischen Stromes, des magnetischen Feldes, der quasistationären Vorgänge der elektromagnetischen Wellen und der Relativitätstheorie. Dazu kommen noch ein Kapitel über Vektor- und Tensorrechnung in dreidimensionalem Raum, Formelzusammenstellung und ein Kapitel über die Lösung der Aufgaben. Hier möchte ich bemerken, dass die geschickte Auswahl der Aufgaben die Nutzbarkeit des Buches beträchtlich erhöht.

Es kann die Frage gestellt werden, und manchmal wird sie auch tatsächlich aufgeworfen, inwiefern die klassische Elektronentheorie in einer modernen Darstellung ihren Platz finden kann. Didaktisch halte ich die Heranziehung der bildhaften Beschreibung der Erscheinungen der Mikrophysik für fast unvermeidlich: unsere Kenntnisse der atomaren Welt führen, nicht nur historisch, sondern methodologisch gesehen, auch heute durch die klassischen Vorstellungen der Elektronentheorie. Durch das so begründete Wissensmaterial werden eben die in weiteren Bänden behandelten modernsten Theorien erst zugänglich.

Im Zusammenhang mit dem Inhalt der weiteren Bände möchte ich hier eine Schwierigkeit erwähnen. Es scheint nämlich fast unmöglich bei einem dreibändigen Buch alle Bände gleichzeitig zu überarbeiten und so Methode und Inhalt gegeneinander vollständig abzustimmen. Mit dem in 1963 erschienenen zweiten und im 1969 erschienenen dritten Band fand auch dieses Problem eine befriedigende Lösung.

Für jeden, der sich in die Grundlagen der klassischen Elektrodynamik vertiefen will, stellt das Buch einen vertrauenswerten Wegweiser dar.

K. SIMONYI

R. C. NEWMAN: Infra-red Studies of Crystal Defects

Taylor and Francis Monographs on Physics. Editor B. R. Coles, Consultant Editor: Sir Neville Mott, F. R. S., Taylor and Francis Ltd. London, 1973

The book deals with the basic problem of detecting and determining the presence and concentration of various impurities in alkaline earth fluorides, alkali halides, silicon, germanium and compound III—V semiconductors. Whereas the investigation of some particular impurities can be successfully carried out by well developed experimental techniques such as electrical conductivity or radioactive tracer methods, infra-red spectroscopy has become increasingly important to learn more about the interactions between various impurities and of impurities with intrinsic defects if more than one impurity is present. A relatively high concentration of impurities may give rise to complicated complexes, which can be revealed only spectroscopically. The purpose of this monograph is to show how infra-red absorption resulting from localized modes of vibration of defects may give useful informations, and enlarge our knowledge on the effects of heat treatment, diffusion, radiation damage and implantation in crystals.

The monograph consists of an introduction and eight chapters dealing with infra-red absorption from a lattice containing point defects, vibrations of an anharmonic oscillator, localized vibrations of hydrogen and deuterium in the alkaline earth fluorides, hydrogen ions in alkali halides, one-phonon infra-red absorption in silicon, radiation damage in silicon, one-phonon absorption in germanium and informations which can be gained of compound III—V semiconductors.

A detailed mathematical treatment of the theory of the vibrations of imperfect lattice is not included, nevertheless the symmetry relations of the oscillators (spherical, cubic, trigonal and tetragonal symmetry) are properly dealt with. The basic ideas of lattice dynamics are reviewed. In the referee's opinion this could have been omitted, since the monograph is apparently written for advanced readers, and lattice dynamics may be found in textbooks anyway.

Though the monograph is intended mainly for research workers, the theory is clearly presented and can be easily followed. The book is certainly stimulating for solid state physicists and chemists who wish to obtain a deeper insight into the lattice dynamics involved with the presence of impurities and complexes formed by them.

Z. MORLIN

P. J. GOODHEW: Electron Microscopy and Analysis

The Wykeham Science Series, General Editors: Sir Neville Mott, F. R. S. and G. R. Noakes Wykeham Publications Ltd., London and Winchester, 1975

The book gives an introductory survey on the principles and experimental techniques of electron microscopy and microanalysis by means of electron optics. It is built up of six chapters, the first two dealing with the basic ideas of electron optics and the interaction of electrons with matter including electron diffraction. The second chapter also includes a description of the properties, generation and deflection of a beam of electrons. The third and fourth chapters describe transmission and scanning electronmicroscopy, the various methods of specimen preparation and examples of application. The fifth chapter discusses the analytical informations which can be obtained from an electron microscope by means of electrondiffraction, secondary electrons and X-ray generation. Finally, electronoptical methods are compared with other techniques.

The book is written to give a summary in the field of up-to-date electronmicroscopy and can be easily understood with some basic background in electronphysics. The book is intelligible, and may be recommended also to chemists, biologists and medical researchers who apply or wish to apply electronoptical methods in their research. Extremely good electronmicrograms, diffraction patterns and drawings help the reader to get well acquainted with the subject.

Z. MORLIN

A. M. CAMPBELL and J. E. EVETTS: Critical Currents in Superconductors

Monographs on Physics No 4. Taylor and Francis Ltd. London

The authors give a wide range survey on the topic of the critical currents in type II superconductors, limiting the contents to those aspects of type II superconductivity which relate directly to flux vortex pinning and transport currents. So the question of flux jumps and instabilities, for instance, are not dealt with.

The nature of the mixed state, the properties of the flux vortex lattice, the driving force and its relation to the transport currents and flux flow are discussed first. The solution of the critical state equation and the distribution of the current are then studied in situations where the pinning force is known. The summation of pinning forces and the various types of vortex-defect interactions are investigated in the next sections.

Experimental methods and results are also treated, such as, for example, the measurement of the vortex structures and Ginzburg—Landau parameters, the experimental confirmation of the critical state model, the measurement of the critical current density and other pinning parameters. Finally a critical assessment of the current agreement between theory and experiment are given.

Some publications that have a direct bearing on subjects treated here are also listed as an addendum to references. These had been published before this book was ready but are not discussed in it any more.

The monograph can be recommended to graduates and researchers active in the field of superconductivity.

I. SKOPÁL

A. BOHR and B. R. MOTTELSON: Struktur der Atomkerne

Akademie-Verlag, Berlin, 1975

This brilliant piece of work of the 1976 Nobel-prize winners is the first volume of a large-scale undertaking, which is planned to cover the topics of single-particle motion in nuclei, nuclear deformations and nucleonic correlations.

The present volume deals with nuclear structure, but the authors also include a summary of the symmetry properties, relevant to nuclear systems. The main theme of the book is nuclear independent-particle motion, leading naturally to single-particle and single-hole configurations, providing detailed and quantitative evidence on independent-particle motion.

An important and valuable feature of the book is the division of the material into three parts: text, illustrative examples and appendices. The text gives a systematic development of the subject, while comparison to experiments and discussion of empirical data is usually placed in sections labelled "Illustrative Examples". The appendices, dealing among others with angular momentum algebra, elements of statistical mechanics, the formulation of electromagnetic and β-decay make the book reasonably self-contained.

The clarity of presentation and the pedagogical care of the authors will make this book extremely useful not only for experimental and theoretical nuclear physicists, but also for researchers of other fields of physics and for graduate students.

J. NÉMETH

J. M. BLAKELY: Introduction to the Properties of Crystal Surfaces

International Series on Materials Science and Technology, Volume 12.
Pergamon Press, Oxford, 1973

The properties of the surface always play a more or less important role in all phenomena occurring in materials. Thus the physics of surfaces is a very interesting part of physics, subject of many books and of many international symposia.

The Introduction to the Properties of Crystal Surfaces by Professor J. M. BLAKELY examines in detail the atomic and electronic structure in the surface region. The treatment

s suitable for senior undergraduates or postgraduates. For this reason the book offers only a general introduction to the subject. But exactly this generality is its high advantage, because the wide range of topics from the macroscopic thermodynamic aspects of the surfaces to the details of the surface electronic structure offers an easily accessible up-to-date knowledge on surface phenomena, such as adsorption, experimental measurements of surface tension in solids, surface relaxation, surface defects, surface atom vibrations, various experimental methods in surface studies and so on. Those who whish to go beyond the scope of this very useful book can study some of the books recommended in the general references.

G. TURCHÁNYI

Printed in Hungary

A kiadásért felel az Akadémiai Kiadó igazgatója — Műszaki szerkesztő: Botyánszky Pál

A kézirat nyomdába érkezett: 1976. VII. 15. — Terjedelem: 6,25 (A/5) ív, 10 ábra

77.3370 Akadémiai Nyomda, Budapest — Felelős vezető: Bernát György

NOTES TO CONTRIBUTORS

I. PAPERS will be considered for publication in Acta Physica Hungarica only if they have not previously been published or submitted for publication elsewhere. They may be written in English, French, German or Russian.

Papers should be submitted to

Prof. I. Kovács, Editor
Department of Atomic Physics, Polytechnical University
1521 Budapest, Budafoki út 8, Hungary

Papers may be either articles with abstracts or short communications. Both should be as concise as possible, articles in general not exceeding 25 typed pages, short communications 8 typed pages.

II. MANUSCRIPTS

1. Papers should be submitted in five copies.

2. The text of papers must be of high stylistic standard, requiring minor corrections only.

3. Manuscripts should be typed in double spacing on good quality paper, with generous margins.

4. The name of the author(s) and of the institutes where the work was carried out should appear on the first page of the manuscript.

5. Particular care should be taken with mathematical expressions. The following should be clearly distinguished, e.g. by underlining in different colours: special founts (italics, script, bold type, Greek, Gothic, etc); capital and small letters; subscripts and superscripts, e.g. x^3, x_3; small l and 1; zero and capital O; in expressions written by hand: e and i, n and u, c and v, etc.

6. References should be numbered serially and listed at the end of the paper in the following form: J. Ise and W. D. Fretter, Phys. Rev., *76*, 933, 1949.

For books, please give the initials and family name of the author(s), title, name of publisher, place and year of publication, e.g.: J. C. Slater, Quantum Theory of Atomic Structures, I. McGraw-Hill Book Company Inc., New York, 1960.

References should be given in the text in the following forms: Heisenberg [5] or [5]

7. Captions to illustrations should be listed on a separate sheet, not inserted in the text.

III. ILLUSTRATIONS AND TABLES

1. Each paper should be accompanied by five sets of illustrations, one of which must be ready for the blockmaker. The other sets attached to the copies of the manuscript may be rough drawings in pencil or photocopies.

2. Illustrations must not be inserted in the text.

3. All illustrations should be identified in blue pencil by the author's name, abbreviated title of the paper and figure number.

4. Tables should be typed on separate pages and have captions describing their content. Clear wording of column heads is advisable. Tables should be numbered in Roman numerals (I, II, III, etc.).

IV. MANUSCRIPTS not in conformity with the above Notes will immediately be returned to authors for revision. The date of receipt to be shown on the paper will in such cases be that of the receipt of the revised manuscript.

Reviews of the Hungarian Academy of Sciences are obtainable at the following addresses:

AUSTRALIA

C. B. D. Library and Subscription Service
Box 4886, G. P. O.
Sydney N. S. W. 2001

Cosmos Bookshop
145 Acland St.
St. Kilda 3182

AUSTRIA

Globus
Höchstädtplatz 3
A—1200 Wien XX

BELGIUM

Office International de Librairie
30 Avenue Marnix
1050-Bruxelles

Du Monde Entier
162 Rue du Midi
1000 – Bruxelles

BULGARIA

Hemus
Bulvar Ruszki 6
Sofia

CANADA

Pannonia Books
P. O. Box 1017
Postal Station "B"
Toronto, Ont. M5T 2T8

CHINA

C N P I C O R
Periodical Department
P. O. Box 50
Peking

CZECHOSLOVAKIA

Mad'arská Kultura
Národní třida 22
115 66 Praha

PNS Dovoz tisku
Vinohradská 46
Praha 2

PNS Dovoz tlače
Bratislava 2

DENMARK

Ejnar Munksgaard
Nörregade 6
DK—1165 Copenhagen K

FINLAND

Akateeminen Kirjakauppa
P. O. Box 128
SF-00101 Helsinki 10

FRANCE

Office International de Documentation et Librairie
48, Rue Gay-Lussac
Paris 5

Librairie Lavoisier
11 Rue Lavoisier
Paris 8

Europeriodiques S. A.
31 Avenue de Versailles
78170 La Celle St. Cloud

GERMAN DEMOCRATIC REPUBLIC

Haus der Ungarischen Kultur
Karl-Liebknecht-Strasse 9
DDR—102 Berlin

Deutsche Post
Zeitungsvertriebsamt
Strasse der Pariser Kommüne 3—4
DDR-104 Berlin

GERMAN FEDERAL REPUBLIC

Kunst und Wissen
Erich Bieber
Postfach 46
7 Stuttgart 5

GREAT BRITAIN

Blackwell's Periodicals
P. O. Box 40
Hythe Bridge Street
Oxford OX1 2EU

Collet's Holdings Ltd.
Denington Estate
London Road
Wellingborough Northants NN8 2QT

Bumpus Haldane and Maxwell Ltd.
5 Fitzroy Square
London W1P 5AH

Dawson and Sons Ltd.
Cannon House
Park Farm Road
Folkestone, Kent

HOLLAND

Swets and Zeitlinger
Heereweg 347b
Lisse

Martinus Nijhoff
Lange Voorhout 9
The Hague

INDIA

Hind Book House
66 Babar Road
New Delhi 1

India Book House
Subscription Agency
249 Dr. D. N. Road
Bombay 1

ITALY

Santo Vanasia
Via M. Macchi 71
20124 Milano

Libreria Commissionaria Sansoni
Via Lamarmora 45
50121 Firenze

JAPAN

Kinokuniya Book-Store Co. Ltd.
826 Tsunohazu 1-chome
Shinjuku-ku
Tokyo 160—91

Maruzen and Co. Ltd.
P. O. Box 5050
Tokyo International 100—31

Nauka Ltd.-Export Department
2—2 Kanda
Jinbocho
Chiyoda-ku
Tokyo 101

KOREA

Chulpanmul
Phenjan

NORWAY

Tanum-Cammermayer
Karl Johansgatan 41—43
Oslo 1

POLAND

Węgierski Instytut Kultury
Marszalkowska 80
Warszawa

BKWZ Ruch
ul. Wronia 23
00—840 Warszawa

ROUMANIA

D. E. P.
Bucureşti

Romlibri
Str. Biserica Amzei 7
Bucureşti

SOVIET UNION

Sojuzpechatj — Import
Moscow

and the post offices in each town

Mezhdunarodnaya Kniga
Moscow G—200

SWEDEN

Almqvist and Wiksell
Gamla Brogatan 26
S—101 20 Stockholm

A. B. Nordiska Bokhandeln
Kunstgatan 4
101 10 Stockholm 1 Fack

SWITZERLAND

Karger Libri AG.
Arnold-Böcklin-Str. 25
4000 Basel 11

USA

F. W. Faxen Co. Inc.
15 Southwest Park
Westwood, Mass. 02090

Stechert-Hafner Inc.
Serials Fulfillment
P. O. Box 900
Riverside N. J. 08075

Fam Book Service
69 Fifth Avenue
New York N. Y. 1003

Maxwell Scientific International Inc.
Fairview Park
Elmsford N. Y. 10523

Read More Publications Inc.
140 Cedar Street
New York N. Y. 10006

VIETNAM

Xunhasaba
32, Hai Ba Trung
Hanoi

YUGOSLAVIA

Jugoslavenska Knjiga
Terazije 27
Beograd

Forum
Vojvode Mišiča 1
21000 Novi Sad

ACTA PHYSICA

ACADEMIAE SCIENTIARUM HUNGARICAE

TOMUS XLI FASCICULUS 2

AKADÉMIAI KIADÓ, BUDAPEST

1976

ACTA PHYS. HUNG. APAHAQ 41 (2) 71–151 (1976)

ACTA PHYSICA

ACADEMIAE SCIENTIARUM HUNGARICAE

SZERKESZTI

KOVÁCS ISTVÁN

Az *Acta Physica* angol, német, francia vagy orosz nyelven közöl értekezéseket. Évente két kötetben, kötetenként 4—4 füzetben jelenik meg. Kéziratok a szerkesztőség címére (1521 Budapest XI., Budafoki út 8.) küldendők.

Megrendelhető a belföld számára az Akadémiai Kiadónál (1363 Budapest Pf. 24. Bankszámla 215-11488), a külföld számára pedig a „Kultúra" Könyv és Hírlap Külkereskedelmi Vállalatnál (1389 Budapest 62, P. O. B. 149. Bankszámla 217-10990 sz.), vagy annak külföldi képviseleteinél és bizományosainál.

The *Acta Physica* publish papers on physics in English, German, French or Russian, in issues making up two volumes per year. Subscription price: $32.00 per volume. Distributor: KULTURA Hungarian Trading Co. for Books and Newspapers (1389 Budapest 62, P. O. Box 149) or its representatives abroad.

Die *Acta Physica* veröffentlichen Abhandlungen aus dem Bereich der Physik in deutscher, englischer, französischer oder russischer Sprache, in Heften die jährlich zwei Bände bilden.

Abonnementspreis pro Band: $32.00. Bestellbar bei: KULTURA Buch- und Zeitungs-Außenhandelsunternehmen (1389 Budapest 62, Postfach 149) oder bei seinen Auslandsvertretungen.

Les *Acta Physica* publient des travaux du domaine de la physique, en français, anglais, allemand ou russe, en fascicules qui forment deux volumes par an.

Prix de l'abonnement: $32.00 par volume. On peut s'abonner à l'Entreprise du Commerce Extérieur de Livres et Journaux KULTURA (1389 Budapest 62, P. O. B. 149) ou chez ses représentants à l'étranger.

«*Acta Physica*» публикуют трактаты из области физических наук на русском, немецком, английском и французском языках.

«*Acta Physica*» выходят отдельными выпусками, составляющими два тома в год.

Подписная цена — $32.00 за том. Заказы принимает предприятие по внешней торговле книг и газет KULTURA (1389 Budapest 62, P. O. B. 149) или его заграничные представительства и уполномоченные.

ACTA PHYSICA

ACADEMIAE SCIENTIARUM HUNGARICAE

TOMUS XLI FASCICULUS 2

AKADÉMIAI KIADÓ, BUDAPEST
1976

ACTA PHYS. HUNG.

INDEX

Acta Physica Academiae Scientiarum Hungaricae, Tomus 41 (2), pp. 71—78 (1976)

WAVE MECHANICS AND THE PHOTON II

THE MANY-BODY ASPECT

By

L. JÁNOSSY

CENTRAL RESEARCH INSTITUTE FOR PHYSICS, BUDAPEST

(Received 6. V. 1976)

The considerations of a previous paper in which we have dealt with the wave mechanical picture of the emission of a photon by a single atom are extended. It is shown how the emission of photons by N independent atoms of a gas can be treated by wave mechanics. The problem of wave functions realized in nature is discussed in some detail.

Introduction

In a previous paper (see [1]) we have discussed a mechanism which gives the mode of the emission of photons by a H-atom with the help of pure wave mechanical considerations.

We have investigated an H-atom in an excited state enclosed into a box with linear dimensions $L \gg r_H$. It was shown that the pure excited state of the atom is highly unstable. Even a very small admixture of a wave function corresponding to a lower state of energy to the wave function of the higher excited state leads to the emission of radiation. The radiation reaction of the system upon itself starts an avalanche. Finally, the excess energy $h\nu$ is emitted in the form of radiation. Moreover, the radiation is emitted into a cone with small opening angle. This process corresponds very closely to what one takes qualitatively to be the emission of a single photon.

Presently we investigate the process where a box contains a gas consisting of N H-atoms, some of which are in excited states. We investigate how far it follows from the wave mechanical description of this system that it emits radiation which can be taken as the emission of successive photons, so that the emission of each photon takes place in a way, similar to that in the case of the single atom.

The problem how to extend the considerations relating to a single atom to that of an ensemble of N atoms is not a trivial one as the system of N atoms has to be described by a collective wave function — and it is not trivial how this wave function has to be chosen.

One finds that there exists a very large number of mathematically possible solutions of the wave equations describing the ensemble of N atoms. Most

of these wave functions, however, describe systems with behaviours very different from the observed behaviour of a gas enclosed in a box.

It is therefore necessary to select from the mathematically possible ones those wave functions which describe the system correctly, i.e. one has to find the wave functions which represent the states realized in nature.

The above problem of selection of the wave function is a general problem of wave mechanics of many body systems — the question of the emission of photons by a gas in an interesting particular case [2].

The choice of the wave function

Presently we construct reasonable types of wave functions representing the ensemble of N H-atoms enclosed into a box. We shall construct two mathematically possible types of wave functions. We believe that the second of the possibilities we consider presently is the one which resembles the wave function realized in nature.

Taking the atoms of the gas to be largely independent of each other it seems reasonable to build up the wave function of the ensemble as a product of two-body wave functions representing single atoms.

Let us write

$$\overset{(2)}{\Psi} = \overset{(2)}{\Psi}(\mathbf{r}^{(1)}, \mathbf{r}^{(2)}, t) \tag{1}$$

for some solution of the two-body hydrogen wave equation; $\mathbf{r}^{(1)}$, $\mathbf{r}^{(2)}$ being the coordinate vectors of proton and electron.

The N-atom wave function will thus be supposed to have the following form:

$$\overline{\Psi} = \overline{\Psi}(\boldsymbol{r}^{(1)}, \boldsymbol{r}^{(2)}, t) = \prod_{\nu=1}^{N} \overset{(2)}{\Psi}(\mathbf{r}_\nu^{(1)}, \mathbf{r}_\nu^{(2)}, t) , \tag{2}$$

where

$$\boldsymbol{r}^{(k)} = \mathbf{r}_1^{(k)}, \mathbf{r}_2^{(k)}, \ldots, \mathbf{r}_N^{(k)} \qquad k = 1, 2$$

are the coordinate vectors of the N protons and the N electrons.

The wave function (2) satisfies the $2N$-body wave equation in a good approximation if $\overset{(2)}{\Psi}$ represents the state of an H-atom enclosed into a box and the interactions between electrons and protons of different atoms are neglected. The approximation is justified if the density of the gas is small, i.e. if

$$N r_H^3 \ll L^3 \tag{3}$$

and one neglects the effect of formation of molecules.

The wave function (1) does not possess the symmetry properties arising from the Pauli principle. A suitable wave function can be obtained in the following usual way. Denote

$$\Psi_{KL} = \Psi_{KL}(\boldsymbol{r}^{(1)}, \boldsymbol{r}^{(2)}, t) = \overset{(2)}{\Psi}(\mathbf{r}_K^{(1)}, \mathbf{r}_L^{(2)}, t)\,; \tag{4}$$

the Ψ_{KL} is independent of the coordinate vectors except those of the K-th proton and the L-th electron.

The Ψ_{KL} can be taken as the elements of an $N \times N$ matrix. A wave function obeying the Pauli principle is thus

$$\Psi = \Psi(\boldsymbol{r}^{(1)}, \boldsymbol{r}^{(2)}, t) = C_N \det \Psi_{KL}\,. \tag{5}$$

If the Ψ_{KL} are mutually orthogonal, i.e. if

$$\int \Psi_{KL}^{*} \Psi_{K'L'} \mathrm{d}^{3N}\boldsymbol{r}^{(1)} \mathrm{d}^{3N}\boldsymbol{r}^{(2)} = \delta_{KK'}\delta_{LL'}\,, \tag{6}$$

then we have

$$C_N = \frac{1}{\sqrt{N!}}\,. \tag{7}$$

We note that if the two-body wave functions are such that

$$\overset{(2)}{\Psi}(\mathbf{r}^{(1)}, \mathbf{r}^{(2)}, t) \sim 0\,,$$

if

$$|\,\mathbf{r}^{(1)} - \mathbf{r}^{(2)}\,| \gg r_H\,, \tag{8}$$

then the orthogonality relation (6) is satisfied in a good approximation for a gas of low density satisfying (3).

With wave functions of the form (4) one can express a large variety of states. More general forms can be obtained as linear combinations of functions of this form.

Particular simple wave functions can be obtained if we start from stationary states of the H-atoms. Considering (5) and (7) the wave functions corresponding to the $\nu\mu$ states can be written as

$$\Psi^{(\nu\mu)} = \frac{1}{\sqrt{N!}} \det \Psi_{KL}^{(\nu\mu)}\,. \tag{9}$$

Thus we obtain a stationary state corresponding to N H-atoms each in the state described by (9). A state in which the N atoms are in various states

(e.g. have a thermal distribution) can be obtained as a linear combination of $\Psi^{\nu\mu}$, as

$$\Psi = \frac{1}{\sqrt{N}} \Sigma c_{\nu\mu} \Psi^{(\nu\mu)} , \tag{10}$$

where the sum is to be extended over N pairs of suffices $\nu\mu$. Because of the normalization we have

$$\Sigma \mid c_{\nu\mu} \mid^2 = N .$$

One may suppose e.g. $\mid c_{\nu\mu} \mid^2 = 1$ and

$$c_{\nu\mu} = c^{i\alpha_{\nu\mu}} , \tag{11}$$

where the $\alpha_{\nu\mu}$ are real phases.

The wave function corresponding to the ν, μ states of the H-atom can be written as (in more detail see [3])

$$\overset{(2)}{\Psi}{}^{\nu\mu} = \frac{1}{L^{3/2}} e^{i(\mathbf{k}_\nu \mathbf{R} - \omega_\nu t)} \cdot \varphi_\mu(\mathbf{s}) e^{-i\bar{\omega}_\mu t} , \tag{12}$$

where $\mathbf{R} = (m_1 \mathbf{r}^{(1)} + m_2 \mathbf{r}^{(2)})/M$ and $\mathbf{s} = \mathbf{r}_1 - \mathbf{r}_2$ with $M = m_1 + m_2$ (Here m_1 and m_2 are the proton and electron mass, respectively) $\varphi_{\nu\mu}$ is the amplitude of the one-body H-wave function with frequency $\bar{\omega}_\mu$ calculated for the reduced mass $m = m_1 m_2/M$.

Taking $\overset{(2)}{\Psi}{}^{(\nu\mu)} = 0$ for points outside the box the wave functions (12) give in a good approximation the stationary states of an H-atom enclosed into the box with sides L. Small corrections which have to be applied mainly near the walls shall be neglected.

With the wave function (12) one finds for the energy of the system

$$U = \hbar \sum_{\nu\mu} (\omega_\nu + \bar{\omega}_\mu) .$$

The above value consists of the kinetic energy

$$K = \frac{1}{2M} \Sigma p_\nu^2 , \qquad p_\nu = \hbar \mathbf{k}_\nu ,$$

of the energy of excitation

$$E = \hbar \Sigma (\bar{\omega}_\mu - \bar{\omega}_0) ,$$

and of the energy of the ground state

$$U_0 = N\hbar\bar{\omega}_0 .$$

The wave function obtained from (10) gives a rather peculiar distribution.

On account of the orthogonality of the $\overset{(2)}{\Psi}{}^{(\nu\mu)}$ we find that the $\Psi^{(\nu\mu)}$ are also mutually orthogonal. One finds thus that although the states (10) are *not* stationary states nevertheless both the three dimensional charge and current densities are constant. Indeed, the density corresponding to the states $\Psi^{(\nu\mu)}$ is constant as those states are stationary. Cross terms where products

$$\Psi^{(\nu\mu)*}\,\Psi^{(\nu'\mu')}$$

when integrated over any of the variables give zero on account of the orthogonality.

Calculating the current densities which contain terms of the form

$$\Psi^{(\nu\mu)*}\,\mathrm{grad}_K\,\Psi^{(\nu'\mu')}$$

the integration over any of the variables $\mathbf{r}_k$, $K' \neq K$ gives a zero factor, and thus the current densities arising from any of the cross terms vanish identically.

The wave function Ψ as given by (10) has the peculiar property that it describes a non stationary state such that it contains fluctuations of current- and charge densities in the $6N$ dimensional configuration space. The projections of these fluctuations upon the three dimensional space vanish, however, identically.

The emission of photons by the ensemble

The state described by (10) is thus not stationary in the ordinary sense, nevertheless it emits no radiation. In analogy with the considerations of the previous paper we find that this state is very unstable. If one of the components $\Psi^{(\nu\mu)}$ of Ψ is modified to a small extent by say the admixture of a lower state, then a radiative process sets in. Indeed, if

$$\overset{(2)}{\Psi}{}^{(\nu\mu)} \to c_0 \overset{(2)}{\Psi}{}^{(\nu\mu)} + c_1 \overset{(2)}{\Psi}{}^{(\nu'\mu')} , \tag{13}$$

where

$$|\,c_0\,|^2 + |\,c_1\,|^2 = 1, \qquad c_1 \sim 0$$

and if the mixture belongs to a stationary state of lower excitation of the H-atom then $\Psi^{(\mu\nu)}$ ceases to be stationary and the avalanche starts which was described in paper [1].

Because of the orthogonality of the states (provided that state ν', μ' causing the perturbation does not occur among the components of Ψ) the radiation interaction is confined largely to the perturbed terms only.

The current density of the perturbed states has an amplitude proportional to

$$\Sigma \Psi^{(\nu\mu)*} I \Psi^{(\nu\mu)} , \tag{14}$$

where

$$I = \sum_{n=1}^{!N} I^{(n)} \tag{15}$$

is the current operator; $I^{(n)}$ gives the current density of the n-th electron. From (10) we see that the current of an electron is proportional to $(1/\sqrt{N})^2 = 1/N$ on account of the factor of normalization. On the other hand the current has N coherent components arising from the components of the operator I. Thus the total electron current contains the factor $N\,1/N = 1$ and thus reduces to that obtained in the two-body treatment.

The avalanche started by the perturbation (13) produces that $\Psi^{(\nu\mu)} \to \Psi^{(\nu'\mu')}$ and the radiation process is much the same in the two-body treatment of the problem.

The total number of photons emitted is proportional to the number of components of Ψ containing excited states. Thus the emission takes place in much the same was as to be expected for independent excited atoms enclosed in the box.

In spite of this property of the wave function thus obtained, we think that the state of the ensemble of N atoms which is realized in nature is given by a different type of function.

Another type of wave function

Although the emission of photons can thus be interpreted in terms of wave functions of the form given by (12), we do not think it likely that the wave function of this form represents the ensemble of N atoms correctly. The difficulty with the above wave function is that it represents a non stationary state of such peculiar configuration that without perturbation it emits no radiation. Such a state must be supposed to be rather unstable not only with respect of the emission of photons caused by the excited H-atoms — but also with respect to thermal radiation.

To demonstrate this point we can construct a wave function Ψ with the help of a two body wave function which does not correspond to a stationary state. The latter wave function Ψ is itself not stationary — but in general it contains oscillating current densities and thus emits radiation. If the en-

semble of atoms described by the latter wave function is enclosed into a box and the box is not transparent for the radiation, a configuration builds up which corresponds to a state of equilibrium of the atoms reacting with their own radiation field.

The wave function (12), (13), (14) represents thus the peculiar state where the whole of the energy of the gas appears in the form of kinetic energy and excitation energy. An alternate wave function built up of non stationary states gives a configuration where the energy is divided between kinetic energy and radiation energy. One expects in the states realized in nature to have equipartition of energy and thus one expects that states are realized which are built up of non stationary two body wave functions.

A wave function Ψ which represents fluctuating densities and currents is obtained from two body functions of the form (12) putting

$$\overset{(2)}{\Psi} = \frac{1}{\sqrt{N}} \sum_{\nu,\mu} c_{\nu\mu} \overset{(2)}{\Psi}{}^{(\nu\mu)}, \quad c_{\nu\mu} = e^{i\varphi_{\nu\mu}}, \tag{16}$$

further

$$\Psi_{KL} = \Psi_{KL}(r^{(1)}, r^{(2)}, t) = \overset{(2)}{\Psi}(\mathbf{r}_K^{(1)}, \mathbf{r}_L^{(2)}, t) \tag{17}$$

and

$$\Psi = \frac{1}{\sqrt{N!}} \det \Psi_{KL}. \tag{18}$$

The wave function Ψ given by (12), (16), (17), (18) contains N atomic states corresponding to the N pairs of suffices ν, μ.

The emissions of photons can be described supposing that $\overset{(2)}{\Psi}$ by a small perturbation receives a further term $c^{(0)}_{\nu'\mu'} \overset{(2)}{\Psi}{}^{(\nu\mu)}$ where

$$c^{(0)}_{\nu'\mu'} \sim 0 .$$

Suppose resonance in the manner described in [1] between the additional state and one of the original states of higher excitation energy. In this case an avalanche starts and it transforms the resonating state ν, μ into ν', μ' with amplitude $| c_{\nu'\mu'} | = 1$. Thus the emission of the photon does not change the type of the configuration.

The emission is exhausted as soon as all the excited states have transformed into lower states. If there is some unspecified perturbation which produces excited states from lower ones then photons are expected to be emitted at a steady rate.

Regarding the intensity of emission in the present case — just as in the former case the current density produced by one pair of states is proportional

to $1/N$. The total current density is the sum of currents of the N electrons; these densities have to be added, therefore the result is independent of N. The emission is thus the same as calculated in the case of one atom in [1].

We see thus that we can describe the ensemble of N atoms either by a collective wave function as given by (9), (10) and (11) or alternatively by a collective wave function given by (9), (16), (17) and (18). In both cases we expect emission of photons in the manner obtained in [1] for one H-atom only.

It seems reasonable to assume that the second type of wave function is nearer to the wave function realized in nature than the first type — since the second type describes a state in which the atoms are interacting with their own radiation field while the first type of wave function describes a rather singular state in which the energy of the system does not contain radiation energy to a noticeable extent.

So as to avoid misconceptions we note that we have merely shown that there exist $6N$ dimensional wave functions which describe states which lead to photon emission much like that considered in [1]. Furthermore, we have given an argument which indicates that the second of the two types of wave functions given above is the more likely to represent the states realized in nature. The possibility cannot be excluded, however, that the wave functions realized in nature have forms differing from both types we have discussed.

REFERENCES

1. L. JÁNOSSY, Acta Phys. Hung., **39**, 109, 1975.
2. L. JÁNOSSY, Acta Phys. Hung., **27**, 35, 1969.
   L. JÁNOSSY, Foundations of Physics, **6**, No. 3.
3. L. JÁNOSSY, Acta Phys. Hung., **37**, 355, 1974.

Acta Physica Academiae Scientiarum Hungaricae, Tomus 41 (2), pp. 79—86 (1976)

PRODUCTION AMPLITUDES IN FIFTH ORDER PERTURBATION THEORY

By

J. CUNNINGHAM

SCHOOL O MATHEMATICS AND COMPUTER SCIENCE, UNIVERSITY COLLEGE OF NORTH WALES, BANGOR, GWYNEDD, U. K.

(Received 13. V. 1976)

A decomposition of the five point single loop amplitude into a sum over four point amplitudes is studied for a variety of physical processes involving pions and nucleons derived from a $\overline{\Psi}\Psi\varphi$ interaction Lagrangian. Consequences for approximate isobar models of production amplitude are discussed.

1. Introduction

The unpleasant analytic properties of fifth order (single loop) production amplitudes are well known (COOK and TARSKI [1], LANDSHOFF and TRIEMAN [2]). In a recent paper the author [3] has suggested that the exploitation of an expansion of the five point amplitude in terms of four point amplitudes might lead to approximate production amplitudes without complex singularities. In the present paper the analytic properties of the exact fifth order amplitudes are studied for a variety of physical processes arising from a trilinear $\overline{\psi}\psi\Phi$ interaction Lagrangian.

2. Reduction formula

The five point single loop amplitude F^5 may be expressed as

$$F^5 = \Delta_5^{-1} \sum_{i=1}^{5} \delta_i F_i \,, \tag{1}$$

where

$$\Delta_5 = \begin{vmatrix} 1 & z_{12} & z_{13} & z_{14} & z_{15} \\ z_{12} & 1 & z_{23} & z_{24} & z_{25} \\ z_{13} & z_{23} & 1 & z_{34} & z_{35} \\ z_{14} & z_{24} & z_{34} & 1 & z_{45} \\ z_{15} & z_{25} & z_{35} & z_{45} & 1 \end{vmatrix} \tag{2}$$

and, e.g.

$$\delta_5 = \begin{vmatrix} \mu_1^{-1} & \mu_2^{-1} & \mu_3^{-1} & \mu_4^{-1} & \mu_5^{-1} \\ 1 & z_{12} & z_{13} & z_{14} & z_{15} \\ z_{12} & 1 & z_{23} & z_{24} & z_{25} \\ z_{13} & z_{23} & 1 & z_{34} & z_{35} \\ z_{14} & z_{24} & z_{34} & 1 & z_{45} \end{vmatrix} \tag{3}$$

the symbols being as defined in reference [3] where references to the derivation of formula (1) may be found.

3. Five point poles

The variables z_{12}, z_{23}, z_{34}, z_{45}, z_{15} are essentially related to the masses of the diagram and will be deemed to be fixed. There remain five independent variables in formula (1) and, with any four fixed, any singularity in F^5 in the complex plane associated with the fifth variable which belongs properly to the leading Landau curve can arise only from the vanishing of Δ_5. It is, therefore, a pole and as such is of little mathematical interest in the application of Cauchy's theorem to derive dispersion relations. We shall take the view that it does not really matter whether this point is real or complex and we shall accept such singularities in the construction of any integral representations.

4. Reality conditions

With a labelling of particles as in [3] we shall discuss a production process in which particles 1 and 5 collide and produce particles 2, 3 and 4. The incident energy E_1 is described by the scalar product variable s_1 or, equivalently, z_{25}; the energies E_3 and E_4 of pairs of adjacent emergent particles are described by the scalar product variables s_3 and s_4 or, equivalently, z_{24} and z_{35}. The scalar product variables s_2 and s_5 or, equivalently, z_{13} and z_{14} describe the momentum transfers T_2 and T_5. The physical values of these variables are restricted by the relations, $i = 1, 3, 4$,

$$E_i : s_i \geq (M_i + M_{i-1})^2 \tag{4a}$$

or

$$z_{i-1,\,i+1} \leq \frac{\mu_{i+1}^2 + \mu_{i-1}^2 - (M_i + M_{i-1})^2}{2\mu_{i+1}\mu_{i-1}}\,, \tag{4b}$$

and, $i = 2, 5$,

$$T_i : s_i \leq (M_i - M_{i-1})^2 \tag{5a}$$

or

$$z_{i-1,\, i+1} \geq \frac{\mu_{i+1}^2 + \mu_{i-1}^2 - (M_i - M_{i-1})^2}{2\mu_{i+1}\mu_{i-1}}\,, \tag{5b}$$

where, as indicated in [3], the μ_i and M_i are respectively the internal and external mass values. We now rewrite Eqs. (1) in the form

$$\begin{aligned} \Delta_5 F^5 = {} & \delta_1 F_1(E_1, E_3, E_4) + \delta_2 F_2(T_2, E_4, T_5) + \\ & + \delta_3 F_3(E_3, T_5, E_1) + \delta_4 F_4(E_4, E_1, T_2) + \delta_5 F_5(T_5, T_2, E_3). \end{aligned} \tag{6}$$

Since we are going to treat interactions deriving from an interaction Lagrangian $\bar{\psi}\psi\Phi$, at each vertex in each diagram two nucleon (mass M) and one pion (mass μ) lines meet; both the stability conditions on the external masses as on the internal masses of F^5 are automatically guaranteed.

We shall now indicate the reasoning behind the results described in Sections 5 and 6 by considering the example of the pseudo amplitude $F_1(E_1, E_3, E_4)$. Similar arguments may be applied to the other pseudo amplitudes and hence to F^5.

Consider first the problem of writing a dispersion relation for F_1 in the variable E_1. As indicated in [3] complex singularities will arise from three point contracted diagrams unless

$$-1 \leq z_{24} \leq 1 \tag{7}$$

and

$$-1 \leq z_{35} \leq 1. \tag{8}$$

This means that to avoid complex singularities the scalar product variables s_3 and s_4 must be restricted to the ranges

$$(\mu_2 - \mu_4)^2 \leq s_3 \leq (\mu_2 + \mu_4)^2 \tag{9}$$

and

$$(\mu_3 - \mu_5)^2 \leq s_4 \leq (\mu_3 + \mu_5)^2\,. \tag{10}$$

Because of (4a) the physical regions of the variables s_3 and s_4 are

$$s_3 \geq (M_2 + M_3)^2 \tag{11}$$

and

$$s_4 \geq (M_3 + M_4)^2\,. \tag{12}$$

Thus (7) and (8) are possible only if

$$\mu_2 + \mu_4 \geq M_2 + M_3 \tag{13}$$

and

$$\mu_3 + \mu_5 \geq M_3 + M_4 . \tag{14}$$

In order to avoid complex singularities arising from four point contracted diagrams it is necessary that

$$\begin{aligned}&(1 - z_{23}^2 - z_{24}^2 - z_{34}^2 + 2z_{23}z_{24}z_{34})\\ &(1 - z_{34}^2 - z_{35}^2 - z_{45}^2 + 2z_{34}z_{35}z_{45}) \geq 0 .\end{aligned} \tag{15}$$

If secondly we wish to consider writing a dispersion relation for F_1 in the variable E_3 the restrictions necessary to avoid complex singularities are

$$-1 \leq z_{25} \leq 1 \tag{16}$$

together with

$$\begin{aligned}&(1 - z_{35}^2 - z_{35}^2 - z_{45}^2 + 2z_{34}z_{35}z_{45})\\ &(1 - z_{23}^2 - z_{25}^2 - z_{35}^2 + 2z_{23}z_{25}z_{35}) \geq 0 .\end{aligned} \tag{17}$$

Finally the restrictions needed to avoid complex singularities of F_1 in the variable E_4 are

$$-1 \leq z_{25} \leq 1 \tag{18}$$

together with

$$\begin{aligned}&(1 - z_{24}^2 - z_{25}^2 - z_{45}^2 + 2z_{24}z_{25}z_{45})\\ &(1 - z_{23}^2 - z_{24}^2 - z_{34}^2 + 2z_{23}z_{24}z_{34}) \geq 0 .\end{aligned} \tag{19}$$

We remark that conditions (16) and (18) are identical and that (17) and (19) may always be satisfied by chosing s_4 and s_3 respectively sufficiently large; this latter result is true because s_1 is bounded by condition (16) or (18).

5. Physical processes

Analyses of the type indicated above have been applied to the following processes:

(a) $$\pi\pi \to \pi\pi\pi$$

for which, for all $i = 1, 2, 3, 4, 5$

$$M_i = \mu$$
$$\mu_i = M$$

(b) $$N\bar{N} \to \pi\pi\pi$$

for which, for $i \neq 1, 5$,

$$M_i = \mu$$

and, for $i \neq 1$,

$$\mu_i = M$$

with $$M_1 = M_5 = M,\ \mu_1 = \mu$$

(c) $$\pi N \to \pi\pi N$$

for which, for $i \neq 4, 5$,

$$M_i = \mu$$

and, for $i \neq 5$,

$$\mu_i = M$$

with $$M_4 = M_5 = M,\ \mu_5 = \mu.$$

The results are tabulated in Tables I, II and III. The three point conditions are both necessary and sufficient to avoid complex branch points. The four point conditions (namely $|s|$ sufficiently large which we have abbreviated in the tables to $s \sim \pm\infty$) on the other hand are not necessary, merely sufficient.

Table I

$\pi\pi \to \pi\pi\pi$

Amplitude	E_1	E_3	E_4
F_1	$4\mu^2 \leq s_3 \leq 4M^2$ $4\mu^2 \leq s_4 \leq 4M^2$	$4\mu^2 \leq s_1 \leq 4M^2$ $s_4 \sim \infty$	$4\mu^2 \leq s_1 \leq 4M^2$ $s_3 \sim \infty$
F_2	—	—	$s_2 = 0$ $s_5 \sim -\infty$
F_3	$4\mu^2 \leq s_3 \leq 4M^2$ $s_5 \sim -\infty$	$4\mu^2 \leq s_1 \leq 4M^2$ $s_5 = 0$	—
F_4	$4\mu^2 \leq s_4 \leq 4M^2$ $s_2 \sim -\infty$		$4\mu^2 \leq s_1 \leq 4M^2$ $s_2 = 0$
F_5	—	$s_2 \sim -\infty$ $s_5 = 0$	
F^5	$4\mu^2 \leq s_3, s_4 \leq 4M^2$ $s_2, s_5 \sim -\infty$	$4\mu^2 \leq s_1 \leq 4M^2$ $s_2 \sim -\infty,\ s_4 \sim \infty$ $s_5 = 0$	$4\mu^2 \leq s_1 \leq 4M^2$ $s_2 = 0,\ s_3 \sim \infty$ $s_5 \sim -\infty$

Table II

$N\bar{N} \to \pi\pi\pi$

Amplitude	E_1	E_3	E_4
F_1	$4\mu^2 \leq s_3 \leq 4M^2$ $4\mu^2 \leq s_4 \leq 4M^2$	$s_1 = 4M^2$ $s_4 \sim \infty$	$s_1 = 4M^2$ $s_3 \sim \infty$
F_2	—	—	$s_2 = (M-\mu)^2$ $s_5 \sim -\infty$
F_3	$4\mu^2 \leq s_3 \leq 4M^2$ $s_5 \sim -\infty$	$s_1 = 4M^2$ $s_5 = (M-\mu)^2$	—
F_4	$4\mu^2 \leq s_4 \leq 4M^2$ $s_2 \sim -\infty$	—	$s_1 = 4M^2$ $s_2 = (M-\mu)^2$
F_5	—	$s_5 = (M-\mu)^2$ $s_2 \sim -\infty$	—
F^5	$4\mu^2 \leq s_3, s_4 \leq 4M^2$ $s_2, s_5 \sim -\infty$	$s_1 = 4M^2, s_2 \sim -\infty$ $s_4 \sim \infty, s_5 = (M-\mu)^2$	$s_1 = 4M^2, s_2 = (M-\mu)^2$ $s_3 \sim \infty, s_5 \sim -\infty$

Table III

$\pi N \to \pi\pi N$

Amplitude	E_1	E_3	E_4
F_1	$4\mu^2 \leq s_3 \leq 4M^2$ $s_4 = (M+\mu)^2$	$s_1 = (M+\mu)^2$ $s_4 \sim \infty$	$s_1 = (M+\mu)^2$ $s_3 \sim \infty$
F_2	—	—	$s_2 = 0$ $s_5 \sim -\infty$
F_3	$4\mu^2 \leq s_3 \leq 4M^2$ $s_5 \sim -\infty$	$s_1 = (M+\mu)^2$ $s_5 = 0$	—
F_4	$s_4 = (M+\mu)^2$ $s_5 \sim -\infty$	—	$s_1 = (M+\mu)^2$ $s_2 = 0$
F_5	—	$s_2 \sim -\infty$ $s_5 = 0$	—
F^5	$4\mu^2 \leq s_3 \leq 4M^2$ $s_2, s_5 \sim -\infty$ $s_4 = (M+\mu)^2$	$s_1 = (M+\mu)^2$ $s_2 \sim -\infty, s_4 \sim \infty$ $s_5 = 0$	$s_1 = (M+\mu)^2$ $s_2 = 0, s_3 \sim \infty$ $s_5 \sim -\infty$

Taking the example of the process $\pi\pi \to \pi\pi\pi$ Table I tells us that dispersion relations in the variable E_1 will not be complicated by complex contours provided that

(i) the emergent energies E_3 and E_4 are restricted to lie below two nucleonic masses, i.e. s_3, $s_4 \leq 4M^2$,

(ii) the momentum transfer variables s_2 and s_5 are restricted to sufficiently large negative values.

6. Isobar models

In conclusion we illustrate the use of these results in the discussion of approximate amplitudes suggested by [3].

First of all we shall suppose that the particles 2 and 3 in the final state are in a $\pi\pi$ resonance and that conditions are such that this configuration dominates the amplitude. We are therefore dealing with an approximate amplitude in which

$$\delta_1 F_1 + \delta_2 F_2 + \delta_4 F_4 + \delta_5 F_5 = 0\,, \tag{20}$$

so that

$$\Delta_5 F^5 = \delta_3 F_3\,. \tag{21}$$

The Tables now imply that dispersion relations in E_1 uncomplicated by complex contours of integration should be possible provided

(i) the $\pi\pi$ resonance has a mass lying between 2μ and $2M$ (say between 270 MeV and 1880 MeV)

(ii) the momentum transfer variable s_5 is sufficiently large and negative.

Secondly we shall suppose that the process is dominated by a final state resonance of the particles 3 and 4. We are now dealing with an approximation in which

$$\delta_1 F_1 + \delta_2 F_2 + \delta_3 F_3 + \delta_5 F_5 = 0\,, \tag{22}$$

so that

$$\Delta_5 F^5 = \delta_4 F_4\,. \tag{23}$$

The Tables now imply that dispersion relations in E_1 uncomplicated by integrations over complex contours are possible when

(i) for processes (a) and (b) the $\pi\pi$ resonance has a mass, as before, lying between 2μ and $2M$ while for process (c) the πN resonance has precisely the mass value $M + \mu$ (say 1075 MeV)

(ii) the momentum transfer variable s_2 is sufficiently large and negative.

Finally if we treat an approximation scheme in which

$$\delta_1 F_1 + \delta_2 F_2 + \delta_5 F_5 = 0\,, \tag{24}$$

so that

$$\Delta_5 F^5 = \delta_3 F_3 + \delta_4 F_4\,, \tag{25}$$

we are demanding that physically in the processes $\pi\pi \to \pi\pi\pi$ and $N\bar{N} \to \pi\pi\pi$ the final states are dominated by $\pi\pi$ resonances in the mass range 270 MeV to 1880 MeV while both momentum transfer variables s_2 and s_5 are large and negative. Various $\pi\pi$ resonances are observed in the stated energy range. Turning, however, to the process $\pi N \to \pi\pi N$ we are requiring dominance of the final state by a $\pi\pi$ resonance in the above range and a πN resonance with a mass value of about 1075 MeV. The lowest lying known resonance of this latter type is the N' (1470) with a mass value of 1435 MeV to 1505 MeV and a width of 165 MeV to 400 MeV.

7. Conclusion

Our calculations suggest that single variable dispersion relations for production amplitudes without complex integration contours may have some limited validity.

For approximation schemes (based on isobar models) for processes such as $\pi\pi \to \pi\pi\pi$ and $N\bar{N} \to \pi\pi\pi$ it seems evident that there is some chance that single variable dispersion relations without complex contours will be valid as long as one or both the E_3 and E_4 final state resonances are dominant. On the other hand while one may be hopeful of making a similar conclusion for $\pi N + \pi\pi\pi$ amplitudes when a $\pi\pi$ final state resonance is dominant one cannot be too hopeful about avoiding complex contours when πN resonances play a significant role.

REFERENCES

1. L. F. Cook and J. Tarski, J. Math. Phys., **3**, 1, 1962.
2. P. V. Landshoff and S. B. Trieman, Nuovo Cimento, **19**, 1249, 1961.
3. J. Cunningham, Acta Phys. Hung., **36**, 401, 1974.

Acta Physica Academiae Scientiarum Hungaricae, Tomus 41 (2), pp. 87—93 (1976)

ON THE GRAVITATIONAL FIELD OF A CHARGED PARTICLE

By

SHRI RAM and J. N. S. KASHYAP

DEPARTMENT OF MATHEMATICS, BANARAS HINDU UNIVERSITY, VARANASI 221005, INDIA

(Received 20. V. 1976)

In this paper the most general spherically symmetric metric, recently defined by SYNGE in Kruskal coordinates, is considered and Einstein—Maxwell equations are imposed which culminates in a prescription for building the most general solutions. The Reissner — Nordström solution is shown to be a special case.

1. Introduction

The most general spherically symmetric space-time is defined by the metric [1]:

$$ds^2 = -2f du dv + r^2(d\theta^2 + \sin^2\theta d\varphi^2)\,, \tag{1.1}$$

where f and r are functions of (u, v). The space-time V_4 is the product of a unit sphere S_2 and a 2-space U_2 in the sense that an event of V_4 corresponds to an ordered pair of points, one on S_2 and the other on U_2. The usual polar coordinates (θ, Φ) belong to S_2 and the coordinates (u, v) are taken on U_2. The minus sign before the first term is of no particular significance but merely a notational convenience. In the 2-space U_2 the lines $u =$ constant, $v =$ constant are zero. The indicial notation for u, θ, Φ and v is

$$x^1 = u, \quad x^2 = \theta, \quad x^3 = \varphi, \quad x^4 = v\,. \tag{1.2}$$

For the line-element (1.1) SYNGE [1] imposed Einstein field equations in vacuo, which culminates in a prescription for building the most general functions f and r. The Kruskal's form of Schwarzschild solution has been shown to be a special case.

In this paper we impose Einstein—Maxwell equations for the space-time characterized by (1.1). A functional relationship between the functions f and r is obtained from which many solutions may be obtained under suitable initial conditions. The Reissner—Nordström solution is found to be a special case. In particular, when the electromagnetic field is absent, we have some results obtained by SYNGE in free space.

2. Field equations

For the metric (1.1) the non-vanishing components of Ricci tensor, R_{ij}, are

$$\begin{aligned} R_{11} &= \frac{2}{r}(r_{11} - r_1 f_1/f)\,, \\ R_{22} &= -1 - \frac{2}{f}(r r_{14} + r_1 r_4), \quad R_{33} = \sin^2\theta \cdot R_{22}\,, \\ R_{44} &= \frac{2}{r}(r_{44} - r_4 f_4/f)\,, \\ R_{14} &= \frac{1}{f}(f_{14} - f_1 f_4/f) + 2 r_1 r_4/r\,. \end{aligned} \tag{2.1}$$

The scalar curvature R is given by

$$R = \frac{2 f_1 f_4}{f_1} - \frac{2 f_{14}}{f^2} - \frac{8 r_{14}}{f r} - \frac{4 r_1 r_4}{f r^2} - \frac{2}{r^2}\,, \tag{2.2}$$

where

$$f_1 = \partial f/\partial u,\ f_{14} = \partial^2 f/\partial u \partial v,\ \text{etc.}$$

We consider here the Einstein—Maxwell field equations in absence of charge-current which are [2]

$$\begin{aligned} R_{ij} &= C E_{ij}\,, \\ (\sqrt{-g}\, F^{ij})_{,j} &= 0\,, \\ F_{[ij,\,k]} &= 0\,, \end{aligned} \tag{2.3}$$

where $C = -8\pi G$, G being the gravitational constant and F_{ij} and E_{ij} are the electromagnetic field and energy tensors, respectively, defined as

$$F_{ij} = \Phi_{i,\,j} - \Phi_{j,\,i}\,, \tag{2.4}$$

$$E_{ij} = -F_{ia} F^a_j + \frac{1}{4} g_{ij} F_{ab} F^{ab}\,. \tag{2.5}$$

Here comma and square bracket denote ordinary differentitaion and anti-symmetrization, respectively.

If we take the electromagnetic 4-potential vector Φ_i as

$$\Phi_i = (0, 0, 0, -K) \tag{2.6}$$

the only non-vanishing component of F_{ij} is F_{14}, given by

$$F_{14} = K_{,1}\,, \qquad F^{14} = -K_{,1}/f^2\,. \tag{2.7}$$

Now, from (2.3), (2.6) and (2.7) we get

$$F_{14} = f\varepsilon/r^2\,, \qquad F^{14} = -\varepsilon/fr^2\,, \tag{2.8}$$

where ε is an arbitrary constant which exhibits the electromagnetic property.

From (2.5) and (2.8) the surviving components of E_{ij} are

$$E_{14} = f\varepsilon^2/2r^4\,, \qquad E_{22} = -\varepsilon^2/2r^4\,, \qquad E_{33} = \sin^2\theta \cdot E_{22}\,. \tag{2.9}$$

Therefore, the field equation (2.3) takes the form

$$r_{11} - r_1 f_1/f = 0\,, \tag{2.10}$$

$$r_{44} - r_4 f_4/f = 0\,, \tag{2.11}$$

$$1 + \frac{2}{f}(rr_{14} + r_1 r_4) = \frac{1}{2}C\varepsilon^2/r^2\,, \tag{2.12}$$

$$\frac{1}{f}(f_{14} - f_1 f_4/f) + \frac{2r_{14}}{r} = -\frac{1}{2}Cf\varepsilon^2/r^4\,. \tag{2.13}$$

From the field equations (2.10) and (2.11) we obtain after integration

$$f = 2B(v)r_1\,, \qquad f = 2A(u)r_4\,, \tag{2.14}$$

where A and B are arbitrary functions of integration. In view of (2.14) the Eq. (2.12) takes the alternative forms:

$$(rr_1)_4 = A\left(\frac{\lambda^2}{r^2} - 1\right)r_4\,, \tag{2.15}$$

$$(rr_4)_1 = B\left(\frac{\lambda^2}{r^2} - 1\right)r_1\,, \tag{2.16}$$

where $\lambda^2 = 1/2\,C\varepsilon^2$. These equations, after integration, provide

$$r_1 = \frac{D}{r} - A\left(1 + \frac{\lambda^2}{r^2}\right)\,, \tag{2.17}$$

$$r_4 = \frac{F}{r} - B\left(1 + \frac{\lambda^2}{r^2}\right)\,, \tag{2.18}$$

where $D[\equiv D(u)]$ and $F[\equiv F(v)]$ are functions of integrations. Differentiating (2.17) and (2.18) with respect to v and u, respectively, and using (2.14) in the derivatives so obtained, we get $D/A = F/B$. Here the left hand side and the right hand side are, respectively, the functions of u and v only, so that there exists a constant k such that

$$D = kA\,, \qquad F = kB\,. \tag{2.19}$$

Substitution of (2.18) in (2.17) and (2.18) gives

$$r_1 = -A\left(1 - \frac{k}{r} + \frac{\lambda^2}{r^2}\right), \tag{2.20}$$

$$r_4 = -B\left(1 - \frac{k}{r} + \frac{\lambda^2}{r^2}\right). \tag{2.21}$$

Putting the value of either r_1 or r_4 from (2.20) and (2.21) in (2.14) we get

$$f = -2AB\left(1 - \frac{k}{r} + \frac{\lambda^2}{r^2}\right). \tag{2.22}$$

Making use of the Eqs. (2.20), (2.21) and (2.22) it is found that Eq. (2.13) is identically satisfied. Thus the problem reduces to the solution of the Eqs. (2.20), (2.21) and (2.22).

We know that

$$\mathrm{d}r = r_1 \mathrm{d}u + r_4 \mathrm{d}v\,, \tag{2.23}$$

which, after using (2.17) and (2.18) gives

$$\frac{r^2 \mathrm{d}r}{r^2 - kr + \lambda^2} = -A\mathrm{d}u - B\mathrm{d}v\,. \tag{2.24}$$

Though the equation (2.24) is integrable, however, to get rid of the tw o constants k and λ setting

$$z = r/k\,, \qquad P(u) = A/k\,, \qquad Q(v) = B/k\,, \qquad \mu = \lambda/k \tag{2.25}$$

in (2.24) we obtain

$$\frac{Z^2 \mathrm{d}Z}{Z^2 - Z + u^2} = -P\mathrm{d}u - Q\mathrm{d}v\,. \tag{2.26}$$

3. Functional relationship

If we relate Z to a real variable H by the differential equation

$$\frac{Z^2 dZ}{Z^2 - Z + \mu^2} = \frac{H dH}{H^2 - \mu^2} \tag{3.1}$$

the Eq. (2.26) provides

$$\frac{H dH}{H^2 - \mu^2} = -P du - Q dv \,. \tag{3.2}$$

All solutions of Eq. (3.1) are comprised in the functional relationship

$$(H^2 - \mu^2)^{1/2} = b(Z^2 - Z + \mu^2)^{1/2} \left[\frac{\left(Z - \frac{1}{2}\right) - \left(\frac{1}{4} - \mu^2\right)^{1/2}}{\left(Z - \frac{1}{2}\right) + \left(\frac{1}{4} - \mu^2\right)^{1/2}} \right] \cdot e^{\frac{\frac{1}{2} - \mu^2}{2\left(\frac{1}{4} - \mu^2\right)^{1/2}}} \tag{3.3}$$

with b as a real constant.

Eq. (3.2) has a solution of the form

$$H^2 - \mu^2 = U^2 V^2 \,, \tag{3.4}$$

where U and V are arbitrary functions of u and v, respectively. Eq. (3.4) after differentiation gives

$$H H_1 = V^2 U U_1 \,, \qquad H H_4 = U^2 V V_4 \,. \tag{3.5}$$

Further, from (3.2) we get

$$-P = \frac{H H_1}{H^2 - \mu^2}, \qquad -Q = \frac{H H_4}{H^2 - \mu^2} \,. \tag{3.6}$$

Therefore, from (3.4), (3.5) and (3.6) we have

$$-P = U_1/U, \qquad -Q = V_4/V \,. \tag{3.7}$$

Also, from Eq. (3.1) we have

$$Z_1 = Z^{-2}(Z^2 - Z + \mu^2) \frac{H H_1}{Z^2 - \mu^2} \,, \tag{3.8}$$

$$Z_4 = Z^{-2}(Z^2 - Z + \mu^2) \frac{H H_4}{H^2 - \mu^2} \,. \tag{3.9}$$

Similarly from (2.22), (2.25) and (3.6) a simple straightforward calculation provides the expression for the function f as

$$f = -2k^2Z^{-2}(Z^2 - Z + \mu^2)\frac{H^2H_1H_4}{(H^2 - \mu^2)^2} . \tag{3.10}$$

Hence for the metric (1.2) compatible with electromagnetic field equations we have

$$r^2 = k^2Z^2,$$

where Z is determined from (3.3) in terms of the function H given by (3.4) and the constant b so that r^2 comes out as a function of (u, v). Consequently the function f can be written in a number of equivalent forms as a function of (u, v). In the next Section we shall obtain the Reissner—Nordström solution in a specific coordinate system. Since the constant of integration b appearing in (3.3) can be absorbed into H we shall take, hereafter, $b = 1$.

4. The Reissner—Nordström solution

On account of (3.7) the Eq. (2.26) becomes

$$\frac{\mathrm{d}U}{U} + \frac{\mathrm{d}V}{V} = \frac{Z^2\mathrm{d}Z}{Z^2 - Z + \mu^2} . \tag{4.1}$$

Also Eq. (2.22) gives

$$f = -2AB\left(1 - \frac{k}{r} + \frac{\lambda^2}{r^2}\right) = -2k^2\frac{U_1V_4}{UV} \cdot \frac{Z^2 - Z + \mu^2}{Z^2} . \tag{4.2}$$

Hence

$$-2f\mathrm{d}u\mathrm{d}v = 4k^2\frac{\mathrm{d}U\mathrm{d}V}{UV} \cdot \frac{Z^2 - Z + \mu^2}{Z^2} . \tag{4.3}$$

Define τ by

$$\frac{-\mathrm{d}U}{U} + \frac{\mathrm{d}V}{V} = \mathrm{d}\tau, \qquad \text{or} \qquad \tau = \log\left(\frac{U}{V}\right) + \text{constant} . \tag{4.4}$$

Then using (4.1) and (5.4), the Eq. (4.3) becomes

$$-2f\mathrm{d}u\mathrm{d}v = k^2\frac{Z^2 - Z + u^2}{Z^2}\left[\left(\frac{Z^2\mathrm{d}Z}{Z^2 - Z + \mu^2}\right)^2 - (\mathrm{d}\tau)^2\right] . \tag{4.5}$$

Therefore, the metric form (1.1) reduces to

$$ds^2 = \left(1 - \frac{k}{r} + \frac{\lambda^2}{r^2}\right)^{-1} dr^2 + r^2(d\theta^2 + \sin^2\theta d\varphi^2) - \left(1 - \frac{k}{r} + \frac{\lambda^2}{r^2}\right) dt^2 , \quad (4.6)$$

where $t = k\tau$.

The line-element (4.6) is the Reissner—Nordström solution for the gravitational field of a charged particle at rest. If $\varepsilon = 0$, one gets the Schwarzschild solution. If k happens to be negative, then it is the gravitational field of a charged particle with negative mass.

*

The authors are thankful to Dr. K. P. SINGH for valuable discussions.

REFERENCES

1. J. L. SYNGE, Annali di Matematica pura ed applicata series IV **98**, 239, 1974.
2. A. S. EDDINGTON, The Mathematical Theory of Relativity, Cambridge, 1954.

Acta Physica Academiae Scientiarum Hungaricae, Tomus 41 (2), pp. 95—105 (1976)

HEAT TRANSFER IN TWO-PHASE LAMINAR FLOW IN A CHANNEL

By

S. N. DUBE and C. L. SHARMA

DEPARTMENT OF MATHEMATICS, HIMACHAL PRADESH UNIVERSITY, SIMLA-5, INDIA

(Received 17. IV. 1976)

Exact solutions of the transient forced convection energy equations of dust particles and of liquid in a channel bounded by two parallel flat plates are obtained in the present investigation when the inlet temperatures vary sinusoidally with time and an interpretation of the case of laminar flows is given.

Nomenclature

$\bar{T}_p$	temperature of dust particle
$\bar{T}$	temperature of liquid
c_p	specific heat of dust particle
c	specific heat of liquid
h	half distance between parallel plates
K_p	thermal conductivity of dust particle
K	thermal conductivity of liquid
$\bar{t}$	time
u_p	velocity of dust particle in $\bar{x}$-direction
u	velocity of liquid in $\bar{x}$-direction
$\bar{u}$	average velocity
x, y	cartesian coordinates ($\bar{x}$: flow direction, $\bar{y}$: distance from channel centre line)
ϱ	liquid density
mN	mass of dust particle per unit volume ($= mN_0$, constant)
μ	coefficient of viscosity of liquid
ν	kinematic coefficient of viscosity
P	Prandtl number ($= \mu c/K$)
R	Reynolds number ($= h\bar{u}/\nu$)
h_p	heat transfer coefficient for flow over dust particle
A_p	surface area of dust particle
V_p	volume of dust particle
T_w	constant wall temperature

The meaning of any other symbols is given in the text as they occur.

1. Introduction

Heat transfer by gas-dust suspensions in pipe flow has been a subject of many studies because of the anticipated large heat-transfer coefficient due to the high volumetric specific heat of dust particles or liquid droplets compared to a gas and the demand for high heat transfer coefficient in gas-cooled reactors. Based on the experimental observations on gas-dust suspensions by FARBAR

and MORLEY [1] and SCHLUDERBERG [2], by JOHNSON [3] on gas suspensions of liquid droplets, and by SALOMONE and NEWMANN [4] on liquid-dust suspensions, TIEN [5, 6] has analysed the heat transfer by a gas-dust suspension in turbulent pipe flow based on a simplified model. In solutions of the transient forced convection energy equations of dust particles and of liquid in a circular pipe, SOO [7] has assumed that the inlet temperatures of dust particles and of liquid are constants across the flow with a specified constant wall temperature.

In the present investigation, exact solutions of the transient forced convection energy equations of dust particles and of liquid with fully developed flow in a parallel plate channel are obtained under prescribed boundary conditions when the inlet temperatures of dust particles and of liquid vary sinusoidally with time and an interpretation of the case of laminar flows is given.

2. Formulation of the problem

We consider the steady laminar flow of a dusty viscous liquid with uniform distribution of dust particles in a parallel plate channel whose sides are separated by distance $2h$. The dust particles and the liquid entering the channel have temperatures which are spatially uniform across the entrance section but vary sinusoidally with time. Therefore we can write the inlet conditions as

$$\bar{T}_p(0, \bar{y}, \bar{t}) = T_0 + (\Delta T)_0 \sin \bar{\omega}\bar{t} \,, \tag{2.1}$$

$$\bar{T}(0, \bar{y}, \bar{t}) = T_0 + (\Delta T)_0 \sin \bar{\omega}\bar{t} \,, \tag{2.2}$$

where T_0 is the cycle mean temperature, $(\Delta T)_0$ is the amplitude and $\bar{\omega}$ is the inlet frequency.

To obtain the heat-transfer performance and the temperatures of dust particles and of liquid it is necessary to set down two energy equations, one for the dust particles and one for the liquid-dust mixture. They are given as

$$\frac{\partial \bar{T}_p}{\partial \bar{t}} + u_p \frac{\partial \bar{T}_p}{\partial \bar{x}} = G(\bar{T} - \bar{T}_p) \,, \tag{2.3}$$

$$\frac{\partial \bar{T}}{\partial \bar{t}} + u \frac{\partial \bar{T}}{\partial \bar{x}} + \frac{mN_0 c_p}{\varrho c}\left(\frac{\partial \bar{T}_p}{\partial \bar{t}} + u_p \frac{\partial \bar{T}_p}{\partial \bar{x}}\right) = \frac{\nu}{P}\frac{\partial^2 \bar{T}}{\partial \bar{y}^2} + \beta_2(\bar{T}_p - \bar{T}) \,, \tag{2.4}$$

where

$$G = \frac{h_p A_p}{mN_0 c_p V_p} \,, \qquad \beta_2 = \frac{mN_0 c_p G}{\varrho c} \,.$$

Simplifying (2.4), we get

$$\frac{\partial \bar{T}}{\partial \bar{t}} + u\frac{\partial \bar{T}}{\partial \bar{x}} = \frac{\nu}{P}\frac{\partial^2 \bar{T}}{\partial \bar{y}^2} + 2\beta_2(\bar{T}_p - \bar{T}) \ . \tag{2.5}$$

The inlet and the boundary conditions of the problem are as follows:

$$\bar{T}_p = T_0 + (\Delta T)_0 \sin \omega \bar{t} \qquad \text{when} \qquad \bar{x} = 0 \ , \tag{2.6}$$

$$\bar{T} = T_0 + (\Delta T)_0 \sin \omega \bar{t} \qquad \text{when} \qquad \bar{x} = 0 \ , \tag{2.7}$$

$$\left(\frac{\partial \bar{T}_p}{\partial \bar{y}}\right)_{\bar{y}=0} = 0 \ , \quad \left(\frac{\partial \bar{T}}{\partial \bar{y}}\right)_{\bar{y}=0} = 0 \ , \quad \bar{T}_p = T_w \ , \quad \bar{T} = T_w \quad \text{at} \quad \bar{y} = h \ , \tag{2.8}$$

$$\bar{t} > 0 \ .$$

The system satisfying (2.3), (2.5) is subjected to the following restrictions (Soo [7]):

(i) Radiation effect is neglected.
(ii) The density of liquid remains constant; thus the velocity distribution is independent of the temperature distribution.
(iii) Liquid property variations are neglected.
(iv) Each dust particle is small and maintains uniform temperature due to its high thermal conductivity K_p.
(v) The liquid and dust particle cloud have similar velocity profiles. The presence of dust particles does not affect the liquid velocity profile.
(vi) The dust particles are uniformly distributed throughout the channel.
(vii) The effect of collision with the wall is neglected.
(viii) The suspension is extremely dilute such that each particle is assumed to see the wall without interference of other particles.
(ix) Fully developed laminar velocity profiles between the parallel plates.
(x) Axial conduction is negligible with respect to bulk transport in the $\bar{x}$-direction. This is a reasonable assumption when Péclét number exceeds 100 [8].
(xi) Thermal resistance of the channel wall is negligible.
(xii) Eddy diffusivity of heat is negligible.

Further, to simplify the method of analysis the case of constant velocity will be considered here and for this purpose we substitute $\bar{u}(u = u_p)$ for the velocity profile in (2.3) and (2.5).

We now introduce the following non-dimensional quantities:

$$\theta = \frac{\bar{T} - T_0}{(\Delta T)_0}, \qquad \theta_p = \frac{\bar{T}_p - T_0}{(\Delta T)_0}, \qquad x = \frac{\bar{x}}{h}, \qquad y = \frac{\bar{y}}{h},$$

$$t = \frac{\nu \bar{t}}{h^2}, \qquad \theta_0 = \frac{T_w - T_0}{(\Delta T)_0}, \qquad \omega = \frac{h^2 \bar{\omega}}{\nu},$$

$$\beta_3 = \frac{h^2 G}{\nu}, \qquad \beta_4 = \frac{2h^2 \beta_2}{\nu}.$$

Equations (2.3) and (2.5) then become

$$\frac{\partial \theta_p}{\partial t} + R \frac{\partial \theta_p}{\partial x} = \beta_3 (\theta - \theta_p), \tag{2.9}$$

$$\frac{\partial \theta}{\partial t} + R \frac{\partial \theta}{\partial x} = \frac{1}{p} \frac{\partial^2 \theta}{\partial y^2} + \beta_4 (\theta_p - \theta). \tag{2.10}$$

The inlet and the boundary conditions reduce to

$$\theta_p = \sin \omega t \quad \text{when} \quad x = 0, \tag{2.11}$$

$$\theta = \sin \omega t \quad \text{when} \quad x = 0, \tag{2.12}$$

$$\left(\frac{\partial \theta_p}{\partial y}\right)_{y=0} = 0, \quad \left(\frac{\partial \theta}{\partial y}\right)_{y=0} = 0, \quad \theta_p = \theta_0, \quad \theta = \theta_0, \quad \text{at} \quad y = 1, \quad t > 0. \tag{2.13}$$

3. Solution

The foregoing problem can be separated into two as follows:

$$\theta_p(x, y, t) = \theta_{p1}(x, y) + \theta_{p2}(x, y, t), \tag{3.1}$$

$$\theta(x, y, t) = \theta_1(x, y) + \theta_2(x, y, t), \tag{3.2}$$

where θ_1, θ_2, θ_{p1} and θ_{p2} satisfy the following problems:

$$R\frac{\partial\theta_{p1}}{\partial x} = \beta_3(\theta_1 - \theta_{p1}) , \tag{3.3}$$

$$R\frac{\partial\theta_1}{\partial x} = \frac{1}{p}\frac{\partial^2\theta_1}{\partial y^2} + \beta_4(\theta_{p1} - \theta_1) , \tag{3.4}$$

$$\theta_{p1} = 0 \quad \text{when} \quad x = 0 , \tag{3.5}$$

$$\theta_1 = 0 \quad \text{when} \quad x = 0 , \tag{3.6}$$

$$\left(\frac{\partial\theta_{p1}}{\partial y}\right)_{y=0} = 0 , \quad \left(\frac{\partial\theta_1}{\partial y}\right)_{y=0} = 0 , \quad \theta_{p1} = \theta_0 , \quad \theta_1 = \theta_0 \quad \text{at} \quad y = 1 . \tag{3.7}$$

$$\frac{\partial\theta_{p2}}{\partial t} + R\frac{\partial\theta_{p2}}{\partial x} = \beta_3(\theta_2 - \theta_{p2}) , \tag{3.8}$$

$$\frac{\partial\theta_2}{\partial t} + R\frac{\partial\theta_2}{\partial x} = \frac{1}{P}\frac{\partial^2\theta_2}{\partial y^2} + \beta_4(\theta_{p2} - \theta_2) , \tag{3.9}$$

$$\theta_{p2} = \sin\omega t \quad \text{when} \quad x = 0 , \tag{3.10}$$

$$\theta_2 = \sin\omega t \quad \text{when} \quad x = 0 . \tag{3.11}$$

$$\left(\frac{\partial\theta_{p2}}{\partial y}\right)_{y=0} = 0 , \quad \left(\frac{\partial\theta_2}{\partial y}\right)_{y=0} = 0 , \quad \theta_{p2} = 0 , \quad \theta_2 = 0 , \quad \text{at} \quad y = 1 , \quad t > 0 . \tag{3.12}$$

Solving Eqs. (3.3) and (3.4) under the conditions (3.5)—(3.7), we get

$$\theta_{p1}(x, y) = \theta_0\left[1 - \frac{4}{\pi}\sum_{n=0}^{\infty}\frac{(-1)^n}{(2n+1)} \cdot \cos\left(\frac{2n+1}{2}\right)\pi y \cdot \frac{\lambda_n e^{-\mu_n x} - \mu_n e^{-\lambda_n x}}{(\lambda_n - \mu_n)}\right] ,$$

$$\theta_1(x, y) = \theta_0\left[1 - \frac{4}{\pi}\sum_{n=0}^{\infty}\frac{(-1)^n}{(2n+1)} \cdot \cos\left(\frac{2n+1}{2}\right)\pi y \cdot A_n(x)\right] ,$$

where

$$A_n(x) = \frac{\lambda_n}{(\lambda_n - \mu_n)}\left(1 - \frac{R\mu_n}{\beta_3}\right) e^{-\mu_n x} - \frac{\mu_n}{(\lambda_n - \mu_n)}\left(1 - \frac{R\lambda_n}{\beta_3}\right) e^{-\lambda_n x} ,$$

$$2\lambda_n = \frac{(\beta_3 + \beta_4)}{R} + \frac{(2n+1)^2\pi^2}{4PR}$$

$$+ \sqrt{\left[\frac{(\beta_3 + \beta_4)}{R} + \frac{(2n+1)^2\pi^2}{4PR}\right]^2 - \frac{(2n+1)^2\pi^2}{PR^2}\beta_3} ,$$

$$2\mu_n = \frac{(\beta_3 + \beta_4)}{R} + \frac{(2n+1)^2\pi^2}{4PR}$$

$$- \sqrt{\left[\frac{(\beta_3 + \beta_4)}{R} + \frac{(2n+1)^2\pi^2}{4PR}\right]^2 - \frac{(2n+1)^2\pi^2}{PR^2}\beta_3} .$$

In obtaining $\theta_{p2}(x, y, t)$ and $\theta_2(x, y, t)$ we define the following auxiliary problems:

$$\frac{\partial\theta'_{p2}}{\partial t} + R\frac{\partial\theta'_{p2}}{\partial x} = \beta_3(\theta'_2 - \theta'_{p2}) , \tag{3.13}$$

$$\frac{\partial\theta'_2}{\partial t} + R\frac{\partial\theta'_2}{\partial x} = \frac{1}{P}\frac{\partial^2\theta'_2}{\partial y^2} + \beta_4(\theta'_{p2} - \theta'_2) , \tag{3.14}$$

$$\theta'_{p2} = \cos\omega t \quad \text{when} \quad x = 0, \tag{3.15}$$

$$\theta'_2 = \cos\omega t \quad \text{when} \quad x = 0, \tag{3.16}$$

$$\left(\frac{\partial\theta'_{p2}}{\partial y}\right)_{y=0} = 0 , \quad \left(\frac{\partial\theta'_2}{\partial y}\right)_{y=0} = 0 , \quad \theta'_{p2} = 0 , \quad \theta'_2 = 0 , \quad \text{at} \quad y = 1 . \tag{3.17}$$

Here we note that the auxiliary problems are similar to the original problems for θ_{p2} and θ_2 except that the periodic condition is shifted by $\pi/2$.

Let us define new temperature functions $\theta_{pc}(x, y, t)$ and $\theta_c(x, y, t)$ such that

$$\theta_{pc} = \theta'_{p2} + i\theta_{p2} , \tag{3.18}$$

$$\theta_c = \theta'_2 + i\theta_2 , \tag{3.19}$$

then the problems given by (3.8)—(3.12) and (3.13)—(3.17) can be combined to give the following problems:

$$\frac{\partial \theta_{pc}}{\partial t} + R\frac{\partial \theta_{pc}}{\partial x} = \beta_3(\theta_c - \theta_{pc}) , \tag{3.20}$$

$$\frac{\partial \theta_c}{\partial t} + R\frac{\partial \theta_c}{\partial x} = \frac{1}{P}\frac{\partial^2 \theta_c}{\partial y^2} + \beta_4(\theta_{pc} - \theta_c) , \tag{3.21}$$

$$\theta_{pc} = e^{i\omega t} \quad \text{when} \quad x = 0 , \tag{3.22}$$

$$\theta_c = e^{i\omega t} \quad \text{when} \quad x = 0 , \tag{3.23}$$

$$\left(\frac{\partial \theta_{pc}}{\partial y}\right)_{y=0} = 0 , \quad \left(\frac{\partial \theta_c}{\partial y}\right)_{y=0} = 0 , \quad \theta_{pc} = 0, \quad \theta_c = 0 , \quad \text{at} \quad y = 1 , \quad t > 0. \tag{3.24}$$

We now assume periodic solutions of the following types:

$$\theta_{pc}(x, y, t) = e^{i\omega t} \quad \Psi(x, y) , \tag{3.25}$$

$$\theta_c(x, y, t) = e^{i\omega t} \quad \Phi(x, y) , \tag{3.26}$$

where the new temperature functions Ψ and Φ satisfy the following problems:

$$i\omega\psi + R\frac{\partial \psi}{\partial x} = \beta_3(\Phi - \psi) , \tag{3.27}$$

$$i\omega\Phi + R\frac{\partial \Phi}{\partial x} = \frac{1}{P}\frac{\partial^2 \Phi}{\partial y^2} + \beta_4(\psi - \Phi) , \tag{3.28}$$

$$\Psi = 1 , \quad \Phi = 1 \quad \text{when} \quad x = 0 , \tag{3.29}$$

$$\left(\frac{\partial \Psi}{\partial y}\right)_{y=0} = 0 , \quad \left(\frac{\partial \Phi}{\partial y}\right)_{y=0} = 0 , \quad \Psi = 0 , \quad \Phi = 0 \quad \text{at} \quad y = 1 . \tag{3.30}$$

Solving Eqs. (3.27) and (3.28) under the conditions (3.29) and (3.30), we get finally

$$\theta_{p2}(x, y, t) = \frac{4}{\pi}\sin\left(\omega t - \frac{\omega}{R}x\right) \cdot \sum_{n=0}^{\infty}\frac{(-1)^n}{(2n+1)} \cdot \cos\left(\frac{2n+1}{2}\right)\pi y \cdot B_n(x) ,$$

$$\theta_2(x, y, t) = \frac{4}{\pi}\sin\left(\omega t - \frac{\omega}{R}x\right) \cdot \sum_{n=0}^{\infty}\frac{(-1)^n}{(2n+1)} \cdot \cos\left(\frac{2n+1}{2}\right)\pi y \cdot A_n(x) ,$$

where

$$B_n(x) = \frac{(\pi_n e^{-\mu_n x} - \mu_n e^{-\lambda_n x})}{(\lambda_n - \mu_n)} .$$

4. Discussion

When the boundary condition on the wall for $\theta_p(x, y, t)$ and $\theta(x, y, t)$ is homogeneous, that is, when θ_0 is zero, then

$$\theta_p(x, y, t) = \theta_{p2}(x, y, t) , \tag{4.1}$$

$$\theta(x, y, t) = \theta_2(x, y, t) . \tag{4.2}$$

$\theta_{p2}(x, y, t)$ and $\theta_2(x, y, t)$ show that the temperatures of dust particles and of liquid decay exponentially along the channel.

For a single-phase system the number of dust particles per unit volume is zero (and so $\beta_4 = 0$). Hence

$$\theta_s(x,y,t) = \frac{4}{\pi} \sin\left(\omega t - \frac{\omega}{R} x\right) \cdot \sum_{n=0}^{\infty} \frac{(-1)^n}{(2n+1)} \cdot \cos\left(\frac{2n+1}{2}\right) \pi y \cdot C_n(x) , \tag{4.3}$$

where

$$C_n(x) = \exp\left[- \frac{(2n+1)^2 \pi^2}{4PR} x \right]$$

and the boundary condition on the wall is homogeneous.

In many applications heat transfer in regions away from the inlet is of interest; for such situations only the first terms in the series (4.1), (4.2) and (4.3) need to be considered. Hence

$$\theta_p(x, y, t) = \frac{4}{\pi} \sin\left(\omega t - \frac{\omega}{R} x\right) \cdot \cos\left(\frac{\pi y}{2}\right) \cdot B_0(x) , \tag{4.4}$$

$$\theta(x, y, t) = \frac{4}{\pi} \sin\left(\omega t - \frac{\omega}{R} x\right) \cdot \cos\left(\frac{\pi y}{2}\right) \cdot A_0(x) , \tag{4.5}$$

$$\theta_s(x, y, t) = \frac{4}{\pi} \sin\left(\omega t - \frac{\omega}{R} x\right) \cdot \cos\left(\frac{\pi y}{2}\right) \cdot C_0(x) , \tag{4.6}$$

where

$$B_0(x) = \frac{(\lambda_0 e^{-\mu_0 x} - \mu e^{-\lambda_0 x})}{(\lambda_0 - \mu_0)},$$

$$A_0(x) = \frac{\lambda_0}{(\lambda_0 - \mu_0)}\left(1 - \frac{R\mu_0}{\beta_3}\right)e^{-\mu_0 x} - \frac{\mu_0}{(\lambda_0 - \mu_0)}\left(1 - \frac{R\lambda_0}{\beta_3}\right)e^{-\lambda_0 x},$$

$$C_0(x) = \exp\left(-\frac{\pi^2}{4PR}x\right),$$

$$2\lambda_0 = \left[\frac{(\beta_3 + \beta_4)}{R} + \frac{\pi^2}{4PR}\right] + \sqrt{\left[\frac{(\beta_3 + \beta_4)}{R} + \frac{\pi^2}{4PR}\right]^2 - \frac{\pi^2}{PR^2}\beta_3},$$

$$2\mu_0 = \left[\frac{(\beta_3 + \beta_4)}{R} + \frac{\pi^2}{4PR}\right] - \sqrt{\left[\frac{(\beta_3 + \beta_4)}{R} + \frac{\pi^2}{4PR}\right]^2 - \frac{\pi^2}{PR^2}\beta_3}.$$

The temperatures at any y, say $y = 0$, are given by

$$\theta_p(x, 0, t) = \frac{4}{\pi}\sin\left(\omega t - \frac{\omega}{R}x\right) \cdot a_p, \tag{4.7}$$

$$\theta(x, 0, t) = \frac{4}{\pi}\sin\left(\omega t - \frac{\omega}{R}x\right) \cdot a, \tag{4.8}$$

$$\theta_s(x, 0, t) = \frac{4}{\pi}\sin\left(\omega t - \frac{\omega}{R}x\right) \cdot a_s, \tag{4.9}$$

where $a_p = B_0(x)$, $a = A_0(x)$, $a_s = C_0(x)$ denote amplitudes of dust particle, liquid-dust mixture and clean liquid (single-phase system), respectively.

Table I

Comparison of the amplitudes for

$$P = 0.73, \quad \beta_3 = 10^5, \quad \frac{\beta_4}{\beta_3} = 0.5, \quad R = 13\,000$$

amplitudes \ x	5	10	15	20	25
a_p	0.99902	0.99802	0.99702	0.99602	0.99502
a	0.99898	0.99798	0.99698	0.99598	0.99498
a_s	0.99870	0.99740	0.99610	0.99480	0.99350

Table II

Comparison of the amplitudes for

$$P = 0.73\,,\quad \beta_3 = 10^5\,,\quad \frac{\beta_4}{\beta_3} = 0.5\,,\quad R = 20\,000$$

amplitudes \ x	5	10	15	20	25
a_p	0.9994499	0.9988849	0.9983199	0.9977549	0.9971899
a	0.9994270	0.9988620	0.9982970	0.9977320	0.9971670
a_s	0.9991550	0.9983100	0.9974650	0.9966200	0.9957750

Table III

Comparison of the amplitudes for

$$P = 0.73\,,\quad \frac{\beta_4}{\beta_3} = 0.5\,,\quad R = 20\,000\,,\quad \beta_3 = 10^9$$

amplitudes \ x	5	10	15	20	25
a_p	0.9994351	0.9988701	0.9983051	0.9977401	0.9971751
a	0.9994350	0.9988700	0.9983050	0.9977400	0.9971750
a_s	0.9991550	0.9983100	0.9974650	0.9946200	0.9957750

Table IV

Comparison of the amplitudes for

$$P = 0.73\,,\quad R = 25\,000\,,\quad \beta_3 = 10^5\,,\quad \frac{\beta_4}{\beta_3} = 0.5$$

amplitudes \ x	5	10	15	20	25
a_p	0.99959	0.99914	0.99869	0.99825	0.99780
a	0.99958	0.99913	0.99868	0.99823	0.99778
a_s	0.99933	0.99865	0.99798	0.99730	0.99663

We observe the following important points:

(a) From Tables I, II and IV it is obvious that the amplitudes a_p, a, a_s increase with the increase of R and

$$a_p > a > a_s\,. \tag{4.10}$$

Table V

Comparison of the amplitudes for

$$P = 0{,}73\,, \quad R = 25\,000\,, \quad \beta_3 = 10^5\,, \quad \frac{\beta_4}{\beta_3} = 0{,}9$$

amplitudes \ x	5	10	15	20	25
a_p	0.99967	0.99933	0.99899	0.99875	0.99831
a	0.99965	0.99931	0.99897	0.99873	0.99829
a_s	0.99933	0.99865	0.99798	0.99730	0.99663

(b) Tables II and III show that a_p decreases with the increase of β_3 (and so β_4), but a increases. Also

$$a_p > a > a_s$$

holds (at least for values of P, β_4/β_3, R and β_3 considered here).

(c) From Tables IV and V we infer that the amplitudes a_p and a increase with the increase of β_4/β_3 and

$$a_p > a > a_s\,.$$

Thus, the effect of dust particle is to flatten the temperature profile and, consequently, to increase the heat transfer.

Equations (4.1), (4.2) and (4.3) suggest that the phase lags are the same for both two-phase and single-phase systems and is a limit due to the nature of the model. Also, as the inlet frequency is increased, phase lag increases and as the Reynolds number R is increased, the phase lag decreases.

REFERENCES

1. L. FARBAR and M. J. MORLEY, Ind. Eng. Chem., **49,** 1143, 1957.
2. D. C. SCHLUDERBERG, The Application of Gas-Ceramic Mixtures to Nuclear Power, Rept. No. CF 55-8-199 ORSORT, AEC, 1955.
3. H. A. JOHNSON, Trans. ASME, **77,** 1257, 1955.
4. J. J. SALOMONE and N. NEWMANN, Ind. Eng Chem. **47,** 283, 1955.
5. C. L. TIEN, Transport Processes in Two-Phase Turbulent Flow, Ph. D. thesis, Princeton University, U.S.A., 1959.
6. C. L. TIEN, Trans. ASME, **83C,** 183, 1961.
7. S. L. SOO, Fluid Dynamics of Multiphase Systems, Blaisdell Publishing Co., London, 1967.
8. P. J. SCHNEIDER, Trans. ASME, **79,** 765, 1957.

Acta Physica Academiae Scientiarum Hungaricae, Tomus 41 (2), pp. 107—123 (1976)

ON THE AB INITIO CRYSTAL ORBITAL METHOD*

By

M. KERTÉSZ

CENTRAL RESEARCH INSTITUTE FOR CHEMISTRY OF THE HUNGARIAN ACADEMY OF SCIENCES, 1525 BUDAPEST

(Received 18. VI. 1976)

A new computer realization of the LCAO Hartree—Fock crystal orbital method using contracted Gaussian orbitals is reported. All integrals over the atomic orbitals are calculated explicitly within a finite interaction range. No approximation with respect to exchange is used. The spin-unrestricted Hartree—Fock-type crystal orbital formalism has been programmed, too. Both programs are limited to quasi one-dimensional systems at present, provide nevertheless a useful tool for the theoretical investigation of the electronic structure of simple polymers and one-dimensional models of solids. Basic information on both programs is documented.

Some numerical aspects, especially the convergency properties of the methods with respect to the number of grid points in the Brillouin zone, the shape of the Fermi surface in the special case of partly filled bands, the starting density matrices in the self-consistent field iteration procedure and the size of the finite interaction range taken into account are discussed. The specific problem of the starting density matrices in the unrestricted HF case are also dealt with. Finally comparison is made with semi-empirical calculations.

1. Introduction

The linear combination of atomic orbitals (LCAO) Hartree—Fock (HF) molecular orbital (MO) as well as crystal orbital (CO) methods appear nowadays well established calculational tools for the investigation of the electronic structure of molecules and solids, respectively. A number of physical observables can be estimated well even from approximate HF wave functions (especially one-particle properties) while others await correlation corrections. Thus it is easy to understand that a large effort has been devoted to the calculation of the LCAO HF CO-s (and energy bands) of many systems. It is not the aim of the present work to review this field, we refer to two review papers only, covering part of the actual calculations [1]. From the methodological point of view these calculations are either semi-empirical using usually one of the integral approximation schemes of the approximate quantum chemical MO methods or are of nonempirical nature. The latter are often termed *ab initio* but use in fact in the majority of cases some kind of approximation scheme [2] for the integrals over the atomic orbitals (AO-s) entering in the LCAO CO formalism. In this paper we shall use the term *ab initio* (in close

* This work was partly performed at the Structural Chemistry Department, B. Kidric Chemical Institute, University of Ljubljana, and supported by the Kidric Fund (Yugoslavia).

analogy to the practice of molecular quantum chemistry) for those schemes only in which all integrals over AO-s are explicitly evaluated (in most cases within a finite neighbour's range of an arbitrary elementary cell). Only very few strictly *ab initio* CO calculations as far as the integrals are concerned have been performed on three dimensional (3-D) solids [3], however, they did not use the standard LCAO HF CO method. The applications to one D (1-D) systems are scarce, too [4—10]. For obvious reasons 1-D systems are much easier to investigate, and therefore in this paper we shall deal mainly with 1-D systems.

It is evident that accurate *ab initio* restricted HF LCAO energy bands are necessary for the improvement and justification of the above mentioned semi-empirical and approximate non-empirical methods. Furthermore, they seem to provide a natural starting point to account for electronic correlation effects (see e.g. [11]).

Another closely related variational method is the spin-unrestricted Hartree—Fock (UFH) method of POPLE, NESBET and BERTHIER [12]. Using different (spatial) orbitals for different spins (DODS, see e.g. [13]) in a one-determinantal many-electron wave-function the UHF method permits one to account for part of the correlation energy. The application of the UHF method to solids [13, 14] seems to be especially attractive as an antiferromagnetic spin structure can be described with it [15]. The DODS method has several different versions (see e.g. [14]) but its full variational form, the UHF CO method, being a straightforward generalization of its restricted form can be applied to solids [10, 16, 17] with comparable efforts to the restricted HF method.

The aim of this paper is to report on a new realization of the *ab initio* restricted HF method (applicable to both strongly and weakly bonded chains), the first realization of the *ab initio* UHF method both restricted to 1-D systems as well as to discuss some convergency properties of the HF CO methods in question.

2. Method of calculation

The equations for the CO coefficients in the restricted HF method are well known [18]. For the spin-unrestricted HF case the corresponding equations are quite similar [16], the difference is only the exchange polarization term [13] in the Fock operator. For the sake of completeness we sketch here an alternative simple derivation [19] of the UHF CO equations (for the general, 3-D, case) by using Bloch function formalism as opposed to the block diagonalization method of BICZÓ et al [16].

We start from a one-determinantal DODS wave function for n_α and n_β electrons with spins α and β, respectively, in each elementary cell which can

be given by using Born—Kármán periodic boundary conditions (N elementary cells being within the Born—Kármán boundaries) as

$$\begin{aligned}\Psi_{\mathrm{DODS}} = \hat{\mathcal{A}}\{&a_{1,k_1}(1)\,\alpha(1)a_{1,k_2}(2)\,\alpha(2)\ldots\\ &\ldots a_{1,k_N}(N)\,\alpha(N)a_{2,k_1}(N+1)\,\alpha(N+1)\ldots a_{2,k_N}(2N)\,\alpha(2N)\ldots\\ &\ldots a_{n_\alpha,k_N}(N\cdot n_\alpha)\,\alpha(N\cdot n_\alpha)\,b_{1,k_1}(N\cdot n+1)\,\beta(N\cdot n+1)\ldots\\ &\ldots b_{n_\beta,k_N}(N\cdot n^*)\,\beta(N\cdot n^*)\}\,.\end{aligned} \tag{1}$$

Here $\hat{\mathcal{A}}$ is the normalized antisymmetrizer, $n^* = n_\alpha + n_\beta$, k_i $(i = 1, 2, \ldots, N)$ are reciprocal wave vectors from the first Brillouin zone (BZ) and the Bloch functions $c_{n,k}(r)$ ($c = a$ and b stand for the orbitals with spins α and β, respectively) are defined in the LCAO form as

$$c_{n,k}(r) = \frac{1}{\sqrt{N}} \sum_R \sum_{\mu=1}^{m} e^{ikR} C_{n,\mu}(k)\,\chi_\mu(r-R)\,, \tag{2}$$

where $\chi_\mu(r)$, $(\mu = 1, 2, \ldots, m)$ are the AO-s in the reference cell, the $C_{n,\mu}(k)$-s are the expansion coefficients of the Bloch functions $a_{n,k}$ and $b_{n,k}$ for spins α and β, respectively. If not specified otherwise, the summations over lattice vectors R are extended over all the lattice points within the Born—Kármán boundaries.

If the number of electrons with different spins in the unit cell is different, the Ψ_{DODS} gives the approximate description of a ferromagnetic state. If, however $n_\alpha = n_\beta$ Ψ_{DODS} corresponds to an antiferromagnetic state [15].* A well-known drawback of the Ψ_{DODS} wave function is that it is not an eigenfunction [13] of the total spin operator. For large systems, however, as proved by UKRAINSKY [20] the energetic properties are not influenced by the presence of the non-singlet components in Ψ_{DODS} [21].

We use the well known Born—Oppenheimer electronic Hamiltonian without nuclear-nuclear repulsion for the system of $N \cdot n^*$ electrons present in N elementary cells (atomic units are used throughout)

$$\hat{H} = -\frac{1}{2}\sum_{i=1}^{N\cdot n^*} \Delta_i - \sum_{i=1}^{N\cdot n^*}\sum_I \frac{Z_I}{|r_i - X_I|} + \sum_{i>j}^{N\cdot n^*} \frac{1}{|r_i - r_j|}\,, \tag{3}$$

where Z_I is the I-th nuclear charge which is in the position X_I. The summation over I is to be extended over all nuclei. Using wave function (1) and the Hamiltonian (3) the variational principle leads to the POPLE—NESBET—

* For sake of simplicity we consider in this paper only this specific case, but neither the UHF CO method nor our programs imply this limitation.

BERTHIER equations [12] for the orbitals

$$\hat{H}^{\sigma}(1)\, c_i(1) = \epsilon_i^{\sigma} c_i(1) \qquad (c_i = a_i \text{ and } b_i \text{ if } \sigma = \alpha \text{ and } \beta\text{, respectively}) \tag{4}$$

where i stands for the pair of quantum numbers n and k, i.e. it labels the electron levels in the whole system of N elementary cells. The Fockian is as usual

$$\hat{H}^{\sigma}(1) = -\frac{1}{2}\Delta_1 - \sum_J \frac{Z_J}{|r_1 - X_J|} + \sum_i^{occ.} (\hat{J}_i - \hat{K}_i^{\sigma}) , \tag{5}$$

with the definition of the Coulomb and exchange operators $\hat{J}_i$ and $\hat{K}_i^{\sigma}$

$$\begin{aligned} \hat{J}_i(1)\,\varphi(1) &= \int \mathrm{d}^3 r \frac{a_i^*(r)\, a_i(r)}{|r - r_1|}\varphi(1) + \int \mathrm{d}^3 r \frac{b_i^*(r)\, b_i(r)}{|r - r_1|}\varphi(1) , \\ \hat{K}_i^{\sigma}(1)\,(1) &= \int \mathrm{d}^3 r \frac{c_i^*(r)\,\varphi(r)}{|r - r_1|} c_i(r_1) \end{aligned} \tag{6}$$

and the summation over i in (5) extends over all the occupied orbital indices.

Starting from the above UHF MO equations one can simply get the UHF CO equations by substituting the Bloch form (2) of the orbitals into (4)—(6). Then the practically manageable LCAO form can be obtained formally by multiplying from left by $\chi_\nu^*(r_1)$ and integrating over $\mathrm{d}^3 r_1$. We write here down the result in an $m \times m$ matrix form (it is of course identical with that of the alternative derivation of BICZÓ et al. [16])

$$\mathbf{H}^{\sigma}(k)\, C_n(k) = \epsilon_n^{\sigma}(k)\, \mathbf{S}(k)\, C_n(k) \qquad (n = 1, 2, \ldots, m) , \tag{7}$$

where* the "k dependent Fock and overlap matrices" are

$$\mathbf{H}(k) = \sum_R^M e^{ikR}\mathbf{H}(R) \qquad \text{and} \qquad \mathbf{S}(k) = \sum_R^M e^{ikR}\mathbf{S}(R) . \tag{8}$$

In the course of the derivation of the equations (7, 8) use is made of the translational symmetry of the system. The elements of the matrices $\mathbf{H}(R)$ and

* The upper limit M indicates that the summations are practically to be extended over finite (M-th) neighbour's interactions only. M should be infinite in principle, but in this paper we restrict ourselves to the finite (M-th) neighbour interaction scheme. It is to be noted that the "interaction domain" must be chosen according to the symmetry of the system [22]. To be consistent, the finite neighbour's approximation must be applied to the nuclear-nuclear repulsion, too.

$\mathbf{S}(R)$ are defined as follows.*

$$h_{\nu\mu}(R) = \left\langle \begin{matrix} 0 \\ \nu \end{matrix} \middle| -\frac{1}{2}\Delta \middle| \begin{matrix} R \\ \mu \end{matrix} \right\rangle - \sum_{I}^{M} \left\langle \begin{matrix} 0 \\ \nu \end{matrix} \middle| \frac{Z_I}{|X_I - r|} \middle| \begin{matrix} R \\ \mu \end{matrix} \right\rangle,$$

$$H^{\sigma}_{\nu\mu}(R) = h_{\nu\mu}(R) + \sum_{R_1 R_2}^{M} \sum_{\gamma\delta} \left\{ [D^{\alpha}_{\gamma\delta}(R_2 - R_1) + D^{\beta}_{\gamma\delta}(R_2 - R_1)] \right. \tag{9}$$

$$\left. \left\langle \begin{matrix} 0 & R \\ \nu & \mu \end{matrix} \middle| \begin{matrix} R_1 & R_2 \\ \delta & \gamma \end{matrix} \right\rangle - D^{\sigma}_{\gamma\delta}(R_2 - R_1) \left\langle \begin{matrix} 0 & R_2 \\ \nu & \gamma \end{matrix} \middle| \begin{matrix} R_1 & R \\ \delta & \mu \end{matrix} \right\rangle \right\},$$

with the following definition of the density matrix elements

$$D^{\sigma}_{\gamma\delta}(R) = \frac{1}{N} \sum_{k}^{occ.} \sum_{n}^{occ.} e^{ikR} C^{*}_{n,\gamma}(k)\, C_{n,\delta}(k) \tag{10}$$

and two-electron integrals are

$$\left\langle \begin{matrix} 0 & R \\ \nu & \mu \end{matrix} \middle| \begin{matrix} R_1 & R_2 \\ \delta & \gamma \end{matrix} \right\rangle = \iint \mathrm{d}^3 r \mathrm{d}^3 r' \chi_{\gamma}(r)\, \chi^{*}_{\mu}(r - R)\, \frac{1}{|r - r'|}\, \chi_{\delta}(r' - R_1)\, \chi^{*}_{\gamma}(r' - R_2)\,. \tag{11}$$

The summation over k, as usual in solid state theory, can be transformed to an integral over the occupied part of the Brillouin zone. This completes the description of the UHF CO equations, which can be solved by the usual self-consistent field (SCF) procedure starting from suitable initial density matrix elements discussed in more detail in § 3c.

The total electronic energy per elementary cell is [16]

$$\frac{E_{el}}{N} = \frac{1}{2N} \sum_{k}^{occ.} \sum_{n}^{occ.} (\epsilon^{\alpha}_{n}(k) + \epsilon^{\beta}_{n}(k)) + \sum_{R}^{M} Tr\left[\mathbf{h}(R)(\mathbf{D}^{\alpha}(R) + \mathbf{D}^{\beta}(R))\right]. \tag{12}$$

As a consequence of the use of a one-determinantal variational trial wave-function, the equations derived are satisfied also by the solutions of the restricted HF equations. Trivially, if the orbitals with different spins coincide ($a_{nk}(r) = b_{nk}(r)$) the above scheme reduces to the RHF CO formalism [18] (using doubly occupied spatial orbitals).

* $|\, R/\mu \,\rangle$ is the μ-th atomic orbital in the elementary cell with lattice vector R.

3. Computational aspects

3.1. Some characteristics of the computer program

Both the above RHF CO equations as well as the analogous UHF ones have been programmed on a CDC 6400 computer. (We have named these two programs BLOCH and UBLOCH, respectively.) The pseudo-eigenvalue equations (7) are essentially complex [see (8)], thus we preferred for their solution the complex matrix diagonalization technique including a Cholesky-type decomposition of the overlap matrix [23] to the more time consuming transformation of the eigenvalue problem of a complex hermitian matrix into an eigenvalue problem of a real matrix of double size combined with the Löwdin orthogonalization technique used by DEL RE et al [18] and ANDRÉ et al [4].

The most crucial point was the choice of the basis set and that of the method of integration over the AO-s. Taking the AO-s as linear combinations of (primitive) Gaussian orbitals, as is well-known, all one- and two-electron integrals can be evaluated analytically. Making the resctriction that the exponents of the primitive Gaussians be equal one can considerably reduce the necessary computer time [24] without decreasing the flexibility of the basis set too much.

For the calculation of the necessary integrals we have adapted the GAUSSIAN 70 MO program system of HEHRE et al. [24]. The following basis sets are thus permitted [25].

1. "Minimal basis set" of Slater-type orbitals (STO) expanded in terms of 2—6 Gaussians (GTO):

2. "Extended basis set", i.e. AO-s consisting of 4 GTO-s for the description of the valence shell (and 4—6 contracted GTO-s for the inner shells) permitting a better description of the valence electron polarization at minimum computational cost by contracting only the inner three primitive GTO-s in the valence part;

3. General contracted Gaussian basis set, which may be taken arbitrarily within the limitations of GAUSSIAN 70.

In the majority of the applications we used the first two basis sets in order to facilitate comparison with earlier calculations on molecules [26], where the GAUSSIAN 70 program proved to be a good compromise with regard to speed and physico-chemical reliability.

The two electron integrals (11) (the number of which is usually very large) are stored on magnetic disc together with their orbital indices having the computational advantage that zero and very small integrals need not be stored and operated upon (the threshold for considering an integral as negligible can be varied over a wide range).

For calculating the Fock matrix elements $H_{\gamma\mu}(R)$ economically it was inevitable to perform an effective classification and administration of the numerous two-electron integrals (11). Thus, in the first neighbour interaction approximation for the one-dimensional case the following types ("classes") had to be dealt with separately: (00 | 00), (10 | 00), (10 | 10), (11 | 00), (11 | 00), (10 | 11) where 0 and 1 stands for any AO in the elementary cell and its first (right) neighbour, respectively. Furthermore, it was necesary to consider also subclasses to make maximum use of the seven index-interchange symmetries of the two-electron integrals (11). For these six classes in the above order the following numbers of subclasses have been considered: 11, 5, 4, 4, 5, 2. (For the reference cell these were identical with those used in the molecular program GAUSSIAN 70.) Each integral contributes to only a few matrix elements $H_{\nu\mu}(R)$ the indices of which it was necessary to determine for each subclass separately.

We have applied our BLOCH programs to several systems: chains of hydrogen atoms with both metallic and molecular crystal type models [6, 10]; hydrogen bonded molecular chains, as hydrogen fluoride [5] and hydrogen cyanide [7]; polyene [8]; polysulfur-nitride chain [9]. The energy band structures as well as other results can be found in these papers. Here we wish to discuss in more detail some computational aspects of the CO method.

The testing of any *ab initio* program presents some technical difficulties. The BLOCH and UBLOCH programs have been tested with the following calculations.

1. In the limit of negligible intercell interactions the results of several molecular calculations have been reobtained by BLOCH and UBLOCH.

2. In the same limit the equidistant H atomic chain dissociates correctly to isolated H atoms using UBLOCH [10].

3. The RHF solution using UBLOCH was the same as that for BLOCH for several systems.

The intercell interactions represented a more difficult problem. These have been tested by the following further calculations.

4. The two electron part has been programmed separately without neither the above-mentioned classification scheme nor the use of the seven symmetry relations for the integral indices. For the same systems these two independent codings led to identical results.

5. Finite clusters of hydrogen-fluoride molecular aggregates have been considered. The total energy per unit cell tends with increasing cluster size very well towards that of the infinite periodic system as can be seen from Fig. 1.

6. A model in which an aggregate of two interacting subunits (HF molecules) is repeated periodically was considered. The distance of these aggregates was taken very large and thus the interaction among them negligible. The

results were independent of the formal choice of the elementary cell, i.e. whether the strong interaction became inter- or intracellular.

7. Results showed all required symmetry properties in all cases (provided that the starting density matrices were of correct symmetry).

For the orientation of the interested reader, we present in Table I the computer times used for the full *ab initio* energy band calculation of some selected systems. All data refer to minimal basis set calculations. (The calculations have been done in collaboration with J. KOLLER and A. AŽMAN.)

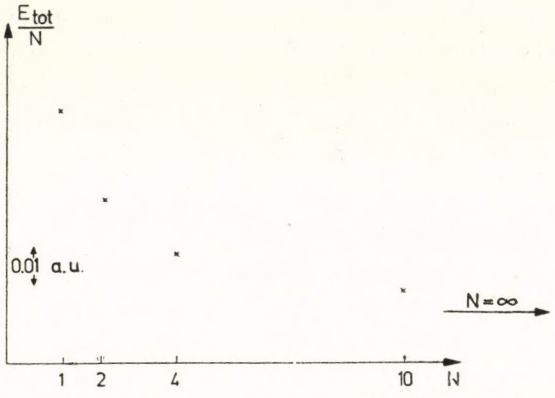

Fig. 1. Total energy per unit cell of increasing clusters of HF molecules converging towards the total energy per elementary cell of the corresponding infinite system. (N is the number of HF units.)

Table I

Computer times necessary for the performance of full *ab initio* crystal orbital calculation for some selected systems (on a CDC 6400, Cyber 70)

System	Number of K grid points in the half Brillouin zone	Number of iterations in the crystal orbital calculation	Number of included a) neighbouring atoms in the main chain b) neighbouring elementary cells	Computer times (in sec)	
				Integral evaluation and molecular calculation used to obtain starting density matrix	Crystal orbital calculation only
Hydrogen fluoride (symmetric nuclear configuration)	7	8	2 (b)	80	65
Hydrogen fluoride (asymmetric nuclear configuration)	7	8	2 (b)	90	240
	7	7	4 (b)	600	1500
Polyene	5	17	1 (a)	20	25
Polysulfur nitride	5	16	3 (a)	400	550
	9	30	2 (a)	70	510
Polyglycine	5	35	2 (a)	360	2500
	5	30	3 (a)	600	2600
Hydrogen atomic chain	61	2	3 (a, b)	120	18
	61	2	15 (a, b)	800	25

3.2. *Convergence problems*

In both methods (RHF and UHF CO) one should reach convergence, with respect to the following four characteristics:

— number of k points in the Brillouin zone (NKP) used in the numerical calculation of the integrals to which the summations in (10) and (12) are transformed;

— shape of the Fermi surface in the case of partly filled bands;

— density matrices in the SCF iteration procedure (see § 3.3 and 3.4);

— number of included neighbours (see § 4).

There is a considerable experience available from semi-empirical band calculations for the choice of NKP according to which relatively few k-points are usually sufficient. We used NKP values between 9 and 25 and in some selected cases even 61. In the majority of the applications we did not require self-consistency with respect to NKP, but on the basis of our experience we tried to choose NKP in all cases to be sufficiently large. The integrations over the BZ have been performed using Simpson's rule.

The shape of the Fermi surface is not the most serious problem for 1-D systems, though in certain cases one can have troubles. E.g. the case of polysulfur-nitride was rather delicate: several starting Fermi "surfaces" failed to lead to self-consistent solution.

3.3. *Choice of the starting density matrices*

We have observed in our *ab initio* HF calculations that usually more iteration steps are necessary than in the analogous semiempirical calculations. The choice of the starting density matrices was found, therefore, to be crucial. In several cases no or extremely slow convergence occurred if we started from the density matrices corresponding to the eigenvectors of the one-electron part of the Fockian (a Hückel-type initial guess). In this respect the following classification of the systems treated by us has proved useful.

(i) Systems consisting of weakly interacting even-electron subunits. Molecular crystals fall within this class including the more strongly interacting hydrogen bonded chains. For these systems the SCF density matrix elements of the elementary cell were used as the intracell elements of the initial density matrix while its intercell elements were taken zero. This choice produced good convergency for all systems of this class. Usually 6—10 iterations were necessary to reach convergency to $5 \cdot 10^{-5}$ in all elements of the density matrix.

(ii) Systems consisting of strongly interacting even-electron subunits. Covalently bonded systems like real regular polymers come under this class possessing elementary cells linked by chemical bonds. These systems are

usually insulators or semiconductors. The starting density is very critical for these systems. E.g. in a calculation for polyglycine using the starting density described above for molecular crystals though self consistency was reached up to $5 \cdot 10^{-3}$ after 30 iterations, the wave-function obtained turned out to be physically unrealistic (electron energy too high, atomic charges too polarized). To overcome this difficulty we propose a simple procedure to construct a better starting density matrix for systems of this class. Taking two interacting elementary cells and supplementing them by fictitious atoms (e.g. hydrogens) we obtain a chemically reasonable closed shell molecule. The density matrix elements taken from a relatively rough approximate MO calculation for this fictitious molecule provide a reasonable initial guess for the polymer. (Elements connecting the fictitious atoms with the original ones are to be omitted, of course.)

(iii) Systems with odd number of electrons in the unit cell (e.g. polymer metals). In order to obtain SCF solutions for these systems sometimes special considerations are necessary due to the combined problem of the starting density matrix and the unknown shape of the Fermi surface. There is a possibility to change both the Fermi surface and the density matrix simultaneously during the SCF iteration procedure. Alternatively, one could change the Fermi surface only after self-consistency with respect to the density has been reached. Several combinations are also possible but neither procedure is necessarily convergent. In case of polysulfur nitride the second iteration scheme led to the SCF solution starting from a Hückel type initial guess in 30 iterations with the difference $8 \cdot 10^{-5}$ in the density matrix elements in the last two steps.

3.4. *Choice of the starting density matrix in the spin-unrestricted Hartree-Fock case*

It is well known that the UHF method as applied to molecules and radicals possesses worse convergency properties than its counterpart RHF method. Especially pronounced is this difference in the case of closed shell systems where the UHF solution can be found sometimes only by the special "optimization of individual orbitals" procedure [27]. Even this method may fail to give a solution *different* from the RHF wave-function [28].

In our practice the following starting densities have been used in all semi-empirical and *ab initio*, molecular and crystal orbital calculations (essentially introducing changes of opposite signs into the diagonal elements)

$$D^{\sigma}_{\gamma\delta}(0) = \frac{1}{2} D^{\mathrm{RHF}}_{\gamma\delta}(0) \pm \delta_{\gamma\delta} l_{\gamma} ,$$

where $+$ $(-)$ stands for $\sigma = \alpha(\beta)$. $D^{\mathrm{RHF}}_{\gamma\delta}(0)$ is the SCF density matrix element of the corresponding RHF solution. The l_{γ}-s are usually subjected to

the restriction $\sum_{\gamma} l_\gamma = 0$. The values l_γ have to be chosen always according to the system forcing the orbitals with different spins to avoid each other as much as possible.

Historically it was just this important type of correlation that was attacked by the several DODS and alternant MO methods [13]. In simple alternant systems the choice $| l_\gamma | = 0.1 \ldots 1.0$ has led usually to convergency, though in some cases it was necessary to try with two or more sets of l_γ values to obtain an UHF solution. In some systems (e.g. linear polyenes) the π-electrons can easily have an alternant structure for the orbitals with different spins, but for the other electrons it may turn out not to be an easy task to find the corresponding alternating densities in order to obtain part of the correlation effect. In certain cases it is even impossible for mathematical reasons to split the orbitals for α and β spins due to the limited size of the basis set (e.g. the core electrons in a minimal basis set calculation).

4. Convergency with respect to the number of neighbours

The finite neighbour's interaction approximation is perhaps the most problematic approximation used in the SCF CO methods in question. This problem is mentioned in almost all papers in this field (see e.g. EUWEMA et al

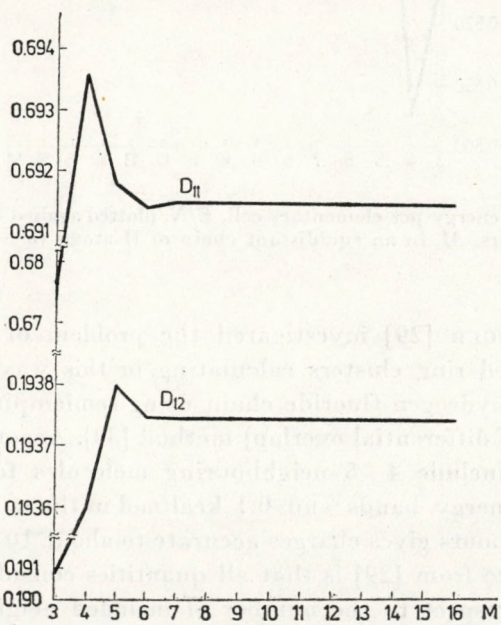

Fig. 2. Density matrix elements D_{11} and D_{12} as function of the number of included neighbours, M, in an equidistant chain of H atoms. (Distance of first neighbours, $a = 1.88$ a.u.)

[2], ANDRÉ et al [4]), but to the author's knowledge a detailed *ab initio* study of this problem is still lacking.

A completely different approach is that of HARRIS and MONKHORST and KUMAR [3] using a modified type of Bloch functions (modulated plane waves) in order to overcome the difficult problem of the evaluation of the multicentre integrals, and the problem of distant neighbours, but their wave function is not of the standard LCAO HF CO type.

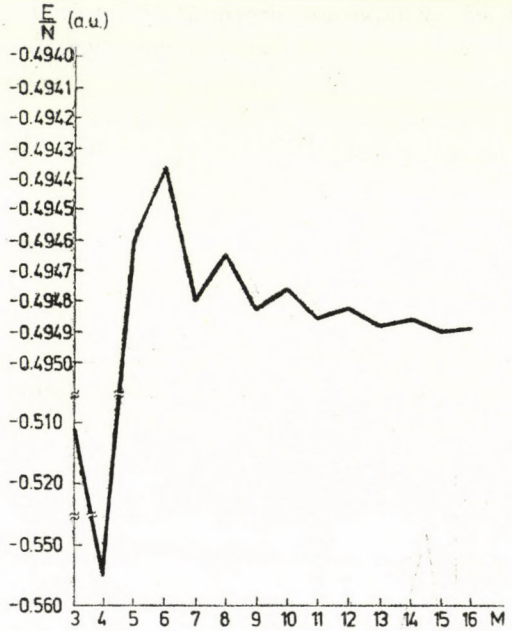

Fig. 3. Total electronic energy per elementary cell, E/N, plotted against the number of included neighbours, M, in an equidistant chain of H atoms ($a = 1.88$ a.u.)

Recently ZUNGER [29] investigated the problem of finite neighbours interaction on closed ring clusters calculating in this way the approximate energy bands of a hydrogen fluoride chain using semiempircial INDO (intermeditate neglect of differential overlap) method [30]. According to his results it was enough to include 4—5 neighbouring molecules for an accuracy of 10^{-4} a.u. in the energy bands and 0.1 kcal/mol in the cohesive energy. The inclusion of 3 neighbours gives charges accurate to about 10^{-3} e. A remarkable property one can see from [29] is that all quantities considered show smooth convergency with respect to the number of included neighbours.

On the other hand SIMMONS et al. [31] obtained rather slow and oscillating convergency for the overlap of the Bloch functions at $k = 0$ using the

usual Gaussian basis set. This convergency was highly improved by truncating the AO-s after 2—4 a.u.

In order to obtain some insight into the convergency properties of the spin restricted SCF CO method we performed a series of *ab initio* energy band calculations on a linear metallic-type chain of H-atoms with nearest neighbour distances of 1.88 a.u. This distance has been found [6] energetically most stable for this system and can therefore be considered as a not-too-weakly

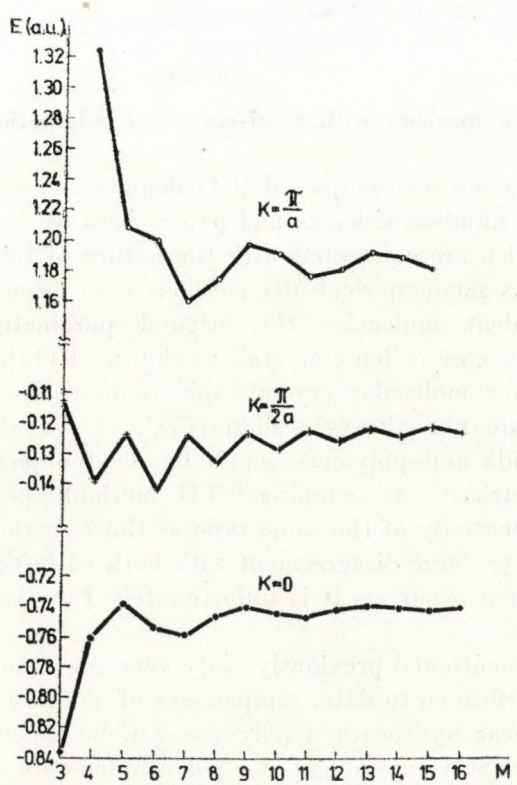

Fig. 4. Three selected energy levels in the H atomic chain, $a = 1.88$ a.u., $E(K = 0)$, $E(K = \pi/2a)$ and $E(K = \pi/a)$ illustrating the behaviour of the energy band (bottom, Fermi level and top) as function of the number of included neighbours, M

interacting model. Minimal STO-4G basis set has been used. Some of the results are represented in Figs. 2—4, where the diagonal and first off diagonal density matrix elements, D_{11} and D_{12}, respectively, total electronic energy per atom E/N and three selected energy levels ($E(K)$ values) are plotted against M, the number of included neighbours.

Considering these result it appears at once, that while the density matrix elements D_{11} and D_{12} converge very quickly the convergence of the energe-

tic quantities is worse. While the total energy changes less than 0.0005 a.u. in going from the 6-th to the 16-th neighbour's interaction, the Fermi level $E(\pi/2a)$ changes about 0.01 a.u. Thus, in general, it may be probable that using a small number of neighbours charge distributions and cohesive energies will be better than energy bands. The empty bands are more sensitive in this respect than the filled ones. This latter observation is in accordance with the experience obtained for several other systems, too. Further investigations of similar type are necessary in order to see how general are the trends found on the simple model considered here.

5. Comparison with semi-empirical calculations

Since *ab initio* and semi-empirical MO calculations have been comparatively analyzed in a number of books and papers here we wish to sketch only some problems which are connected with the nature of solids considered by the CO method. As semiempirical MO methods have been parametrized for the case of covalent molecules the original parametrizations lead to wrong results in the case of ionic crystals as shown in [32]. Moreover, it was found that even for molecular crystals the unmodified semiempirical MO parametrizations are not always realistic [33].

Covalent solids and polymers would be ideal objects for the use of "molecular-parametrized" semiempirical CO methods as the interactions in the solid are essentially of the same type as those in the molecules. Even in this case, however, large disagreement with both *ab initio* calculations and experiment can often occur, as it is unfortunately the case for many molecules, too.

As we have mentioned previously, only very few true *ab initio* calculations have been performed to date, comparisons of *ab initio* and semiemprical results for two linear hydrocarbon polymers can be found in [34, 35]. (In [35] the results of ESCA experiments for polyethylene are interpreted on the basis of different CO calculations.) The general trend found in these comparative studies was that the forbidden gap in the CNDO/2 method is too large, while in the extended Hückel (EH, [35]) method it is too small as compared with the corresponding *ab initio* results. (This is in accordance with the tendencies found for the difference of the orbital energies of the highest occupied and lowest empty levels of molecules.) The improved CNDO/SW (Sichel—Whitehead [36]) method gave centres of gravity of the bands more similar to *ab initio* than the original CNDO/2. (It is to be noted that the EH method, being not an SCF one, fails for strongly polarized systems.) Other parametrizations considered in the above comparisons gave smaller gaps than *ab initio*. The results of SAMO (simulated *ab initio* MO [34]) method agree rather well

with the *ab initio* results for polyethylene in the first cell approximation, but the discrepancy with the second neighbour approximation may indicate the failure of the SAMO method as applied to solids.

A rather close qualitative agreement between the *ab initio* and CNDO/2 results has been found recently [5] for a hydrogen fluoride chain with respect to both the energy band schemes and cohesion energies. It is worth noting that both in these calculations on hydrogen fluoride chain and in our recent *ab initio* band calculation for hydrogen cyanide chains [7] some possible proton positions have been considered and of these the most stable nuclear configuration was the experimentally observed one. (For the latter system no semiempirical work is known to the author.) Recently we have published energy bands of polysulfur nitride [9], too. The *ab initio* and CNDO/2 bands show a similar qualitative pattern but there are considerable quantitative differences. The *ab initio* charge distribution seems to be, however, much more reasonable as expected and with respect to stability problems the *ab initio* method is superior to both EH and CNDO/2 [37].

We feel that work is still to be done in order to have more confidence in applying semiempirical quantum chemical parametrizations of CO methods to solid-state calculations especially for van der Waals crystals. For these problems *ab initio* results are in need to have a basis of comparisons.

6. Concluding remarks

The *ab initio* crystal method can now be applied as a routine aid for the investigation of the electronic structure of simple one-dimensional systems with arbitrary type of interaction between the elementary cells in both restricted and unrestricted Hartree—Fock schemes without further approximation on exchange using contracted Gaussian basis sets.

The method may also help in improving semiempirical band calculational methods which still retain their importance due to the high expenses of *ab initio* calculations for large systems. Another promising methodological possibility offered by our BLOCH program would be to compare strict *ab initio* results with other approximate non-empirical schemes [2] mentioned in the Introduction.

The problem of broken-symmetry solutions is common to all Hartree—Fock schemes. The spin-unrestricted solution may break also the spatial symmetry of the one-particle wave functions by concentrating the Bloch functions with spins up and down on different sublattices. Even in the spin-restricted Hartre—Fock case one can find, as is well known, broken-symmetry solutions. In our *ab initio* treatment of the equidistant H chains [6] and polyene [8] besides the symmetric (metallic) solution also broken-symmetry (insulat-

ing) solutions with a lower energy have been found indicating the instability of the equidistant nuclear configurations.

The convergency properties of the methods have been found sometimes worse than those of analogous methods for molecules and especially for metallic type systems special convergency considerations are necessary. The convergency as function of the number of included neighbours seems to be the most problematic point in the method. A model calculation on a chain of H-atoms in this paper showed that sometimes several (at least 10), neighbours are necessary to reach even a rather moderate accuracy of ~ 0.5 eV for the energy bands.

The spin-unrestricted version of the LCAO Hartree–Fock method which includes that part of the electronic correlation which may be associated with an antiferromagnetic spin structure has convergency properties comparable to the restricted version. The correlation energy one can include is not too large (e.g. $\sim 34\%$ of the estimated correlation energy in the case of an equidistant H atomic chain [10]) but is still encouraging regarding that the spin-unrestricted HF method retains the one-particle picture.

Several applications of our *ab initio* programs BLOCH and UBLOCH described in this paper are in progress: infinite cumulene, polyacetylene, polyglycine [38], formic acid chain, homopolynucleotides, the backbone of a diacetylene polymer etc. are being studied. Work is planned to calculate correlation corrections using Wannier functions calculated from the SCF Bloch functions. Simple physical observables as dipole moments [39] and Compton profiles will be also calculated.

Acknowledgement

The author is deeply indebted to Prof. A. Ažman and Dr. J. Koller for their enthusiastic collaboration which enabled him to perform this work. His stay in Ljubljana, Yugoslavia, where the computations have been performed was made possible by the kind hospitality of Prof. D. Hadži whose interest in hydrogen bonded chains led to several investigations on these systems referred to in the text. We thank for the contribution of Prof. E. Zakrajsek to this work, who provided his fast complex matrix diagonalizer program including a Cholesky-type decomposition before publication. The author has profited very much from the discussions with Drs G. Biczó, I. Mayer and S. Suhai. Very useful conversations with Prof. P. Pulay on the integral problem of *ab initio* quantum chemistry are gratefully acknowledged.

REFERENCES

1. A. B. Kunz, in: Elementary Excitations in Solids, Molecules and Atoms, Part A, Ed. J. T. Devreese, A. B. Kunz and T. C. Collins, Plenum Press, London, 1974. p. 195; B. J. Duke, Ann. Repts. Progr. Chem. A., The Chem. Soc. **68**, 3, 1971.
2. R. N. Euwema, D. L. Wilhite and G. T. Surratt, Phys. Rev., **B7**, 818, 1973; A. B. Kunz, Phys. Rev., **B7**, 5369, 1973; L. Piela, L. Pietronero and R. Resta, Phys. Rev., **B7**, 5321, 1973 and **B9**, 5332, 1974; H. Stoll and H. Preuss, Int. J. Quant. Chem., **9**, 775, 1975; J. Delhalle, J. M. Andre, S. Delhalle, C. P. Malherbe, F. Clarisse, G. Leroy, P. Peeters, Theoret Chim. Acta (Berl) **43**, 215, 1977. L. Piela, J. Phys. C., Solid State Phys., **8**, 2606, 1975; F. E. Harris, L. Kumar and H. J. Monkhorst, Phys. Rev., **B7**, 2850, 1973.

3. L. KUMAR, H. J. MONKHORST and F. E. HARRIS, Phys. Rev., **B9**, 4084, 1974 and references therein.
4. J. M. ANDRÉ and G. LEROY, Chem. Phys. Lett., **5**, 71, 1970;
J. M. ANDRÉ and G. LEROY, Int. J. Quantum Chem., **5**, 557, 1971;
E. CLEMENTI, J. Chem. Phys., **54**, 2492, 1971.
A. KARPFEN, Thesis Vienna, 1976.
A. BLUMEN and C. MERKEL, Chem. Phys. Lett., **45**, 47, 1977.
5. M. KERTÉSZ, J. KOLLER and A. AŽMAN, Chem. Phys. Lett., **36**, 576, 1975.
6. M. KERTÉSZ, J. KOLLER and A. AŽMAN, Theoret, Chim. Acta, (Berl.), **41**, 89, 1976.
7. M. KERTÉSZ, J. KOLLER, A. AŽMAN and E. ZAKRAJSEK, Z. Naturforsch., **31a**, 637, 1976.
8. M. KERTÉSZ, J. KOLLER and A. AŽMAN, J. Chem. Phys., 1. August, 1977.
9. M. KERTÉSZ, J. KOLLER, A. AŽMAN and S. SUHAI, Phys. Lett. **A55**, 107, 1975.
10. M. KERTÉSZ, J. KOLLER and A. AŽMAN, Phys. Rev., **B14**, 76, 1976.
11. H. J. MONKHORST and J. ODDERSHEDE, Phys. Rev. Lett., **30**, 797, 1973;
S. T. PANTELIDES, D. J. MIKISH and A. B. KUNZ, Phys. Rev., **B10**, 2602, 1974;
N. E. BRENER, Phys. Rev., **B11**, 929, 1975.
12. G. BERTHIER, J. Chim. Phys., **51**, 363, 1954;
J. A. POPLE and R. K. NESBET, J. Chem. Phys., **22**, 571, 1954.
13. J. C. SLATER, Rev. Mod. Phys., **25**, 199, 1953;
P. O. LÖWDIN, J. Appl. Phys. Suppl., **33**, 251, 1962;
R. PAUNCZ, The Alternant Molecular Orbital Method, Saunder, Philadelphia, 1967.
14. J. L. CALAIS and G. SPERBER, Int. J. Quant. Chem., **7**, 501, 1973.
15. I. A. MISURKIN and A. A. OVCHINNIKOV, Mol. Phys., **27**, 237, 1974.
16. G. BICZÓ, G. DEL RE and J. LADIK, 1972, unpublished.
17. M. KERTÉSZ, J. LADIK and S. SUHAI, Acta Phys. Hung., **36**, 77, 1974.
18. G. DEL RE, J. LADIK and G. BICZÓ, Phys. Rev., **155**, 997, 1967.
19. M. KERTÉSZ, Thesis, 1971.
20. I. I. UKRAINSKY, Int. J. Quant. Chem., **6**, 473, 1972.
21. I. MAYER and M. KERTÉSZ, Int. J. Quant. Chem., **10**, 961, 1976.
22. S. F. O'SHEA and D. P. SANTRY, Chem. Phys. Lett., **25**, 169, 1974.
I. I. UKRAINSKY, Theoret. Chim. Acta (Berl.) **28**, 139, 1975.
23. E. ZAKRAJSEK, Quantum Chemistry Program Exchange, QCPE Indiana Univ., submitted.
E. ZAKRAJSEK and J. ZUPAN, Ann. Soc. Sci. Bruxelles, **89**, 337, 1975.
24. W. J. HEHRE, W. A. LATHAN, R. DITCHFIELD, M. D. NEWTON and J. A. POPLE, QCPE, Indiana Univ. No. 236.
25. W. J. HEHRE, R. F. STEWART and J. A. POPLE, J. Chem. Phys., **51**, 2657, 1969;
W. J. HEHRE, R. DITCHFIELD, R. F. STEWART and J. A. POPLE, J. Chem. Phys., **52**, 2769, 1970.
26. W. J. HEHRE and W. A. LATHAN, J. Chem. Phys. **56**, 5255, 1972, and references therein.
27. I. MAYER, Acta Phys. Hung., **34**, 83, 1973.
28. I. MAYER, Acta Phys. Hung., **39**, 133, 1975.
29. A. ZUNGER, J. Chem. Phys., **63**, 1713, 1975.
30. See e.g. I. N. LEVINE, Molecular Spectroscopy, Wiley-Interscience, 1975, pp. 73—76.
31. J. E. SIMMONS, C. C. LIN, D. F. FONQUET, E. E. LAFON and R. C. CHANEY, J. Phys. C.: Solid State Phys., **8**, 1549, 1975.
32. J. O. HEAD, K. A. R. MITCHELL and M. L. WILLIAMS, Mol. Phys., **29**, 1929, 1975.
33. J. J. KATZ, S. A. RICE, S. I. CHOI and J. JORTNER, J. Chem. Phys., **39**, 1683, 1963.
34. J. M. ANDRÉ, G. S. KAPSOMENOS and G. LEROY, Chem. Phys. Lett., **8**, 195, 1971;
B. J. DUKE and O'LEARY, Chem. Phys. Lett., **20**, 459, 1973.
D. BLOOR, Chem. Phys Lett., **40**, 323, 1976.
35. J. DELHALLE, J. M. ANDRÉ, S. DELHALLE, J. J. PIREAUX, R. CANDANO and J. J. VERBIST, J. Chem. Phys., **60**, 595, 1974.
36. J. M. SICHEL and M. A. WHITEHEAD, Theoret. Chim. Acta., (Berl.) **11**, 220, 1968.
37. M. KERTÉSZ, S. SUHAI, A. AŽMAN, D. KOCJAN and Á. I. KISS, Chem. Phys. Lett. **44**, 53, 1976.
38. M. KERTÉSZ, J. KOLLER and A. AŽMAN, Nature (London), 1977.
39. M. KERTÉSZ, J. KOLLER and A. AŽMAN, J. Mol. Struct. **36**, 366, 1977.

Acta Physica Academiae Scientiarum Hungaricae, Tomus 41 (2), pp. 125—136 (1976)

CHARACTERIZATION OF CHARGE DISTRIBUTION IN TERMS OF LOCALIZED ORBITALS

By

E. KAPUY, ZS. OZORÓCZY and C. KOZMUTZA

QUANTUM THEORY GROUP, INSTITUTE OF PHYSICS, TECHNICAL UNIVERSITY OF BUDAPEST
BUDAPEST

(Received 2. VII. 1976)

Localized orbital densities have been investigated in a series of ten-electron hydrides. It has been found that changes in the central atom nuclear charge cause systematic modifications in the localized electronic structure. The charge distributions of localized orbitals have been analyzed using their electric moments.

Introduction

The wavefunction of a closed shell system in the independent particle model is approximated by a single determinant of one-particle functions. The canonical molecular orbitals (CMO) are the solution of the pseudoeigenvalue problem: the well-known Hartree—Fock—Roothaan method uses atomic orbitals (AO) to construct the molecular ones [1].

The CMO's conform to the symmetry restrictions and they extend usually over the whole system. Even though the analysis of canonical orbitals provides information on the electronic structure of individual systems, real and actual problems in chemistry are often connected with the comparison of different molecules. The localization of electron distribution makes it possible to come closer to classical chemical concepts, investigate related molecular systems, study transferable properties and has some further advantages. Each localized molecular orbital (LMO) yields significant charge density only in distinct regions of a system. Thus one expects to use LMO's or their characteristic features determined for small systems as "starting points" in a preliminary study of related larger molecules [2, 3].

In order to investigate the localized orbitals and their characteristics systematic work has been done on a series of ten-electron systems. Ab initio molecular orbital calculations have been carried out for the ten-electron hydrides derivable from C, N, O, F and Ne using basis sets of (13s7p/4s) Gaussians contracted to [4s2p/2s]. The bond lengths and bond angles were fixed at the experimental values of the neutral species [4].

The proton affinities, the ionization potentials and the molecular dipole moments have been discussed in recent papers [5, 6, 7]. The localized orbitals

of the ten-electron systems studied have been analyzed in terms of first and second electric moments of their charge distribution [7, 8]. The first moment vector $\langle \mathbf{r} \rangle$ with the origin at the central nucleus, determines the length of the centroid of charge $\langle r \rangle$ of a localized orbital. The eigenvalues $\langle x'^2 \rangle$, $\langle y'^2 \rangle$, $\langle z'^2 \rangle$ of the second moment θ tensor can be represented by an ellipsoid with semiaxes $\langle x'^2 \rangle^{\frac{1}{2}}$, $\langle y'^2 \rangle^{\frac{1}{2}}$, $\langle z'^2 \rangle^{\frac{1}{2}}$ where the origin of the coordinate system is usually shifted onto the centre of the charge distribution [9].

The electric moments of a charge distribution can be related to the statistical moments of probability theory [8]. This mathematical background offers the possibility of using the electric moments of localized orbital densities for characterizing molecular electronic structures. Thus the mean features of the localized moments can also be used for analyzing the various types of localized orbitals.

In the present paper the systematic modifications in the electron distribution of the LMO densities caused by changes in the central atom nuclear charge are investigated. The changes of the molecular environments are discussed in terms of localized moments and of their characteristics.

1. Construction of localized orbitals

The molecular orbital calculations were performed using the IBMOL-IV program [10]. The localized orbitals were obtained by EDMISTON—RUEDENBERG energy localization criterion [11]. The studied ten-electron systems can be grouped into five symmetry point groups, the localized orbitals corresponding to these series are the following:

K_h core, four lone pair LMO's
$C_{\infty v}$ core, three lone pair LMO's, one bond pair LMO
C_{2v} core, two lone and two bond pair LMO's
C_{3v} core, one lone pair LMO, three bond pair LMO's
T_d core, four bond pair LMO's.

The transformation matrices of AO basis to CMO and CMO basis to LMO, respectively, are in good agreement with earlier investigations [12, 13, 14, 15]. The calculated coefficients for the AO → CMO and CMO → LMO matrices on the example of H_2O molecule are given in Table I.

2. Interaction energies of electrons on localized orbitals

The total energy of a closed shell system containing $2N$ electrons

$$E = \hat{H}(0) + 2\sum_{i=1}^{N} \langle \varphi_i \mid \hat{H}(1) \mid \varphi_i \rangle + \sum_{i,j=1}^{N} \langle \varphi_i \varphi_j \mid \sigma_{12}^{-1}(2 - \hat{P}_{12}) \mid \varphi_i \varphi_j \rangle \qquad (1)$$

Table I

Transformation matrices for the H_2O molecule
AO to CMO

Basis function		$1a_1$	$2a_1$	$1b_2$	$3a_1$	$1b_1$
S	(0)	+0.044006	−0.008621	0.0	−0.003119	0.0
S'	(0)	+0.981333	−0.232763	0.0	−0.083741	0.0
S''	(0)	+0.010774	+0.650577	0.0	+0.252617	0.0
S'''	(0)	−0.004730	+0.294719	0.0	+0.270435	0.0
S	(H1)	+0.000026	+0.135915	−0.255611	−0.143433	0.0
S'	(H1)	+0.001144	−0.012522	−0.093975	−0.110493	0.0
S	(H2)	+0.000026	+0.135915	+0.255611	−0.143433	0.0
S'	(H2)	+0.001144	−0.012522	+0.093975	−0.110493	0.0
PX	(0)	0.0	0.0	−0.277285	0.0	0.0
PX'	(0)	0.0	0.0	−0.518776	0.0	0.0
PY	(0)	0.0	0.0	0.0	0.0	+0.360029
PY'	(0)	0.0	0.0	0.0	0.0	+0.770638
PZ	(0)	−0.002492	−0.055817	0.0	0.305897	0.0
PZ'	(0)	0.001222	−0.121473	0.0	0.615870	0.0

CMO to LMO

Canonical orbital	Core	Bond 1	Bond 2	Lone 1	Lone 2
$1a_1$	+0.990912	+0.053419	+0.053419	+0.078696	+0.078696
$2a_1$	−0.125331	0.579098	+0.579098	+0.395969	+0.395969
$1b_2$	0.0	−0.707107	+0.707107	0.0	0.0
$3a_1$	−0.048841	−0.402234	−0.402234	+0.580530	+0.580530
$1b_1$	0.0	0.0	0.0	−0.707107	+0.707107

can be expressed using the Coulomb integrals

$$\langle \varphi_i \varphi_j \mid \varphi_i \varphi_j \rangle \qquad \forall\, i, j \tag{2}$$

and the exchange integrals

$$\langle \varphi_i \varphi_j \mid \varphi_j \varphi_i \rangle \qquad \forall\, i, j \tag{3}$$

between the $\{\varphi_k\}$ functions of a given basis set [1].

The single-determinant wavefunction is invariant under the localization transformation in the case of closed shell systems, while the Coulomb

self-repulsion terms increase and the non-diagonal exchange terms decrease during the energy localization procedure [11]. The diagonal elements of the Coulomb matrices over the localized orbitals of ten-electron hydrides studied represent the self-repulsion energies of the core, bond and lone pair LMO's (Table II).

The self-repulsions of core as well as bond and lone pair LMO's are increasing with the nuclear charge of the central atom within each symmetry point group. The core self-interaction integrals are much larger than the terms

Table II

Self-interaction energies of electrons on localized orbitals

Systems		Core self	Bond self	Lone self
	C^{4-}	3.5454	—	0.5281
	N^{3-}	4.1882	—	0.6978
K_h	O^{2-}	4.8371	—	0.8386
	F^-	5.4874	—	1.0041
	Ne	6.1385	—	1.1785
	HC^{3-}	3.5569	0.5997	0.5574
	HN^{2-}	4.2043	0.6265	0.7399
$C_{\infty v}$	HO^-	4.8500	0.7316	0.8818
	HF	4.4941	0.8953	1.0396
	HNe^+	6.1418	1.0734	1.2017
	H_2C^{2-}	3.5646	0.6305	0.5809
	H_2N^-	4.2097	0.6982	0.7612
C_{2v}	H_2O	4.8525	0.8128	0.9047
	H_2F^+	5.4966	0.9607	1.0688
	H_2Ne^{2+}	6.1421	1.1243	1.2174
	H_3C^-	3.5669	0.6540	0.6023
	H_3N	4.2083	0.7420	0.7797
C_{3v}	H_3O^+	4.8512	0.8580	0.9280
	H_3F^{2+}	5.4958	1.0023	1.0826
	H_3Ne^{3+}	6.1414	1.1585	1.2325
	H_4C	3.5670	0.6700	—
	H_4N^+	4.2006	0.7702	—
T_d	H_4O^{2+}	4.8495	0.8898	—
	H_4F^{3+}	5.4946	1.0344	—
	H_4Ne^{4+}	6.1399	1.1855	—

corresponding to the interactions in the valence shell. The values of self-interaction of the lone pairs are always smaller than those of the bond LMO's in a given species: a lone pair LMO density is less concentrated than the bond pair LMO. The electron density of the latter is better localized for the proton provides a positive nuclear charge (i.e. there are additive basis functions for describing the LMO distribution).

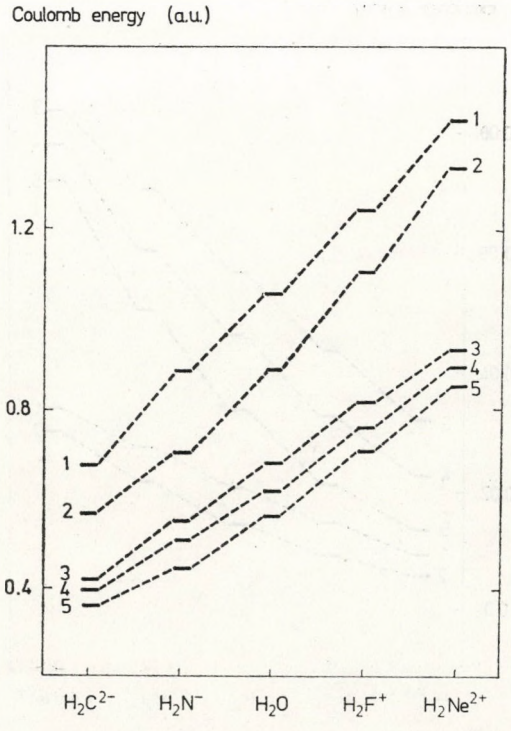

Fig. 1. Coulomb interaction energies of localized orbitals (1 : Lone/Core, 2: Bond/Core, 3: Lone/Lone, 4: Bond/Lone, 5: Bond/Bond)

The non-diagonal Coulomb and exchange terms characterize the interactions between the various types of localized orbitals. The Coulomb interactions change systematically with the central nucleus within each symmetry point group (on the example of C_{2v} group the changes are shown in Fig. 1). The interaction energies show certain regularity in each series, for the Coulomb energies the following order was obtained:

$$\text{lone/core} > \text{bond/core} > \text{lone/lone} > \text{bond/lone} > \text{bond/bond}$$

The exchange integrals are larger within the valence shell than between the core and the valence shell localized orbitals, as expected. Fig. 2 represents

the exchange terms for the molecules of C_{2v} point group. The

$$\text{lone/lone} > \text{bond/lone} > \text{bond/bond} \tag{4a}$$

order holds again, whereas the lone/core and bond/core exchange interactions are smaller (but still lone/core > bond/core integrals), showing a systematic

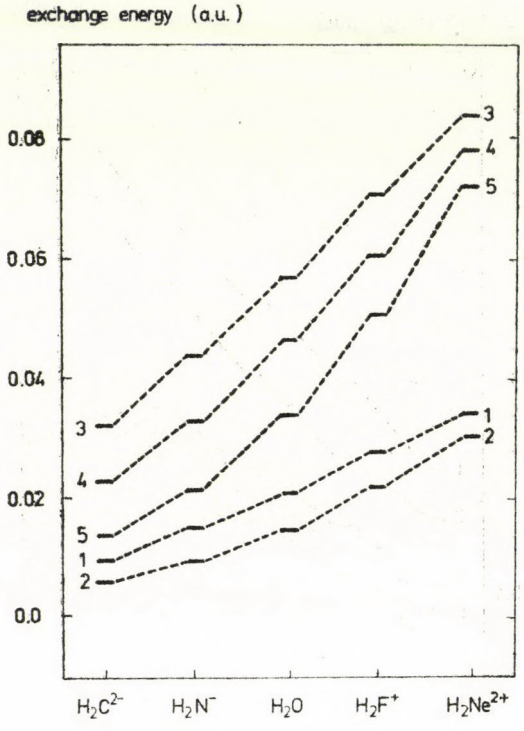

Fig. 2. Exchange interaction energies of localized orbitals (1: Lone/Core, 2: Bond/Core, 3: Lone/Lone, 4: Bond/Lone, 5: Bond/Bond)

change with increasing atomic number of the central nucleus. The results suggest that one should expect a similar relationship while analyzing the localized orbitals in terms of localized moments and their mean features.

3. Characteristics of localized moments viz. the change of central atom nuclear charge

It is interesting to compare the angles between the centroid of charge vectors of different LMO's [16, 17, 18, 19]. A study on neutral ten-electron systems as well as the investigation of the localized orbitals of hydrides with

increasing proton number have shown that the angles between the three combinations of bond and lone pair centroid vectors keep the

$$\text{lone/lone} > \text{bond/lone} > \text{bond/bond} \tag{4b}$$

order [8]. The relationship (4b) is expected because of the inequalities of (4a). Similar regularity has been found while investigating the centroid vector

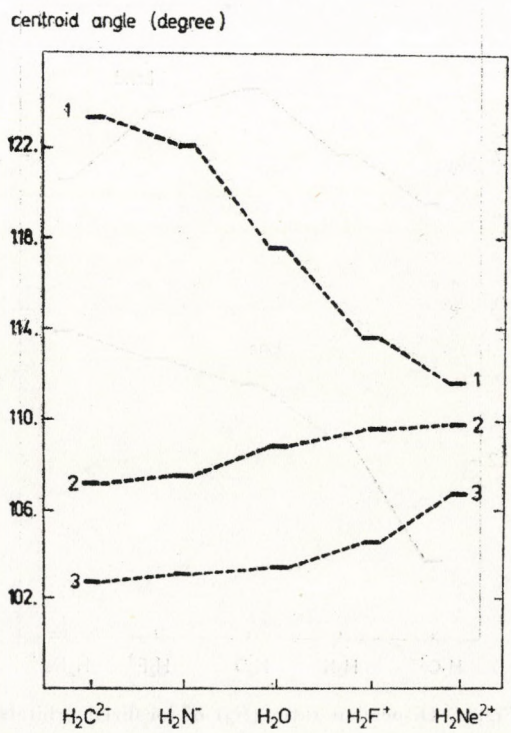

Fig. 3. Angles between the centroid vectors of localized orbitals (1: Lone/Lone, 2: Bond/Lone, 3: Bond/Bond)

angles of the ten-electron hydrides belonging to the C_{2v} symmetry point group (Fig. 3). It should be noted that fix valence angle has been taken for all five species of C_{2v} group, the experimental bond angle (104.52°) of the water molecule. Therefore the angles between the bond pair LMO centroid vectors do not differ too much, while the lone/lone angles decrease strongly with increasing central atom nuclear charge, as expected.

The first electric moments of bond and lone pair LMO's show significant difference as well as the angles between the centroid vectors. The second electric moments, however, are more sensitive to the geometry data and the basis

set. It is evident, because the higher is the order of an electric moment it describes the more distant regions from the centroid of the given orbital. E.g. the dispersion ratio, R_d (as defined in (8)) shows systematic changes in the series of neutral systems as well as in the case of the hydrides with increasing proton number, but no regularity holds for the molecules of C_{2v} group included in the calculations (Fig. 4). The discrepancies are certainly due to

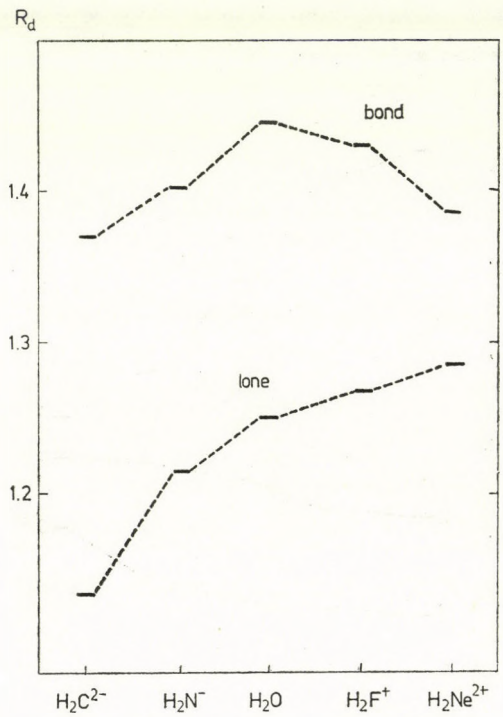

Fig. 4. Dispersion ratio (R_d) of localized orbitals

the geometry and basis set dependence. Further study in these directions is in progress.

In addition to the use of first and second electric moments of localized orbital distribution, other characteristics of the localized moments can also be introduced. These quantities obtained by the combination of the electric moments of different order [8] may be suitable for analyzing the LMO densities.

The ratio of the absolute value of centroid of charge vector and the major semiaxis, the quantity $\langle r\rangle_i/\langle x'^2\rangle_i^{\frac{1}{2}}$ show the asymmetry of the i-th localized orbital. A similar interpretation can be given to the quantity $(\langle r\rangle_i - \langle x'^2\rangle_i^{\frac{1}{2}})/\langle y'^2\rangle_i^{\frac{1}{2}}$ which makes a comparison between the magnitudes

of first and second moment components. This so called orbital distortion, D_{orb}, is the less the more spherical distribution has the given LMO (it can also be negative). The orbital asymmetry, A_{orb}, as well as the orbital distortion keep similar orders while investigating these quantities for the bond and lone pair LMO densities of the ten-electron hydrides of the C_{2v} symmetry point group (Figs. 5 and 6). The charge distribution of a bond pair LMO elongates

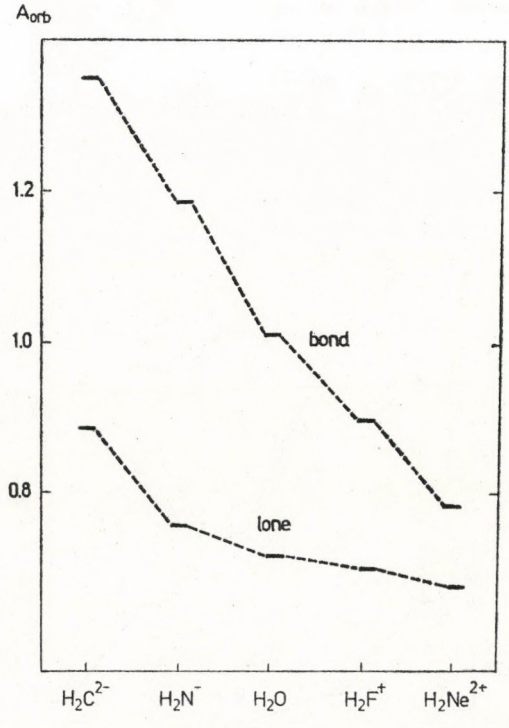

Fig. 5. Orbital asymmetry (A_{orb}) of localized orbitals

more away from the central atom nucleus and decreases appreciably with the change of molecular environment, i.e. increasing nuclear charge of the heavy atom, the lone pair LMO densities are closer to spherical symmetry.

It has been shown that there is also a significant gap between bond and lone pair LMO densities if they are calculated over density contours [20]. Similar results were obtained from a numerical integration of the inside and the surface of electron density contours for some neutral molecules. Some earlier investigations have already shown that the bond and lone pair LMO's can be characterized by main features of their electric moments [7, 8, 20].

The orbital asymmetry and the orbital distortion in the case of ten-electron hydrides studied vary systematically — like in the C_{2v} group's species

presented — for each LMO of the K_h, $C_{\infty v}$, C_{3v} and T_d symmetry point groups. The deformation of both bond and lone pair LMO densities decreases with increasing central nuclear charge, as expected. The effective solid angle, Ω_{eff}, is also suitable for characterizing a localized orbital, it can be calculated using the first and second electric moments. These angles, presented in the series of C_{2v} group in Fig. 7. vary little for lone pair LMO's, but increase significantly for bond pair LMO's. Similar regularity holds within the other four symmetry point groups, too. It should be emphasized that not only the first and second electric moments of LMO's can be related to mathematical variables, but they are, as one-electron properties, expected to be determined to a good approximation by ab initio calculations (BRILLOUIN theorem [21]).

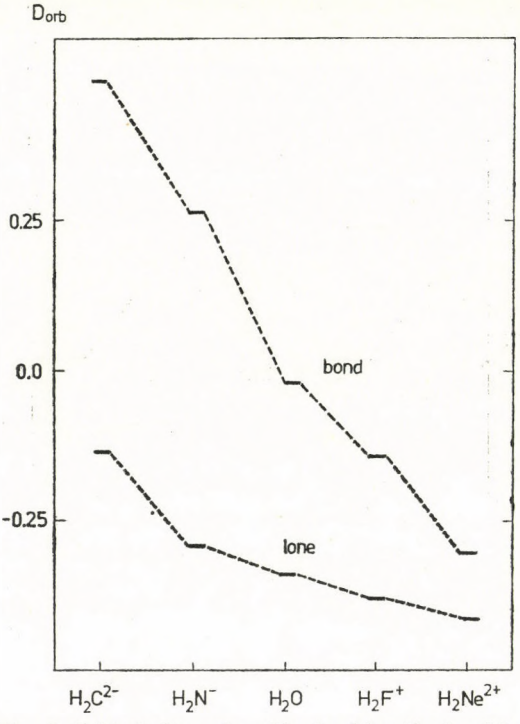

Fig. 6. Orbital distortion (D_{orb}) of localized orbitals

These systematic changes of localized moments with varying central atom nuclear charge (in the present paper) and proton number (in [8]) are expected, because similar relationships hold between the energy interaction terms of studied ten-electron systems. The characterization of charge distribution can be done using some quantities derived from the electric moments of localized orbitals: in the case of ten-electron hydrides the change of these features of LMO's (Figs. 4, 5, 6, 7) are in agreement with the variation of Coulomb and exchange energy integrals (Table II, Figs. 1, 2).

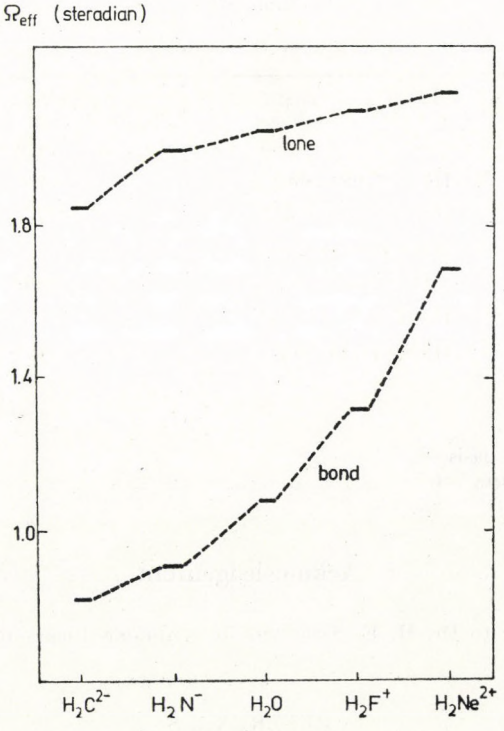

Fig. 7. **Effective solid angle (Ω_{eff}) of localized orbitals**

4. The influence of geometry and basic set

It has already been pointed out that the electric moments of charge distribution are sensitive to the basis set chosen [22, 23]. The effect of the geometry on the electric moments has not yet been investigated in previous references.

The calculated equilibrium geometry is expected to be near the experimental one for a molecule, using ab initio calculations. In the case of ten-electron systems we have taken experimental data for the geometries, the total energy minima, however, have also been determined for the neutral species (Table III). The calculated equilibrium in each case is in modest agreement with the expectation. Therefore it is hoped that the geometry effects do not influence strongly the results obtained for the localized moments. The basis set dependence may be more dangerous, but the characteristics proposed, as they are ratios, are expected to be suitable for analyzing LMO densities. The influence of geometry variation is under investigation and a study on the basis set dependence is also planned.

Table III

Calculated equilibrium of the studied neutral systems

System	Geometry data in the calculated equilibrium	Total energy (in a. u.) in the Equ. calc.	Equ. exp.
CH_4	$\overline{HC} = 2.054$ bohr	− 40.186000	− 40.185944
NH_3	$\overline{HN} = 1.924$ bohr	− 56.173377	− 56.170648
	$NHN \sphericalangle = 112.51°$		
H_2O	$\overline{HO} = 1.845$ bohr	− 76.012339	− 76.010814
	$HOH \sphericalangle = 109.03°$		
HF	$\overline{HF} = 1.746$ bohr	−100.03271	−100.03267
Ne	—	−128.54467*	−128.54337**

* noncontracted basis set
** contracted basis set

Acknowledgement

Thanks are due to Dr. M. E. STEPHENS for valuable discussions.

REFERENCES

1. E. KAPUY and E. TÖRÖK: Quantum Theory of Atoms and Molecules (in Hungarian). Akadémiai Kiadó, Budapest, 1975.
2. H. WEINSTEIN, R. PAUNCZ and M. COHEN, Adv. Mol. Phys., **7**, 97, 1971.
3. W. ENGLAND, L. S. SALMON and K. RUEDENBERG, Fortschritte der chemischen Forschung, **23**, 31, 1971.
4. Interatomic Distances Suppl., No. 18, The Chem. Soc., London, 1965.
5. R. DAUDEL, C. KOZMUTZA and E. KAPUY, Chem. Phys. Letters, **36**, 555, 1975.
6. E. KAPUY, M. A. ROBB, R. DAUDEL, C. KOZMUTZA and I. G. CSIZMADIA (in preparation).
7. R. DAUDEL, M. E. STEPHENS, C. KOZMUTZA, E. KAPUY, J. D., GODDARD, and I. G. CSIZMADIA, Int. J. Quant. Chem., (accepted for publication).
8. E. KAPUY, C. KOZMUTZA and M. E. STEPHENS, Theoret. Chim. Acta, Berlin **43**, 175, 1976.
9. M. A. ROBB, W. J. HAINES and I. G. CSIZMADIA, J. Am. Chem. Soc., **95**, 42, 1973.
10. A. VEILLARD, IBMOL-Version 4. Special IBM Technical Report, San José, California, 1968.
11. C. EDMISTON and K. RUEDENBERG, Rev. Mod. Phys., **35**, 457 1963; J. Chem. Phys., **43**, S97, 1965.
12. C. EDMISTON and K. RUEDENBERG, Quantum Theory of Atoms, Molecules and the Solid State, p. 263, 1966.
13. M. A. ROBB and I. G. CSIZMADIA, Int. J. Quant. Chem., **4**, 365, 1970.
14. W. VON NIESSEN, J. Chem. Phys., **56**, 4290, 1972.
15. W. VON NIESSEN, Theoret. Chim. Acta (Berl.) **29**, 29, 1973.
16. P. TH. VAN DUIJNEN and D. B. COOK, Mol. Phys., **21**, 475, 1971.
17. S. WILSON and J. GERRATT, Mol. Phys., **30**, 789, 1975.
18. A. HINCHLIFFE and P. R. HUGHES, J. Mol. Structure, **32**, 79, 1976.
19. M. A. ROBB, Ph. Thesis, University of Toronto, 1970.
20. M. E. STEPHENS, E. KAPUY and C. KOZMUTZA (in preparation).
21. L. BRILLOUIN, Actualités sci. et ind., No. 71 (1933); No. 159 (1934).
22. T. H. DUNNING, J. Chem. Phys., **53**, 2823, 1970, **55**, 3958, 1971.
23. T. H. DUNNING, R. W. PITZER and S. AUNG, J. Chem. Phys., **57**, 5044, 1972.

Acta Physica Academiae Scientiarum Hungaricae, Tomus 41 (2), pp. 137—144 (1976)

THE APPLICATION OF SU (1,1) SPIN COEFFICIENTS FOR SPACE LIKE SYMMETRY

By

B. LUKÁCS

CENTRAL RESEARCH INSTITUTE FOR PHYSICS, HIGH ENERGY PHYSICS DEPARTMENT
BUDAPEST

(Received in revised form 26. VII. 1976)

If the space-time has a space-like Killing symmetry, the three-dimensional spin coefficient technique, which was useful for time-like symmetry, can be applied again. This paper contains the spin coefficient forms of the Einstein equation and the Ricci and Weyl tensors.

1. Introduction

Solution of the Einstein equations have long been studied in the literature. Various methods have been applied to find solutions of these equations. The spin coefficient technique developed by NEWMAN and PENROSE [1] is one of them. By means of this technique several new solutions have been found [2]. On the other hand, PERJÉS has shown that if the space-time has a Killing symmetry, it is useful to reformulate the gravitational equations in a three-dimensional "background" space and to apply the spin coefficient technique in three dimensions [3]. This method has given solutions, which could not have been obtained in the four-dimensional NP formalism [4], [5], [6]. But this new formalism has been worked out in the stationary case only.

The massive objects whose gravitational fields are sufficiently strong to have a non-Newtonian character show axial symmetry. Adapting the PERJÉS formalism to the case of space-like symmetry, it will be possible to investigate time-dependent solutions in a new way. This may be useful, for example, in the description of the gravitational collapse.

This paper contains the equations of the spin coefficient method adapted to the 3-dimensional relativity theory when the symmetry is space-like, i.e. the Killing equation

$$K_{\mu;\nu} + K_{\nu;\mu} = 0 \tag{1.1}$$

has a space-like solution K^μ and the Lie derivatives of all field quantities vanish along this K^μ vector field.

2. Three-dimensional relativity theory

The derivation of the equations of the 3-dimensional relativity is similar to the procedure written down in [3] therefore we survey only some important points.

The coordinate system can be chosen in such a way that

$$K^\mu = \delta^\mu_3 \,. \tag{2.1}$$

From Eqs. (1.1), (2.1) we find that

$$g_{\mu\nu,3} = 0 \,. \tag{2.2}$$

Eq. (2.2) shows that

$$T_{\mu\nu,3} = 0 \,. \tag{2.3}$$

The condition (2.1) is preserved by the following transformations:

$$x^{3'} = x^3 + F(x^i) \,, \tag{2.4a}$$

$$x^{i'} = x^{i'}(x^k) \,, \tag{2.4b}$$

$$i = 0, 1, 2 \,.$$

In this paper we shall use such coordinate systems in which condition (2.1) is fulfilled.

Let us write the line element of the 4-dimensional space-time in the form:

$$\begin{aligned} d\tilde{s}^2 &= f(\mathrm{d}z + \omega_r \mathrm{d}x^r)^2 - f^{-1}\mathrm{d}s^2 \,, \\ \mathrm{d}s^2 &= g_{ik}\mathrm{d}x^i\mathrm{d}x^k \,, \\ x^3 &= z \,, \end{aligned} \tag{2.5}$$

where a tilde denotes the 4-dimensional quantities. This form is general because $f = K_\varrho K^\varrho > 0$. g_{ik} is a symmetric tensor of signature $(+, -, -)$. f, ω_i, g_{ik} are independent of z. f is a scalar, ω_i is a 3-vector, g_{ik} is a symmetric tensor with respect to the transformations (2.4b) and they transform under (2.4a) as follows:

$$\begin{aligned} f' &= f \,, \\ \omega'_i &= \omega_i - F_{,i} \,, \\ g'_{ik} &= g_{ik} \,. \end{aligned} \tag{2.4c}$$

We shall consider g_{ik} as the metric tensor of the 3-dimensional background space.

Now we introduce the following quantities:

$$G_i = (2f)^{-1} \cdot (f'_{,i} + i\varphi_i) ,$$
$$\varphi_i = \epsilon_{ikl}\omega^{k|l} f^{+2}\sqrt{g} . \tag{2.6}$$

Here the stroke | denotes the 3-dimensional covariant derivation, $v_i = g_{ik}v^k$. The new form for the Einstein equations is:

$$G^r{}_{|r} + (\bar{G}^r - G^r)\, G_r = -f^{-2}\tilde{R}_{33} ,$$
$$G_{i|k} - G_{k|i} + G_i\bar{G}_k - G_k\bar{G}_i = -i\epsilon_{ikl}\tilde{R}^l_3\sqrt{g}f^{-2} . \tag{2.7}$$
$$R_{ik} + G_i\bar{G}_k + \bar{G}_iG_k = f^{-2}(g_{ir}g_{ks}\tilde{R}^{rs} - g_{ik}\tilde{R}_{33}) .$$

R_{ik} is the 3-dimensional Ricci tensor. $\tilde{R}_{\mu\nu}$ can be obtained by means of $\tilde{T}_{\mu\nu}$ considering Eq. (2.5). These equations were published by PERJÉS in 1970 [3]. The form of the equations of "3-dimensional relativity theory" is independent of the signature of $\tilde{K}_\varrho\tilde{K}^\varrho$, but having applied the spin coefficient technique to the spacelike symmetric case, the spin coefficient equations differ from those of [3]. Now we are going to calculate these equations.

3. The complex triad formalism

We have to construct the 3-dimensional analogues of the NEWMAN—PENROSE spin coefficients. For that purpose we introduce a complex basic vector triad in the background space with the following orthonormalization:

$$z^i_p = (l^i, m^i, \bar{m}^i) , \qquad l^i \text{ is real},$$
$$p = 0, +, -,$$
$$g_{mn} = z_{mr}z^r_n = \begin{bmatrix} 1 & 0 & 0 \\ 0 & 0 & -1 \\ 0 & -1 & 0 \end{bmatrix} . \tag{3.1}$$

The connection with the NEWMAN—PENROSE null tetrad [1] is:

$$\tilde{l}^\mu = (l^i; f^{-1} - l^r\omega_r) ,$$
$$\tilde{m}^\mu = \sqrt{-f}\,(m^i; -m^r\omega_r) , \tag{3.2}$$
$$\tilde{n}^\mu = -\frac{1}{2}f\tilde{l}^\mu + \tilde{K}^\mu .$$

Similarly to the NEWMAN—PENROSE method we introduce the differential operators:

$$D \equiv l^r \frac{\partial}{\partial x^r} ; \qquad \delta \equiv m^r \frac{\partial}{\partial x^r} . \tag{3.3}$$

From Eq. (3.2) it can be seen that their connection with the NEWMAN—PENROSE operators is the following:

$$\tilde{D} = D ; \qquad \tilde{\delta} = \sqrt{-f}\delta ; \qquad \tilde{\Delta} = -\frac{1}{2} f D ; \tag{3.4}$$

because all quantities are independent of the coordinate z.

The complex rotational coefficients can be introduced similarly as in the stationary case. They are antisymmetric in their first and second indices because of the normalization. Eq. (3.1) shows that writing $-$ instead of $+$ we get the complex conjugate quantity. Thus we have 1 imaginary and 4 complex rotational coefficients:

$$\begin{gathered} \gamma_{mnp} = z_{mi|k} z^i_n z^k_p , \\ \gamma_{+00} \equiv \varkappa , \qquad \gamma_{+0-} \equiv \varrho , \\ \gamma_{+0+} \equiv \sigma , \qquad \gamma_{+--} \equiv \tau , \\ \gamma_{+-0} \equiv \epsilon . \end{gathered} \tag{3.5}$$

The correspondence between these rotational coefficients and the NEWNAN—PENROSE spin coefficients can be established using the definition of the spin coefficients [1] and the formulae (3.5), (3.2), (3.1). We obtain the following result:

$$\begin{aligned} \tilde{\alpha} &= -\frac{\sqrt{-f}}{2}\left(\tau + \frac{1}{2} G_- - \frac{1}{2}\bar{G}_-\right), \\ \tilde{\beta} &= \frac{\sqrt{-f}}{2}\left(\bar{\tau} - \frac{1}{2} G_+ - \frac{3}{2}\bar{G}_+\right), \\ \tilde{\gamma} &= \frac{f}{4}\left(\epsilon + \frac{1}{2} G_0 + \frac{3}{2}\bar{G}_0\right), \\ \tilde{\epsilon} &= -\frac{1}{2}\left(\epsilon + \frac{1}{2} G_0 - \frac{1}{2}\bar{G}_0\right), \\ \tilde{\varkappa} &= -\frac{1}{\sqrt{-f}}(\varkappa - 2\bar{G}_+) , \end{aligned} \tag{3.6}$$

$$\tilde{\lambda} = -\frac{f}{2}\bar{\sigma}\,,$$

$$\tilde{\mu} = -\frac{f}{2}(\bar{\varrho} - G_0)\,,$$

$$\tilde{\nu} = \frac{(-f)^{3/2}}{4}(\bar{\varkappa} - 2\bar{G}_-)\,,$$

$$\tilde{\pi} = \frac{\sqrt{-f}}{2}\bar{\varkappa}\,; \tag{3.6}$$

$$\tilde{\varrho} = -\varrho + \bar{G}_0\,,$$

$$\tilde{\sigma} = -\sigma\,,$$

$$\tilde{\tau} = -\frac{\sqrt{-f}}{2}\varkappa\,.$$

Similarly, we can calculate the commutators of the (3.6) differential operators using the formulae (3.1), (3.3), (3.5) [7].

$$\begin{aligned}(D\delta - \delta D)\varphi &= \left[-(\bar{\delta} + \epsilon)\delta - \sigma\delta + \varkappa D\right]\varphi\,,\\ (\delta\bar{\delta} - \bar{\delta}\delta)\varphi &= \left[\tau\delta - \bar{\tau}\bar{\delta} - (\varrho - \bar{\varrho})D\right]\varphi\,.\end{aligned} \tag{3.7}$$

Now we can write down the new form of the Einstein equations for the space-like symmetric case.

4. The new form of the Einstein equations

First we project the Eqs. (2.7) on the complex vector triad. The result is the same as in the [3] (but in the formulae lower index "3" is replaced by "0"):

$$\lambda \equiv f^{-2}\tilde{R}_{33}\,,$$

$$\chi_p = f^{-2}\tilde{R}^{l}_{3}z_{pl}\,, \tag{4.1}$$

$$2\Phi_{mn} = f^{-2}(\tilde{R}^{ik} - g^{ik}\tilde{R}_{33})\,z_{mi}z_{nk}\,.$$

Now we can apply the method described [3]. It is necessary to decompose the three-dimensional Riemann tensor into irreducible parts and to act with the Ricci identity on the basic vectors z^{i}_{m} [7]. The triad components of Eqs.

(2.7 a-b) give further equations:

$$
\begin{aligned}
D\varrho - \bar{\delta}\varkappa &= \varkappa\tau + \varkappa\bar{\varkappa} - \varrho^2 - \sigma\bar{\sigma} - G_0 G_0 + \Phi_{00}\,, \\
D\sigma - \delta\varkappa &= -(\varrho + \bar{\varrho} + 2\epsilon)\,\sigma - \varkappa\bar{\tau} + \varkappa^2 + 2G_+\bar{G}_+ - 2\Phi_{++}\,, \\
D\tau - \bar{\delta}\epsilon &= -\varkappa\bar{\sigma} + \bar{\varkappa}\varrho + \epsilon\tau + \bar{\varkappa}\epsilon - \varrho\tau + \bar{\varrho}\bar{\tau} - \bar{G}_0 G_- - G_0\bar{G}_- + 2\Phi_{0-}\,, \\
\delta\varrho - \bar{\delta}\sigma &= 2\sigma\tau - (\varrho - \bar{\varrho})\,\varkappa - G_0\bar{G}_+ - \bar{G}_0 G_+ + 2\Phi_{0+}\,, \\
\delta\tau + \bar{\delta}\bar{\tau} &= -2\tau\bar{\tau} - \sigma\bar{\sigma} - \varepsilon(\varrho - \bar{\varrho}) + \varrho\bar{\varrho} - G_0\bar{G}_0 - G_-\bar{G}_+ - \bar{G}_- G_+ + \\
&\quad + \Phi_{00} + 2\Phi_{+-}\,, \qquad (4.2) \\
DG_0 - \delta G_- - \bar{\delta}G_+ &= (-\varrho - \bar{\varrho} + G_0 - \bar{G}_0)\,G_0 + (\bar{\varkappa} + \tau - G_- + \bar{G}_-)\,G_+ + \\
&\quad + (\varkappa + \bar{\tau} - G_+ + \bar{G}_+)\,G_- - \lambda\,, \\
\delta G_0 - DG_+ &= \sigma G_- + (\bar{\varrho} + \bar{G}_0 + \epsilon)\,G_+ - (\varkappa + \bar{G}_+)\,G_0 - \chi_+\,, \\
\bar{\delta}G_0 - DG_- &= (\varrho + \bar{G}_0 - \epsilon)\,G_- + \bar{\sigma}G_+ - (\bar{\varkappa} + \bar{G}_-)\,G_0 + \chi_-\,, \\
\bar{\delta}G_+ - \delta G_- &= (\bar{\tau} + \bar{G}_-)G_- - (\tau + \bar{G}_-)\,G_+ + (\varrho - \bar{\varrho})\,G_0 + \chi_0\,.
\end{aligned}
$$

The nonvanishing components of the Weyl tensor can be obtained from the NEWMAN—PENROSE equations, using Eqs. (3.4), (3.6). If the energy-momentum tensor vanishes they have the following form:

$$
\begin{aligned}
\Psi_0 &\equiv -\tilde{C}_{\alpha\beta\gamma\delta}\tilde{l}^\alpha\tilde{m}^\beta\tilde{l}^\gamma\tilde{m}^\delta = 2\{-\delta\bar{G}_+ - (G_+ + 2\bar{G}_+ - \bar{\tau})\,\bar{G}_+ + \sigma\bar{G}_0\}\,, \\
\Psi_1 &\equiv -\tilde{C}_{\alpha\beta\gamma\delta}\tilde{l}^\alpha\tilde{n}^\beta\tilde{l}^\gamma\tilde{m}^\delta = \sqrt{-f}\{-D\bar{G}_+ - (2\bar{G}_0 + G_0 + \epsilon)\,\bar{G}_+ + \varkappa\bar{G}_0\}\,, \\
\Psi_2 &\equiv -\frac{1}{2}\tilde{C}_{\alpha\beta\gamma\delta}(\tilde{l}^\alpha\tilde{n}^\beta\tilde{l}^\gamma\tilde{n}^\delta - \tilde{l}^\alpha\tilde{n}^\beta\tilde{m}^\gamma\bar{\tilde{m}}^\delta) = \frac{f}{2}\{D\bar{G}_0 - \bar{\varkappa}\bar{G}_+ - \\
&\quad - \varkappa\bar{G}_- + 2\bar{G}_-\bar{G}_+ + (G_0 + \bar{G}_0)\,\bar{G}_0\}\,, \qquad (4.3) \\
\Psi_3 &\equiv \tilde{C}_{\alpha\beta\gamma\delta}\tilde{l}^\alpha\tilde{n}^\beta\tilde{n}^\gamma\bar{\tilde{m}}^\delta = \frac{(-f)^{3/2}}{2}\{-D\bar{G}_- - (G_0 + 2\bar{G}_0 - \epsilon)\,\bar{G}_- + \bar{\varkappa}\bar{G}_0\}\,, \\
\Psi_4 &\equiv -\tilde{C}_{\alpha\beta\gamma\delta}\tilde{n}^\alpha\bar{\tilde{m}}^\beta\tilde{n}^\gamma\bar{\tilde{m}}^\delta = -\frac{f^2}{2}\{\delta\bar{G}_- + (2\bar{G}_- + G_- - \tau)\,\bar{G}_- - \bar{\sigma}\bar{G}_0\}\,.
\end{aligned}
$$

5. Eigenrays

The Eqs. (4.2) can be simplified by some kind of convenient choice of basic vectors. In stationary case it was useful to take the basic vector l^i as tangent to the eigenray congruence of the gravitational field [3]. If we choose l^i in the same way in the space-like symmetric case as in the stationary one,

we get the same, pure algebraical requirement for this vector:

$$f_{,i} - (f_{,r}l^r)\, l_i + \epsilon_{irs}\varphi^r l^s \sqrt{g} = 0 \,. \tag{5.1a}$$

This requirement can be fulfilled, except for the following special cases:

$$f_{,i} = 0 \,, \qquad \varphi_r\varphi^r \leq 0 \,,$$

or

$$f_{,i} \neq 0 \,, \qquad \varphi^i = 0 \,, \qquad f_{,r}f_{,s}g^{rs} \leq 0 \,, \tag{5.1b}$$

or

$$f_{,i} \neq 0 \,, \qquad \varphi^i \neq 0 \,, \qquad f_{,r}f_{,s}g^{rs} = \varphi_r\varphi^r = f_{,r}\varphi^r = 0 \,.$$

Projecting Eq. (5.1a) onto the basic vector triad z_m^i, it takes the simple form:

$$G_- = 0 \,. \tag{5.1c}$$

Now l^i has been fixed. The quantity ϵ can be made zero by a complex rotation of the vector m^i and still remains:

$$m' = m(\cos C^\circ + i \sin C^\circ) \tag{5.2}$$

where C° is real and $DC^\circ = 0$. If one of the quantities G_+, $\varkappa$, σ has a phase factor exp. $i\chi^\circ$ which is independent of time (i.e. $D\chi^\circ = 0$), this χ° can be made zero by the complex rotation (5.2).

The geometrical meaning of the rotational coefficients is similar as in the stationary case. If $\varkappa = 0$, the eigenray congruence is geodesic in the background space-time, and then $\mathrm{Re}\varrho$ gives the divergence, $\mathrm{Im}\varrho$ gives the rotation and $|\sigma|$ gives the shear of the congruence.

It is possible to classify the space-like symmetric solutions similarly to the NEWMAN—PENROSE classification. Defining the quantity M

$$M \equiv \tilde{\varrho}\bar{\tilde{\varrho}} - \tilde{\sigma}\bar{\tilde{\sigma}} \tag{5.3}$$

the solution is

spherical, if $M \neq 0$,

cylindrical, if $M = 0$, but $\tilde{\varrho}\bar{\tilde{\varrho}} + \sigma\bar{\tilde{\sigma}} \neq 0$,

plane wave, if $\tilde{\varrho} = \tilde{\sigma} = 0$,

where $\tilde{\varrho} = \bar{G}_0 - \varrho$, $\tilde{\sigma} = -\sigma$. However, we note that this classification does not refer to the rays (as the NP classification does) but to the 4-dimensional images of the eigenrays (see Eq. (3.2)). When $\sigma = 0$, the eigenrays coincide with the 3-dimensional projections of the rays and the two classifications

are equivalent. If $\varkappa = \sigma = 0$, it can be seen from Eq. (4.3) that $\Psi_0 = \Psi_1 = 0$, thus the space is algebraically special.

Our field equations can be handled similarly as their analogues in stationary case. Unpublished calculations show that they can be solved if the gravitational field has timelike geodesic and/or shearfree eigenrays.

Acknowledgements

I would like to thank Drs. Z. PERJÉS and J. KÓTA for illuminating discussions.

REFERENCES

1. E. T. NEWMAN and R. PENROSE, J. Math. Phys., **3**, 566, 1962.
2. T. W. J. UNTI and R. J. TORRENCE, J. Math. Phys., **7**, 535, 1966.
3. Z. PERJÉS, J. Math. Phys., **11**, 3383, 1970.
4. Z. PERJÉS, Phys. Rev. Lett., **27**, 1668, 1971.
5. J. KÓTA and Z. PERJÉS, J. Math. Phys., **13**, 1695, 1972.
6. B. LUKÁCS and Z. PERJÉS, GRG Journal, **4**, 161, 1973.
7. Z. PERJÉS, Acta Phys. Hung., **32**, 207, 1972.

Acta Physica Academiae Scientiarum Hungaricae, Tomus 41 (2), pp. 145—147 (1976)

COMMUNICATIO BREVIS

EFFECT OF SOLVENT ON POLARIZATION OF FLUORESCENCE OF RHODAMINE-B

By

M. L. PANDYA* and M. K. MACHWE

DEPARTMENT OF PHYSICS AND ASTROPHYSICS, DELHI UNIVERSITY, DELHI, INDIA

(Received 14. VI. 1976)

Introduction

The polarization of fluorescence of molecules in solution has been reported to depend upon various factors viz. viscosity of the solvent [1]; migration of the excited state energy from the originally excited molecule to a neighbouring molecule [2]; shape and size of the fluorescent molecule [3]; temperature, etc. In the present report the effect of dipole moment of the solvent as an extrinsic cause of depolarization has been dealt with.

Experimental

The polarization of Rhodamine-B in different solvents (conc. $\sim 10^{-5}$ g/cc) has been measured at room temperature ($\sim$20 °C) with an Aminco Bowman spectrophotofluorometer. In each case, the excitation and emission peaks were located and then keeping the excitation and emission monochromators to the longest wavelength, the polarization was determined by the method adopted in [4]. The effect of scattered light and background for each solvent was checked by using pure solvent in the cell and setting the excitation and emission monochromators at values used in the polarization measurements. The contribution of this effect to the intensity of fluorescence was found to be less than 0.5%.

Results

The results obtained for polarization along with the peak excitation and emission wavelengths are given in Table I.

* Permanent address: Department of Physics M. M. College, Modinagar. Distt. Meerut (U. P.) India

Discussion

From Table I it is seen that the observed variation in polarization cannot be accounted for as viscosity effect alone because in this case a plot between $1/p$ and $1/n$ (Perrin plot) will not be linear. The electromagnetic coupling of neighbouring molecules and its depolarization effect due to energy migration is small on account of low concentration. It is, therefore, likely that the observed variation in polarization is due to the dipole moment of the solvent. The variation in polarization in the solvents listed in the Table shows that the percentage polarization is lower in a solvent of higher dipole moment. Though the solvents chosen have low viscosity, even then some change in

Table I

Solvent	Dipole moment (5,6)	Viscosity (5,6)	λ_{ex} (nm)	λ_{em} (nm)	% P
Formamide	3.25	3.307	566	576	5.0
Water	3.0	1.002	562	574	3.2
Acetic anhydride	2.8	0.90	570	580	3.7
n-butanol	1.67	2.9	548	564	6.3
Ethanol	1.68—1.70	1.197	562	572	7.4
Methanol	1.65	0.597	556	568	4.2

percentage polarization may be there due to change of viscosity. In the case of water and acetic anhydride, the viscosities are of nearly the same order, the percentage polarization in acetic anhydride (lower dipole moment) is greater than in water (higher dipole moment). Again, in the case of water and ethanol, the viscosities are of the same order, but the percentage polarization in ethanol (lower dipole moment) is greater than in water. In the case of water and methanol, the viscosity of water is higher than that of methanol. If it had been a viscosity effect, the percentage polarization in water should have been greater than in methanol. But the observed percentage polarization is higher in methanol. This can be accounted for as due to the effect of dipole moment. Similarly the pairs methanol and acetic anhydride. ethanol and formamide all establish that the variation in percentage polarization can be explained on the basis of the effect of dipole moment of the solvent. The effect can be explained as follows:

During the short interval of time in which the absorption of excitation energy takes place, the dipole moment of the solute molecule remains unchanged But just before a radiative transition takes place, the solute molecule gets itself reoriented in the surrounding solvent medium due to dipole-dipole

interaction to get a new equilibrium position, thus resulting in fluorescence depolarization. The Brownian rotation tends to destroy this equilibrium orientation and causes further depolarization. If the dipole moment of the solute molecule in the excited state is different from that in the ground state, the orientation of the molecule in the equilibrium excited state will be different from the Franck—Condon excited state. Therefore, the Brownian rotation will add to the dipole-dipole interaction, thereby increasing the depolarization with a consequent decrease in the value of polarization. The dipole-dipole interaction for a given solute depends upon the dipole moment of the solvent.

Acknowledgement

The authors are thankful to Dr. L. S. KOTHARI, Professor & Head, Department of Physics & Astro-Physics, Delhi University, for providing the necessary facilities for the experimental work. One of us (MP) gratefully acknowledges the financial assistance rendered by the University Grants Commission. Delhi.

REFERENCES

1. F. J. PERRIN, Phys. Radium, **7**, 370, 1926.
2. G. WEBER, Adv. in Protein Chem. **8**, 415, 1953; **75**, 335, 1960.
3. S. S. RATHI and M. K. MACHWE, Phys. Letters. **25A**, 41, 1967.
4. T. AZUMI and S. P. MCGLYNN, J. Chem. Phys., **37**, 2413, 1962.
5. Handbook of Chemistry and Physics (Chemical Rubber Publishing Co., Cleveland, Ohio).
6. G. W. C. KAYE and T. H. LABY, Tables of Physical and Chemical Constants, 1966.

RECENSIONES

F. S. LEVIN and H. FESHBACH:

Reaction Dynamics

Documents on Modern Physics Series, Gordon and Breach Science Publishers Ltd. London, 1973

The book represents the the main part of the authors' lectures at the Latin American School of Physics held in 1968. In the first part written by P. S. LEVIN an attempt is made to survey recent developments in direct nuclear reaction theory. Emphasis is focussed on the comparison of theory and experiment.

In the second part H. FESHBACH reviews recent developments in the general theory of nuclear reactions. Since his original work which appeared in 1958 various new insight both published and unpublished have been gained at MIT. The article brings these various elements together in review of what has been accomplished and in order to show how they describe nuclear reactions and how these elements might be used to calculate cross-sections from fundamental nuclear interactions.

P. BOSCHÁN

L. D. LANDAU and E. M. LIFSCHITZ:

Theoretische Physik-kurzgefasst, Vol. II., Quantentheorie

Akademie Verlag, Berlin, 1975 (In deutscher Sprache herausgegeben von Dr. Siegfried Matthies)

and

L. D. LANDAU and E. M. LIFSHITZ:

A Shorter Course of Theoretical Physics, Volume 2: Quantum Mechanics

Pergamon Press, Oxford — New York — Toronto — Sydney 1974 (Translated from the Russian by J. B. Sykes and J. S. Bell)

Since the publication of the first volume of the "Shorter Course" we have been waiting for the next concise volumes. No doubt, the Course of Theoretical Physics by LANDAU and LIFSHITZ presents a rich and stimulating account of the subject. As a broad view of everywhere connected texture of active physical thought, the Course has been and remains for a long time the guide of physicists' generations in the Soviet Union as well as in the rest of the world (esp. due to the efforts of Pergamon Press, Akademie Verlag and the Soviet Publishing House Mir, which had the book translated into French.) The Shorter Course itself was promised to serve the "non-specialists of theoretical branches" in physics and we may add chemistry, biology and engineering sciences. Such an effort is extremely rare in the literature though there is a growing need for it. The reviewer believes that he is not alone to welcome the Authors' and the Publishers' achievement and to thank for the excellent work of the Translators.

The second volume of the "Shorter Course" retains the following sections from the third volume of the longer Course (treating nonrelativistic quantum mechanics): Basic Concepts of QM — Conservation Laws in QM — Schrödinger Equation — Perturbation Theory — Spin — Identity of Particles — The Atom — The Diatomic Molecule — Elastic Collisions — Inelastic Collisions. The reduction is realized not only by dropping some too special sections but also by rewriting part of the text to be self-contained and clear (in the spirit of

LANDAU). The presentation of the relativistic quantum theory slightly changes the style, since its aim is to present the fundamentals of the theory without entering every where into complex details of the applications and so it is obliged to present the theory by expounding the physical hypotheses and the logical structure (under headings such as: Photons — Dirac's Equation — Particles and Antiparticles — Electrons in an External Field — Radiation — Feynman Diagrams).

Both the German and the English translation have been published in the spirit of the late Professor LANDAU, offering a stimulating example of his striving for clarity, his efforts to simplify what appeared to be complex and so to reveal the laws of nature in thir true simplicity and beauty.

I. ABONYI

H. M. NUSSENZWEIG:

Introduction to Quantum Optics

Gordon and Breach Science Publishers Ltd, London, 1975

The book was published as an umpteenth volume of a series entitled Documents on Modern Physics. Due to some previous experiences on the series I took it in my hand with certain aversion. While reading this feeling disappeared completely and was replaced by recognition. Briefly: in the vast literature dealing with this topics it occupies a very honourable place, it is very useful as a textbook for students, handbook for young research workers, and for specialists as a kind of memory supplement, too (with perhaps an additional non-linear optics textbook). Let us see what this opinion is based on:

In the last fifteen years together with lasers also the detection techniques developed very rapidly. Lasing can be achieved from picosecond to CW operation, from infrared to vacuum UV, from milliwatt to gigawatt output power. The detection of very weak and extremely strong signals has become equally possible. These, altogether have led to the discovery of quite new phenomena (non-linear optics, laser Raman-spectroscopy,holographic interferometry etc.). In the same time the theory has undergone a very significant development as well. The statistical description of the light field, the quantum theory of coherence (coherent states), the understanding of the behaviour of non-linear, non-equilibrium systems (lasers), the theory of the non-linear interaction of light with matter all represent the result of this period. The general term for all these topics is quantum optics. The working tools of the theory in this field are quantum electrodynamics and statistical mechanics.

The book should be equally well called the textbook of quantum optics and as all textbooks it is mainly of theoretical character. From the above topics the following are considered in detail.

Chapter 1 introduces the notion of classical coherence (spatial and temporal coherence) through the correlation functions of the light field. Chapter 2 gives the generalization of the classical coherence for the quantum case with the help of the correlation functions of quantized fields. It points out also the relationship between correlation functions and measurements. Chapter 3 deals with the detailed investigation of that state of the electromagnetic field in which the previously introduced "degree of coherence" is unity (coherent state). In Chapter 4 the statistical properties of natural (thermal) light and other photonstatistics are considered. Chapters 5, 6 and 7 describe the phenomenological, semiclassical and quantum theory of lasers, respectively. The subject matter accessible thus far in the form of articles only is treated here very systematically, striving for clarity and with special regard to some interesting problems (optical resonators, threshold theory, linewidth). Chapter 8 (which is actually the last one) introduces other collective coherent and correlation phenomena (superradiance, photon-echo, self-induced transparency).

Thus the book offers a nearly complete review of quantum optics. What one could object is that the description of non-linear optics (e.g. higher harmonic generation, non-linear absorption, light scattering and parametric processes) is omitted, however, it should well be worth at least one chapter. Nevertheless this failure is partly compensated for by the very complete literature cited.

As a conclusion we can state that the work by all means fills a gap existing in the literature, it follows a uniform treatment and merits the attention of the specialist working in this field. It seems to be suitable for the purposes of a course as well.

J. BERGOU

J. M. IRVINE:

Nuclear Structure Theory

Pergamon Press Ltd, Oxford, 1972

This book is basically different from any conventional textbook on nuclear structure. Especially Part I presenting a large compilation of experimental data in an unsophisticated manner and, as far as possible, without any theoretical interpretation or comment, seems to be rather unusual in the literature on nuclear theory. It is, however, an excellent guide to the phenomena which nuclear structure theories must seek to explain. Extensive mass tables and energy level diagrams are also included in order to increase the usefulness of the book as a reference work. Part I also contains a brief review of the properties of elementary particles, together with a short description of the meson theory of nuclear forces.

Part II presents an account of the nuclear many-body problem. Several theories, designed to explain gross nuclear properties, such as binding energies, charge and mass distributions etc. are treated in a clear and reasonably selfcontained manner. Part II provides a good foundation for the various nuclear models, discussed in Part III.

Part IV deals with the technology of nuclear structure theory. It reviews mathematical techniques and formalism widely used in calculations, such as occupation number representation, angular momentum algebra, application of group theoretical methods to nuclear structure and scattering theory.

The monograph exhibits the author's own way of looking at nuclear physics. This unique point of view makes the book not only useful for university lecturers, research workers and students, but also highly enjoyable and fascinating.

J. NÉMETH

Printed in Hungary

A kiadásért felel az Akadémiai Kiadó igazgatója — Műszaki szerkesztő: Botyánszky Pál
A kézirat nyomdába érkezett: 1976. VIII. 22. — Terjedelem: 7,25 (A/5) ív, 11 ábra

77.3490 Akadémiai Nyomda, Budapest — Felelős vezető: Bernát György

NOTES TO CONTRIBUTORS

I. PAPERS will be considered for publication in Acta Physica Hungarica only if they have not previously been published or submitted for publication elsewhere. They may be written in English, French, German or Russian.

Papers should be submitted to

Prof. I. Kovács, Editor
Department of Atomic Physics, Polytechnical University
1521 Budapest, Budafoki út 8, Hungary

Papers may be either articles with abstracts or short communications. Both should be as concise as possible, articles in general not exceeding 25 typed pages, short communications 8 typed pages.

II. MANUSCRIPTS

1. Papers should be submitted in five copies.

2. The text of papers must be of high stylistic standard, requiring minor corrections only.

3. Manuscripts should be typed in double spacing on good quality paper, with generous margins.

4. The name of the author(s) and of the institutes where the work was carried out should appear on the first page of the manuscript.

5. Particular care should be taken with mathematical expressions. The following should be clearly distinguished, e.g. by underlining in different colours: special founts (italics, script, bold type, Greek, Gothic, etc); capital and small letters; subscripts and superscripts, e.g. x^3, x_3; small l and 1; zero and capital O; in expressions written by hand: e and i, n and u, c and v, etc.

6. References should be numbered serially and listed at the end of the paper in the following form: J. Ise and W. D. Fretter, Phys. Rev., *76*, 933, 1949.

For books, please give the initials and family name of the author(s), title, name of publisher, place and year of publication, e.g.: J. C. Slater, Quantum Theory of Atomic Structures, I. McGraw-Hill Book Company Inc., New York, 1960.

References should be given in the text in the following forms: Heisenberg [5] or [5]

7. Captions to illustrations should be listed on a separate sheet, not inserted in the text.

III. ILLUSTRATIONS AND TABLES

1. Each paper should be accompanied by five sets of illustrations, one of which must be ready for the blockmaker. The other sets attached to the copies of the manuscript may be rough drawings in pencil or photocopies.

2. Illustrations must not be inserted in the text.

3. All illustrations should be identified in blue pencil by the author's name, abbreviated title of the paper and figure number.

4. Tables should be typed on separate pages and have captions describing their content. Clear wording of column heads is advisable. Tables should be numbered in Roman numerals (I, II, III, etc.).

IV. MANUSCRIPTS not in conformity with the above Notes will immediately be returned to authors for revision. The date of receipt to be shown on the paper will in such cases be that of the receipt of the revised manuscript.

Reviews of the Hungarian Academy of Sciences are obtainable at the following addresses:

AUSTRALIA

C. B. D. Library and Subscription Service
Box 4886, G. P. O.
Sydney N. S. W. 2001

Cosmos Bookshop
145 Acland St.
St. *Kilda 3182*

AUSTRIA

Globus
Höchstädtplatz 3
A—1200 Wien XX

BELGIUM

Office International de Librairie
30 Avenue Marnix
1050-Bruxelles

Du Monde Entier
162 Rue du Midi
1000—Bruxelles

BULGARIA

Hemus
Bulvar Ruszki 6
Sofia

CANADA

Pannonia Books
P. O. Box 1017
Postal Station "B"
Toronto, Ont. M5T 2T8

CHINA

C N P I C O R
Periodical Department
P. O. Box 50
Peking

CZECHOSLOVAKIA

Mad'arská Kultura
Národní třida 22
115 66 Praha

PNS Dovoz tisku
Vinohradská 46
Praha 2

PNS Dovoz tlače
Bratislava 2

DENMARK

Ejnar Munksgaard
Nörregade 6
DK—1165 Copenhagen K

FINLAND

Akateeminen Kirjakauppa
P. O. Box 128
SF-00101 Helsinki 10

FRANCE

Office International de Documentation et Librairie
48, Rue Gay-Lussac
Paris 5

Librairie Lavoisier
11 Rue Lavoisier
Paris 8

Europeriodiques S. A.
31 Avenue de Versailles
78170 La Celle St. Cloud

GERMAN DEMOCRATIC REPUBLIC

Haus der Ungarischen Kultur
Karl-Liebknecht-Strasse 9
DDR—102 Berlin

Deutsche Post
Zeitungsvertriebsamt
Strasse der Pariser Kommüne 3—4
DDR-104 Berlin

GERMAN FEDERAL REPUBLIC

Kunst und Wissen
Erich Bieber
Postfach 46
7 Stuttgart 5

GREAT BRITAIN

Blackwell's Periodicals
P. O. Box 40
Hythe Bridge Street
Oxford OX1 2EU

Collet's Holdings Ltd.
Denington Estate
London Road
Wellingborough Northants NN8 2QT

Bumpus Haldane and Maxwell Ltd.
5 Fitzroy Square
London W1P 5AH

Dawson and Sons Ltd.
Cannon House
Park Farm Road
Folkestone, Kent

HOLLAND

Swets and Zeitlinger
Heereweg 347b
Lisse

Martinus Nijhoff
Lange Voorhout 9
The Hague

INDIA

Hind Book House
66 Babar Road
New Delhi 1

India Book House
Subscription Agency
249 Dr. D. N. Road
Bombay 1

ITALY

Santo Vanasia
Via M. Macchi 71
20124 Milano

Libreria Commissionaria Sansoni
Via Lamarmora 45
50121 Firenze

JAPAN

Kinokuniya Book-Store Co. Ltd.
826 Tsunohazu 1-chome
Shinjuku-ku
Tokyo 160—91

Maruzen and Co. Ltd.
P. O. Box 5050
Tokyo International 100—31

Nauka Ltd.-Export Department
2—2 Kanda
Jinbocho
Chiyoda-ku
Tokyo 101

KOREA

Chulpanmul
Phenjan

NORWAY

Tanum-Cammermayer
Karl Johansgatan 41—43
Oslo 1

POLAND

Węgierski Instytut Kultury
Marszalkowska 80
Warszawa

CKP I W
ul. Towarowa 28
00—958 Warsaw

ROUMANIA

D. E. P.
Bucureşti

Romlibri
Str. Biserica Amzei 7
Bucureşti

SOVIET UNION

Sojuzpechatj — Import
Moscow

and the post offices in each town

Mezhdunarodnaya Kniga
Moscow G—200

SWEDEN

Almqvist and Wiksell
Gamla Brogatan 26
S—101 20 Stockholm

A. B. Nordiska Bokhandeln
Kunstgatan 4
101 10 Stockholm 1 Fack

SWITZERLAND

Karger Libri AG.
Arnold-Böcklin-Str. 25
4000 Basel 11

USA

F. W. Faxon Co. Inc.
15 Southwest Park
Westwood, Mass. 02090

Stechert-Hafner Inc.
Serials Fulfillment
P. O. Box 900
Riverside N. J. 08075

Fam Book Service
69 Fifth Avenue
New York N. Y. 1003

Maxwell Scientific International Inc.
Fairview Park
Elmsford N. Y. 10523

Read More Publications Inc.
140 Cedar Street
New York N. Y. 10006

VIETNAM

Xunhasaba
32, Hai Ba Trung
Hanoi

YUGOSLAVIA

Jugoslavenska Knjiga
Terazije 27
Beograd

Forum
Vojvode Mišiča 1
21000 Novi Sad

ACTA PHYSICA

ACADEMIAE SCIENTIARUM HUNGARICAE

TOMUS XLI FASCICULUS 3

AKADÉMIAI KIADÓ, BUDAPEST

1976

ACTA PHYS. HUNG. APAHAQ 41 (3) 153–229 (1976)

ACTA PHYSICA

ACADEMIAE SCIENTIARUM HUNGARICAE

SZERKESZTI

KOVÁCS ISTVÁN

Az *Acta Physica* angol, német, francia vagy orosz nyelven közöl értekezéseket. Évente két kötetben, kötetenként 4—4 füzetben jelenik meg. Kéziratok a szerkesztőség címére (1521 Budapest XI., Budafoki út 8.) küldendők.

Megrendelhető a belföld számára az Akadémiai Kiadónál (1363 Budapest Pf. 24. Bankszámla 215-11488), a külföld számára pedig a „Kultúra" Könyv és Hírlap Külkereskedelmi Vállalatnál (1389 Budapest 62, P. O. B. 149. Bankszámla 217-10990 sz.), vagy annak külföldi képviseleteinél és bizományosainál.

The *Acta Physica* publish papers on physics in English, German, French or Russian, in issues making up two volumes per year. Subscription price: $32.00 per volume. Distributor: KULTURA Hungarian Trading Co. for Books and Newspapers (1389 Budapest 62, P. O. Box 149) or its representatives abroad.

Die *Acta Physica* veröffentlichen Abhandlungen aus dem Bereich der Physik in deutscher, englischer, französischer oder russischer Sprache, in Heften die jährlich zwei Bände bilden.

Abonnementspreis pro Band: $32.00. Bestellbar bei: KULTURA Buch- und Zeitungs-Außenhandelsunternehmen (1389 Budapest 62, Postfach 149) oder bei seinen Auslandsvertretungen.

Les *Acta Physica* publient des travaux du domaine de la physique, en français, anglais, allemand ou russe, en fascicules qui forment deux volumes par an.

Prix de l'abonnement: $32.00 par volume. On peut s'abonner à l'Entreprise du Commerce Extérieur de Livres et Journaux KULTURA (1389 Budapest 62, P. O. B. 149) ou chez ses représentants à l'étranger.

«*Acta Physica*» публикуют трактаты из области физических наук на русском, немецком, английском и французском языках.

«*Acta Physica*» выходят отдельными выпусками, составляющими два тома в год.

Подписная цена — $32.00 за том. Заказы принимает предприятие по внешней торговле книг и газет KULTURA (1389 Budapest 62, P. O. B. 149) или его заграничные представительства и уполномоченные.

ACTA PHYSICA

ACADEMIAE SCIENTIARUM HUNGARICAE

TOMUS XLI FASCICULUS 3

AKADÉMIAI KIADÓ, BUDAPEST

1976

ACTA PHYS. HUNG.

INDEX

Acta Physica Academiae Scientiarum Hungaricae, Tomus 41 (3), pp. 153—158 (1976)

ON THE INERTIAL-GRAVITATIONAL FIELD

By

L. D. RAIGORODSKI

DEPARTMENT OF PHYSICS, LENINGRAD SHIPBUILDING INSTITUTE, LENINGRAD, USSR

(Received 14. IV. 1976)

The physical significance of the inertial-gravitational field is discussed.

The method best suited for the study of the properties of any physical field (or the properties of space-time, i.e. the gravitational field) is the investigation of characteristics of the motion of test particles moving in the field (or in the curved space-time) under examination.

The most complete information about the field (about the geometry of the space-time) can be obtained from the comparison of world-lines of test objects.

In the case of an electromagnetic field the role of test objects is played by the small point charges and exhaustive information about the field can be obtained from the comparison of the behaviour of the test charges moving in the field studied with the behaviour of the neutral (uncharged) particles moving freely in the same field (because they do not interact with the field). These uncharged particles constitute the frame of reference.

In studying the properties of the space-time (gravitational field) it is impossible in general to discern the test particles from particles belonging to (or forming) the frame of reference, because "gravineutral" physical objects (i.e. particles without mass) do not exist, and the concept of the frame of reference in the curved space-time becomes indeterminate. The only way to study the gravitational field (or the corresponding properties of the curved space-time) is the comparison of properties of the free (geodesic) motion of the test particles moving along the adjacent world-lines. In this case the "frame of reference" consists of test particles placed on the infinitesimal hypersurface orthogonal to the world-line of the chosen test particle — observer. It is important that if the whole collection of test particles (the cloud of dust-like matter) moves in the homogeneous gravitational field and the "external" reference points are missing (or they are included in the system of test particles in question) then there is no possibility to ascertain the properties of this field. Moreover, it is impossible to discover whether this system moves in the homogeneous gravitational field or freely in the flat space-time.

However, the cloud consisting of noninteracting identifiable test particles (noncoherent fluid) is the most perfect test object for the investigation of the

properties of space-time (inertial and gravitational fields). The comparison of neighbour world-lines of test particles can provide all information available in principle about the properties of the space-time in the region filled by the noncoherent fluid.

The theory of the gravitational and the inertial fields is based on the geodesic principle.

In accordance with this principle the motion of test particles in the gravitational field is the free motion of these particles in the curved space-time and the geodesic equations are the equations of motion in the gravitational field:

$$\frac{Du^i}{ds} = \frac{du^i}{ds} + \Gamma^i_{kl} u^k u^l = 0, \tag{1}$$

where s is a canonical parameter (the proper time), D/ds is the operator of the absolute derivative with respect to s, Γ^i_{kl} are Christoffel symbols,

$$u^i = \frac{dx^i}{ds} \tag{2}$$

are components of the 4-velocity of the test particle,

$$u_i u^i = g_{ik} u^i u^k = -1. \tag{3}$$

g_{ik} is the metric tensor. The usual summation convention is used.

The equations of motion (1) are the geodesic equations of the first kind.

However, so long as we suppose that the using of the collection of particles (the cloud of dust) in the capacity of the test object is more effective than one particle, it is worth-while to use the geodesic equations in the following form [1]:

$$G_{ki} u^k = 0 \tag{4}$$

(the geodesic equations of the second kind), where

$$G_{ki} = u_{i,k} - u_{k,i}. \tag{5}$$

(A comma denotes the partial derivative).

The geodesic equations of the second kind (4) are the degenerate Lorentz type equations of motion. They are the equations of stream-lines in the noncoherent fluid consisting of identifiable test particles moving in the curved space-time. We interpret the skew-symmetric tensor G_{ik} (5) as the "4-strength" of a hypothetical inertial-gravitational vector field [2]. Components of the 4-velocity of particles of the dust-like matter moving in the field are the inertial-gravitational potentials.

"Although the four dimensional formulation of Einstein's theory is perfect from a geometrical point of view, it cannot disclose all physical aspects

without the introduction of a physical frame of reference (preferred or not) which gives rise to the local separation of space from time. This frame which according to one's approach can be represented by a tetrad field or even by a simple unit vector field, is (...) an essential physical element..." (CATTANEO [3]).

We suppose that the inertial-gravitational field has the same physical significance as CATTANEO's unit vector field.

Let us discuss the meaning of the characteristics of the inertial-gravitational field G_{ki}.

World-lines of particles of the dust-like matter (stream-lines in the non-coherent fluid) form a congruence and if test particles move freely in the space-time their world-lines form a geodesic congruence (in accordance with the geodesic principle).

A congruence of world-lines can be normal or non-normal.

By definition a congruence of world-lines is normal if there exists a family of hypersurfaces to which these world-lines (stream-lines) are orthogonal. A geodesic congruence is normal if and only if the rotation of a unit 4-vector u_i (2) tangent to the world-lines (geodesics) of the congruence is equal to zero

$$u_{i,k} - u_{k,i} = G_{ki} = 0\,. \tag{6}$$

But if

$$G_{ki} \neq 0\,, \tag{7}$$

then the congruence is non-normal and it means that there exists no hypersurface to which each curve of the congruence is orthogonal.

Hypersurfaces orthogonal to geodesic lines of a normal geodesic congruence are loci of synchronous points and any one of them can be brought into coincidence with any other by a translation that is by a motion in which all points of the hypersurface (and test particles placed in each of them) describe the equal distance along their geodesic world-lines [4]. Hypersurfaces orthogonal to geodesics of the normal geodesic congruence are equipotential hypersurfaces;

$$u_i = \frac{\partial \varphi}{\partial x^i} \tag{8}$$

(φ is a scalar function) and from (6)

$$u_{i,k} - u_{k,i} = 0\,; \quad u_{i;k} = u_{k;i}$$

and geodesic equations are given by

$$u_{i;k}\, u^k = u_{k;i}\, u^k \equiv 0\,. \tag{9}$$

The tensor G_{ki} (5) is the covariant characteristics of the congruence, and the geodesic equations of the second kind (4) may be regarded as of great

importance as they contain the information about the type of the congruence to which the geodesics belong.

But, in general, there is a great number of geodesic congruences and the quantities G_{ki} are different for different geodesic congruences and so the physical interpretation of the tensor G_{ki} is not obvious.

To make the tensor G_{ki} the invariant characteristic of the inertial-gravitational field it is necessary to introduce an additional condition: at infinity where the space-time is flat and the metric is Galilean, test particles form the "flat" cloud of the dust-like matter and each of them is placed in one of centres of the spatial cubical lattice and $u_i(x) = \text{const}_i$. (The possibility and the necessity of the introduction of this and any other conditions can be the subject of a special discussion).

If the properties of space-time are such that world-lines of particles of the dust-like matter moving freely (from infinity) in the space-time form the non-normal congruence ($G_{ki} \neq 0$) then we say that the cause of this is the inertial-gravitational field. The rotational motion of the clouds of test particles is the indication of the presence of the inertial-gravitational field.

If the space-time admits only normal congruences of world-lines of test particles then the inertial-gravitational field is absent ($G_{ki} = 0$). Layers of test particles move translationally in the space-time of such structure.

Equations of the inertial-gravitational field can be derived from the variational principles.

There are two acceptable Lagrangians of the inertial-gravitational field

$$\Lambda^{\mathrm{I}}_{(i-g)} = a\, G^{ij} G_{ij} \sqrt{-g} \tag{10}$$

and

$$\Lambda^{\mathrm{II}}_{(i-g)} = a\,(G^{ij} G_{ij} + 2H^2) \sqrt{-g}\,, \tag{11}$$

where $a = c^4/4\pi k$, k is a Newton's constant of gravity, g is the determinant of g_{ik},

$$H = u_{k;k} \tag{12}$$

(A semicolon denotes the covariant derivative).

Let us use the action principle

$$\delta S = 0\,, \tag{13}$$

where

$$S = \frac{1}{c} \int \Lambda_\Sigma \, d\Omega \tag{14}$$

and $d\Omega = dx^0 dx^1 dx^2 dx^3$;

$$\Lambda_\Sigma = \Lambda_{(i-g)} + \Lambda_{(m)}\,. \tag{15}$$

$\Lambda_{(m)}$ is the Lagrangian characterizing all other physical objects besides the inertial-gravitational field.

Taking into account the peculiarities of variational properties of inertial-gravitational potentials u_i [5] and using in (14) and (15) the field Lagrangians (10) and (11) we obtain from (13) equations of the inertial-gravitational field in two corresponding forms

$$G^{ml}{}_{;l}\,\pi_{m\cdot ik} = \frac{1}{a}(\Theta_{ik} + \tau_{ik}) \tag{16}$$

and

$$G^{ml}{}_{;l}\,\pi_{m\cdot ik} - H_{,m}\,u^m\,p_{ik} = \frac{1}{a}(\hat{\Theta}_{ik} + \tau_{ik}), \tag{16a}$$

where

$$\Theta_{ik} = a\left(G_{il}\,G_k^{\cdot l} - \frac{1}{4}\,g_{ik}\,G^{lm}\,G_{lm}\right) \tag{17}$$

and

$$\hat{\Theta}_{ik} = \Theta_{ik} + \frac{1}{2}\,g_{ik}\,H^2 \tag{17a}$$

are two forms of the energy-momentum tensor of the inertial-gravitational field; τ_{ik} is a tensor characterizing all other physical objects as sources of the inertial-gravitational field;

$$\pi_{m\cdot ik} = u_m\,u_i\,u_k + g_{mi}\,u_k + g_{mk}\,u_i, \tag{18}$$

$$p_{ik} = g_{ik} + u_i\,u_k \tag{19}$$

is the operator of the projection in the three-dimensional space orthogonal to the world-line of the observer moving with one of a number test particles. This 3-space is the "empirical" space of the observer.

From the equations of the inertial-gravitational field one can find components of the metric tensor of the space-time curved g_{ik}, potentials u_i, and components of the metric tensor of the three-dimensional empirical space of the observer h_{ik}:

$$h_{ik} = g^{lm}\,p_{li}\,p_{mk} = p_{ik}\,. \tag{20}$$

The foundation of the theory of the inertial-gravitational field is the geodesic principle, but the interpretation of this principle in the theory presented here and in the previous papers differs from the traditional one. We use the geodesic equations in the form of the degenerated Lorentz type equations of motion (the geodesic equations of the second kind (4)) and interpret the

tensor G_{ik} by the analogy with the electromagnetic tensor as the "4-strength" of the hypothetical inertial-gravitational vector field. The essence of this theory is contained in the field equations (16) or (16a) and (5). These equations include the quasi-Maxwell type equations of the field and equations of motion in the field [1, 2]. Note that there is a possibility to connect the inertial-gravitational vector field with the tetrad field (the field of tetrads may be neither orthogonal nor normal (cf [3]), but the theory of the inertial-gravitational field is not, generally speaking, the "vector retelling" of Einstein's theory of gravitation (cf[6,7])).

The modified form of the field Lagrangian and corresponding field equations are the objects of further investigations.

REFERENCES

1. L. D. RAIGORODSKI, Phys. Letters, **32A**, 527, 1970; Acta Phys. Hung., **33**, 63, 1973.
2. L. D. RAIGORODSKI, Acta Phys. Hung., **37**, 139, 1974; Gen. Relat. and Grav., **6**, 1975.
3. C. CATTANEO, Ann. Inst. Henri Poincaré, **6**, 1, 1966.
4. L. P. EISENHART, Riemannian geometry (Princeton University Press, Princeton), 1926.
5. L. D. RAIGORODSKI, Izv. VUZ. SSSR, Fizika, **11**, 110, 1974.
6. F. A. E. PIRANI, «Les Theor. relat. de la Grav.», C.N.R.S., Paris, 1962.
7. H. DEHNEN, Z. Phys., **199**, 360, 1967.

Acta Physica Academiae Scientiarum Hungaricae, Tomus 41 (3), pp. 159—163 (1976)

INNER-SHELL IONIZATION BY ELECTRONS IN THE 300—600 keV REGION

By

B. SCHLENK, D. BERÉNYI, S. RICZ, A. VALEK and G. HOCK

INSTITUTE OF NUCLEAR RESEARCH OF THE HUNGARIAN ACADEMY OF SCIENCES (ATOMKI), 4001 DEBRECEN

(Received 14. VI. 1976)

A measuring set-up at a Cockcroft—Walton accelerator is described for the determination of electron impact inner-shell ionization cross-section detecting the X-rays by Si(Li) solid-state detector. The K-shell electron impact ionization cross-sections for Ag in the region from 300 to 600 keV were determined and compared with the earlier experimental and the calculated theoretical values.

1. Introduction

Most of the relatively few measurements on inner-shell ionization by electron impact (cf. surveys in [1—3]) have been carried out using scintillation X-ray detectors. On the other hand, especially few reliable cross-section values are available in the several hundred keV region of the bombarding electrons.

That is why we intended to use the Cockroft — Walton generator of ATOMKI accelerating electrons for electron impact inner-shell ionization measurement with Si(Li) semiconductor X-ray detection techniques.

In this paper we report first of all on the measuring arrangement and procedure including the scattering chamber, the efficiency calibration of the detector, the thickness determination of the target foil, etc. We also report on the results of measurement of the K-shell ionization cross-section for Ag in the energy region of the bombarding electrons from 300 to 600 keV.

2. Experimental arrangement and procedure

Electrons were accelerated by the Cockcroft—Walton generator of the Institute. The electron beam after passing a 90° magnet as well as a focusing and collimating system hit the target placed in the centre of the scattering chamber having a diameter of 18 cm. The high voltage of the generator was measured to 1% accuracy by a rotary-type voltmeter calibrated with elastically scattered electrons on thin foil. The energy of these scattered electrons

was measured by a Si(Li) detector of room temperature calibrated in energy with radioactive β sources and connected to the scattering chamber at an angle 45°.

A semiconductor Si(Li) X-ray spectrometer with a surface of 50 mm^2 cooled by liquid nitrogen was used to detect the X-rays originated from the target. It was placed at a distance of 48 cm from the target and it was mounted to the scattering chamber at an angle of 90° with respect to the incident beam. The Be window on the face of the detector was 0.025 mm thick. The whole arrangement is schematically shown in Fig. 1. In the tube between the scatter-

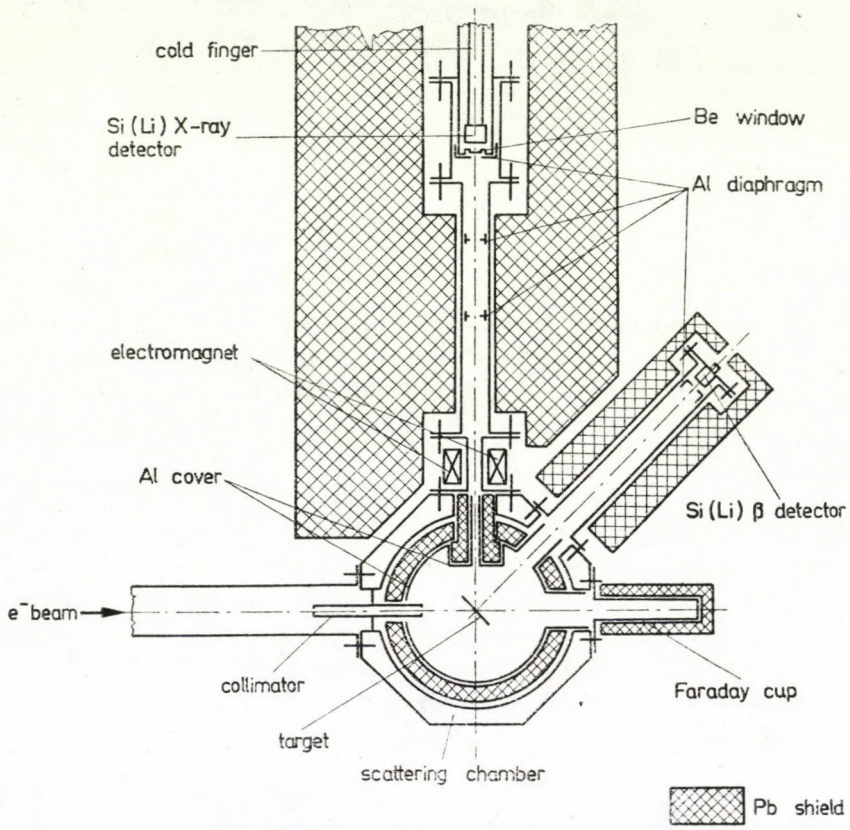

Fig. 1. Sketch of the experimental arrangement

ing chamber and the detector a high vacuum (cca. 10^{-5} Hgmm) was maintained as in the scattering chamber. At the same time the tube and the detector were surrounded by a lead shield of 15—20 cm thickness to reduce the background mainly due to external bremsstrahlung. The electrons scattered from the target

were swept by a small electro-magnet preventing electrons to get to the Si(Li) detector.

The whole charge in the electron beam was collected by the insulated scattering chamber and a Faraday cup and it was measured by a current integrator. The Faraday cup outside and the scattering chamber inside were shielded with lead of about 2 cm thickness for correct charge collection. In addition, the inner surface of the chamber was lined with an aluminium layer of 1 mm thickness in order to reduce the background originated from the scattered electrons. During the course of the measurements the typical electron beam current was 30—50 nA.

The targets were self-supporting foils of about 150—300 $\mu g/cm^2$ thick prepared by vacuum evaporation techniques. The thickness of the targets was determined by direct weighing using a micro-balance.

The absolute efficiency of the detector having a resolution (FWHM) of 320 eV at 6.4 keV was determined by means of standard calibrated radioactive sources of ^{137}Cs, ^{241}Am and ^{57}Co, ^{54}Mn from IAEA, Vienna and OHM, Budapest, respectively.

3. Measurements and results

For the determination of cross-section the following formula was used

$$\sigma = \frac{N_x}{N_e n \varepsilon \omega_K},$$

where N_x is the number of X-rays detected (pulses under the respective peak in the X-ray spectrum), N_e is the number of the bombarding electrons, n is the number of atoms per cm^2 in the target, ε is the efficiency of the X-ray detector and finally, ω_K is the fluorescence yield [4].

Table I

K-shell ionization cross-section for Ag ($\omega_K = 0.834$)

Energy (keV)	Cross-section (barn)		
	Experimental	Theoretical[a]	Theoretical[b]
300	55.9±5.6	54.20	48.19
400	53.0±5.3	52.43	47.20
500	50.2±5.0	51.61	46.88
600	52.1±5.2	51.33	46.88

[a] KOLBENSTVEDT theory
[b] PESSA and NEWELL theory

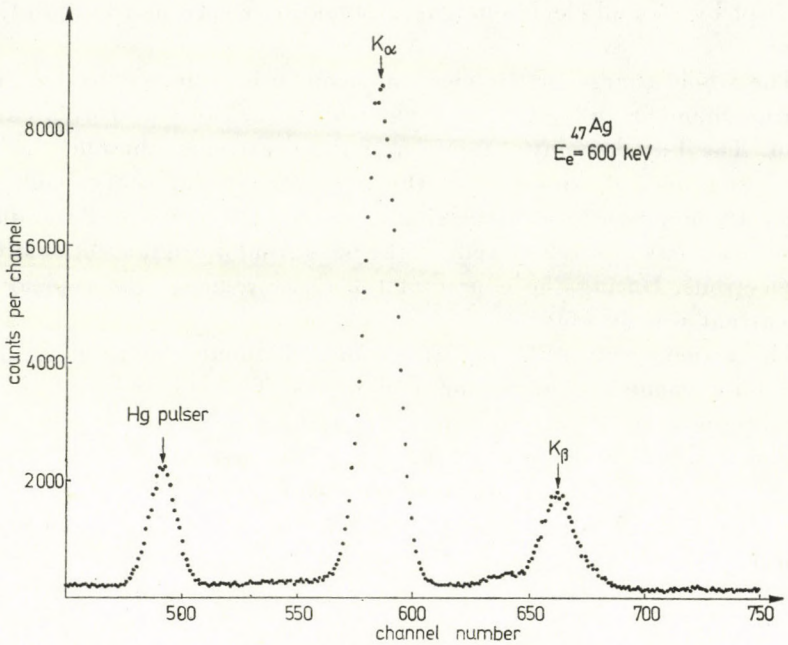

Fig. 2. K—X-ray spectrum from silver target by electron impact

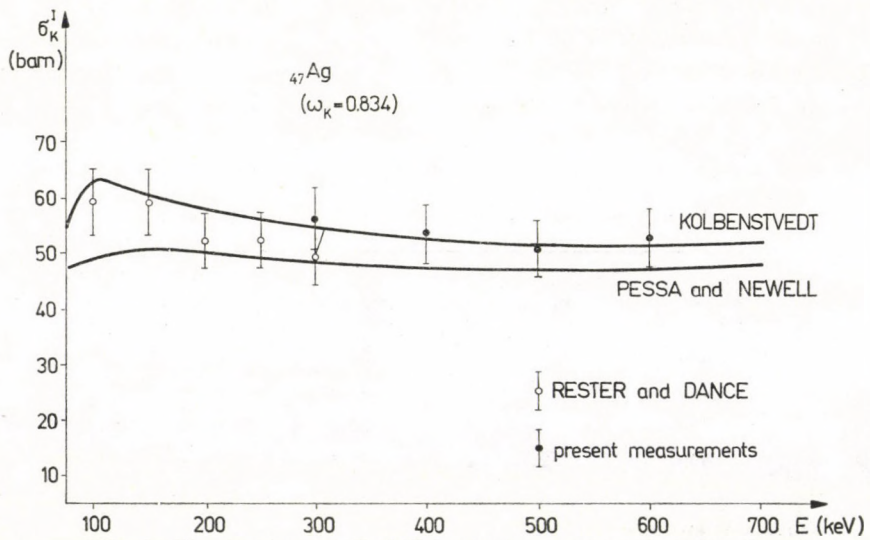

Fig. 3. Electron impact K-shell ionization cross-sections for silver

The K-shell ionization cross-section for Ag was determined in the energy region from 300 to 600 keV of the bombarding electrons. A typical X-ray spectrum in the region of the Ag K—X-rays is shown in Fig. 2.

The cross-section values are given in Table I and plotted in Fig. 3. The present experimental values were compared with the most reliable earlier experimental values of REster and DANCE [5] and with the theoretical values calculated from KOLBENSTVEDT's revised theory [6] and that of PESSA and NEWELL [7]. As can be seen the agreement is fairly good with the previous experiment and also with the theoretical values of KOLBENSTVEDT.

In the estimation of the error of the present experimental values, the main contributions came from the spectrum analysis (background subtraction), from the measurement of the target thickness and from the efficiency calibration of the detector. Thus the total error is estimated to be about 10 per cent.

REFERENCES

1. C. B. O. MOHR, Adv. in Atomic and Molecular Phys. **4**, 221, 1968.
2. H. S. W. MASSEY and E. H. S. BURHOP, "Electronic and Ionic Impact Phenomena". Vol. I. Oxford Univ. Press, Oxford, 1969 p. 158.
3. C. J. POWELL, Rev. Mod. Phys., **48**, 33, 1976.
4. W. BAMBYNEK, B. CRASEMANN, R. W. FINK, H. U. FREUND, H. MARK, C. D. SWIFT, R. E. PRICE and P. V. RAO, Rev. Mod. Phys., **44**, 716, 1972.
5. D. M. REster and W. E. DANCE, Phys. Rev., **152**, 1, 1966.
6. L. M. MIDDLEMAN, R. L. FORD and R. HOFSTADTER, Phys. Rev., *A***2**, 1429, 1970.
7. W. M. PESSA and W. R. NEWELL, Phys. Scripta, **3**, 165, 1971.

Acta Physica Academiae Scientiarum Hungaricae, Tomus 41 (3), pp. 165—171 (1976)

LATTICE DYNAMICAL STUDY OF PLATINUM

By

R. C. Rai and M. P. Hemkar

PHYSICS DEPARTMENT, UNIVERSITY OF ALLAHABAD, ALLAHABAD, INDIA

(Received 18. VI. 1976)

A modified angular force model which takes into account the effect of electron-ion interaction on the basis of Sharma and Joshi model along with the ion-ion central and de Launay type angular interaction, has been applied to investigate the phonon dispersion curves, vibrational spectrum and specific heat of platinum. The calculated results show satisfactory agreement with the experimental data.

1. Introduction

In spite of the significant advances made in the recent past, the lattice dynamics of metallic crystals remains one of the most interesting field of investigation to undertake. The theory is still far from a stage of completion and phenomenological force models based on empirical relations are still necessary for a proper understanding of the vibrational properties. It is well known that the Cauchy relation ($C_{12} = C_{44}$) does not hold for metals and Fuchs [1] attributed the cause of this failure to the presence of conduction electrons. Quite recently, Behari and Tripathi [2—5] have investigated the lattice dynamics of several body-centred and face-centred cubic metals using a modified form of a non-central force model which takes into account de Launay [6] type angular forces and Sharma and Joshi [7] type volume forces along with the ion-ion central interaction. It was emphasized that the Cauchy discrepancy in metals arises because of the angular interaction between a pair of ions and the presence of electron gas. The frequencies calculated on this approach were found to show good agreement with the recent experimental neutron scattering data for almost all the cases. In a recent study, we have utilized this model as well to explain many other solid state phenomena for a number of cubic metals [8, 9]. In view of the relative success and simplicity of this model, it was thought of interest to employ it to other complicated cases of transition metals. In the present communication we have considered platinum for lattice dynamical study, because of its high stiffness constants C_{11} and C_{12} and departure from Cauchy relation which is is very much greater in it than in copper ($C_{12}/C_{442} = 1.53$ for Cu and 3.82 for Pt). It shows that angular forces are more important in platinum. Thus platinum is a suitable metal to test the validity of modified angular force model. On the basis of this model we have

calculated phonon dispersion relations, frequency spectrum and the specific heat of platinum. An independent stimulus to the present study was also imparted by the availability of experimental dispersion curves from neutron scattering [12] and specific heat data [10].

2. Secular determinant

The secular equation for the determination of vibration frequencies can be written as:

$$| D(q) - 4\pi^2 \nu^2 m I | = 0 , \tag{1}$$

where I is the unit matrix of order three and m is the mass of the atom. The elements D_{ij} of the dynamical matrix D can be expressed as the sum of the three interaction terms as explained above. The expressions for two typical elements of the dynamical matrix for *fcc* structure are given by:

$$D_{ii}(q) = 2(\alpha_1 + \alpha')[2 - C_i(C_j + C_k)] + 4\alpha_2 S_i^2 + 4\alpha'(1 - C_j C_k) + \\ + 4\alpha''(S_j^2 + S_k^2) + 2a^3 q_i^2 K_e G^2(q r_0) , \tag{2(a)}$$

$$D_{ij}(q) = 2(\alpha_1 - \alpha') S_i S_j + 2a^3 q_i q_j K_e G^2(q r_0) , \tag{2(b)}$$

where

$$C_i = \cos a q_i , \; S_i = \sin a q_i , \; G(x) = \frac{3(\sin x - x \cos x)}{x^3} .$$

r_0 is the radius of the Wigner — Seitz sphere, $2a$ the lattice constant, $q(|q| = 2\pi/\lambda)$ the phonon wave-vector, α_1, α_2 (radial); α', α'' (angular) and K_e (corresponding to the bulk modulus of the electron gas) are the five force constants. These constants are determined by expanding the elements of the determinant in the long wave-length limit and relating them to the three elastic constants and two zone boundary frequencies (ν_L, ν_T) in [ζ00] direction. The resulting relations are

$$aK_e = \frac{2\pi^2 m(\nu_L^2 - \nu_T^2) - 2a(C_{44} + C_{12})}{(\pi^2 G^2 - 2)} , \tag{3(a)}$$

$$\alpha_1 = \frac{1}{8}[6m\pi^2 \nu_L^2 - 4m\pi^2 \nu_T^2 - 3a K_e \pi^2 G^2] , \tag{3(b)}$$

$$\alpha_2 = \frac{1}{8}[a K_e \{\pi^2 G^2 - 4\} - 2\pi^2 \nu_L^2 m + 4a C_{11}] , \tag{3(c)}$$

$$\alpha' = \frac{1}{8}\left[4m\,\pi^2\,\nu_T^2 - 2m\,\pi^2\,\nu_L^2 + a\,K_e\,\pi^2\,G^2\right], \qquad 3(d)$$

$$\alpha'' = \frac{1}{2}\left[a\,C_{44} - \frac{1}{2}\,m\,\pi^2\,\nu_T^2\right]. \qquad 3(e)$$

The relevant constants and calculated values of the various force constants are presented in Table I.

Table I

Constants and calculated parameters for platinum

Constants/Parameters	
Constants	
C_{11} (10^{11} dyn cm^{-2})	34.67
C_{12} (10^{11} dyn cm^{-2})	25.07
C_{44} (10^{11} dyn cm^{-2})	7.65
$2a$ (10^{-8} cm)	3.923
L (10^{12} Hz)	5.8
T (10^{12} Hz)	3.84
Calculated parameters	
aK_e (10^3 dyn cm^{-2})	−12.4065
1 (10^3 dyn cm^{-1})	69.2143
2 (10^3 dyn cm^{-1})	9.2847
(10^3 dyn cm^{-1})	−7.3723
(10^3 dyn cm^{-1})	−4.2716

3. Numerical computation

Frequency versus wave vector dispersion relations for platinum along the symmetry directions [ζ00], [ζζ0], and [ζζζ] have been determined from the solutions of secular determinant (1) along these directions. Experimental values of the elastic constants used in the computation have been taken from the work of MACFARLANE et al. [10].

To compute the frequency modes of lattice vibration, the simplest and the most straightforward method is the Blackman root sampling technique, in which the first Brillouin zone is divided into evenly spaced miniature cells. Here we have taken the axes of these cells to be 1/20th of the ordinary reciprocal cell. This gives 24000 frequencies corresponding to the 8000 points of the miniature lattices lying within the first Brillouin zone. From symmetry considerations these 8000 points are reduced to only 262 non-equivalent points (including the origin) for a face centred lattice lying within the 1/48th part of the first Brillouin zone which is irreducible under the symmetry operations that leave the roots of the secular equation unchanged. The frequencies have

been calculated for these non-equivalent points from the secular determinant (1). Each frequency has been weighted according to the symmetrically equivalent points. The importance of giving correct weights to various points has been emphasized by DAYAL and SHARAN [11]. A total of 24000 frequencies is obtained. These frequencies represent the complete vibration spectrum. After dividing the entire frequency range into a number of intervals, the smooth curve that fits into the resulting histogram has been constructed and shown in Fig. 2. It shows the two peaks characteristic of the frequency spectrum with the higher peak being sharper and towards the higher frequency side of the spectrum. It agrees well with the test that of anisotropy factor $A = 2C_{44}/(C_{11} - C_{12})$ is greater than unity, the higher peak is found towards the high frequency end.

Using the frequency spectrum the lattice specific heat at constant volume has been calculated in the usual way. The specific heat results calculated from the frequency spectrum are expressed in terms of the conventional Debye temperature θ_D.

4. Results and discussion

The theoretically calculated phonon-dispersion curves are shown in Fig. 1, where we have also plotted the experimental values obtained by the inelas-

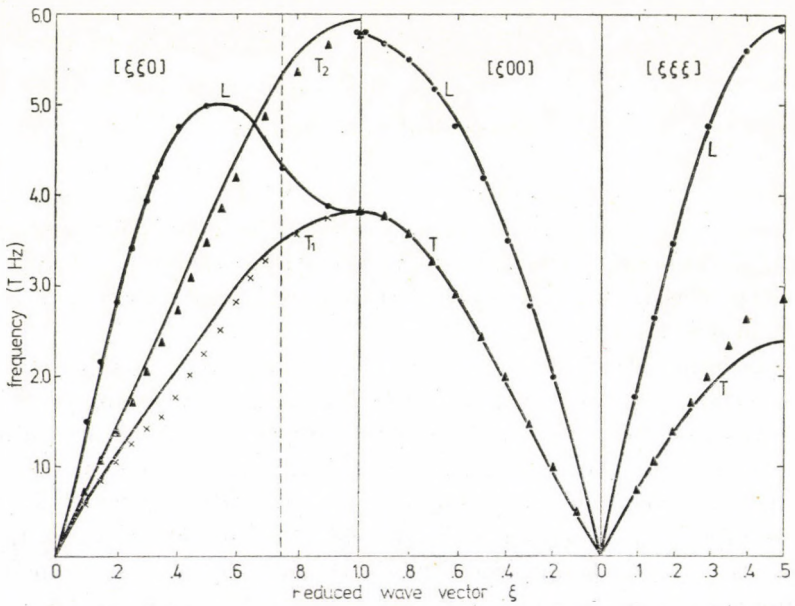

Fig. 1. Phonon dispersion curves at 90 °K in the three symmetry directions in platinum The experimental results are due to DUTTON et al. L and T correspond to the longitudinal and transverse modes

tic scattering of thermal neutron by DUTTON et al. [12]. Fig. 1 shows a fairly good agreement between theoretical and experimental results. Along 110 direction the calculated curves slightly violate the symmetry properties of a face centred structure. This deviation may be attributed to the assumption of short-range interatomic forces and to the approximate calculation of the electron lattice interaction. The analysis of the experimental data on Born—Von Kármán theory indicates that interatomic forces in platinum are of a fairly long range nature. The incomplete *d*-electronic shells which characterise the transition metals and which are responsible for their large cohesive energies (MOTT [13]) also make an important contribution to their lattice dynamical properties.

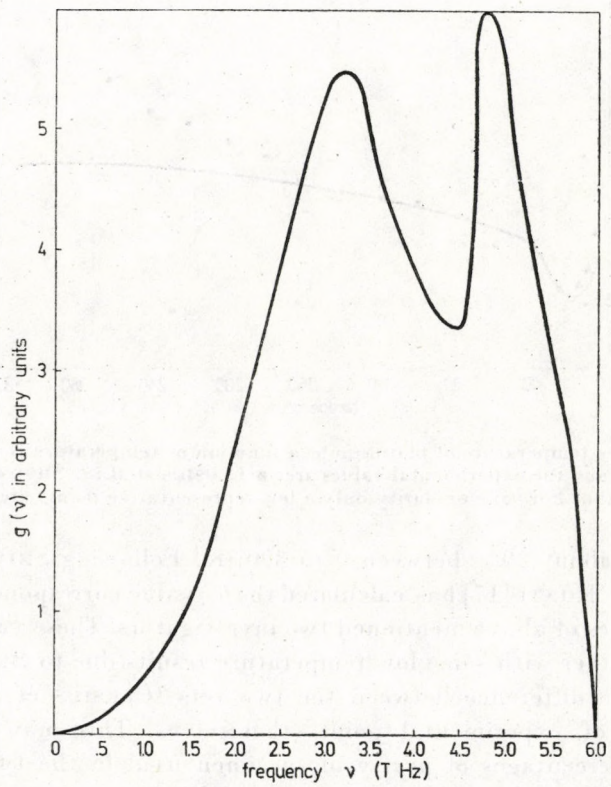

Fig. 2. The frequency spectrum of platinum

The calorimetric Debye temperature θ_D, calculated from frequency distribution is shown in Fig. 3. along with the experimental results. The specific heat of platinum has been measured by several investigators over the course of years, mostly at low temperatures. For a review of these measurements, reference may be made to FELDMAN and HORTON [14]. Only two recent

measurements [15, 16] extend to temperatures greater than 25 °K, but even these two experimental results cannot be used directly to compare with the theoretical ones. CLUSIUS et al. [15] and SHOEMAKE and RAYNE [16] have used different values of δ, the coefficient of the electronic specific heat (C_E) term, to reduce their data. SHIMIZU and KATSUKI have shown that δ decreases

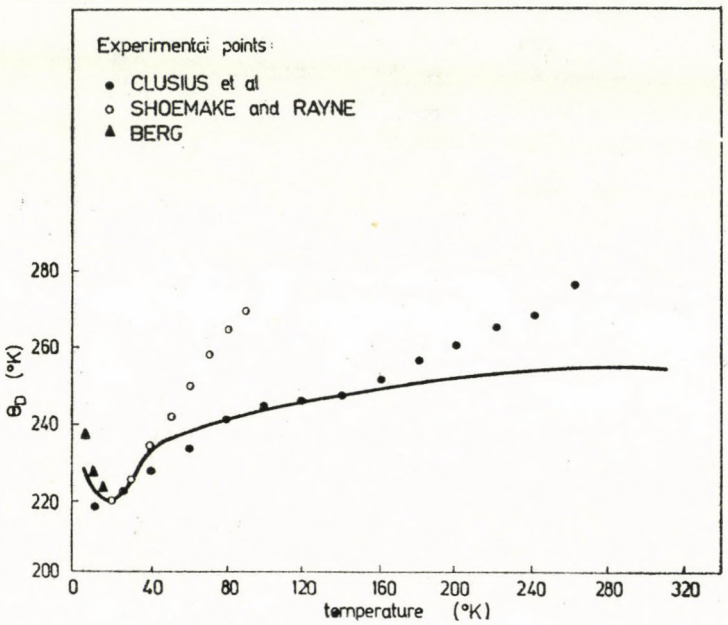

Fig. 3. The Debye temperature of platinum as a function of temperature. The solid line is the theoretical curve and the experimental values are: • CLUSIUS et al.; o SHOEMAKE and RAYNE; ▲ BERG. For sake of clarity only a few representative points are shown.

substantially about 20% between 0 to 300 °K. Following SHIMIZU and KATSUKI's method KONTI [17] has calculated the θ_D value corresponding to the specific heat values of above mentioned two investigators. These values are shown in Fig. 3, together with some low temperature results due to BERG [18]. There is considerable difference between the two sets (CLUSIUS et al., SHOEMAKE and RAYNE) of experimental points themselves. This may be attributed to different percentages of purity of specimen used in the two experiments and some error in the measurement of energy. However, our calculated result is in reasonable agreement to that of CLUSIUS et al. at moderate temperature and at very low temperature with that of SHOEMAKE and RAYNE and that of BERG. In order to get a better agreement between theoretical and experimental θ_D, a precise measurement of the specific heat of platinum over an extended temperature interval (0 to $\sim$300 °K) and a more accurate calculation of the variation of the electronic specific heat with temperature than the existing

one would be desirable. However, as things stand it emerges from the present study that the lattice vibrations in platinum could be explained satisfactorily by the modified angular force model of BEHARI and TRIPATHI.

Acknowledgements

The authors record their sincere thanks to Prof. VACHASPATI, Head of the Physics Department, Allahabad University, for encouragement and providing facilities for the study. One of us (R.C.R.) withes to thank Dr. J. PRAKASH and Mr. V. P. SINGH for useful discussions during the course of investigation.

REFERENCES

1. K. FUCHS, Proc. R. Soc. *A* **153,** 622, 1936.
2. J. BEHARI, and B. B. TRIPATHI, J. Phys. Soc. Japan, **28,** 346, 1970**a.**
3. J. BEHARI and B. B. TRIPATHI, J. Phys. C, **3,** 659, 1970**b.**
4. J. BEHARI and B. B. TRIPATHI, J. Phys. F, **1,** 19, 1971**a.**
5. J. BEHARI and B. B. TRIPATHI, Ind. J. Pure and Appl. Phys., **9,** 1037, 1971**b.**
9. J. DE LAUNAY, J. Chem. Phys. **21,** 1975, 1953; J. DE LAUNAY, "Solid State Physics", Ed. F. Seitz and D. Turnbull, Academic Press, New York, 1956 Vol. 2 p. 219.
7. P. K. SHARMA and S. K. JOSHI, J. Chem. Phys., **39,** 2633, 1963; **40,** 662, 1964.
8. S. CHANDRA and M. P. HEMKAR, Ind. J. Pure and Appl. Phys. **11,** 635, 1973.
9. J. PRAKASH, L. P. PATHAK and M. P. HEMKAR, Austr. J. Phys., **28,** 57, 1975.
10. R. F. MAC FARLANE, J. A. RAYNE and C. K. JONES, Phys. Letters, **18,** 91, 1965.
11. B. DAYAL and B. SHARAN, Proc. Roy. Soc., A **259,** 361, 1960.
12. D. H. DUTTON, B. N. BROCKHOUSE and A. P. MILLER, Can. J. Phys., **50,** 2915, 1972.
13. N. F. MOTT, Rep. Progr. Phys., **25,** 218, 1962.
14. J. L. FELDMAN and G. K. HORTON, Phys. Rev., **137,** A 1106, 1965.
15. K. CLUSIUS, C. G. LOSA and P. FRANZOSINI, Z. Naturforsch, **12***a*, 34, 1957.
16. G. E. SHOEMAKE and J. A. RAYNE, Phys. Letters, **26***A*, 222, 1968.
17. A. KONTI, J. Chem. Phys., **55,** 3997, 1971.
18. W. T. BERG, J. Phys. Chem. Solids, **30,** 69, 1969.

Acta Physica Academiae Scientiarum Hungaricae, Tomus 41 (3), pp. 173—185 (1976)

INTRODUCTION TO SPINORS AND PETROV TYPES IN GENERAL RELATIVITY

By

Z. PERJÉS

CENTRAL RESEARCH INSTITUTE FOR PHYSICS, BUDAPEST

(Received 29. VII. 1976)

An introduction to spinor methods in general relativity is presented. Gravitational equations are reformulated in spinor terms. The way of classifying gravitational fields with respect to the algebraic type of the curvature tensor is discussed. The use of Petrov classification is demonstrated on the example of the peeling-off theorem.

I

The late HERMAN WEYL remarked in his famous book "Classical Groups": "*In every Euclidean field we can construct the spin representation; the Euclidean nature of the field is essential . . . In some way Euclid's geometry must be deeply connected with the existence of the spin representation*" (He called any flat space, irrespectively of the signature of the metric, an Euclidean space).

These results of WEYL have generally been interpreted to prohibit the existence of spinors in curved space. On the other hand, we encounter many recent results in General Relativity based on the use of spinors. I only want to mention a work which is probably the most significant. NEWMAN and PENROSE had developed a spinor method by which a lot of important discoveries about the nature of gravitational field have been obtained [1].

As a preparation of our main topic, I would like to show how it is possible that — despite of the above quoted statements of WEYL — spinors could have been so successfully fitted into the theory of General Relativity. Our second point will be the thorough reformulation of EINSTEIN's gravitational equations in terms of spinors. This was the real turning-point since that the significance of spinors in the theory became generally recognized.

We shall finally see the elegance and ease achieved by use of spinors on the example of the PETROV classification of gravitational fields. The original route of classifying will be replaced by the more perspicuous spinor methods. All these matters are mainly based on the above mentioned paper of PENROSE, excepting only the following discussion of the wayout from WEYL's sceptic conclusions.

II

Let us consider the space-time, as a curved four dimensional manifold, for which it is possible to introduce in each point a *tetrad* of linearly independent basic vectors **X**; **Y**; **Z** and **T** and the normalization can be chosen such that

$$\mathbf{X}^2 = \mathbf{Y}^2 = \mathbf{Z}^2 = -1\,, \quad \mathbf{T}^2 = 1$$

further the vectors are orthogonal to each other. All these orthogonality properties can be summarized in a single equation:

$$g_{\nu\mu} = -X_\mu X_\nu - Y_\mu Y_\nu - Z_\mu Z_\nu + T_\mu T_\nu\,.$$

We can easily check that this equation contains all the orthogonality properties. For example we multiply by X^ν:

$$g_{\mu\nu}\,\mathbf{X}^\nu = -(\mathbf{X}\,\mathbf{X})\,\mathbf{X}_\mu - (\mathbf{X}\,\mathbf{Y})\,\mathbf{Y}_\mu - (\mathbf{X}\,\mathbf{Z})\,\mathbf{Z}_\mu + (\mathbf{X}\,\mathbf{T})\,\mathbf{T}_\mu\,.$$

From the linear independence of the basis vectors it follows that

$$1 + (\mathbf{X}\,\mathbf{X}) = (\mathbf{X}\,\mathbf{Y}) = (\mathbf{X}\,\mathbf{Z}) = (\mathbf{X}\,\mathbf{T}) = 0\,.$$

We can rotate the base vectors at will independently in the various points of the space-time. Let me illustrate this situation on the symbolical Fig. 1.

Fig. 1. Orientation of orthonormal frames in different space-time points

Consider now point *P*. We can express each of the new **X′**; **Y′**; **Z′** and **T′** base vectors obtained by an arbitrary rotation, in terms of the old ones:

$$\mathbf{X}' = \alpha_{11}\,\mathbf{X} + \alpha_{12}\,\mathbf{Y} + \alpha_{13}\,\mathbf{Z} + \alpha_{14}\,\mathbf{T}\,.$$
$$\cdots$$

To see the structure of the tetrad rotation group, we observe that the metric can equally well be put down in terms of the new tetrad, such that

$$\begin{aligned} g_{\mu\nu} &= -X_\mu X_\nu - Y_\mu Y_\nu - Z_\mu Z_\nu + T_\mu T_\nu = \\ &= -X'_\mu X'_\nu - Y'_\mu Y'_\nu - Z'_\mu Z'_\nu + T'_\mu T'_\nu\,. \end{aligned}$$

The transformations which preserve the above quadratic form are just the Lorentz transformations. Identifying **X**, **Y**, etc. with the orthogonal coordinates x, y etc., respectively, all properties of Lorentz transformations can be trans-

ferred to the tetrad rotation group. We must not, however, confuse the tetrad transformations with the coordinate transformations in the curved space. These latter affect the base vectors in the well-known way:

$$X'_\mu \ldots = \frac{\partial x^\nu}{\partial x'^\mu} X_\nu .$$

Now we construct a 2×2 Hermitean matrix from the basis vectors as follows:

$$\underline{M} = \frac{1}{\sqrt{2}} \begin{bmatrix} \mathbf{T} + \mathbf{Z} & \mathbf{X} - i\mathbf{Y} \\ \mathbf{X} + i\mathbf{Y} & \mathbf{T} - \mathbf{Z} \end{bmatrix}.$$

That means, $\underline{M}$ is a matrix, the elements of which are vectors. What are the transformation properties of $\underline{M}$? For coordinate transformations we obviously have:

$$\underline{M}'_\mu = \frac{\partial x^\nu}{\partial x'^\mu} \underline{M}_\nu .$$

To see the tetrad transformation rules for $\underline{M}$, we recall that replacing the elements of $\underline{M}$ by the rectilinear coordinates x, y etc., we arrive at a complex two-dimensional representation of the Lorentz group:

$$\underline{M}'_{AB'} = \Lambda^R_A \underline{M}_{RS'} \bar{\Lambda}^{S'}_{B'} \qquad \begin{matrix} A, \ldots = 0, 1 \\ B', \ldots = 0', 1' . \end{matrix}$$

Here Λ is a 2×2 unimodular matrix, and the row indices of $\underline{M}$ which transform with the adjoint of Λ, are distinguished by a prime. In general, any two component quantity ξ_A which transforms as

$$\xi'_A = \Lambda^B_A \xi_B$$

is called a (first rank) spinor. All the rules of this kind of spinor calculus are easily inferred from the usual flat-space one using the correspondence between base vectors and rectilinear coordinates. We summarize these rules in the following: Primed spinors transform like

$$\bar{\xi}_{A'} = \bar{\Lambda}^{B'}_{A'} \xi_{B'} ,$$

the components of primed spinors can be taken the complex conjugate of the unprimed components. Spinor indices are raised and lowered by the antisymmetric metric spinors

$$\varepsilon_{AB} = \varepsilon_{A'B'} = \varepsilon^{AB} = \varepsilon^{A'B'} = \begin{bmatrix} 0 & 1 \\ -1 & 0 \end{bmatrix}$$

such that, e.g., $\xi^A \eta_A$ is an invariant.

The action of a combined tetrad- and coordinate transformation on the matrix $\underline{M}$ is written as follows;

$$M'_{\mu A B'} = \frac{\partial x^\nu}{\partial x'^\mu} \Lambda^R_A M_{\nu R S'} \bar{\Lambda}^{S'}_{B'} .$$

In terms of the orthogonality properties of the base, we can verify that $\underline{M}_\mu$ satisfies

$$M_{\mu A C'} M^{C'}_{\nu B} + M_{\mu A C'} M^{C'}_{\mu B} = g_{\mu\nu} \varepsilon_{AB} .$$

This relation shows that, in our calculus, $\underline{M}$ takes over the role of the Pauli matrices. However, as is well-known, in the usual flat-space spinor calculus, the form of Pauli matrices is independent of the coordinate system. To see the relation between the flat-space calculus and the generalized one which we want to use, let us confine ourselves to Minkowskian coordinates. We may ask if it is possible to combine the two kinds of transformations such that, as a result, the form of $\underline{M}$ be unchanged. As is known, for Lorentz transformations this can be achieved. This is easily seen if we move the base vectors and coordinate axes together (Fig. 2).

It is clear, that if we rotate both the axes and the base together, then the *new* **X′**, **Y′**, . . . vectors will have the same components in the *new* coordinates as the *old* basis in the *old* coordinates, therefore the form of $\underline{M}$ is preserved

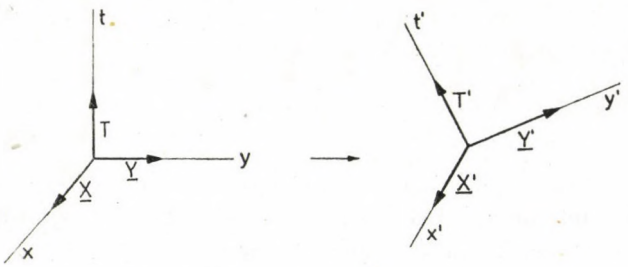

Fig. 2. Simultaneous rotation of base vectors and coordinate axes

This is just the well-known property of Pauli matrices in the usual flat-space spinor calculus. Therefore in the following we shall always write $\underline{M}_\mu = \underline{\sigma}_\mu$. Of course, in curved space we cannot stick to the rule that the components of $\underline{\sigma}_\mu$ be coordinate invariant, but, by dropping this requirement we will be allowed to perform coordinate and spin (tetrad) transformations quite independ-

ently. In the following, we may forget about tetrads and the construction of $\underline{\sigma}$'s. We must bear in mind only that there exists a set of the Hermitean matrices $\underline{\sigma}_\mu$ satisfying

$$\sigma_{\mu AC'}\sigma_{\nu B}^{C'} + \sigma_{\nu AC'}\sigma_{\mu B}^{C'} = g_{\mu\nu}\,\varepsilon_{AB}$$

in terms of which any tensor can be expressed equivalently as the set of its spinor components. For example:

$$\Phi_{\mu\nu} \leftrightarrow \Phi_{AB\dot{C}\dot{D}} \equiv \Phi_{\mu\nu}\,\sigma_{AB\dot{C}}\,\sigma_{CD\dot{C}}\,.$$

The spinor algebra has some special features which arise essentially from the identity

$$\varepsilon_{A[B}\varepsilon_{CD]} = 0\,.$$

(Bracket denotes antisymmetrization). This identity is easily checked if we recall that the indices can take only two distinct values (0 and 1), yet the antisymmetrized quantities vanish unless all the enclosed indices are distinct. The most important consequence of this identity is that antisymmetric tensors are equivalent to symmetric second-rank spinors. We can prove this if we contract the above identity with the spinor equivalent of $F_{\mu\nu} = -F_{\nu\mu}$.

$$F_{AB\dot{C}\dot{D}} = F_{\mu\nu}\,\sigma^{\mu AB'}\,\sigma^{\nu CD'}$$

and subtract the complex conjugate of the equation so obtained. As a result we have

$$F_{AB'CD\dot{C}} = \frac{1}{2}\,(\varepsilon_{AC}\,\bar{\Phi}_{B'D'} + \varepsilon_{B\dot{C}D'}\,\Phi_{AC})\,,$$

where

$$\Phi_{AC} = F_{AR'C}^{R'}\,.$$

We can construct the spinor representation of the curvature tensor along the same lines. The curvature tensor has, as it can be proven by direct computation, the symmetry properties

$$\begin{aligned} R_{\alpha\beta\gamma\delta} &= -R_{\alpha\beta\delta\gamma}\,,\\ R_{\alpha\beta\gamma\delta} &= R_{\gamma\delta\alpha\beta}\,,\\ R_{\alpha[\beta\gamma\delta]} &= 0\,. \end{aligned}$$

Using the above construction for representing antisymmetric tensors with symmetric second rank spinors, we obtain

$$R_{AE'BF'CG'DH'} = \Psi_{ABCD}\,\varepsilon_{E'F'}\,\varepsilon_{G'H'} + \varepsilon_{AB}\,\varepsilon_{CD}\,\overline{\Psi}_{E'F'G'H'} + \\ + \varepsilon_{CD}\,\Phi_{ABG'H'}\,\varepsilon_{E'F'} + \varepsilon_{AB}\,\bar{\Phi}_{E'F'CD}\,\varepsilon_{G'H'} + \\ + 2\Lambda\,(\varepsilon_{AC}\,\varepsilon_{BD}\,\varepsilon_{E'F'}\,\varepsilon_{G'H'} + \varepsilon_{AB}\,\varepsilon_{CD}\,\varepsilon_{E'H'}\,\varepsilon_{G'F'})\,.$$

Here the totally symmetric fourth-rank spinor Ψ_{ABCD} is defined thus:

$$\Psi_{ABCD} = C_{\alpha\delta\gamma\delta}\,\sigma^{\alpha}_{AE'}\,\sigma^{\beta E'}_{B}\,\sigma^{\gamma}_{CG'}\,\sigma^{\delta G'}_{D}\,.$$

$C_{\alpha\beta\gamma\delta}$ is the trace-free part of the curvature tensor and it is called *Weyl tensor or conform tensor*. This latter name stems from a symmetry property of $C_{\alpha\beta\gamma\delta}$ which momentarily is of no interest for us. In vacuum the Einstein equations reduce to $R_{\mu\nu} = 0$ and thus the traces of $R_{\alpha\beta\gamma\delta}$ all vanish, therefore in empty space we have $C_{\alpha\beta\gamma\delta} = R_{\alpha\beta\gamma\delta}$. This means that in vacuum the curvature tensor corresponds to the spinor Ψ_{ABCD}.

In the above equation the mixed fourth rank spinor $\Phi_{ABC'D'}$ represents the trace-free part of Ricci tensor $R_{\alpha\beta}$ as follows;

$$2\Phi_{ABC'D'} = \left(R_{\mu\nu} - \frac{1}{4}\,g_{\mu\nu}\,R\right)\sigma^{\mu}_{AC'}\,\sigma^{\nu}_{BD'}\,.$$

Finally, Λ is related to the curvature invariant R by

$$\Lambda = \frac{R}{24}\,.$$

III

The spinor representation of curvature tensor gives us the clue for classifying the gravitational fields with respect to the algebraic properties of this tensor. But before doing this, I want to accomplish the reformulation of gravitational equations in spinor language. First of all we obviously need some rules of spinor analysis. As is easily seen, the partial derivatives of spinors (e.g. $\partial_\mu \xi_A$) do not transform like covariant quantities. Just as for tensors, we must introduce the covariant derivative of a spinor. Again I do not want to go into the details of building up spinor analysis, I only would like to point out, that similarly to tensor analysis, we stipulate the following properties for covariant spinor derivatives [3]:

1. Linearity: $\nabla_\mu(\xi \ldots + \eta \ldots) = \nabla_\mu \xi \ldots + \nabla_\mu \bar{\xi} \ldots$
2. Leibnitz rules: $\nabla_\mu(\xi \ldots \eta \ldots) = \xi \ldots \nabla_\mu \eta + (\nabla_\mu \xi \ldots)\eta \ldots$
3. Be partial derivative on scalars: $\nabla_\mu \varphi = \varphi,_\mu$
4. Be real operation: $\overline{\nabla_\mu \xi} \ldots = \nabla_\mu \bar{\xi} \ldots$
5. The covariant derivative of the fundamental quantities $\sigma_{\mu AB'}$ and ε_{AC} should vanish:

$$\nabla_\nu \sigma_{\mu AB'} = \nabla_\nu \varepsilon_{AC} = 0 .$$

There is another version of spinor analysis, where the vanishing of $\nabla_\nu \varepsilon_{AC}$ is not required. This version was intended to include the electromagnetic four-potential into the geometry, but has the drawback that spinor indices under covariant derivatives cannot be raised and lowered. PENROSE has shown [2] that electromagnetic phenomena can be treated satisfactorily simply even if $\nabla_\nu \varepsilon_{AB} = 0$ holds.

Properties 1–5 imply that the covariant derivative of a first rank spinor has the form

$$\nabla_\mu \xi_B = \partial_\mu \xi_B - \Gamma^C_{\mu B} \xi_C ,$$

where the spinor affine connection, $\Gamma^C_{\mu B}$ is written

$$\Gamma^C_{\mu B} = \frac{1}{2} \sigma^{CR'}_\varrho (\sigma^\tau_{BR'} \Gamma^\varrho_{\mu\tau'} + \partial_\mu \sigma^\varrho_{BR'}).$$

The derivation rules for higher rank spinors follow from property 2.

We are now in position to translate differential relations of general relativity to spinor language. We have two important identities. The Ricci identity prescribes how the second covariant derivatives acting on a vector v_λ commute:

$$\nabla_\mu \nabla_\nu \nabla_\lambda - \nabla_\nu \nabla_\mu v_\lambda = R^\sigma_{\lambda\mu\nu} v_\varrho .$$

The curvature tensor, by construction, satisfies the Bianchi identity:

$$\nabla_{[\lambda} R_{\mu\nu]\varrho\sigma} = 0 .$$

The spinor translations of these identities read as follows;

$$\left.\begin{aligned} \nabla_{H(E'} \nabla^H_{F')} \xi_D &= \Phi_{DBE'F'} \xi^B \\ \nabla^{P'}_{(A} \nabla_{B|P'|} \xi_{C)} &= -\Psi_{ABCD} \xi^D + 2\Lambda \xi_{(A} \varepsilon_{B)C} \end{aligned}\right\} \text{ Ricci,}$$

$$\left.\begin{aligned} \nabla^{D}_{E'} \Psi_{ABCD} &= \nabla^{F}_{(C'} \Phi_{AB)E'F'} \\ \nabla^{BF'} \Phi_{ABE'F'} &= -3\nabla_{AE'} \Lambda \end{aligned}\right\} \text{ Bianchi.}$$

Here the "spinor derivatives" are defined by

$$\nabla_{AE'} \equiv \sigma^\mu_{AE} \nabla_\mu$$

and the parentheses denote symmetrization with the appropriate normalization factors, e.g. $\xi_{(AB)} = 1/2!(\xi_{AB} + \xi_{BA})$. Subscripts for which the symmetrization does not hold are separated by strokes.

We have now four differential identities upon which the Einstein equations are to be imposed:

$$R_{\mu\nu} - \frac{1}{2} g_{\mu\nu} R = - \varkappa T_{\mu\nu} .$$

These equations mean algebraic conditions on the quantities $\Phi_{ABC'D'}$ and Λ. For example, in empty space we have

$$\Phi_{ABC'D'} = \Lambda = 0 .$$

Thus in vacuum the field equations take the form:

$$\nabla^{D}_{E'} \Psi_{ABCD} = 0 \qquad + \text{Ricci identities.}$$

We now see that the vacuum gravitational fields are massless fourth rank spinor fields (that means, this field is of spin 2) which satisfy a covariant spinor wave equation.

The spinorial form of the gravitational equations is the starting point of the NEWMAN—PENROSE equations [1]. It is not my purpose here to give a detailed account of the NEWMAN—PENROSE method. I would like only to mention, that in the spin space, just like in the usual four dimensional space-time, it is possible to introduce a basis. This now consists of two independent spinors. All spinor quantities are expressed in terms of their projections on this basic *dyad*. The NEWMAN—PENROSE equations are essentially the dyad projections of the above spinor relations. They are extensively used for treating problems in General Relativity.

IV

Now, let us turn our attention to the classification of gravitational fields. This task was first undertaken by PETROV [4]. We shall not follow his rather complicated method but rather use spinor techniques which enabled PENROSE [2] to refine and simplify the original PETROV classification.

I have shown previously, that the decomposition of the curvature tensor in terms of irreducible spinors yields three quantities which correspond to the conformal tensor, Ricci tensor and curvature scalar, respectively. The latter quantities are locally fixed by the EINSTEIN equations for any given distribution of matter. The only quantity which essentially describes the gravitational field is the conformal tensor or the corresponding spinor $\overline{\Psi}_{ABCD}$. In addition, for empty space this tensor is the curvature itself. Therefore we shall consider the local properties of this quantity.

As PIRANI has remarked [3], one of the most elegant results of the spinor algebra is the decomposition of any symmetric spinor into the symmetrized product of first-rank spinors. Let $\varphi_{ABC\ldots}$ be an arbitrary symmetric (that means, irreducible) spinor with p indices. Consider the expression

$$\varphi(\xi) = \varphi_{ABC\ldots}\, \xi^A\, \xi^B\, \xi^C \ldots,$$

where ξ^A is a first rank spinor. Writing $z = \xi^1/\xi^0$ and separating the factor $(\xi^0)^p$ in φ we get

$$\varphi(\xi) = (\xi^0)^p\, P(z),$$

where P is a complex polynomial expression in z. We can factorize P as

$$P(z) = (\alpha_1 z - \alpha_0)(\beta_1 z - \beta_0) \ldots$$

such that for φ we may write

$$\varphi(\xi) = (\alpha_A\, \xi^A)(\beta_B\, \xi^B) \ldots .$$

Since ξ^A is arbitrary,

$$\varphi_{ABC\ldots} = \alpha_{(A}\beta_B \ldots \pi_{P)}.$$

Thus we have obtained the *canonical decomposition* of the symmetric $\varphi_{ABC\ldots}$ into the symmetrized product of first rank spinors. The spinors $\alpha_A, \beta_B, \ldots$ are called *principal spinors* and are determined up to a (complex) scalar factor. They need not be all distinct.

Any first rank spinor α_A determines a real light-like vector l_μ by

$$l_\mu = \alpha_A\, \sigma_\mu^{AB'}\, \bar{\alpha}_{B'}.$$

That the vector l_μ is light-like, follows from the fundamental properties of the $\underline{\sigma}$ matrices (see above) from which the necessary relation

$$\sigma_{AB'\mu}\, \sigma_{CD'}{}^{\mu} = \varepsilon_{AC}\, \varepsilon_{B'D'}$$

can be obtained.

Thus we see that the canonical decomposition of irreducible spinor of rank p gives at least one but at most p real null directions. Let us now consider the curvature spinor Ψ_{ABCD}. Obviously, there are six different possibilities. The type and name of the various classes is shown in Fig. 3.

The historical names for the various types will be explained later. The interrelation among PETROV types can be visualized on the PENROSE diagram (Fig. 4). Here the arrows show the direction of increasing specialization.

It is usual to call type I *algebraically general* and the remaining types *algebraically special.*

The physical significance of the PETROV classification very strikingly reveals in the "*peeling-off*" *theorem.* This theorem states that the gravitational radiational field of a localized source can be divided into shells with different PETROV types. The situation can be visualized on the qualitative picture of Fig. 5 in the ordinary three-dimensional space.

Type	Name	Symbolically
$\Psi_{ABCD} = \alpha_{(A}\beta_B\gamma_C\delta_{D)}$	I	[1111]
$\Psi_{ABCD} = \alpha_{(A}\alpha_B\beta_C\gamma_{D)}$	II	[211]
$\Psi_{ABCD} = \alpha_{(A}\alpha_B\beta_C\beta_{D)}$	D	[22]
$\Psi_{ABCD} = \alpha_{(A}\alpha_B\alpha_C\beta_{D)}$	III	[31]
$\Psi_{ABCD} = \alpha_{(A}\alpha_B\alpha_C\alpha_{D)}$	N	[4]
0	0	[-]

Fig. 3. PETROV types

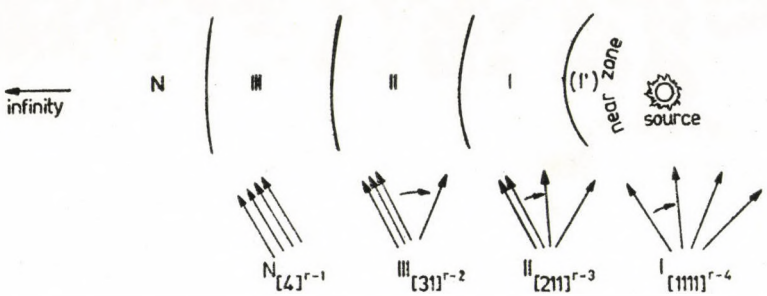

Fig. 4. PENROSE diagram

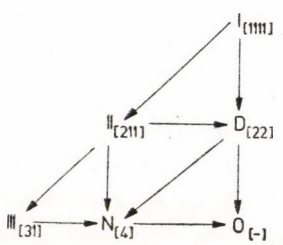

Fig. 5. The "peeling-off" theorem

This picture reflects that the curvature tensor of the radiation field can be written in the form

$$R_{\alpha\beta\gamma\delta} = \frac{N_{\alpha\beta\gamma\delta}}{r} + \frac{\mathrm{III}_{\alpha\beta\gamma\delta}}{r^2} + \frac{\mathrm{II}_{\alpha\beta\gamma\delta}}{r^3} + \frac{\mathrm{I}_{\alpha\beta\gamma\delta}}{r^4} + 0\,(r^{-5})\,.$$

Here r is an invariantly defined distance, the so-called affine distance along the lightlike radial geodesics. The r-independent coefficients belong to the PETROV types indicated. As we move from outwards to the source, the type of the gravitational field becomes more and more general. At large distances, where the type is N, all the principal directions coincide but as we approach the source, they gradually peel off.

This theorem was originally established by ROY SACHS. The proof was considerably shortened by NEWMAN and PENROSE [1]. Even in this form the calculations are rather involved and therefore in this introductory discussion it is of no use to go into details. However, we may recall that the electromagnetic radiation (in its classical version) behaves in a very similar fashion. The electromagnetic field can be represented by a second rank spinor for which we have two types altogether: the two principal spinors either coincide or not. Accordingly, the radiation zone separates into the algebraically general near zone and the degenerate radiation zone.

To demonstrate further the interplay between the type of curvature and physical processes, I would like to mention the famous GOLDBERG—SACHS theorem. According to this, a vacuum gravitational field is algebraically special if and only if it admits a shearfree light-like geodesic congruence.

We get some insight into the meaning of this theorem, if we consider a family of space-time filling light-like geodesics, called a light-like *congruence*. The curves have the tangent vector l_μ. We can imagine this system as a bundle of light rays passing through the region of space-time considered. We put an infinitesimal disc at distance r orthogonally to the rays and consider the shape of the shadow cast at $r + dr$ behind the disc. (Fig. 6). Expanding the boundary of the shadow into Legendre polynomials and neglecting higher order terms, the shape will be of the form of an ellipse with the eccentricity $\varepsilon = \sqrt{2\sigma}dr$, where the *shear* σ of the congruence is defined by

$$2\sigma^2 = l_{(\mu;\nu)}\, l^{\mu;\,\nu} - \frac{1}{2}\, l^{\mu}_{\ ;\mu}{}^{;\nu}.$$

It is interesting to classify the known exact solutions of the gravitational equations according to the PETROV type of the curvature tensor. By direct calculation we can prove that the KERR solution [6] (the stationary field of a rotating body) is of type D. Since the KERR metric goes over to the Schwarz-

schild one in the static (nonrotating) limit, the Schwarzschild metric is also of type D. There exist plane wave solutions of the vacuum Einstein equations which were found first by BRINKMAN and were investigated later by KUNDT. These plane wave solutions are of type N. Quite recently W. KINNERSLEY

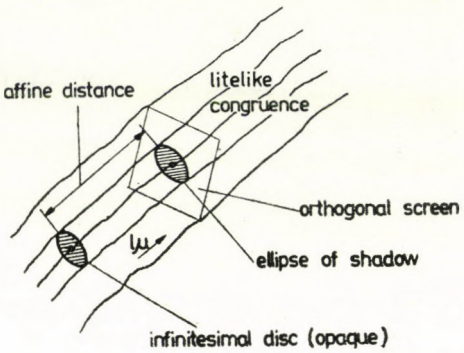

Fig. 6. Measurement of the shear σ

succeeded to find all type D metrics in explicit form. It is an interesting consequence of his work that it turned out that the KERR metric exhausts all type D fields which can represent the field of a reasonable source. This fact and other features of the KERR metric indicate that this solution plays a very fundamental role in nature.

There are also type I solutions known. WEYL has completely solved the static axially symmetric gravitational equation in empty space. WEYL's fields with a very few exceptions are of type I. Recently KÓTA and I found type I stationary solutions of the vacuum Einstein equations [7], which are not equivalent to any other metrics previously obtained. However, we do not know what kind of source can produce these latter gravitational fields. The metrics exhibit rather pathological behaviour.

Finally, I would like to stress that everything that can be done with spinor methods can also be achieved by conventional tensor calculus, although in many cases the use of spinor calculus is much more simple. Thus the PETROV classification in its original form was developed by conventional methods. I do not find it particularly useful to go here into the details of this rather complicated approach to PETROV types. However, the essence of this approach can be depicted in a way which does not show the covariance of the classification [5].

The curvature tensor is a quantity, symmetric in the first and second pair of indices. As these pairs are skewsymmetric, we may represent them in a six dimensional space according to the following rule:

$\mu\nu$	23	13	12	14	24	34
M	1	2	3	4	5	6

From the symmetry properties of $R_{\mu\nu\alpha\beta}$ follows that the 6×6 matrix representation of the curvature tensor can be partitioned in the following manner:

$$R_{AB} = \begin{bmatrix} \underline{M} & \underline{N} \\ \underline{N} & -\underline{M} \end{bmatrix}.$$

$\underline{M}$ and $\underline{N}$ are symmetric and trace-free (3×3) matrices. We can construct a complex (3×3) matrix $\underline{P}$:

$$\underline{P} = \underline{M} + i\underline{N}\,.$$

The PETROV classification arises now from the eigenvalue problem of this complex matrix. Depending on the number of the linearly independent eigenvectors the type is III (one independent eigenvector), II [2] or I [3]. If any two of the eigenvalues coincide, the type is D. If all three eigenvalues vanish, the type is N.

REFERENCES

1. E. T. NEWMAN and R. PENROSE, J. Math. Phys., **3**, 566, 1962.
2. R. PENROSE, Ann. Phys., **10**, 171, 1960.
3. F. A. E. PIRANI, in the Lectures on General Relativity, 1964.
4. A. Z. PETROV, Einstein Spaces, M. Physmat ed., 1961.
5. F. A. E. PIRANI, in the Recent Developments in General Relativity, 1962.
6. R. P. KERR, Phys. Rev. Letts., **11**, 237, 1963.
7. J. KÓTA and Z. PERJÉS, J. Math. Phys., **13**, 1695, 1972.

Acta Physica Academiae Scientiarum Hungaricae, Tomus 41 (3), pp. 187—194 (1976)

A HAMILTONIAN FORMULATION IN MAGNETOFLUID DYNAMICS

By

I. MERCHES

FACULTY OF PHYSICS, ALEXANDRU IOAN CUZA UNIVERSITY, IASI, ROMANIA

(Received 29. VII. 1976)

By using a special set of "generalized electromagnetic antipotentials", a Hamiltonian formulation is given for an inviscid, infinitely conducting fluid, undergoing an isentropic motion in an electromagnetic field. The concept of a "combined field" is used to consider the interaction between the electromagnetic field and charges (or currents). The equation of conservation of energy of the total system is obtained, as an application of the theory.

1. Introduction

Hamiltonian formulations in hydrodynamics and electrodynamics, separately, have been known for many years (see e.g. [1] and [2]). Recently, by using the concept of "combined field", we presented a symmetric Hamiltonian formulation in the electrodynamics of charged moving fluids [3].

In this paper we have constructed a suitable Hamiltonian density, leading to the equation of motion of our physical model. This has been done by using special sets of field potentials.

2. Basic equations

In 1963, CALKIN [4] wrote the source equations of the electromagnetic field in a form suitable for an action principle, by means of the so-called "polarization" **P**. Following CALKIN's formulation, we showed [5] that the electromagnetic field **E**,**B**, interacting with a charged, moving fluid, can be described in terms of the "generalized electromagnetic antipotentials" **M** and ψ

$$E_j = \varepsilon_0^{-1}(\varepsilon_{jkm}\,\partial_k M_m - P_j)\,, \tag{1}$$

$$B_j = \mu_0(\partial_j \psi + \varepsilon_{jkm} P_k v_m + \partial_t M_j)\,, \tag{2}$$

where ε_{jkm} is the Levi-Civita symbol with $\varepsilon_{123} = +1$, ∂_j is the partial derivative with respect to x_j $(j = 1, 2, 3)$, ∂_t is the partial derivative with respect

to time, ε_0 and μ_0 are the permittivity and the permeability of the medium, respectively. The generalized antipotentials **M** and ψ satisfy the homogeneous d'Alembert wave equations $\Box M_j = 0$, $\Box \psi = 0$, if and only if they are related by the Lorentz-type condition

$$\partial_j M_j + \varepsilon_0 \mu_0 \partial_t \psi = 0 . \tag{3}$$

The conservation of the fluid mass is given by the equation of continuity

$$\partial_t \varrho + \partial_j (\varrho v_j) = 0 , \tag{4}$$

while the conservation of the entropy (the motion is isentropic) is shown by the equation

$$\partial_t S + v_j \partial_j S = 0 , \tag{5}$$

where S is the entropy per unit mass (specific entropy).

We are now prepared to construct a suitable Hamiltonian density for the investigated fluid.

3. The Hamiltonian formulation

We shall develop our theory in two different cases:

a) The Hamiltonian formalism is based on the physical assumption that the charges and/or currents do not interfere explicitly in the Lagrangian density. The "polarization" **P** is used to define the generalized electromagnetic antipotentials, but it will not be present in the final result.

b) The construction of the Lagrangian density is based on the idea of "combined field", given as a combination between the electromagnetic field **E**, **B** and the "polarization" field **P**, $\mathbf{P} \times \mathbf{v}$. In this case, the Hamiltonian density contains both fields.

a) We shall use the Lagrangian density of such a fluid, given already in a previous paper [5], but in a slightly modified form. In view of (1)—(5) we have

$$\begin{aligned} L = {} & \frac{1}{2} \mu_0 \sum_j (\partial_j \psi + \varepsilon_{jkm} P_k v_m + \partial_t M_j)^2 - \frac{1}{2\varepsilon_0} \sum_j (\varepsilon_{jkm} \partial_k M_m - P_j)^2 - \\ & - \frac{1}{2\varepsilon_0} (\partial_j M_j + \varepsilon_0 \mu_0 \partial_t \psi)^2 + \frac{1}{2} \varrho v_j v_j - \varrho \varepsilon + \\ & + \varrho(\partial_t \alpha + v_j \partial_j \alpha) - \beta \varrho (\partial_t S + v_j \partial_j S) , \end{aligned} \tag{6}$$

where $\varepsilon(\varrho, S)$ is the specific internal energy. It is obvious that the Lagrangian density (6) is written as a combination between two Lagrangian densities, corresponding to the hydrodynamic [6] and the electrodynamic [2] behaviour of the fluid, respectively. In view of the Euler—Lagrange equations

$$\frac{\partial L}{\partial \sigma_\nu} - \frac{\partial}{\partial x_k}\left(\frac{\partial L}{\partial \sigma_{\nu,k}}\right) - \frac{\partial}{\partial t}\left(\frac{\partial L}{\partial \sigma_{\nu,t}}\right) = 0\,, \tag{7}$$

($k = 1, 2, 3$) and the thermodynamic fundamental equation for reversible processes

$$TdS = d\varepsilon + pd\left(\frac{1}{\varrho}\right), \tag{8}$$

one gets from (6) (see [5]):

$$\partial_j B_j = 0\,, \tag{9}$$

$$\varepsilon_{jkm}\,\partial_k E_m + \partial_t B_j = 0\,, \tag{10}$$

$$E_j + \varepsilon_{jkm}\, v_k\, B_m = 0\,, \tag{11}$$

$$v_j + \partial_j \alpha - \beta\,\partial_j S + \varrho^{-1}\,\varepsilon_{jkm}\, B_k\, P_m = 0\,, \tag{12}$$

$$\frac{1}{2}\, v_j v_j + v_j\,\partial_j \alpha + \partial_t \alpha - \varepsilon - \frac{1}{\varrho}\, p = 0\,, \tag{13}$$

$$\partial_t \beta + v_j\,\partial_j \beta = T\,. \tag{14}$$

As was shown [5], by eliminating the Lagrangian multipliers from (9)—(14) one obtains the equation of motion in MHD

$$\varrho(\partial_t v_s + v_k\,\partial_k v_s) = -\partial_s p + \varepsilon_{skm}\, j_k\, B_m\,. \tag{15}$$

This investigation tells us that the Lagrangian density (6) is suitable for a Hamiltonian formulation.

The generalized momenta p_{M_j}, p_φ, p_α, p_S, corresponding to the field variables M_j,ψ,α,S, are then

$$\begin{aligned} p_{M_j} &= B_j\,; \quad & p_\varphi &= -\mu_0(\partial_j M_j + \varepsilon_0\,\mu_0\,\partial_t \psi) = 0\,, \\ p_\alpha &= \varrho\,; \quad & p_S &= -\beta\varrho\,. \end{aligned} \tag{16}$$

If we denote by q^i the general coordinates, and by p_i their conjugate momenta, the Hamiltonian density is

$$\mathcal{H} = \sum_i p_i \partial_t q^i - L = B_j \partial_t M_j - \mu_0(\partial_j M_j + \varepsilon_0 \mu_0 \partial_t \psi)\, \partial_t \psi +$$

$$+ \varrho\, \partial_t \alpha - \beta \varrho\, \partial_t S - \frac{1}{2\mu_0} B_j B_j + \frac{1}{2} \varepsilon_0 E_j E_j - \frac{1}{2} \varrho\, v_j v_j + \varrho \varepsilon -$$

$$- \varrho(\partial_t \alpha + v_j \partial_j \alpha) + \beta \varrho(\partial_t S + v_j \partial_j S)$$

or, after performing some reduction

$$\mathcal{H} = \frac{1}{2\mu_0} B_j B_j + \frac{1}{2} \varepsilon_0 E_j E_j - B_j \partial_j \psi - \tag{17}$$

$$- \frac{1}{2\varepsilon_0} \left[\sum_i (\partial_j M_j)^2 - \varepsilon_0^2 \mu_0^2 (\partial_t \psi)^2 \right] + \frac{1}{2} \varrho\, v_j v_j + \varrho\, \varepsilon\,.$$

The Hamiltonian of the system fluid + field is then

$$Q = \int \left(\frac{1}{2\mu_0} B_j B_j + \frac{1}{2} \varepsilon_0 E_j E_j + \frac{1}{2} \varrho\, v_j v_j + \varrho\, \varepsilon \right) d\mathbf{x}\,, \tag{18}$$

and denotes the energy of the total field, as expected. In the derivation of (18) we made the supposition that the potentials M_j and ψ vanish on the boundary of the integration domain.

Next step is now to write the Hamiltonian density (17) in terms of the field variables M_j, ψ, α, S, and the conjugate momenta p_{M_j}, p_ψ, p_α, p_S. We have then

$$\mathcal{H} = \frac{1}{2\mu_0} P_{M_j} P_{M_j} + \frac{1}{2\varepsilon_0} \sum_j (\varepsilon_{jkm} \partial_k M_m - P_j)^2 - p_{M_j} \partial_j \psi +$$

$$+ \frac{1}{2\varepsilon_0 \mu_0} p_\psi (\partial_j M_j - \varepsilon_0 \mu_0 \partial_t \psi) + \tag{19}$$

$$+ \frac{1}{2} p_\alpha \sum_j \left(-\partial_j \alpha - \frac{1}{p_\alpha} p_S \partial_j S - \frac{1}{p_\alpha} \varepsilon_{jkm} p_{M_k} P_m \right)^2 + p_\alpha\, \varepsilon(p_\alpha, S)\,.$$

Hamilton's canonical equations [2]

$$\partial_t q^i = \frac{\partial \mathcal{H}}{\partial p_i}\,; \qquad \partial_t p_i = - \frac{\partial \mathcal{H}}{\partial q^i} + \frac{\partial}{\partial x_k} \left(\frac{\partial \mathcal{H}}{\partial q^i{}_{,k}} \right) \tag{20}$$

lead to the following relations:

$$\partial_t p_{M_j} = - \varepsilon_{jkm} \partial_k E_m\,, \tag{21}$$

$$\partial_t M_j = \mu_0^{-1} p_{M_j} - \partial_j \psi - \varepsilon_{jkm} P_k v_m , \tag{22}$$

$$\partial_t p_\psi = -\partial_j p_{M_j} , \tag{23}$$

$$\partial_t \psi = -(2\varepsilon_0 \mu_0)^{-1} (\partial_j M_j - \varepsilon_0 \mu_0 \partial_t \psi), \tag{24}$$

$$\partial_t p_\alpha = -\partial_j (\varrho v_j) , \tag{25}$$

$$\partial_t \alpha = -\frac{1}{2} v_j v_j - v_j \partial_j \alpha + \varepsilon + \frac{1}{p_\alpha} p , \tag{26}$$

$$\partial_t p_S = -T p_\alpha - \partial_j (p_S v_j) , \tag{27}$$

$$\partial_t S = -v_j \partial_j S . \tag{28}$$

In addition to this, if p_{P_j} is the generalized momentum associated with the polarization P_j, we still have

$$\partial_t p_{P_j} = 0 = E_j + \varepsilon_{jkm} v_k p_{M_m} . \tag{29}$$

By making allowance for (16), it is easy to show that the system of equations (21)—(29) is just the system (9)—(14), containing in excess the Lorentz condition (3), and the equation of continuity (4). Consequently, we have refound the equation of motion (15).

b) The discussion of the second case is similar. As was shown [3], the combined field is given by

$$H_j = \varepsilon_{jkm} \partial_k C_m ; \qquad D_j = -\partial_j \varphi - \varepsilon_0 \mu_0 \partial_t C_j , \tag{30}$$

where C_j and φ are the vector and scalar potentials of the combined field, respectively. The Lagrangian density can be written as

$$L^c = \frac{1}{2\varepsilon_0} \sum_j (-\partial_j \varphi - \varepsilon_0 \mu_0 \partial_t C_j)^2 - \frac{1}{2} \mu_0 \sum_j (\varepsilon_{jkm} \partial_k C_m)^2 - \tag{31}$$

$$- \frac{1}{2} \mu_0 (\partial_j C_j + \partial_t \varphi)^2 + \frac{1}{2} \varrho v_j v_j - \varrho \varepsilon + \varrho (\partial_t \alpha + v_j \partial_j \alpha) - \beta \varrho (\partial_t S + v_j \partial_j S) .$$

By taking φ, C_j, P_j, and v_j as variational parameters, one gets from (7) and (31):

$$\partial_j D_j = 0 , \tag{32}$$

$$\varepsilon_{jkm} \partial_k H_m - \partial_t D_j = 0 , \tag{33}$$

$$D_j + \varepsilon_0 \mu_0 \varepsilon_{jkm} v_k H_m = 0 , \tag{34}$$

$$v_j + \partial_j \alpha - \beta \partial_j S + \mu_0 \varrho^{-1} \varepsilon_{jkm} H_k P_m = 0 . \tag{35}$$

We therefore arrived at the source equations of the electromagnetic field [3], [4], a generalization of Ohm's law for infinite conductivity [7], and a generalization of the Clebsch's transformation in the presence of both the electromagnetic and "polarization" fields. The variation of ϱ and S leads to the equations (13) and (14). In particular, if charges and currents are absent, the "polarization" field $\mathbf{P}$, $\mathbf{P}\times\mathbf{v}$ vanishes, and equations (32)—(35) turn into (9)—(12), as expected. The generalized momenta p_{M_j}, p_φ will be replaced by p_{C_j}, p_φ, corresponding to the field variables C_j, φ, while p_α and p_S remain unchanged. The Hamiltonian density is then

$$\mathcal{H}^c = \frac{1}{2}\mu_0 H_j H_j + \frac{1}{2\varepsilon_0} D_j D_j + \mu_0 \varepsilon_{jkm} H_j P_k v_m + \\ + \frac{1}{2}\varrho v_j v_j + \varrho\varepsilon + \frac{1}{\varepsilon_0} D_j \partial_j \varphi + \frac{1}{2}\mu_0 [\sum_j (\partial_j C_j)^2 - (\partial_t \varphi)^2]. \tag{36}$$

The third term in (36) gives the interaction between the electromagnetic and the "polarization" fields. The energy of the total system is obtained by integrating (36) over a certain domain $\mathfrak{D}$. In this case the last three terms vanish and we are left with

$$Q^c = \int \left(\frac{1}{2}\mu_0 H_j H_j + \frac{1}{2\varepsilon_0} D_j D_j + \mu_0 \varepsilon_{jkm} H_j P_k v_m + \frac{1}{2}\varrho v_j v_j + \varrho\varepsilon \right) d\mathbf{x}, \tag{37}$$

or, written in a more symmetric form

$$Q^c = \int \left(\frac{1}{2} H_j B_j + \frac{1}{2} D_j E_j + \frac{1}{2}\varrho v_j v_j + \varrho\varepsilon \right) d\mathbf{x}, \tag{38}$$

where Eq. (34) has been used. If the "polarization" of the medium is negligible, the Hamiltonian (38) turns into the "classical" form (18), which proves the theory.

N. B. It is easy to see that the Lagrangian densities considered in this paper are relativistic invariants. Indeed, we can write for the first two terms in (31)

$$\frac{1}{2\varepsilon_0} D_j D_j - \frac{1}{2}\mu_0 H_j H_j = -\frac{1}{4}\mu_0 F_{ik} F_{ik}, \tag{39}$$

where F_{ik} is the combined field tensor [8]. The rest of the terms in (31) are constructed by means of either equations of conservation or quantities like ϱ, ε, S, p, which are supposed to be invariant with respect to the Lorentz transformation. The Lorentz invariance of the Lagrangian density (6) is obvious.

4. Application. The equation of conservation of energy

As we have shown [7], the combined field D,H is described by the following equations of evolution:

$$\varepsilon_0 \mu_0 \partial_t H_j + \varepsilon_{jkm} \partial_k D_m = 0 , \tag{40}$$

$$\partial_t D_j - \varepsilon_{jkm} \partial_k H_m = 0 . \tag{41}$$

The equation of motion of the fluid in the combined field is then

$$\varrho(\partial_t v_S + v_k \partial_k v_S) = -\partial_S p + \mu_0 \varepsilon_{Skm} j_k H_m . \tag{42}$$

In view of (5), (8), (33), (34), (40), (41), (42), and by means of some vector algebra, it is not difficult to perform the partial derivative with respect to time of the energy (38). The result is

$$\partial_t Q^c = \frac{1}{2\varepsilon_0} \int j_k D_k \, d\mathbf{x} - \int \pi_j^c \, dS_j - \int \varrho \left(\frac{1}{2} v_k v_k + w \right) v_j \, dS_j , \tag{43}$$

where $w = \varepsilon + p/\varrho$ is the specific enthalpy, and

$$\pi_j^c = \frac{1}{2} \varepsilon_{jkm} \left(E_k H_m + \frac{1}{\varepsilon_0 \mu_0} D_k B_m \right) \tag{44}$$

is the Poynting-like vector of the combined field.

Discussion. Equation (43) is a generalization of the equation of conservation of energy in magnetofluid dynamics. The concept of "combined field" makes it possible to consider the "polarization" of the medium, i.e. charges and/or currents. Written in this form, the equation of conservation of energy is a better approach to reality. If $\mathbf{P} = 0$ (i.e. $\mathbf{j} = 0$, $\varrho_e = 0$) $\mathbf{\Pi}^c$ turns into the usual Poynting vector $\mathbf{\Pi} = \mu_0^{-1} \mathbf{E} \times \mathbf{B}$, and Eq. (43) becomes

$$\partial_t \int \left(\frac{1}{2\mu_0} B_j B_j + \frac{1}{2} \varepsilon_0 E_j E_j + \frac{1}{2} \varrho v_j v_j + \varrho \varepsilon \right) d\mathbf{x} = \\ = - \int \left[\pi_j + \varrho \left(\frac{1}{2} v_k v_k + w \right) v_j \right] dS_j , \tag{45}$$

which is a well-known equation of conservation. We could have arrived at the same equation starting with (18) and following the same procedure as for (43).

5. Conclusion

It was the purpose of the present paper to prove the usefulness of both the "generalized electromagnetic antipotentials" and the concept of "combined field" in the development of the Hamiltonian formalism in magnetofluid dynamics. This method allows a symmetric Hamiltonian formulation, and enables us to take into consideration the interaction between a continuous system (the electromagnetic field) and point charges (or currents). An important result of this investigation is the generalized Ohm's law for infinite conductivity (34), which is useful in the study of the force-free combined field [7]. The Hamiltonian formalism also leads to the equation of conservation of energy (43) for the system: fluid + charges + currents + electromagnetic field, as a final proof of our theory.

REFERENCES

1. H. Itô, Prog. Theor. Phys., **9**, 117, 1953.
2. W. Yourgrau and S. Mandelstam, Variational Principles in Dynamics and Quantum Theory, New York, Pitman, 1960.
3. I. Merches, J. Plasma Phys., **15**, 49, 1976.
4. M. G. Calkin, Can. J. Phys., **41**, 2241, 1963.
5. I. Merches, Phys. Fluids, **12**, 2225, 1969.
6. J. W. Herivel, Proc. Camb. Phil. Soc., **51**, 344, 1955.
7. I. Merches, Phys. Letters, **55A**, 98, 1975.
8. I. Merches, Phys. Letters, **34A**, 132, 1971.

Acta Physica Academiae Scientiarum Hungaricae, Tomus 41 (3), pp. 195—200 (1976)

ZEMPLÉN'S THEOREM FOR THE SHOCK WAVES OF COLLISIONLESS ANISOTROPIC PLASMAS

By

M. DOBRÓKA

TECHNICAL UNIVERSITY FOR HEAVY INDUSTRY, DEPARTMENT OF PHYSICS, MISKOLC

(Received 4. VIII. 1976)

The consequences of the second law of thermodynamics are treated in the case of the shock waves of collisionless plasmas in the Chew—Goldberger—Low approximation. The density and at least one of the two pressures are found to have a positive jump on the strong discontinuity surface.

In an earlier paper we discussed the shock jump conditions in a collisionless anisotropic plasma and gave the classification of shock waves of this medium (the so-called CGL-plasma) [1]. It is well known, however, that the conservation equations give no conditions sufficient to select the only shock wave solutions which can exist in nature. An additional condition must be imposed, which is generally the second law of thermodynamics. GY. ZEMPLÉN was the first to discuss the consequence of this law for hydrodynamical shock waves. According to ZEMPLÉN's theorem the density and the pressure in hydrodynamics is greater behind of the strong discontinuity surface (positive side) than ahead of it (negative side). This theorem was extended to the case of magnetohydrodynamics by J. SZABÓ [2]. Because of the strong magnetic field there are two pressures in CGL approximation: $P_\perp$ and $P_{||}$, measured along with and traverse to the magnetic field. The pressure tensor is highly dependent on the magnetic field direction

$$P_{ik} = \frac{P_{||} - P_\perp}{H^2} H_i H_k + P_\perp \delta_{ik},$$

where H is the magnetic field and δ_{ik} is the Kronecker symbol. Our problem is how to formulate ZEMPLÉN's theorem in this case.

The CGL equations are consistent with the assumption of a two-temperature Maxwellian velocity distribution function:

$$f(\mathbf{r}, \mathbf{v}, t) = n(\mathbf{r}, t) \left(\frac{2\pi k T_{||}}{M}\right)^{1/2} \frac{2\pi k T_\perp}{M} \exp\left\{-\frac{M}{2k}\left[\frac{\mathbf{u}_\perp - \mathbf{v}_\perp}{T_\perp} + \frac{(\mathbf{u}_{||} - \mathbf{v}_{||})^2}{T_{||}}\right]\right\},$$

where M is the mass of ions, $\mathbf{v}(\mathbf{r},t)$ is the fluid velocity, $n(\mathbf{r},t)$ is the particle density, $P_{||} = nkT_{||}$ and $P_{\perp} = nkT_{\perp}$. On the basis of Boltzmann's H-function two entropy densities (entropy per unit mass) can be defined [3]:

$$S_{||} = \frac{1}{3} C_v \ln \frac{P_{||} H^2}{\varrho^3},$$

$$S_{\perp} = \frac{2}{3} C_v \ln \frac{P_{\perp}}{\varrho H},$$

where $\varrho = nM$ and C_v is the specific heat. The total entropy is

$$S = S_{||} + S_{\perp} = C_v \ln \frac{P_{||}^{1/3} P_{\perp}^{2/3}}{\varrho^{5/3}},$$

which gives the well known relation

$$S = C_v \ln \frac{P}{\varrho^{5/3}},$$

when $P_{||} = P_{\perp} = p$.

In accordance with the second law of thermodynamics the entropy of the fluid cannot decrease, when it flows through the shock front, or in other words: the entropy density has a non negative jump on the discontinuity surface:

$$[S] \geq 0.$$

If, as in [1], the conservation of the mean magnetic moment is required in the shock front as well, we can write $[S_{\perp}] = 0$. After this, the additional condition imposed by the second law of thermodynamics is

$$\left[\frac{P_{||} H^2}{\varrho^3}\right] \geq 0. \tag{1}$$

Introducing the notions

$$x = \frac{\varrho_+}{\varrho_-} \quad \text{and} \quad y = \frac{H_+}{H_-}$$

we can write the condition (1) as

$$\frac{P_{||+}}{P_{||-}} y^2 - x^3 \geq 0. \tag{2}$$

(The indices (+) and (−) designate the positive and negative sides of the discontinuity surface.)

By means of the shock jump conditions, the ratio $P_{||+}/P_{||-}$ can be expressed. The shock jump conditions are [1]:

$$[\sigma] = 0\,,$$

$$[H_n] = 0\,,$$

$$\sigma[\mathbf{v}] + \left[\left(\frac{1}{4\pi} - \frac{P_{||} - P_{\perp}}{H^2}\right)\mathbf{H}\,H_n - \left(P_{\perp} + \frac{H^2}{8\pi}\right)\mathbf{n}\right] = 0\,, \tag{3}$$

$$\sigma[\mathbf{H}\,\tau] + H_n[\mathbf{v}] = 0\,, \tag{4}$$

$$\sigma\left[\left(\frac{1}{2}\varrho\mathbf{v}^2 + \frac{1}{2}P_{||} + P_{\perp} + \frac{H^2}{8\pi}\right)\tau\right] + \left[\left(\frac{1}{4\pi} - \frac{P_{||} - P_{\perp}}{H^2}\right)(\mathbf{H}\,\mathbf{v})\,H_n - \left(P_{\perp} + \frac{H^2}{8\pi}\right)v_n\right] = 0\,, \tag{5}$$

$$\left[\frac{P_{\perp}}{\varrho H}\right] = 0\,,$$

where $\tau = 1/\varrho$, $\sigma = \varrho\theta$ and θ is the velocity of the discontinuity surface relative to the fluid, $\mathbf{n}$ is the unit normal vector of the discontinuity surface oriented towards the direction of the motion of plasma particles.

Multiplying Eq. (3) with $\bar{\mathbf{v}} = 1/2(\mathbf{v}_+ + \mathbf{v}_-)$ we can find

$$\frac{1}{2}\sigma[\mathbf{v}^2] = -\left[\left(\frac{1}{4\pi} - \frac{P_{||} - P_{\perp}}{H^2}\right)\mathbf{H}\right]H_n\,\bar{\mathbf{v}} + \left[P_{\perp} + \frac{H^2}{8\pi}\right]\mathbf{v}_n\,.$$

With the aid of this equality Eq. (5) can be written in the form:

$$\sigma\left[\left(\frac{1}{2}P_{||} + P_{\perp} + \frac{H^2}{8\pi}\right)\tau\right] - \left[\left(\frac{1}{4\pi} - \frac{P_{||} - P_{\perp}}{H^2}\right)\mathbf{H}\right]\bar{\mathbf{v}}\,H_n + \left[P_{\perp} + \frac{H^2}{8\pi}\right]\mathbf{v}_n + \left[\left(\frac{1}{4\pi} - \frac{P_{||} - P_{\perp}}{H^2}\right)(\mathbf{H}\,\mathbf{v})\right] \times H_n - \left[\left(P_{\perp} + \frac{H^2}{8\pi}\right)v_n\right] = 0\,. \tag{6}$$

Making use of the identities

$$[\mathbf{a}\,\mathbf{b}] = \bar{\mathbf{a}}[\mathbf{b}] + \bar{\mathbf{b}}[\mathbf{a}]\,, \tag{7}$$

$$\frac{1}{4}[\mathbf{a}][\mathbf{b}] = (\bar{\mathbf{a}}\bar{\mathbf{b}}) - \bar{\mathbf{a}}\bar{\mathbf{b}}, \tag{8}$$

we get

$$\sigma\left[\left(\frac{1}{2}P_{\parallel} + P_{\perp} + \frac{H^2}{8\pi}\right)\tau\right] + \left\{\left(\frac{1}{4\pi} - \frac{P_{\parallel} - P_{\perp}}{H^2}\right)\vec{H}\right\}[\vec{v}]\,H_n -$$

$$- \overline{\left(P_{\perp} + \frac{H^2}{8\pi}\right)}\,[v_n] = 0\,. \tag{9}$$

By means of Eqs. (4), (7), (8) we can transform Eq. (9) to the form not containing the components of velocity:

$$\sigma\left\{\left[\left(\frac{1}{2}P_{\parallel} + P_{\perp}\right)\tau\right] + \bar{P}_{\perp}[\tau] + \frac{1}{16\pi}[\vec{H}]^2[\tau] + \overline{\left(\frac{P_{\parallel} - P_{\perp}}{H^2}\vec{H}\right)}[\vec{H}\,\tau]\right\} = 0\,. \tag{10}$$

This equation gives the well known result

$$\sigma\left\{\frac{1}{K-1}[p\tau] + \bar{p}[\tau] + \frac{1}{16\pi}[\vec{H}]^2[\tau]\right\} = 0\,,$$

when $P_{\parallel} = P_{\perp} = p$ and $K = 5/3$ [2].

After a simple calculation, excluding the contact discontinuities, where $\sigma = 0$, we find from Eq. (10), that

$$\frac{P_{\parallel +}}{P_{\parallel -}} = \frac{y}{2y - \alpha x}\{h(y^2 - 2\alpha y + 1)(x - 1) + p[x^2(y - \alpha) + 2x(1 - y) +$$

$$+ \alpha y - 1] + 2x - \alpha y\}\,, \tag{11}$$

where

$$h = \frac{H^2}{16\pi P_{\parallel -}}, \quad p = \frac{P_{\perp -}}{P_{\parallel -}} \quad \text{and} \quad \alpha = \frac{\mathbf{H}_+\,\mathbf{H}_-}{H_+\,H_-}.$$

The substitution of Eq. (11) into the inequality (2) gives

$$\frac{y^3}{2y - \alpha x}\{h(y^2 - 2\alpha y + 1)(x - 1) + p[y(x^2 - 2x + \alpha) -$$

$$- (\alpha x^2 - 2x + 1)] + 2x - \alpha y\} - x^3 \geq 0\,. \tag{12}$$

As h and p depend only on the state parameters of the negative side and the inequality (12) must hold at all possible values of these quantities we get the following conditions:

$$\frac{1}{2y - \alpha x}(x^2 - y^2)\{\alpha(x^2 + y^2) - 2xy\} \geq 0\,, \tag{13}$$

$$\frac{y^3}{2y - \alpha x}(y^2 - 2\alpha y + 1)(x - 1) \geq 0\,, \tag{14}$$

$$\frac{y^3}{2y - \alpha x}\{y(x^2 - 2x + \alpha) - (\alpha x - 2x + 1)\} \geq 0\,. \tag{15}$$

An elementary calculation shows that the condition (13) holds only in the case, when $2y - \alpha x > 0$, so we find from (14), that

$$x \geq 1\,.$$

This means, that the density is always greater behind the shock than ahead. From the inequality (15) we find, that

$$y \geq g(x, \alpha) \equiv \frac{\alpha x^2 - 2x + 1}{x^2 - 2x + \alpha}\,.$$

If $\alpha < 0$, it can be seen from (13), that $y \geq x$. The range of x, y parameters where the inequalities (13)—(15) hold is plotted in Fig. 1. By means of the equality

$$\frac{P_{\perp +}}{P_{\perp -}} = xy$$

follows that $P_\perp$ has a positive jump on the discontinuity surface in this case. From the inequality (2) we can find that $P_{\perp +}/P_{\perp -} \geq 1$ when $y \leq x^{3/2}$ (region I in Fig. 1), while $P_{||}$ can have a negative jump in the region II, where $y > x^{3/2}$.

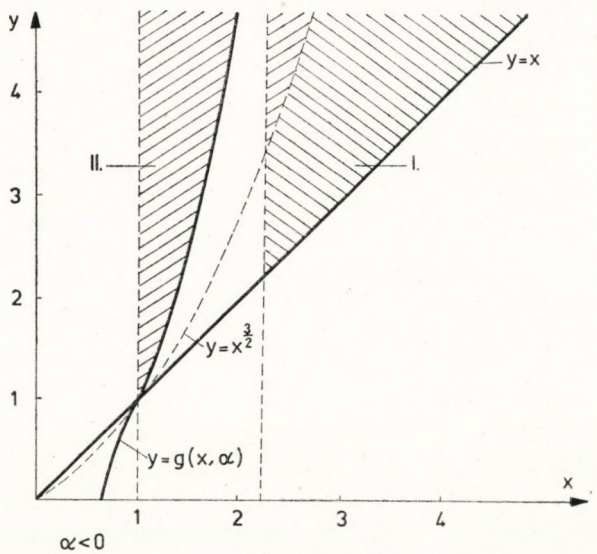

Fig. 1

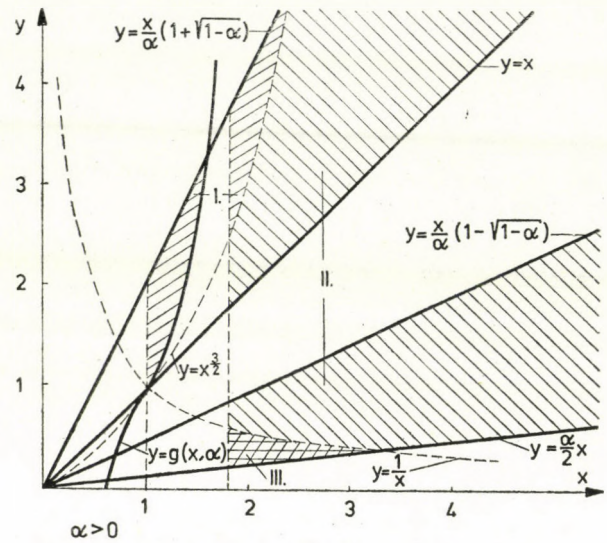

Fig. 2

If $\alpha > 0$ the inequality (13) holds in two distinct ranges of the $\{x, y\}$ plane (Fig. 2). In the region I $P_{||+}/P_{||-} \leq 1$ may be valid, while in the regions II—III we find that $P_{||+}/P_{||-} > 1$. If $\alpha > 0$ there always exists a range of x, y parameters (III), where $P_{\perp+}/P_{\perp-} \leq 1$.

As a result ZEMPLÉN's theorem can be formulated for CGL plasmas as follows: the shock waves of the CGL plasmas are compression waves. The density and at least one of the two pressures are greater on the positive side of the discontinuity surface than on the negative one.

Acknowledgement

The author wishes to thank Dr. JÁNOS SZABÓ for suggesting the problem and encouragement. Thanks are also due to PÉTER RAISZ for helpful discussions in mathematics.

REFERENCES

1. M. DOBRÓKA, Acta Phys. Hung., **38**, 55, 1975.
2. J. SZABÓ, Acta Phys. Hung., **17**, 75, 1963.
3. B. ABRAHAM-SHRAUNER, J. Plasma Phys., **1**, 361, 1967.

Acta Physica Academiae Scientiarum Hungaricae, Tomus 41 (3), pp. 201—209 (1976)

THE UNIVERSE AS A BOLYAI—LOBACHEVSKY VELOCITY SPACE

By

S. J. PROKHOVNIK

SCHOOL OF MATHEMATICS, UNIVERSITY OF NEW SOUTH WALES, SYDNEY, AUSTRALIA*

(Received 12. VIII. 1976)

It is shown that a uniformly-expanding universe, governed by the Cosmological Principle, exhibits a velocity space described by the hyperbolic geometry of J. BOLYAI and N. LOBACHEVSKY. This geometry provides a mathematical description of the free paths of light-rays and of material bodies, and has considerable theoretical, epistemological and practical implications. Its application is of particular importance for astronomical observations involving cosmological distances; this is exemplified in relation to the estimation of the size of objects (QSOs) with large ($z > 1$) redshifts. It is suggested that Bolyai—Lobachevskian geometry is of general relevance to any expanding model of the universe.

1. Basic assumptions

In the face of the great wealth of new astronomical observations and discoveries over the last few decades, the evidence continues to support the view that the observable universe can be considered as a homogeneous and expanding system of fundamental particles (the galaxies or clusters of such) governed by the Cosmological Principle. This Principle embodies the assumptions that the laws of nature as we know them appear to operate throughout the observable universe, and that the universe would have the same isotropic appearance for any fundamental observer, that is from the viewpoint on any fundamental particle.

The apparent expansion may be described by Hubble's Law:

$$w = Hr = r/T, \tag{1}$$

where w is the recession velocity of a distant galaxy estimated from Doppler red-shift measurements, r is its distance estimated from its apparent intensity and H is the Hubble constant whose most-recently estimated value is about 50 km/sec per megaparsec. T, the reciprocal of H, has the dimension of time and its corresponding value is about 2×10^{10} years.

There is a growing consensus [1] among astronomers that the expansion appears to be very close to uniform, in conformity with strong theoretical

* During 1976 with the Department of Philosophy, London School of Economics, Houghton Street, London, WC2A 2AE.

arguments [2, 3] for a zero value of the deceleration parameter q_0. The assumption of uniform expansion provides a simple physical interpretation of T: it can then be considered as the age of the universe measured from the time when it commenced expanding from a highly dense state. In such a context the ratio r/w provides a cosmic measure of time, t, having a universal significance for all observers.

We will consider a model of the universe based on the above assumptions which are now widely accepted and in general conformity with the astronomical evidence.

2. Mathematical formulation of the model

The model of the universe described above may be represented by a General Relativistic type metric, named after its independent proposers H. G. ROBERTSON and A. G. WALKER. This representation incorporates a scale-factor $R(t)$ corresponding to the nature of the expansion assumed and also a curvature parameter k whose value is taken as constant in view of the assumed homogeneity of our model universe.

The reference frame is based on the set of fundamental particles-cum-observers constituting the model, and clearly any one of these, say F_0, can be taken as the origin of the frame. In terms of spherical polar space co-ordinates, the ROBERTSON—WALKER metric is then given by

$$ds^2 = dt^2 - \frac{R^2(t)}{c^2\left(1 + \frac{1}{4}kr^2\right)^2}(dr^2 + r^2 d\Theta^2 + r^2 \sin^2\Theta d\Phi^2), \tag{2}$$

where r, Θ, are tΦhe fixed co-moving co-ordinates of any fundamental particle or observer relative to F_0 at the origin of the system, and t its cosmic time co-ordinate.

The curvature parameter k may take values of 0, $+1$ or -1 depending on whether the geometry of the model's 3-space is assumed to be Euclidean, spherical or hyperbolic, respectively. Since this metric obtains equally and isotropically for all fundamental observers, the interval ds is invariant with respect to all such observers in conformity with General Relativity.

For the uniformly-expanding model described above, we may take $R(t) = t$ and $k = 0$. Further, the fixed co-ordinate r associated with any fundamental particle, or observer can be taken, in our context, as equivalent to its constant recession velocity w relative to F_0. We will call w the Hubble measure of the recession velocity, it being based on a cosmological red-shift observation. We can now also define another radial co-ordinate r such that

$$r = \mathbf{r}t = wt \ , \tag{3}$$

so that r is the time-dependent distance of a given fundamental particle from F_0, and (3) can be considered as an expression of Hubble's Law with $t \sim 2 \times 10^{10}$ years at present .

We note that $\mathbf{r}$ or w, though fixed with respect to a given fundamental particle, takes different values for a set of such particles along (say) the path of a light-ray emanating radially from F_0. The path of such a ray constitutes a geodesic with $ds = 0$, and $d\Theta = d\Phi = 0$ also since the path is radial. Remembering that for our model $R(t) = t$ and $k = 0$, (2) then becomes:

$$0 = c^2dt^2 - t^2d\mathbf{r}^2 \ ,$$

with solution

$$\mathbf{r} = w = c \log (t/t_0) \, , \tag{4}$$

where t_0 is the cosmic time epoch of the transmission of the ray at F_0, and t is the epoch at which the ray reaches a fundamental particle receding from F_0 with velocity w. It follows that the distance travelled by the light-ray is given by

$$r = \mathbf{r}t = ct \log (t/t_0) \, . \tag{5}$$

The results (4) and (5) also follow [4] from the direct application of McCrea's Hypothesis [5] — that light passes every fundamental particle in its path with the velocity c — to a uniformly-expanding set of particles. The equivalence of these two approaches is perhaps not surprising, since the metric (2) employs a specific and unique cosmological reference frame, and the constant c, in this context, clearly represents the velocity of light with respect to this frame. Hence the Robertson—Walker metric implies the existence of an expanding fundamental reference frame for light propagation.

The result (4) enables us to show [4] that the recession velocity measure w is related to the corresponding Einstein measure* v by

$$w = c \tan \mathbf{h}^{-1}(v/c) = c \log \sqrt{\frac{1 + v/c}{1 - v/c}} \, . \tag{6}$$

From this it is easily shown [4] that the set of fundamental observers are Lorentz-equivalent, in conformity with their assumed cosmological equivalence. Note that this result is unique: it could not follow without the assumption of uniform expansion.

* The Einstein measures of the co-ordinates of a distant event are based on defined operations employing reflecting light-signals, standards clocks and measuring rods.

From (4) and (6), it also follows in the usual way that the cosmological Doppler effect is given by

$$\frac{\lambda}{\lambda_0} = \frac{R(t)}{R(t_0)} = \frac{t}{t_0} = e^{w/c} = \sqrt{\frac{1 + v/c}{1 - v/c}}, \tag{7}$$

where λ_0 and λ are the respective emitted and received corresponding wavelengths of a light-ray transmitted between two fundamental particles whose mutual recession velocity is w or v depending on the manner of measurement. It is seen that the values of v are restricted to $-c < v < c$, but that the corresponding values of w have no finite limit.

3. The geometry of geodesics

For our present purpose, the most important consequence of (4) is its application to the behaviour of geodesics. Consider then four fundamental observers A, B,C and D, as in Fig. 1, such that the mutual recession of A and D is w, of B and C also w, of A and B it is u, and of D and C also u. Thus A,B,C

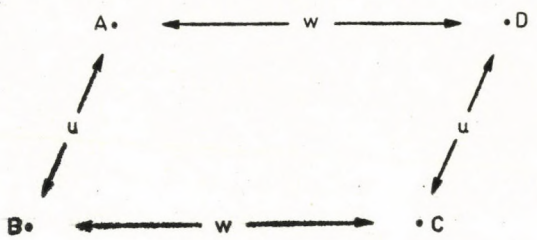

Fig. 1. Parallelogram of recession velocities

and D lie on the vertices of a parallelogram of recession velocities, and at any given epoch of cosmic time, t, their space-intervals of separation, wt and ut, also form a parallelogram.

Now imagine that at cosmic time T a light-ray passes A in the direction towards D, and a second light-ray passes B in the direction towards C. It follows from (4) that the rays will reach C and D at cosmic time $Te^{w/c}$. The resulting light-paths might be considered parallel; yet on leaving A and B these paths are separated by a distance uT, whereas on reaching D and C the paths are separated by the greater distance $uTe^{w/c}$.

Travelling backwards along these paths we note that the distance between them decreases by a factor of $e^{-w/c}$ for a length of path corresponding to a recession velocity w. Hence no matter how large we take w in either direction the paths will not meet, even though in the backwards direction the sum of the co-interior angles made by a transverse light-path is less than two right-angles.

The parallel light-paths of our cosmology have geometrical properties identical to those of parallel lines in hyperbolic geometry first discovered by JÁNOS BOLYAI in 1823 (when he communicated his results to his father, FARKAS BOLYAI, himself an eminent mathematician and friend of GAUSS), and independently by NICOLAI LOBACHEVSKY. The latter published his findings in 1826 and again in a shorter version in 1829 which came under general notice outside Russia only many years later. JÁNOS BOLYAI's outline of his new geometry appeared in 1832 as a twenty-four page appendix to a book on geometry by his father, FARKAS. Both of these men deserve full credit and honour for this achievement.

An important concept employed by them was the horocycle (or paracycle according to BOLYAI), the line which cuts a bundle of coplanar parallel lines orthogonally; the corresponding surface for a three-dimensional bundle of such lines is known as a horosphere (parasphere). Applying the horocycle concept to define the (varying) distance between parallel lines, they showed that for such lines in hyperbolic space the distance between them increases (or in the opposite direction decreases) by a factor $e^{x/\varkappa}$ as we move a distance x along a line and where $\varkappa$ is a constant. From this property all the relations of hyperbolic trigonometry follow readily [6].

It is seen that this geometry applies precisely to the geodesics of our cosmological model. However, in respect to our universe the exponential relation does not involve distances and an arbitrary constant $\varkappa$, but instead recession velocities and the universal light-velocity constant c; so that, for instance, the angle* of parallelism, α, of the light-paths described above is given by

$$\cos\alpha = \tanh(u/c). \tag{8}$$

Thus our model manifests a hyperbolic velocity-space whose geodesics conform precisely to Bolyai—Lobachevskian geometry.

4. Physical implications of a hyperbolic velocity space

The geometry of Bolyai—Lobachevsky is not merely a mathematical tool or convenience in the description of a uniformly-expanding universe; it describes precisely the behaviour of light-paths in such a universe. The geometry shows what happens when the passage of a light-ray is constrained by the (uniform) expansion of the substratum in which it propagates. The divergence of 'parallel' light-rays is inevitable is such a universe and is in principle observable.

* This is the acute interior angle made by one light-path with a transverse (light-path) which is at right-angles with a parallel light-path.

Thus consider our parallel light-rays associated with Fig. 1 from the viewpoint of one of the observers, say A. According to A, the light-ray travelling towards D maintains a fixed direction, the same direction as that of the mutual recession separating A and D. However from A's viewpoint, the light-ray travelling from B to C is diverging, as in Fig. 2, relative to the (light-ray)

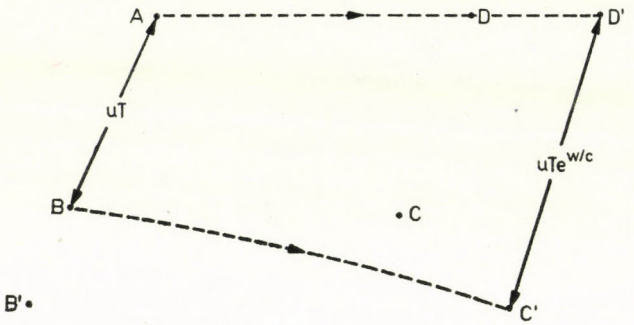

Fig. 2. Observer A's viewpoint of parallel light-rays and of separation distances. B′, C′ and D are the respective positions, relative to A, of observers B, C and D when the light-rays from A and B reach D and C, respectively. Note that C′ is on the radial extension of the line from A to C

line linking A to D, in accordance with the recession of C (the ray's destination) from D. Reciprocally, observer B would of course observe the ray from A to D bending away from the fixed direction of B to C.

The divergence of parallel light-rays in this way would appear to constitute a clear test of the nature of cosmological geometry, as was indeed recognised by GAUSS. Unfortunately the direct observation of such divergence, or of associated phenomena, is well beyond our present practical capacity, since the expected divergence could only assume an observably significant character over enormous distances corresponding to recession velocities comparable to c. Thus recollecting the value of the Hubble constant ($H \sim 50$ km sec per megaparsec), parallel light-rays travelling a distance of three million light-years would only diverge to the extent of about one part in six thousand ($\sim e^{1/6000} - 1$); and it follows from (8) that the angle of parallelism of two light-rays separated by this same enormous distance would differ from a right-angle by less than 0.01°. It is seen that for all local purposes, including those even on the galactic scale, our cosmological hyperbolic velocity-space reduces indistinguishably to a Euclidean space. This was forseen by BOLYAI who noted the limit equivalence of the two types of space as $\varkappa \to \infty$.

Both BOLYAI and LOBACHEVSKY also deduced another association between these two types of space, that is that the surface of any horosphere is governed by Euclidean geometry. In our context this means that at any given instant of cosmic time, this geometry applies precisely for the description of the spa-

tial relationships of our universe; so that we are certainly entitled to consider our four observers of Fig. 1 as lying on the vertices of an Euclidean parallelogram. We note, in this regard, that our cosmological hyperbolic velocity-space is four-dimensional, and that the 'surface' of its horospheres, corresponding to fixed instants of cosmic time, is three-dimensional.

Geodesics are equivalent to the 'straight lines' in a given space — the 'shortest distance' between two points in it. Hence we might expect that they should represent not only the paths of light-rays but of any freely moving body. This result is indeed confirmed elsewhere [7] by showing that our velocity-space can also be considered as a universal acceleration field; this field constrains the motion of both light-rays and material bodies in accordance with the results (4) and (5) above, except that for bodies the initial velocity replaces the constant c.

Hyperbolic geometry thereby assumes a physical significance in respect to all free motion in our uniformly expanding universe. It is of interest that the universal acceleration field, directly associated with Bolyai—Lobachevskian geometry, can be considered [7] as a valid basis for gravitational phenomena in terms of a value of G given by

$$G = \left(\frac{4}{3}\pi\varrho_0 T^2\right)^{-1},$$

where T is the reciprocal of the Hubble constant (or rather parameter), and ϱ_0 is the density of the universe at cosmic time T.

5. Astronomical implications

The Euclidean notion for the addition (and subtraction) of space-intervals applies along any straight line of hyperbolic space; such a line corresponds to a free path (of light or a material body) in our context, where the length of the path is measured in terms of the recession velocity obtaining between fundamental observers at the two ends of the interval. Thus if in a given direction, the Hubble recession velocities of two fundamental particles are w_1 and w_3 (with $w_1 < w_3$), then their relative recession velocity w_2 will satisfy the simple relation $w_3 = w_1 + w_2$.

On account of (6), this is equivalent to

$$c\,\mathrm{tanh}^{-1}(v_3/c) = c\,\mathrm{tanh}^{-1}(v_1/c) + c\,\mathrm{tanh}^{-1}(v_2/c) =$$

$$= c\,\mathrm{tanh}^{-1}\left[\frac{(v_1 + v_2)/c}{1 + v_1 v_2/c^2}\right];$$

so that the relativistic formula, relating the Einstein measures of recession velocities in a given direction, is equivalent to a simple addition formula for the corresponding Hubble measures. ROBB [8] appears to have been the first to recognize that the function $c \tanh^{-1}(v/c)$ has hyperbolic geometry properties and he named it the 'rapidity'. BOYER [9] has employed these properties to derive the formula for astronomical aberration and to disclose the basis of the Thomas precession effect, and, from quite a different standpoint, FOCK [10] has also linked Special Relativity with a hyperbolic velocity-space in the treatment of his gravitational theory. In the context of our approach the 'rapidity' function and its associated properties assume a tangible significance in terms of the cosmological behaviour of light-rays and freely-moving bodies.

As seen above, it would require millions of years of observation with hypersensitive astronomical techniques to detect the slight divergence of parallel light-rays posited by our cosmological model; however, modern astronomical observations of galaxies and quasars at cosmological distances may provide indirect evidence of the geometry of light-rays. For example, the Quasi-stellar objects OH471 and OQ172 were observed by BROWNE et al. [11] to have red-shifts of 3.40 and 3.53, respectively. They also found that the angular diameters of these objects were less than 1/2 arc sec ,"which in a Friedmann universe with $H_0 = 50$ km s^{-1}Mpc^{-1} and $q_0 = +1$ implies a linear diameter less than 2.5 kpc" [11].

The appropriate hyperbolic trigonometric formula* for the analysis of this data is

$$\sinh(d/2c) = \sinh(w/c) \sin(\alpha/2), \tag{9}$$

where $\alpha \leq 1/2$ arc sec, d is the recession velocity measure of the diameter of the observed object, and for $z = 3.4$ we have $e^{w/c} = 4.4$ and $\sinh(w/c) \sim 2.1$. Expressing α in radians and in view of the smallness of the arguments, we may take

$$\sin(\alpha/2) \sim 1.25 \times 10^{-6} \qquad \text{and} \qquad \sinh(d/2c) \sim d/2c,$$

so that (9) yields

$$d \leq 5 \times 10^{-6} c(\text{km/sec}) = 1.5 \text{ (km/sec)},$$

which is equivalent to a diameter of 30 kpc on taking $H = 50$ km/sec per Mpc.

This result is more consistent than that of BROWNE et al. [11], with the observed objects having galactic dimensions, as might be expected [12] from the common association of QSOs with galaxies at cosmological distances. It is

* Note that, to the first order, (9) is equivalent to the Euclidean formula $d = 2w \sin(\alpha/2)$.

suggested that hyperbolic trigonometry will provide a more consistent interpretation of observations of very distant ($z > 1$) objects than is otherwise possible.

Hyperbolic geometry is exactly applicable to the description of free paths in a uniformly-expanding universe and, as mentioned above, the uniformity assumption ($q_0 = 0$) appears to be well-supported by observation. However even if the expansion were finally found to be not precisely uniform, hyperbolic geometry would still provide an excellent approximation to the velocity-space of our universe; for in a universe where energy propagates with respect to an expanding reference frame, parallel light-rays must diverge according to an exponential (or, at least, quasi-exponential) law. Hence the new mathematical vistas, revealed by J. BOLYAI and N. LOBACHEVSKY, will remain of cosmological relevance as long as our universe is expanding.

Acknowledgement

The author is indebted to Professor K. P. KOVÁCS for his suggestions and encouragement in preparing this paper.

REFERENCES

1. A. SANDAGE, Astrophys. J., **202,** 563, 1975.
2. S. J. PROKHOVNIK, Int. J. Th. Phys., **9,** 291, 1974.
3. A. D. ALLEN, Found. Phys., **6,** 59, 1976.
4. S. J. PROKHOVNIK, The Logic of Special Relativity. Cambridge University Press, Cambridge, 1967.
5. W. H. MCCREA, Proc. Math. Soc. Univ. of Southampton, **5,** 15, 1962.
6. S. KULCZYCKI, Non-Euclidean Geometry, Pergamon, Oxford, 1961.
7. S. J. PROKHOVNIK, Nature, **225,** 359, 1970.
8. A. A. ROBB, Geometry of Space and Time, Cambridge University Press, Cambridge, 1963.
9. R. H. BOYER, Amer. J. Phys., **33,** 910, 1965.
10. V. FOCK, The Theory of Space, Time and Gravitation, Pergamon, Oxford, 1959.
11. I. W. A. BROWNE et al., Nature, **244,** 19, 1973.
12. M. ROWAN-ROBINSON, Nature, **262,** 97, 1976.

Acta Physica Academiae Scientiarum Hungaricae, Tomus 41 (3), pp. 211—218 (1976)

AN UNPUBLISHED IDEA OF D. R. HARTREE AND ITS EXTENSION

By

L. JÁNOSSY

CENTRAL RESEARCH INSTITUTE FOR PHYSICS, BUDAPEST

(Received in revised form 14. IX. 1976)

According to an unpublished suggestion of HARTREE the improper integrals expressing the electromagnetic potentials should be interpreted in terms of polar coordinates around the singularity. It is shown that with the help of this suggestion the well-known relations of electrodynamics can be obtained in a consequent manner — and it is shown that when there might be doubt of how to interpret singularities — the physically correct interpretation can be obtained.

Introduction

More than thirty years ago I gave lectures on electrodynamics at the University of Manchester using lecture notes prepared by D. R. HARTREE. These notes contained an idea which I have not met elsewhere but which I think is of importance. Presently I reproduce the consideration and extend it to some extent.

I

The electrostatic potential of a charge distribution can be written as

$$\Phi(\mathbf{r}) = \int \frac{\varrho(\mathbf{r}')}{|\mathbf{r} - \mathbf{r}'|} d^3\mathbf{r}' . \tag{1}$$

For values of $\mathbf{r}$ so that $\varrho(\mathbf{r}) \neq 0$ the right hand expression is an improper integral and its numerical value can be given only if we add to (1) the definition of how this improper integral should be interpreted.

For this purpose it is convenient to introduce polar coordinates, thus in place of (1) we may write

$$\Phi(\mathbf{r}) = \int_0^{2\pi} d\varphi \int_0^{\pi} \sin\vartheta d\vartheta \int_0^{R_0} \varrho(\mathbf{r} + \mathbf{R}) R dR , \tag{2}$$

where R_0 is the radius of a sphere containing the whole of the charge distribution.

We note that (1) and (2) give identical results for values of $\mathbf{r}$ so that $\varrho(\mathbf{r}) = 0$ more precisely if

$$\varrho(\mathbf{r}') = 0 \quad \text{for} \quad |\mathbf{r} - \mathbf{r}'| < a,$$

where a is a length greater than zero.

The potential inside the charge distribution can be *defined* as to be represented by (2). The definition (2) can be recommended for two important reasons:

1) We show presently that $\Phi(\mathbf{r})$ given by (2) obeys the Laplace—Poisson equation

$$\nabla^2\Phi(\mathbf{r}) = -4\pi\varrho(\mathbf{r}) \tag{3}$$

both inside and outside the charge distribution.

2) The field strength

$$\mathbf{E} = -\text{grad}\,\Phi, \tag{4}$$

calculated from the potential as defined by (2) agrees with the experimental findings.

It is important to emphasize that the improper integral (1) from the purely mathematical point of view (as any improper integral) could be interpreted in a fashion different from (2) — in the latter case Φ defined by the alternate method may not possess the properties 1) and 2).

The use of polar coordinates in potential theory is a well-known method. The point made by HARTREE is, however, that the use of polar coordinates does not simply represent a convenient mathematical method — but it really contains a physical assumption about the nature of the field.

To show that using the hypothesis (2) of how to interpret the improper integral (1), we obtain the well-known mathematical formalism without having to evaluate improper integrals. We reproduce in petit the well-known procedures so as to show that once the singularity is eliminated postulating (2) — only regular expressions have to be dealt with.

II

The Laplace—Poisson equation

To show that (2) obeys the Laplace—Poisson equation we note that, (2) being an integral the integrand of which possesses no singularity, we can differentiate the relation (2) and interchange the order of integration and differentiation. Remembering that

$$\nabla_{\mathbf{r}}^2\,\varrho(\mathbf{r} + \mathbf{R}) = \nabla_{\mathbf{R}}^2\varrho(\mathbf{r} + \mathbf{R}),$$

where the suffices **r** and R signify that the operator ∇^2 has to be taken to operate on those coordinates, we have

$$\nabla_{\mathbf{r}}^2 \Phi(\mathbf{r}) = \int_0^{2\pi} d\varphi \int_0^{\pi} \sin\vartheta \, d\vartheta \int_0^{R_0} (\nabla_{\mathbf{R}}^2 \varrho(\mathbf{r} + \mathrm{R})) R dR \,. \tag{5}$$

Using the well-known relation

$$\nabla_{\mathbf{R}}^2 \varrho = \frac{1}{R^2} \frac{\partial}{\partial R} \left(R^2 \frac{\partial \varrho}{\partial R} \right) + \frac{1}{R^2 \sin\vartheta} \frac{\partial}{\partial \vartheta} \left(\sin\vartheta \frac{\partial \varrho}{\partial \vartheta} \right) + \frac{1}{R^2 \sin^2\vartheta} \frac{\partial^2 \varrho}{\partial \varphi^2} = \mathrm{I} + \mathrm{II} + \mathrm{III} \,.$$

the integral (5) can be separated into three terms. As can be seen easily neither of the terms contain singularities and therefore the order of integrations can be interchanged. Thus

$$\int_0^{2\pi} \frac{\partial^2 \varrho}{\partial \varphi^2} d\varphi = \frac{\partial \varrho}{\partial \varphi} \Big|_0^{2\pi} = 0$$

and

$$\int_0^{\pi} \frac{\partial}{\partial \vartheta} \left(\frac{1}{R} \sin\vartheta \frac{\partial \varrho}{\partial \vartheta} \right) = \frac{1}{R} \sin\vartheta \frac{\partial \varrho}{\partial \vartheta} \Big|_0^{\pi} = 0$$

the latter relation is correct including $R = 0$. We have thus $\mathrm{II} = \mathrm{III} = 0$. Further

$$\int_0^{R_0} \frac{1}{R} \frac{\partial}{\partial R} \left(R^2 \frac{\partial \varrho}{\partial R} \right) dR = \int_0^{R_0} R \left(\frac{\partial^2 \varrho}{\partial R^2} + 2 \frac{\partial \varrho}{\partial R} \right) dR = R \frac{\partial \varrho}{\partial R} \Big|_0^{R_0} + \int_0^{R_0} \frac{\partial \varrho}{\partial R} \, dR = -\varrho(\mathbf{r}),$$

where we suppose

$$\frac{\partial \varrho}{\partial R} = 0, \quad \varrho = 0 \quad \text{for} \quad r = R_0 \,.$$

We see thus that (2) satisfies indeed the Laplace—Poisson relation (3).

Dipole fields

The field of a polarized dielectric can be regarded as that of a dipole density $\mathbf{P}(\mathbf{r})$; the field of the dielectric can thus be derived from a potential

$$\Phi_P(\mathbf{r}) = \int \frac{\mathbf{P}(\mathbf{r}') (\mathbf{r} - \mathbf{r}')}{|\mathbf{r} - \mathbf{r}'|} d^3\mathbf{r}' \,. \tag{6}$$

Outside the dielectric the integral (6) can be transformed integrating by parts; one finds thus

$$\Phi_P(\mathbf{r}) = - \int \frac{\operatorname{div} \mathbf{P}(\mathbf{r}')}{|\mathbf{r} - \mathbf{r}'|} d^3\mathbf{r}' \,.$$

Thus the field of the dielectric outside the dielectric can be derived from a fictive charge distribution

$$\varrho_P(\mathbf{r}) = -\operatorname{div} \mathbf{P}(\mathbf{r}) \,, \tag{7}$$

the so-called Poisson distribution. The integrand (6) is highly singular at $\mathbf{r}' = \mathbf{r}$ if $\mathbf{P}(\mathbf{r}) \neq 0$ thus inside the dielectric the right hand expression is an improper integral. The latter integral can be interpreted again in accord with HARTREE's suggestion in terms of polar coordinates.

We may thus write

$$\Phi_P(\mathbf{r}) = \int_0^{2\pi} d\varphi \int_0^{\pi} \sin\vartheta \, d\vartheta \int_0^{R_0} \frac{\mathbf{P}(\mathbf{r}+\mathbf{R})\,\mathbf{R}}{R} \, dR \,. \tag{8}$$

The integrand of the above integral is regular; we can make use of the identity

$$\frac{\mathbf{P}\,\mathbf{R}}{R} = R \operatorname{div} \mathbf{P} - R^2 \operatorname{div} \frac{\mathbf{P}}{R} \tag{9}$$

which is valid in the limit $R \to 0$ also; introducing (9) into (8) we may integrate by parts just as in the previous case, and find thus

$$\Phi_P(\mathbf{r}) = -\int_0^{2\pi} d\varphi \int_0^{\pi} \sin\vartheta \, d\vartheta \int_0^{R_0} (\operatorname{div} \mathbf{P}) \, R \, dR \,. \tag{10}$$

Thus comparing with (2) and (3) we find

$$\begin{aligned} \nabla^2 \Phi_P(\mathbf{r}) &= -4\pi \varrho_P \,, \\ \varrho_P &= -\operatorname{div} \mathbf{P} \,. \end{aligned} \tag{11}$$

The field of the polarized atoms of a dielectric is obtained to be equal of the Poisson charge ϱ_P. The above result is valid outside the dielectric. Inside the dielectric it is valid if the improper integral, which is obtained by integrating over the dipole density, is interpreted in terms of polar coordinates in the form (8).

III

The definitions are not trivial ones, according to which certain improper integrals have to be interpreted in terms of polar coordinates around the singularity. To see this we consider two mathematically possible treatments of a dipole field and show that we are led to different results according to how we interpret certain improper integrals.

The field of a point dipole $\mathbf{M}$ (we shall think of magnetic dipoles, this is, however, unimportant from the purely mathematical point of view) can be given by two different expressions, namely as

$$\operatorname{grad} \frac{\mathbf{M}\mathbf{r}}{r^3} \quad \text{or} \quad \operatorname{rot} \frac{\mathbf{r} \times \mathbf{M}}{r^3} \,. \tag{12}$$

Both expressions are singular at $r = 0$. Both give, however, the same distribution for $r > 0$. According to the two expressions (12) we can give the field of a dipole distribution as

$$\mathbf{B} = \operatorname{rot} \mathbf{A}$$

with

$$\mathbf{A} = \int \operatorname{rot} \frac{\mathbf{R} \times \mathbf{M}(\mathbf{r} - \mathbf{R})}{R^3} \, d^3\mathbf{R} \tag{13}$$

or

$$\mathbf{H} = -\text{grad}\, \Omega$$

with

$$\Omega = \int \frac{\mathbf{M}(\mathbf{r}+\mathbf{R})\,\mathbf{R}}{R^3}\, d^3\mathbf{R}\,. \tag{14}$$

We write **H** and **B** to remind of the alternative mathematical definitions. Outside the dipole distribution the integrals (13) (14) are regular and we find

$$\mathbf{H}(\mathbf{r}) = \mathbf{B}(\mathbf{r}) \qquad \text{if} \qquad \mathbf{M}(\mathbf{r}) \neq 0. \tag{15}$$

Inside the distribution the integrals are improper ones, both can be interpreted introducing polar coordinates around the singularity. In this manner we can by definition give definitive values to the fields **H** and **B**. The result of this procedure leads, however, to different results according to whether we fix the value of (13) as of (14) by introducing polar coordinates.

Indeed, writing (13) and (14) in polar coordinates and taking the rot resp. grad of the integrals, we can interchange the order of differentiation and integration as the integrands are regular. We thus find as the result of simple calculations

$$\mathbf{B} = \text{rot}\, \mathbf{A} = \int_0^{2\pi} d\varphi \int_0^{\pi} \sin\vartheta\, d\vartheta \int_0^{R_0} (\text{rot rot}\, \mathbf{M}(\mathbf{r}+\mathbf{R}))\, R\, dR\,,$$

$$\mathbf{H} = -\text{grad}\, \Omega = \int_0^{2\pi} d\varphi \int_0^{\pi} \sin\vartheta\, d\vartheta \int_0^{R_0} (\text{grad div}\, \mathbf{M}(\mathbf{r}+\mathbf{R}))\, R\, dR\,.$$

(The operators under the integral are supposed to act upon **R**).

We have thus

$$\mathbf{B} - \mathbf{H} = -\int_0^{2\pi} d\varphi \int_0^{\pi} \sin\vartheta d\vartheta \int_0^{R_0} (\nabla^2 \mathbf{M})\, R dR = 4\pi \mathbf{M}\,.$$

Thus according to which of the expressions (11) of the dipole field we start — regularizing the improper integral by introducing polar coordinates — we come to a different value for the field inside the polarized medium. We arrive thus according to which of the definitions we choose to the "magnetic field strength" **H** or to the magnetic displacement **B**.

Introducing polar coordinates in certain improper integrals we can define their numerical values uniquely. This procedure is, however, not a formal procedure but it can be shown that this intepretation of certain improper integrals leads to values in agreement with experience. This can be seen to be the case in the following manner.

The interpretation of (1) in form (2) leads to the potential distribution $\Phi(\mathbf{r})$ obeying the Laplace—Poisson relation (3). The Laplace—Poisson relation

(apart from an additional constant) has a unique solution, thus mathematically the expression (2) gives the only solution of (3).

That this solution describes the field inside a charge distribution correctly, can be seen considering a charged conductor. In the state of electrostatic equilibrium the electric field inside the conductor must vanish, thus

$$\mathbf{E} = 0$$

inside the conductor. It follows thus that

$$\operatorname{div} \mathbf{E} = 0$$

inside the conductor and therefore in accord with (3)

$$\varrho = 0 \ .$$

The latter property of the distribution of the electrostatic field was first proved to be correct by CAVENDISH and is one of the common experiences of electrostatics. If we were to replace (2) by some expression in which the singularity of the integrand is interpreted in a different way, then the potential would not necessarily obey the Laplace—Poisson equations and even in the state of equilibrium charge densities were to be expected inside a conductor.

Considering the case of a magnetic dipole distribution experimental results prove that the force upon a charge moving through a magnet is given by

$$\mathbf{F} = \frac{e}{c} (\mathbf{v} \times \mathbf{B}) \ .$$

Such experiments are e.g. the deflection of fast charged particles passing through a permanent magnet. Similarly experiments on the change of polarization of a neutron beam passing through a permanent magnet proves that a magnetic field of strength **B** (and not of H) acts upon the magnetic moments of the neutrons. In the electrical case one suspects that the field acting on a particle penetrating into a dielectric is given by $e\mathbf{E}$; experiments to clear this question would be very desirable.

From the above consideration one is thus led to conclude that results in agreement with experiments are obtained if we calculate the magnetic field inside the magnet from (13) and not from (14); similarly in the dielectric we have to calculate the field from Φ_P as given by (10). Thus the magnetic field inside a magnet is obtained from an effective current density

$$\mathbf{i}_{\text{eff}} = \operatorname{rot} \mathbf{M} \ , \tag{16}$$

the electric field in a dielectric from the effective charge density

$$\varrho_P = -\operatorname{div}\mathbf{P}\,. \tag{17}$$

In both cases the improper integrals giving the field strength inside the distribution have to be normalized by introducing polar coordinates.

IV

Introducing polar coordinates to define the improper integral a straightforward derivation of the retarded potential expressions is also obtained. The problem is to show that the wave equation

$$\nabla^2\Phi - \frac{1}{c^2}\ddot{\Phi} = -4\pi\varrho \tag{18}$$

s satisfied by the retarded potential

$$\Phi(\mathbf{r}, t) = \int \frac{\varrho(\mathbf{r}', t')}{|\,r - r'\,|}\, d^3r' \qquad t' = t - |r - r'\,|/c\,. \tag{19}$$

The integral (19) (being an improper one) does not define unambiguously the retarded potential $\Phi(\mathbf{r},t)$. An unambigous definition is, however, obtained if we use again HARTREE's procedure and define the integral (19) by introducing polar coordinates. Thus we replace the definition (19) by

$$\Phi(\mathbf{r},t) = \int_0^{2\pi} d\varphi \int_0^{\pi} \sin\vartheta d\vartheta \int_0^{R_0} \varrho(\mathbf{r} + \mathbf{R}, t - R/c)\, RdR\,. \tag{19a}$$

Outside the charge distribution (19) and (19a) give identical values; inside the distribution (19a) gives a definite meaning to the improper integral.

To show that (19a) satisfies indeed (18) it is convenient to rewrite (19a) as

$$\Phi\,(\mathbf{r},\, t) = \int_0^{2\pi} d\varphi \int_0^{\pi} \sin\vartheta\; d\vartheta \int_0^{R_0} \overline{\varrho}\;(\mathbf{r},\, \mathbf{R},\, t)\, R\; dR \tag{20}$$

with

$$\overline{\varrho}(\mathbf{r},\, \mathbf{R},\, t) = \varrho\,(\mathbf{r} + \mathbf{R},\, t - R/c)\,. \tag{21}$$

We may now apply the Laplace operator to both sides of (20). Since the integrand of (20) is regular we can interchange the order of integration and differentiation, we have thus

$$\nabla^2_{\mathbf{r}}\,\Phi(\mathbf{r},\, t) = \int_0^{2\pi} d\varphi \int_0^{\pi} \sin\vartheta\; d\vartheta \int_0^{R_0} \nabla^2_{\mathbf{r}}\,\overline{\varrho}(\mathbf{r},\, \mathbf{R},\, t)\, R\, dR. \tag{22}$$

As the result of a short calculation one finds, using the rules of partial differentiation, that

$$\nabla_{\mathbf{r}}^2 \bar{\varrho} = \nabla_R^2 \bar{\varrho} + \frac{2}{c} \frac{\partial}{\partial t} \left(\frac{1}{R} \frac{\partial \bar{\varrho}}{\partial R} \right) + \frac{1}{c^2} \frac{\partial^2 \bar{\varrho}}{\partial t^2} . \tag{23}$$

Introducing (23) into (22) the integral can be split into the sum of three integrals $I_1 + I_2 + I_3$ according to the terms on the right hand side of (23). Using the method of part I, the first integral is found to have a value

$$I_1 = -4\pi\bar{\varrho}(\mathbf{r}, 0, t) = -4\pi\varrho(\mathbf{r}, t) .$$

The third integral can be evaluated by taking the $\partial^2/\partial t^2$ operator before the integral; one thus finds

$$I_3 = \frac{1}{c^2} \frac{\partial^2}{\partial t^2} \Phi(I, t) .$$

Finally one finds integrating by parts that

$$I_2 = 0$$

thus

$$\nabla^2 \Phi(\mathbf{r}, t) = -4\pi\varrho(\mathbf{r}, t) + \frac{1}{c^2} \ddot{\Phi}(\mathbf{r}, t),$$

therefore (20) is indeed a solution of (18).

In the above derivation the introduction of polar coordinates is essentia[1] as the operations we have carried out would not be unambiguous if we were to start from (19) in place of (20) without specifying how to interpret the singularity of (19),

In many textbooks other considerations are given with the purpose to show that (19) gives a solution of (18). Thus the integral (19) is extended into a small sphere around r and the retardation is neglected in this region. The integral outside the sphere is shown to give the effect of retardation. The above method is rather unsatisfactory both from the mathematical and from the physical point of view. We think that this latter method contains in a hidden way at least partly the assumption according to which the improper integral has to be interpreted in terms of polar coordinates. It seems to us more satisfactory to start from the assumption that the singularity has to be interpreted in polar coordinates so as to arrive to a correct description of the phenomena.

This procedure of interpreting certain integrals in terms of polar coordinates must be taken not as a procedure which can be justified by mathematical argument — but it rather contains an empirically justified physical assumption as to the structure of the sources of the electromagnetic field. Thus replacing the not well defined expression (19) by the well defined equation (10) we can prove, using exact mathematical methods, that (20) indeed gives a solution of (18).

Acta Physica Academiae Scientiarum Hungaricae, Tomus 41 (3), pp. 219—224 (1976)

COMMUNICATIO BREVIS

COMBINED FREE AND FORCED CONVECTION MAGNETOHYDRODYNAMIC FLOW THROUGH TWO PARALLEL POROUS WALLS

By

L. M. SRIVASTAVA

DEPARTMENT OF MATHEMATICS, INDIAN INSTITUTE OF TECHNOLOGY KANPUR
KANPUR, INDIA

(Received 17. VI. 1976)

1. Introduction

The investigation of natural convection effects in forced horizontal flows is of great physical interest. This is the case in nuclear-reactor applications, particularly when dealing with after shut down cooling problems. SPARROW et al. [1] has shown that in case of horizontal flows of low Prandtl number fluids, the bouyancy forces cannot be neglected as they significantly affect the flow field. GILL and CASAL [2] also proved that the effects of the buoyancy forces are highly important in case of the horizontal flows of low Prandtl number fluids. All low Prandtl number fluids are electrically conducting and hence their flow is affected by transversely applied magnetic field. This property has been utilised profitably in magnetohydrodynamic channel flows. But all attempts to analyse the mhd flows were without considering the buoyancy forces. This led GUPTA [3] to investigate the effect of buoyancy forces on a forced convection flow through a horizontal channel with nonconducting walls. Recently JANA [4] extended the GUPTA's problem by considering horizontal conducting walls.

The present paper is concerned with the study of forced flow of electrically conducting fluid between two parallel porous non-conducting walls, one of which is at rest and the other moving parallel to itself, with a linear axial temperature variation including buoyancy forces. The flow takes place in the presence of uniform vertical magnetic field.

2. Mathematical problem and its solution

Consider the flow of an electrically conducting fluid between two horizontal parallel nonconducting porous walls, the upper wall moving with a constant velocity u_0. The x and y axes are taken along and transverse to the

parallel plates with the origin on the lower plate. It is assumed that a uniform magnetic field H_0 is acting along the y axis. At a sufficiently large distance from the entry, the flow will be fully developed and in the steady state we can take all physical variables depending on y only. Then the governing equations can be written as [3]

$$\varrho_0 V_0 \frac{du}{dy} = -\frac{\partial p}{\partial x} + \mu \frac{d^2u}{dy^2} - \sigma\mu_e^2 H_0^2 u\,, \tag{1}$$

$$0 = -\frac{\partial p}{\partial y} - \varrho g\,, \tag{2}$$

$$\varrho_0 c\left(u\frac{\partial T}{\partial x} + V_0\frac{\partial T}{\partial y}\right) = k\frac{\partial^2 T}{\partial y^2} + \mu\left(\frac{\partial u}{\partial y}\right)^2 + \sigma\mu_e^2 H_0^2 u^2\,. \tag{3}$$

The equation of state under the Boussinesq approximation is assumed to be

$$\varrho = \varrho_0[1 - \beta(T - T_0)]\,, \tag{4}$$

where T is the temperature, β is the coefficient of the thermal expansion and σ_0, T_0 are the density and the temperature in the reference state.

Combining Eqs. (1) and (2)

$$V_0\frac{d^2u}{dy^2} - \frac{g}{\varrho_0}\frac{\partial\varrho}{\partial x} = \frac{d^3u}{dy^3} - \nu\frac{\sigma\mu_e^2 H_0^2}{\varrho_0}\frac{du}{dy}\,. \tag{5}$$

Introducing the following dimensionless variables

$$u = u_0\omega\,, \quad Y = h\eta, \quad x = P_e h\xi\,.$$

Eq. (5) reduces to

$$\frac{d^3W}{d\eta^3} - \frac{V_0 h}{\nu}\frac{d^2W}{d\eta^2} - \frac{g\beta h^2}{\nu\varrho_e u_0}\frac{\partial}{\partial\xi}(T - T_0) - \frac{\sigma\mu_e^2 H_0^2 h^2}{\varrho_e\nu}\frac{dW}{d\eta} = 0\,. \tag{6}$$

Assuming that the wall temperature has a uniform radient A_1 along the x-direction the temperature of the fluid can be assumed as

$$T - T_0 = A_1\xi + Y(\eta)\,. \tag{7}$$

Hence Eq. (6) reduces to

$$\frac{d^3W}{d\eta^3} - R_s\frac{d^2W}{d\eta^2} - M^2\frac{dW}{d\eta} - G = 0\,, \tag{8}$$

where

$$R_s = \frac{V_0 h}{\nu}, \quad M = \left(\mu_e^2 H_0^2 h^2 \frac{\sigma}{\mu}\right)^{1/2}, \quad G = \left(\frac{g\beta h^2 A_2}{u_0 \nu}\right), \quad A_2 = \frac{A_1}{P_e}. \tag{9}$$

Eq. (7) shows that the positive and negative values of A_1 correspond to heating and cooling, respectively, along the channel walls. Since $P_e > 0$, it then follows from (9) that $G \gtrless 0$ depending on whether the channel walls are uniformly heated or cooled in the axial direction.

The equation of energy in non-dimensional form, including viscous and ohmic dissipation is

$$\frac{d^2\Phi}{d\eta^2} = P_r R_s \frac{d\Phi}{d\eta} + W - B_r\left[\left(\frac{dW}{d\eta}\right)^2 + M^2 W^2\right], \tag{10}$$

where

$$Y(\eta) = A_1 \Phi(\eta); \quad P_e \frac{u_0 h c \varrho_0}{k}; \quad B_r = \frac{\mu u_0^2}{k A_1} \quad \text{and} \quad P_r = \frac{\nu \varrho_0 c}{k}.$$

The boundary conditions available on velocity W are the no slip conditions, at the walls and the conservation of mass flow, i.e.

$$W(0) = 0, \; W(1) = 1, \; \int_0^1 W d\eta = 1. \tag{11}$$

The boundary conditions for Φ are given by

$$\Phi(0) = 0; \; \Phi(1) = \frac{Y(1)}{A_1} = N \text{ (wall temperature parameter)}. \tag{12}$$

The solution of (8) subject to the boundary conditions (11) gives the velocity distribution and is given by

$$= A\left[\frac{R_s}{e^2} \cosh n \sqrt{\frac{R_s^2 + 4M^2}{4}} - 1\right] + \frac{R_s}{Be^2} \sin h\eta \sqrt{\frac{R_s^2 + 4M}{4}} - \frac{G\eta}{M^2}, \tag{13}$$

where

$$A = \frac{1 + c}{(e^a \cosh b - 1)} - \frac{e^a \sinh b}{(e^a \cosh b - 1)} \times$$

$$\times \left[\begin{array}{c} -\frac{1}{2}(M^2 c + 2M^2)(e^a \cosh b - 1) + \\ + (1 + c)\{e^a(b \sinh b - a \cosh b) - M^2 + a\} \\ \hline (e \cosh b - 1)\{e(s \sinh b - b \cosh b) + b\} + \\ + e^a \sinh b\{e^a(b \cosh b - a \cosh b) - M^2 + a\} \end{array}\right];$$

$$B = \left[\begin{array}{c} -\frac{1}{2}(M^2c + 2M^2)(e^a \cosh b - 1) + \\ + (1+c)\{e^a(b \sinh b - a \cosh b) - M^2 + a\} \\ \hline [(e^a \cosh b - 1)\{e(a \sinh b - b \cosh b) + b\} + \\ + e^a \sinh b\{e(b \cosh b - a \cosh b) - M^2 + a^2\}] \end{array} \right];$$

$$a = \frac{R_s}{2}; \quad b = \sqrt{\frac{R_s^2 + 4M^2}{4}} \quad \text{and} \quad c = \frac{G}{M^2}.$$

The solution of (10) subject to the boundary conditions (12) gives the temperature distribution and is given by

$$\Phi = c_0 \exp\{m\eta\} + b_0 b_1 \eta + b_2\eta^2 + b_3\eta^3 + b_4 \exp\{2a\eta\} + b_5 \exp\{a\eta\} \sinh b\eta$$
$$b_6 \exp\{a\eta\} \cosh b\eta + b_7 \exp\{2a\eta\} \sinh 2b\eta + b_8 \exp\{2a\eta\} \cosh 2b\eta +$$
$$+ b_9 \cdot \eta \exp\{a\eta\} \sinh b\eta + b_{10}\eta \exp\{a\eta\} \cos h\, b\eta, \tag{14}$$

where

$$b_0 = -\frac{1}{m^4}(6a_3 + 2a_2m + a_1m^2 + a_0m^3); \quad b_1 = -\frac{1}{m^3}(6a_3 + 2a_2m + a_1m^2);$$

$$b_2 = -\frac{1}{m^2}(3a_3 + a_2m); \quad b_3 = -\frac{1}{m}a_3; \quad b_4 = \frac{a_4}{2a - m};$$

$$b_5 = \frac{1}{\{(a-m)^2 - b^2\}^2}[\{(a-m)^2 - b^2\}(a-m)a_5 -$$
$$- \{(a-m)^2 - b^2\}ba_6 - \{(a-m)^2 + b^2\}a_9 + 2(a-m)ba_{10}];$$

$$b_6 = -\frac{1}{\{(a-m)^2 - b^2\}^2}[\{(a-m)^2 - b^2\}ba_5 - \{(a-m)^2 - b^2\}$$
$$\times (a-m)a_6 - 2(a-m)ba_9 + \{(a-m)^2 + b^2\}a_{10}];$$

$$b_7 = \frac{1}{(2a-m)^2 - (2b)^2}[(2a-m)a_7 - 2ba_8];$$

$$b_8 = \frac{1}{(2a-m)^2 - (2b)^2}[(2a-m)a_8 - 2ba_7];$$

$$b_9 = \frac{1}{(a-m)^2 - b^2}[(a-m)a_9 - ba_{10}];$$

$$b_{10} = \frac{1}{(a-m)^2 - b^2}[(a-m)a_{10} - ba_9];$$

$$c_0 = \frac{1}{1-e^m}[b_1 + b_2 + b_3 + b_4(e^{2a} - 1) + b_5 e^a \sin hb +$$

$$+ b_6(e^a \cosh b - 1) + b_7(e^{2a} \sinh 2b) + b_8(e^{2a} \cosh 2b - 1) +$$

$$+ b_9 e^a \sinh b + b_{10} e^a \cos hb - N]\,; \quad m = P_r \cdot R_s\,;$$

$$a_1 = -\frac{1}{M^4}(B_r M^6 A^2 + B_r G^2 + AM^4)\,; \quad a_2 = -\frac{1}{2M^2}(B_r M^4 + G)\,;$$

$$a_3 = -\frac{B_r G^2}{3M^2}\,; \quad a_4 = \frac{B_r}{4a}[A^2b^2 + B^2a^2 + M^2B^2 - A^2a^2 - B^2b^2 - M^2A^2]\,;$$

$$a_5 = -\frac{a}{M^2}\left[B + \frac{2GB_r}{M^2}(Ab + Ba) + 2B_r M^2 AB\right] +$$

$$+ \frac{b^2}{M^2}\left[A + \frac{2GB_r}{M^2}(Aa + Bb) - 2B_r M^2 A^2\right] - \frac{B_r G}{M^4}[a^2B + b^2B - 2abA]\,;$$

$$a_6 = \frac{b}{M^2}\left[B + \frac{2GB_r}{M^2}(Ab + Ba) + 2B_r M^2 AB\right] -$$

$$- \frac{a}{M^2}\left[A + \frac{2GB_r}{M^2}(Aa + Bb) + 2B_r M^2 A^2\right] - \frac{B_r G}{M^4}[a^2A + b^2A - 2abB]\,,$$

$$a_7 = \frac{B_r}{4M^2}[-b\{+A^2b^2 + B^2a^2 + M^2B^2 + A^2a^2 + B^2b^2 + M^2A^2\} +$$

$$+ 2a\{(Ab + Ba)(Aa + Bb) + M^2AB\}]\,;$$

$$a_8 = \frac{1}{4M^2}[2b\{Ab + Ba)(Aa + Bb) + M^2AB\} -$$

$$- 2aB_r\{A^2b^2 + B^2a^2 + M^2B^2 + A^2a^2 + B^2b^2 + M^2A^2\}]\,;$$

$$a_9 = \frac{B_r G}{M^2}[Ab - Ba] \text{ and } a_{10} = \frac{B_r G}{M^2}[Aa + Bb]\,,$$

The Drag-Coefficients at the two walls ($\eta = 0$ and $\eta = 1$) are given from (13) as

$$\left(\frac{dW}{d\eta}\right)_{\eta=0} = Aa + Bb - \frac{G}{M^2} \text{ and } \left(\frac{dW}{d\eta}\right)_{\eta=1} = (Ab + Ba)e^a \sinh b +$$

$$+ (Aa + Bb) - \frac{G}{M^2}. \tag{15}$$

The expressions for the heat transfer at the two walls from (14) are

$$\left(\frac{d\Phi}{d\eta}\right)_{\eta=0} = c_0 m + b_1 + 2ab_4 + bb_6 + ab_6 + 2bb_7 + 2ab_8 + b_{10} \qquad (16)$$

and

$$\left(\frac{d\Phi}{d\eta}\right)_{\eta=1} = c_0 me^m + b_1 + 2b_2 + 3b_3 + 2ab_4 e^{2a} + [be^a \cosh b + ae^a \sinh b]\, b_5 +$$
$$+ [be^a \sinh b + ae^a \cosh b]b_6 + [2be^{2a} \cosh 2b + 2ae^{2a} \sinh 2b] + b_7 +$$
$$+ [2be^{2a} \sinh 2b + 2ae^{2a} \cosh 2b]b_8 + [be^a \cosh b + ae^a \sinh b + e^a \sinh b]b_9 +$$
$$+ [be^a \sinh b + ae^a \cosh b + e^a \cosh b]b_{10}. \qquad (17)$$

Acknowledgement

I wish to express my sincere thanks to Professor JAGDISH LAL, D. Sc., Director, Indian Institute of Technology, Kanpur for his help and guidance in the preparation of this paper.

REFERENCES

1. E. M. SPARROW, R. EICHORN and J. L. GREGG, Phys. Fluids, **2**, 319, 1959.
2. W. N. GILL and A. D. CASAL, A. I. Chem. Eng. J., **8**, 513, 1962.
3. A. S. GUPTA, Z. angew. Math. Phys., **20**, 506, 1969.
4. R. N. JANA, Z. angew. Math. Phys., **26**, 315, 1975.

RECENSIONES

E. KAPUY and F. TÖRÖK: Quantum Theory of Atoms and Molecules

Akadémiai Kiadó, Budapest 1975, 620 pages
(in Hungarian)

The aim of the book is to provide an introduction into the quantum theory of atoms and molecules and to serve as a reference book for advanced research workers on the subject.

After a brief historical survey the elements of classical mechanics are given with an experimental background of the quantum theory.

To lay the mathematical foundation the basis of linear operators in linear spaces is given with matrix representation and infinite dimensional spaces including a survey of the properties of important orthonormalized functions.

In the next paragraph the properties of wave functions, the principle of superposition, the statistical interpretation, physical properties and operators, the changing of the state with time, the foundations of representation theory and the interrelation between quantum and classical mechanics are presented in detail. Subsequently, the most important simple solvable cases are reviewed and the basis of spin theory is given.

The many-body problem in quantum theory and the Pauli principle are treated in detail and the separation of the variables in the Born—Oppenheimer approximation is analysed carefully.

Variational method and perturbation theory are treated and group theory and symmetry properties are dealt with in sufficient detail for the beginner to get a good working knowledge of the topic.

In the next four paragraphs the mathematical apparatus of the theory is further developed. Eigenfunctions of the operators of the spin, evaluation of matrix elements with determinants, density matrices and the occupation number representation are treated with basis functions and the one- and two-particle integrals of the independent particle method.

In the following two paragraphs a short review of the electronic structure of atoms is given with a more detailed presentation of the electronic structure of molecules beginning from the diatomic molecules and ending at π-electron systems, including localization, hybridization and the population analysis.

The Coulomb correlation of electrons in atoms and molecules is treated and methods of relative coordinates, configuration interactions, the multiconfiguration self-consistent field, perturbation theory and some other theories are reviewed.

Methods dealing with systems of many electrons such as the Xα-method, pseudopotentials and the all electron methods CNDO, INDO, MINDO, OCILO, EHT are mentioned with the π-electronmethods as the Hückel method, PPP method and AMO and NPSO method and crystal field theory and ligand field theory.

Short paragraphs deal with topics like the interactions of molecules with electromagnetic fields, weak interactions as the van der Waals one and the hydrogen bond, the interpretation of the chemical bond, molecular spectra and chemical reactions.

In the Appendix coordinate systems, relativistic corrections, the character tables of the important point groups and values of the physical constants are given.

At the end of each paragraph the authors give many references, some review articles and books for further reading.

The well written book may be recommended to chemists, physicists and spectroscopists interested in the physics of molecules. Because of the detailed, textbook-like nature of the first part and the enormous amount of material presented in the second part the book may serve well both undergraduate and graduate students as well as research workers.

R. GÁSPÁR

P. GOMBÁS and D. KISDI: Wave Mechanics and its Applications

Akadémiai Kiadó, Budapest, 1973. pp. XII + 235.

The Publishing House of the Hungarian Academy of Sciences has published the English translation of the successful book of the late Prof. P. GOMBÁS and his co-worker, Dr. D. KISDI. The first edition had been originally written and published in Hungarian, in 1967; later it was translated into German and published in cooperation with the Springer Publishing House, Vienna, 1969.

During the past few decades a considerable number of text-books on quantum mechanics have appeared. Owing to its individual features the book reviewed here deserves special appreciation; earlier editions met with merited success. According to the preface, the endeavour of the authors was to give an introduction to quantum mechanics and its applications to atoms. However, the book offers appreciably more than that.

Giving a non-axiomatic development of quantum mechanics, the book starts from the knowledge of fundamental experimental facts, then through classical physical analogies and a short discussion of the Bohr—Sommerfeld theory it gets as far as the Schrödinger equation. These are treated in the three chapters of the first part of the book. The second part also consists of three chapters, the first of which presents examples, which are exactly solvable with Schrödinger's equation; the second gives the quantummechanical discussion of the scattering problem, the third treats the perturbational and variational methods and some of their typical applications.

The authors' aim was to develop the physical considerations and to explain the physical characteristics of substance by using a moderate and non-formal mathematical apparatus with clear and logical interpretation. Their choice of subject covers the field of non relativistic quantum mechanics almost completely, including the most important approximative methods necessary for applications. Moreover, the selected examples provide a firm basis for many important concepts of nuclear as well as solid state physics. So the book is a good introduction for a young researcher, wishing to become better acquainted with the literature of the subject.

The authors presented all this rich subject matter in a comparatively easily readable form taking up altogether 235 pages. In view of the moderate size of the book it can perhaps be noted that it would be desirable to introduce Dirac symbols and the basic ideas of relativistic quantum mechanics in the same masterful style. Recent theoretical research achieved many results in the field of the quantum-mechanical treatment of the many-electron systems, in addition to the one-electron approximation. This is also a chapter to be taken into account in a possible new edition.

Owing to the good selection of the subject and the consequent logical treatment, the book may be recommended to students in physics and chemistry and to young researchers in all fields of modern science.

A. KÓNYA

A. STOLZ: Einführung in die Vielelektronentheorie der Kristalle

Akademie-Verlag, Berlin, 1974. XII + 329 pages

The author, Dr. rer. nat. habil HUBERTUS STOLZ, one of the heads of the Central Institute for Electronphysics of the Academy of Sciences of the GDR, summarised in this book his lectures held at Humboldt University. The book differs in many points from the numerous monographs on solid state physics recently published.

It breaks with the practice often followed by similar books, which aim at completeness and attempt to treat the basic experimental facts as well as several applications of the theoretical methods. Instead of this, this book concentrates on an appropriate and didactically correct review of the Green-function formalism, the quantum field method for treating the electrons in crystals. The quasi-particle picture of the crystal electrons, the theory of elementary excitations and some applications of fundamental importance are all based on this method.

Modern experimental reaerch in the field of solid state physics demonstrates more and more effects, which cannot be theoretically explained by the one-particle approximation but which are typically many-particle effects. This is why the methods, ideas and results of the

quantum mechanics of many-body systems should be introduced into solid state physics. Most of the monographs on solid state physics, some of the textbooks too, deal with this problem only briefly, only few good summaries are available on this subject.

Under these circumstances the book of H. STOLZ can be welcomed with pleasure. Its well arranged structure and clear discussion is praiseworthy. In spite of its good qualities the book is not an easily readable one. The reason for this is its subject, the close concentration on the theme, and the omission of the fundamental introduction. It can be recommended to solid state physicists, theoretical physicists and university students, who have completed their basic studies in solid state physics and quantummechanics.

The subject of the book is divided into the following 12 chapters:

1. Electrons in perfect crystals (8 pages);
2. Field-theoretical description of many electron systems (12 pages);
5. Green functions (22 pages);
4. Hartree—Fock approximation for a system of electrons in crystals (17 pages);
5. Screened Coulomb interaction (22 pages);
6. Electron-hole propagators and Bethe—Salpeter equation (24 pages);
7. Quasi-particle picture of the electrons in crystals (40 pages);
8.—9. Interaction with electromagnetic field I—II (71 pages);
10. Fundamental principles of the exciton theory (40 pages);
11. Fundamental principles for Landau—Silin theory of metallic electrons (28 pages);
12. The effective crystal-potential (11 pages).

A. KÓNYA

N. F. MOTT: Metal—Insulator Transitions

Taylor and Francis Ltd., London, 1974

Solid materials occurring in nature can easily be classified into the categories of metals and non-metals or insulators. The two types of materials are thought to be characterized by their electronic structures in such a way that non-metals must have non-overlapping, completely full and empty bands whereas in metals the Fermi energy lies somewhere in the middle of the conduction band, allowing full and empty states within the same band. Like all simple classifications, this one is not quite correct. There are solid materials showing transition from the metallic state to the non-metallic one and vice versa. A particular case, nickel oxide, should be metallic according to the simple band model because the eight electrons of the Ni^{2+} ion would only partly fill the *d* band, this material, however, is definitely a non-metal.

Professor MOTT's name is well known among solid state physicists; he was one of the initiators of the investigations concerning metal—non-metal transitions. It is for this reason that this phenomenon is frequently known as the MOTT transition. The book has therefore been written by the person who knows the story from the beginning and who participated in the development of this extremely interesting field of solid state physics.

The book contains six chapters. For information on their subject matter, one can do no better than to quote the author. "Chapter 1 deals with the phenomena which can be described in terms of a model of non-interacting electrons, including metal — insulator transitions due to band crossing such as that shown by some divalent metals under pressure. It also describes the behaviour of electrons in a non-crystalline medium and the Anderson transition, including that in liquids. Chapter 2 discusses first the interaction of electrons with phonons, particularly the mass enhancement by polaron formation, and also the band crossing transition in Ti_2O_3. Then various phenomena due to electron—electron interaction are introduced, including exciton formation, the properties of excitons in metals and the Nozières peak at an absorption edge, electron—electron collisions and the effect on the resistance (Baber scattering), and an introduction to the Hubbard intra-atomic energy U. Chapter 3 deals with magnetic moments; ferro- and antiferromagnetic coupling in non-metallic oxides are first described, followed by the Anderson—Wolff condition for the formation of moments in metals. The Kondo effect is relevant to some of the properties of materials near the metal—insulator transition and an outline of the physics of this phenomenon is given. We also describe the interaction between moments in spin glasses and amorphous antiferromagnets. A brief section on metallic ferromagnets is introduced, mainly in order to discuss nearly ferromagnetic materials where the

Pauli paramagnetism can be indefinitely enhanced without any large effect on the density of states or electronic specific heat; in this they are in strong contrast to the highly correlated nearly antiferromagnetic materials where both are enhanced. Chapter 4 introduces the metal—insulator transition due to correlation, and starts with the Hubbard model in which only intra-atomic correlation is included. The sequence antiferromagnetic insulator—antiferromagnetic metal—normal metal is described, and the comparison between the highly correlated nearly antiferromagnetic and nearly ferromagnetic metals is again made. In the former the spin-flip on strongly occupied centres is compared with the Kondo behaviour. The chapter also describes Wigner and Verwey transitions with applications to Fe_3O_4, vanadium bronzes and the transitions in some rare-earth compounds. Chapter 5 applies the ideas of Chapter 4 to the well-known transitions in such materials as V_2O_3, VO_2 and NiS. Finally, Chapter 6 discusses doped semiconductors and other disordered systems such as $La_{1-x}Sr_xVO_3$, VO_x and metal-ammonia solutions where both correlation and Anderson localization play a part."

Professor MOTT has succeeded in giving a consistent model to describe the metal—insulator transitions in his book. As a result of his being so well informed down to the minutest detail he is able to illustrate the complex theoretical treatment by concrete examples without using the difficult formal treatment. In reality, this book is a collection of physical ideas with examples to illustrate them. This book is indispensable for the specialist; il is also extremely useful for a student endeavouring to learn the subject.

B. VASVÁRI

GUSTAV E. R. SCHULZE: **Metallphysik**

Akademie-Verlag, Berlin, 1974

This book is the essentially unchanged second edition of the late Professor SCHULZE's work that first appeared in 1967. The book is basically a handbook — the author having aspired to completeness in collecting the basic knowledge about metals. At the same time in the individual main parts of the book Professor SCHULZE goes so much into detail that these parts can be regarded as a monograph of the subjects. The volume contains much more information than needs to be learned by the average university student so it is a good introductory work for those who wish to deal with the special subject of metal physics in a more detailed way.

The book has nearly 500 pages and consists of four main sections. After a short introduction to the most characteristic metallic properties the first section is devoted to the description of crystal lattices and their symmetry properties including some basic group-theoretical concepts. This is followed by a detailed description of the individual lattice structures not only in the case of simple metals but also for complex alloys. The thermodynamic treatment of the different crystallographic phases with questions relating to melting and solidification closes the main part.

The second section describes the mechanical and thermal properties of ideal crystals, starting with the classical treatment of elasticity. This is followed by the description of lattice dynamics, lattice heat capacity and thermal conductivity on the basis of the atomistic model.

The third section contains the description of atomic motions in real crystal lattices, such as diffusion and the diffusionless matter transport (glide processes, work hardening).

The fourth section deals with electronic and magnetic properties. The quantum-mechanical pictures of the electron structures of metals including some very new result for the binding energy are first summarized, then follows the treatment of electronic properties such as conductivity, the electron emission from metallic surfaces, optical properties. Magnetic phenomena are treated by returning to macroscopic properties and using the atomistic interpretation.

Each chapter contains quite a number of exercises. A wealth of clear figures and detailed tables are to be found in the text illustrating the treatment. A trilingual (German, Russian, English) subject index completes the book.

Professor SCHULZE's handbook will be very useful for university students as well as metal physicists and metallurgists.

B. VASVÁRI

R. HANBURY BROWN:

The Intensity Interferometer and its Application to Astronomy

Taylor and Francis, London, 1974.

The reading of this book offers simultaneously the benefit of understanding physical ideas and the enjoyment of being a companion — though only spiritually — to pioneers of science. The intensity interferometer proposed by the author seems to be the only effective tool for measuring the angular size of faraway visible and radio stars while the laboratory measurements carried out on the basis of the ideas originating from stellar interferometry led to the increase of our knowledge on the coherence of light, i.e. on nature itself.

The light interference measurements carried out by a Michelson interferometer provide information on the spectrum of atomic transitions, moreover the interference phenomenon can be applied for *length measurements* too. But both applications are influenced by the size of the light source. This is an undesirable factor in spectral and *length measurements* but Michelson turned this disadvantage into a valuable tool constructing the stellar interferometer for measuring the angular size of stars.

The stellar interferometer, however, is affected by spurious variations of the armlength and the refraction index of air, limiting the accuracy of the instrument. It was on the initiative of the author that thorough theoretical and experimental work has been carried out on the intensity interferometer. It consists of two square law detectors and the high speed electronics measuring the correlation signal of the detectors. This signal is proportional to the degree of spatial coherence of the light source i.e. to its angular size. Thus the difficulties connected with the phase of the electromagnetic field can be avoided.

After a historical introduction the monography gives the physical outlines of wave and intensity correlation. In Chapters 6 and 7 the author reviews the experiments carried out both with visible light and radio waves. The big interferometer constructed on the principle of intensity correlation was built up at Narrabi (Australia). It consists of two mosaic concave mirrors (intensity interferometers do not require monolithic mirrors) with a diameter 6,5 m built on two tracks moving in a circle of a diameter of 188 m. The signal of a pair of photomultipliers placed in the foci of the mirrors was then led to an electronic correlation circuitry.

The angular diameter of 32 stars between $0.5-6\times10^{-3}$ sec of arc are listed, showing the possibilities of the interferometer. Where a significant difference of the correlation signal from unity was observed (for zero delay between the signals) the presence of multiple stars could be concluded. The efficiency of the method was amply demonstrated by observing from the periodic variation of the correlation signal the rotation of a binary star (known from spectroscopic measurements).

P. VARGA

Printed in Hungary

A kiadásért felel az Akadémiai Kiadó igazgatója. Műszaki szerkesztő: Botyánszky Pál
A kézirat nyomdába érkezett: 1976. X. 26. — Terjedelem: 7 (A/5) ív, 16 ábra
77.3770 Akadémiai Nyomda, Budapest — Felelős vezető: Bernát György

NOTES TO CONTRIBUTORS

I. PAPERS will be considered for publication in Acta Physica Hungarica only if they have not previously been published or submitted for publication elsewhere. They may be written in English, French, German or Russian.

Papers should be submitted to

Prof. I. Kovács, Editor
Department of Atomic Physics, Polytechnical University
1521 Budapest, Budafoki út 8, Hungary

Papers may be either articles with abstracts or short communications. Both should be as concise as possible, articles in general not exceeding 25 typed pages, short communications 8 typed pages.

II. MANUSCRIPTS

1. Papers should be submitted in five copies.

2. The text of papers must be of high stylistic standard, requiring minor corrections only.

3. Manuscripts should be typed in double spacing on good quality paper, with generous margins.

4. The name of the author(s) and of the institutes where the work was carried out should appear on the first page of the manuscript.

5. Particular care should be taken with mathematical expressions. The following should be clearly distinguished, e.g. by underlining in different colours: special founts (italics, script, bold type, Greek, Gothic, etc); capital and small letters; subscripts and superscripts, e.g. x^3, x_3; small l and 1; zero and capital O; in expressions written by hand: e and i, n and u, c and v, etc.

6. References should be numbered serially and listed at the end of the paper in the following form: J. Ise and W. D. Fretter, Phys. Rev., *76*, 933, 1949.

For books, please give the initials and family name of the author(s), title, name of publisher, place and year of publication, e.g.: J. C. Slater, Quantum Theory of Atomic Structures, I. McGraw-Hill Book Company Inc., New York, 1960.

References should be given in the text in the following forms: Heisenberg [5] or [5]

7. Captions to illustrations should be listed on a separate sheet, not inserted in the text.

III. ILLUSTRATIONS AND TABLES

1. Each paper should be accompanied by five sets of illustrations, one of which must be ready for the blockmaker. The other sets attached to the copies of the manuscript may be rough drawings in pencil or photocopies.

2. Illustrations must not be inserted in the text.

3. All illustrations should be identified in blue pencil by the author's name, abbreviated title of the paper and figure number.

4. Tables should be typed on separate pages and have captions describing their content. Clear wording of column heads is advisable. Tables should be numbered in Roman numerals (I, II, III, etc.).

IV. MANUSCRIPTS not in conformity with the above Notes will immediately be returned to authors for revision. The date of receipt to be shown on the paper will in such cases be that of the receipt of the revised manuscript.

Reviews of the Hungarian Academy of Sciences are obtainable at the following addresses:

AUSTRALIA

C. B. D. Library and Subscription Service
Box 4886, G. P. O.
Sydney N. S. W. 2001

Cosmos Bookshop
145 Acland St.
St. Kilda 3182

AUSTRIA

Globus
Höchstädtplatz 3
A—1200 Wien XX

BELGIUM

Office International de Librairie
30 Avenue Marnix
1050-Bruxelles

Du Monde Entier
162 Rue du Midi
1000—Bruxelles

BULGARIA

Hemus
Bulvar Ruszki 6
Sofia

CANADA

Pannonia Books
P. O. Box 1017
Postal Station "B"
Toronto, Ont. M5T 2T8

CHINA

C N P I C O R
Periodical Department
P. O. Box 50
Peking

CZECHOSLOVAKIA

Mad'arská Kultura
Národní třida 22
115 66 Praha

PNS Dovoz tisku
Vinohradská 46
Praha 2

PNS Dovoz tlače
Bratislava 2

DENMARK

Ejnar Munksgaard
Nörregade 6
DK—1165 Copenhagen K

FINLAND

Akateeminen Kirjakauppa
P. O. Box 128
SF-00101 Helsinki 10

FRANCE

Office International de Documentation et Librairie
48, Rue Gay-Lussac
Paris 5

Librairie Lavoisier
11 Rue Lavoisier
Paris 8

Europeriodiques S. A.
31 Avenue de Versailles
78170 La Celle St. Cloud

GERMAN DEMOCRATIC REPUBLIC

Haus der Ungarischen Kultur
Karl-Liebknecht-Strasse 9
DDR—102 Berlin

Deutsche Post
Zeitungsvertriebsamt
Strasse der Pariser Kommüne 3—4
DDR-104 Berlin

GERMAN FEDERAL REPUBLIC

Kunst und Wissen
Erich Bieber
Postfach 46
7 Stuttgart 5

GREAT BRITAIN

Blackwell's Periodicals
P. O. Box 40
Hythe Bridge Street
Oxford OX1 2EU

Collet's Holdings Ltd.
Denington Estate
London Road
Wellingborough Northants NN8 2QT

Bumpus Haldane and Maxwell Ltd.
5 Fitzroy Square
London W1P 5AH

Dawson and Sons Ltd.
Cannon House
Park Farm Road
Folkestone, Kent

HOLLAND

Swets and Zeitlinger
Heereweg 347b
Lisse

Martinus Nijhoff
Lange Voorhout 9
The Hague

INDIA

Hind Book House
66 Babar Road
New Delhi 1

India Book House
Subscription Agency
249 Dr. D. N. Road
Bombay 1

ITALY

Santo Vanasia
Via M. Macchi 71
20124 Milano

Libreria Commissionaria Sansoni
Via Lamarmora 45
50121 Firenze

JAPAN

Kinokuniya Book-Store Co. Ltd.
826 Tsunohazu 1-chome
Shinjuku-ku
Tokyo 160—91

Maruzen and Co. Ltd.
P. O. Box 5050
Tokyo International 100—31

Nauka Ltd.-Export Department
2—2 Kanda
Jinbocho
Chiyoda-ku
Tokyo 101

KOREA

Chulpanmul
Phenjan

NORWAY

Tanum-Cammermayer
Karl Johansgatan 41—43
Oslo 1

POLAND

Węgierski Instytut Kultury
Marszalkowska 80
Warszawa

CKP I W
ul. Towarowa 28
00—958 Warsaw

ROUMANIA

D. E. P.
Bucureşti

Romlibri
Str. Biserica Amzei 7
Bucureşti

SOVIET UNION

Sojuzpechatj — Import
Moscow

and the post offices in each town

Mezhdunarodnaya Kniga
Moscow G—200

SWEDEN

Almqvist and Wiksell
Gamla Brogatan 26
S—101 20 Stockholm

A. B. Nordiska Bokhandeln
Kunstgatan 4
101 10 Stockholm 1 Fack

SWITZERLAND

Karger Libri AG.
Arnold-Böcklin-Str. 25
4000 Basel 11

USA

F. W. Faxon Co. Inc.
15 Southwest Park
Westwood, Mass. 02090

Stechert-Hafner Inc.
Serials Fulfillment
P. O. Box 900
Riverside N. J. 08075

Fam Book Service
69 Fifth Avenue
New York N. Y. 1003

Maxwell Scientific International Inc.
Fairview Park
Elmsford N. Y. 10523

Read More Publications Inc.
140 Cedar Street
New York N. Y. 10006

VIETNAM

Xunhasaba
32, Hai Ba Trung
Hanoi

YUGOSLAVIA

Jugoslavenska Knjiga
Terazije 27
Beograd

Forum
Vojvode Mišiča 1
21000 Novi Sad

Acta Phys. Hung. Tom. 41. No. 3. Budapest, 31. V. 1977 **Index: 26.025**

ACTA PHYSICA

ACADEMIAE SCIENTIARUM HUNGARICAE

TOMUS XLI FASCICULUS 4

AKADÉMIAI KIADÓ, BUDAPEST
1976

ACTA PHYS. HUNG. APAHAQ 41 (4) 231—318 (1976)

ACTA PHYSICA

ACADEMIAE SCIENTIARUM HUNGARICAE

SZERKESZTI

KOVÁCS ISTVÁN

Az *Acta Physica* angol, német, francia vagy orosz nyelven közöl értekezéseket. Évente két kötetben, kötetenként 4—4 füzetben jelenik meg. Kéziratok a szerkesztőség címére (1521 Budapest XI., Budafoki út 8.) küldendők.

Megrendelhető a belföld számára az Akadémiai Kiadónál (1363 Budapest Pf. 24. Bankszámla 215-11488), a külföld számára pedig a „Kultúra" Könyv- és Hírlap Külkereskedelmi Vállalatnál (1389 Budapest 62, P. O. B. 149. Bankszámla 217-10990 sz.), vagy annak külföldi képviseleteinél és bizományosainál.

The *Acta Physica* publish papers on physics in English, German, French or Russian, in issues making up two volumes per year. Subscription price: $32.00 per volume. Distributor: KULTURA Hungarian Trading Co. for Books and Newspapers (1389 Budapest 62, P. O. Box 149) or its representatives abroad.

Die *Acta Physica* veröffentlichen Abhandlungen aus dem Bereich der Physik in deutscher, englischer, französischer oder russischer Sprache, in Heften die jährlich zwei Bände bilden.

Abonnementspreis pro Band: $32.00. Bestellbar bei: KULTURA Buch- und Zeitungs-Außenhandelsunternehmen (1389 Budapest 62, Postfach 149) oder bei seinen Auslandsvertretungen.

Les *Acta Physica* publient des travaux du domaine de la physique, en français, anglais, allemand ou russe, en fascicules qui forment deux volumes par an.

Prix de l'abonnement: $32.00 par volume. On peut s'abonner à l'Entreprise du Commerce Extérieur de Livres et Journaux KULTURA (1389 Budapest 62, P. O. B. 149) ou chez ses représentants à l'étranger.

«*Acta Physica*» публикуют трактаты из области физических наук на русском, немецком, английском и французском языках.

«*Acta Physica*» выходят отдельными выпусками, составляющими два тома в год.

Подписная цена — $32.00 за том. Заказы принимает предприятие по внешней торговле книг и газет KULTURA (1389 Budapest 62, P. O. B. 149) или его заграничные представительства и уполномоченные.

ACTA PHYSICA

ACADEMIAE SCIENTIARUM HUNGARICAE

TOMUS XLI FASCICULUS 4

AKADÉMIAI KIADÓ, BUDAPEST
1976

ACTA PHYS. HUNG.

INDEX

Acta Physica Academiae Scientiarum Hungaricae, Tomus 41 (4), pp. 231—239 (1976)

A HYDRODYNAMIC MODEL OF FREE CONVECTIVE MASS TRANSFER

By

M. F. KOTKATA and Y. K. BADAWY

PHYSICS DEPARTMENT, FACULTY OF SCIENCE, AIN-SHAMS UNIVERSITY, CAIRO, EGYPT

(Received 3. VI. 1976)

The hydrodynamical flow due to the free convection in electrolysing cells with plane vertical electrodes model is revealed by a shadow Schlieren method. Electrolyte composition ranges from 0.01 to 0.50 M $CuSo_4$ in 1.5 M H^7So_4 under limiting currents for the deposition of copper between 0.32—35.7 mA/cm^2.

The data of the mass transfer have been verified by the empirical formula

$$Nu = 0.22\ (Sc \cdot Gr)^{0.29},$$

where Nu, Sc and Gr represent the NUSSELT, SCHMIDTH and GRASHOF mass transfer numbers.

Flow to solution of different concentrations near both cathode and anode has been studied to confirm the presence of a "back-flow". The recorded back-flow was found to grasp the original flow leading to some stratification of the cell liquid. Insertion of a centred-glass diaphragm, to separate the cathode compartment from the anode, has a qualitative influence on the back-flow phenomenon.

Introduction

The need to use electrochemical systems as models for analogous problems in mass and heat transfer has shown the importance of hydrodynamic studies of the electrolysing cells. An application of electrochemical mass transfer probes has been made by HANRATTY et al. [1] to measure the velocity gradient at a wall as to study the influence of drag-reducing polymers.

The first concept of the analogy between heat and mass transfer was proposed by AGAR [2]. Then, a correlation between the heat and mass transfer problem has been carried out by many workers using different models. Heat and mass transfer under simultaneous free and forced convection was studied by BAIRIEV et al. [3] and others [4, 5]. Also, the heat transfer coefficients were determined by analogy from mass transfer data with the aid of photometric measurements [6].

The most convenient method for studying rates of mass transfer by free convection mechanism measures the maximum rate of the electrode reaction, i.e. the limiting current, which may be maintained in the steady state. The rate of mass transfer from an electroyte to a solid can be related to the overall concentration difference between bulk solution and electrode interface,

$$N = K_L(C_b - C_i)\,.$$

The theoretical maximum current density is that which would reduce the concentration at the electrode interface C_i to zero [7]. This means that every ion near the electrode is instantaneously removed by reaction. So, the mass transfer coefficient K_L, which depends on hydrodynamical conditions [8], may be expressed in terms of the limiting current density I_L,

$$K_L = I_L(1 - t)/ZFC_b.$$

The transfer number of copper ($t_{Cu^{++}}$) could be neglected as it amounts to less than 1.5% even at the highest concentration of copper sulphate [9].

For vertical plane electrodes, DELAHY and TOBIAS [10] show that the local limiting current density $(I_L)_x$ for a discharge of copper ions at a distance X from the lower end of the cathode is represented by the relation

$$(I_L)_x = KZF\left(\frac{g\alpha D^3}{\nu^2}\right)^{1/4} C_b^{5/4} X^{-1/4},$$

where ν is the kinematic viscosity, g the acceleration of gravity, α the densification coefficient relates density changes $(\varrho_b - \varrho_i)$ to concentration changes, and K is a numerical constant which depends on the solution of the differential equations describing the mass transfer problem. The last relation may be written as

$$(I_L)_x = CX^{-1/4}.$$

Experiment

Fig. 1 illustrates the elevation and side views of the working holder used for the assembled cell. It is composed essentially of a cell holder and another to control the Haber-Luggin Capillary (HLC) in three independent directions. Necessary equipment is provided for the measurements of the total current and cathode potential at different points on the cathode relative to the bulk electrolyte solution in the cell.

A rectangular cell made of flow-free optical glass of dimensions $12.2 \times \times 11.8 \times 2.4$ cm^3 has been constructed for the deposition of copper from copper sulphate with sulphuric acid as a supporting electrolyte. The anode and the cathode are parallel plane plates made of electrolytic copper sheets of 0.4 cm thickness, 2.3 cm width and 10.2 cm height. Each electrode is held in place in a plexiglass holder. The backsides of the electrodes are covered with an insulating material to avoid any side reactions providing two-dimensional flow. The potential at any point near the cathode surface is measured using the HLC tubes made of pyrex-glass with the required precautions [11]. The

HLC is held in place parallel to the vertical mid-line of the cathode surface and adjusted at 1 mm away from it.

Fresh solutions prepared with different materials have been considered to realise a constant state polarization potential of the cathode during the electro-deposition. Molarities of Cu^{++} in the acidified copper sulphate solutions are estimated by the analytical iodine-thiosulphate method.

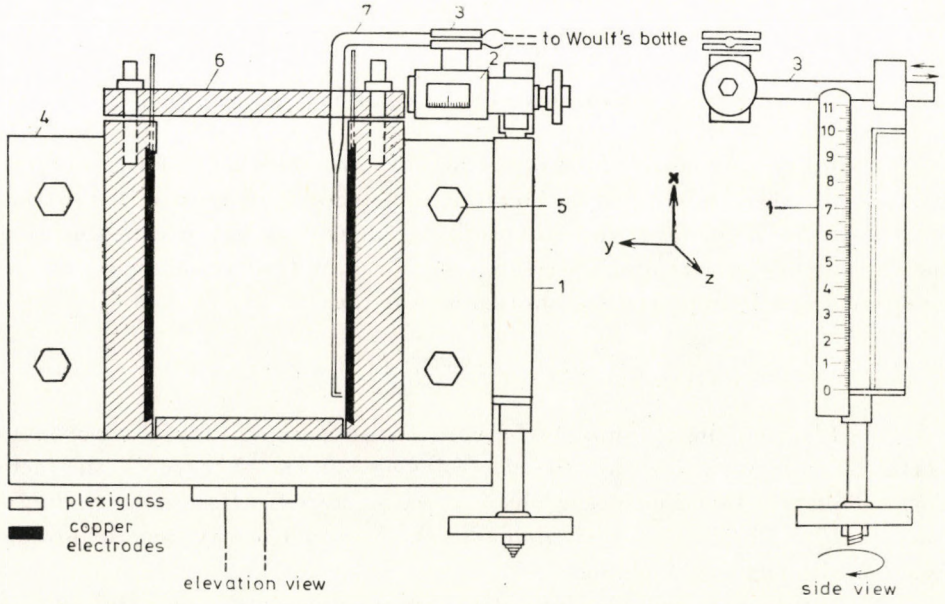

Fig. 1. Elevation and side views of the working holder used for the assembled cell. 1. vertical scale moves in x-direction; 2. vertical scale moves in y-direction; 3. capillary holder moves in z-direction; 4. steel cell frame; 5. frame screw; 6. assembled cell; 7. H. L. capillary

The potential value at zero current is recorded and, then, subtracted, with proper sign from the potential at the different current values. Thus, any static potential difference due to variation in the surface structure of the electrodes could be accounted for. The electric circuit is then immediately closed and current is passed through the cell. Potential is changed in steps of 25 mV each 1/2 minute and actual potentials are recorded with the aid of a Vibrating Reed Electrometer, of error less than 2%, till. hydrogen evolution takes place. Temperature is recorded during runs of the experiment for the subsequent evaluation of liquid properties.

Current—Potential measurements have been taken at different locations (0.5, 3.6, 6.6, and 9.7 cm) along the cathode (10.2 cm long). At each location, the experiment was repeated 2—4 times using fresh solution and freshly prepared polished cathodes. The reproducibility of successive limiting current measurement has been found to be within 1—2%.

To study the effect of separating the cathode compartment from that of the anode, a centred glass diaphragm has been used. The diaphragm's dimensions are: 0.8 cm thickness, 2.3 cm width, 14 cm height. The sizes of the adhering pyrexglass grains varied between 0.20—0.208 mm.

The hydrodynamical flow of the fluid inside the cell has been recorded by considering a shadow Schlieren method. This method is similar to that developed by SCHMIDTH [12] to study the thermal boundary layer, and later confirmed by GRIGULL [13].

Mass transfer calculations

Experimental measurements of the current-potential taken at different points along the cathode surface indicate no detectable changes in the limiting current value. This means that the limiting current density is constant along the surface of the cathode. Therefore, the constant C of the limiting current equation must be replaced by another factor $C(x)$, i.e.

$$(I_L)_x = C(x)X^{-1/4}.$$

As $(I_L)_x$ has been found to be constant, experimentally, so, the factor $C(x)$ must vary with X within the electrolysing cell. In other words, the factor $C(x)$, which is a function of the physical parameters C_b, D, α and c, increases somewhat with increasing the cathode height X in such a way that the product $C(x) \cdot X^{-1/4}$ remains unchanged.

Such behaviour of the limiting current constancy along the cathode height has been found over the whole compositional range studied; 0.0098 to 0.514 M/L $CuSo_4$ in approximately 1.5 M/L H_2So_4. Fig. 2 gives the average current—potential curves of the considered concentrations from which the limiting current values have been evaluated and given in Table I together with the corresponding physical properties estimated from the reported experimental data [5, 14] after correction for the measuring temperatures.

Dependence of the limiting current density of the present vertical electrode model on the bulk concentration of the reacting ionic species, Cu^{++}, can be represented by the linear equation

$$(I_L)_V \simeq C_b^{5/4}$$

which differs from that for a horizontal electrode model [15], where

$$(I_L)_H \simeq C_b^{4/3}.$$

It is customary to represent the limiting current data in terms of the three characteristic dimensionless mass transfer numbers; SCHMIDTH, NUSSELT

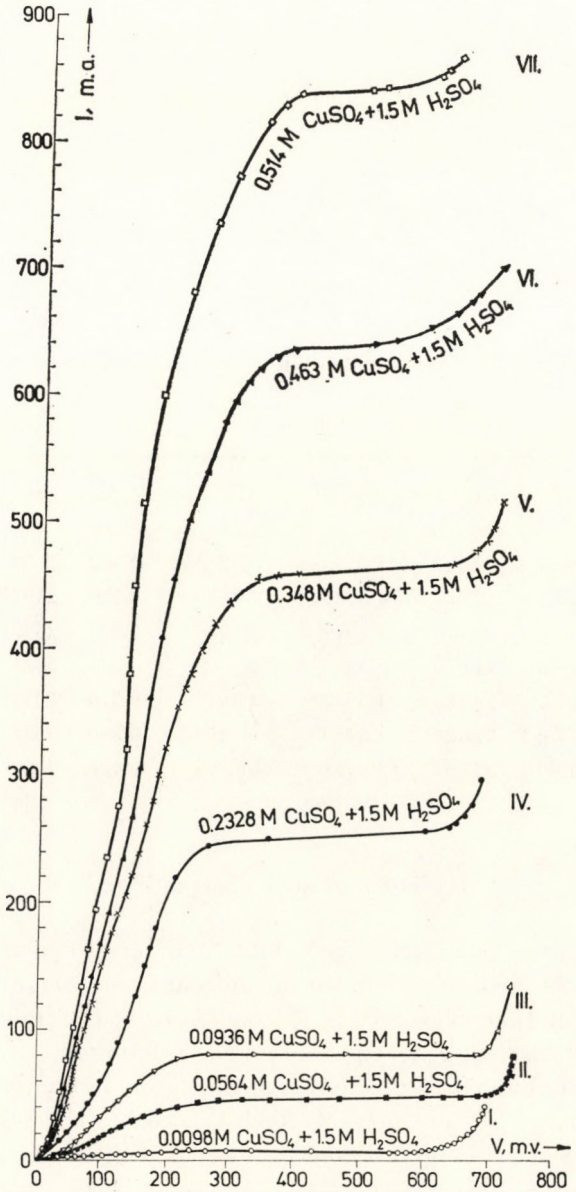

Fig. 2. Current—Potential curves for determination of the limiting current for the different concentrations

and GRASHOF by an empirical relation of the form

$$Nu = K(Sc \cdot Gr)^n,$$

where the constants K and n are evaluated from the experimental data, and

the characteristic numbers are defined by

$$Sc = \nu/D, \qquad Nu = I_V l/ZFDC_b,$$
$$Gr = gl^3(\varrho_b - \varrho_i)/\varrho\nu^2,$$

where Z is the valency, l the electrode height and F the Faraday constant. An IBM programmed computer has been used to indicate that

$$Nu = 0.2221(Sc \cdot Gr)^{0,2890}$$

which is comparable to that for the inclined parallel electrodes model [16].

Table I

No.	$CuSo_4$ Molarity C_b	Temp. °C	I_L mA/Cm²	$\nu \times 10^2$ cm²/sec	$\frac{\varrho_b - \varrho_i}{\varrho_i} \times 10^3$	$D \times 10^5$ cm²/sec	Sc	Nu	$Gr \times 10^{-7}$
I	0.0098	16.8	0.318	1.3736	1.248	0.542	2534	310.7	0.68788
II	0.0564	16.1	2.127	1.3739	7.959	0.529	2597	369.3	4.33208
III	0.0936	16.1	3.574	1.3949	19.318	0.520	2683	443.5	10.32530
IV	0.2328	17.2	11.050	1.4514	26.399	0.514	2824	488.4	14.34306
V	0.3480	17.7	19.684	1.5087	39.647	0.510	2958	576.9	18.11470
VI	0.4630	17.0	27.128	1.5450	50.870	0.500	3090	711.7	22.16757
VII	0.5140	18.0	35.734	1.6151	56.896	0.488	3309	742.9	22.74789

Hydrodynamical observations

Observations of flow of the cell fluid from zero current to the limiting current value have been recorded. As the current flows, there will be an initial depletion of the metal ions, Cu^{++}, in the region where the fluid is in immediate contact with the cathode. As the metal ion is depleted, the fluid density is reduced and consequently a convective flow occurs as a result of buoyancy forces. Such convective flow supplies fresh solution to the electrode interface, thus, the mass transfer is represented by molecular diffusion alone. The layers of solution flowing along the electrode surface undergo greater depletion as they rise to greater heights, and the convective current is continuously increased by the movement of additional bulk solution into the depleted regions.

However, the recorded Schlieren photos have shown that the original flow, at the surface of the cathode, transfers not only solution of low concentrations but it also transfers part of denser solution towards the free surface of the electrolyte. The transfer of denser solution is due mainly to the strong effect of the hydrodynamic boundary layer of the electrolyte used which is

much broader than that of the diffusion boundary layer, $\delta_h > \delta_d$ [17]. The instability of the heigher density portions of the solution near the upper surface of the cell liquid results in a "back-flow" which retransfers the denser solution downwards from the upper corner of the cathode. Similarly, the solution of lower density which is carried by the original flow on the anode will be retransferred upwards beginning from the lower corner of the anode.

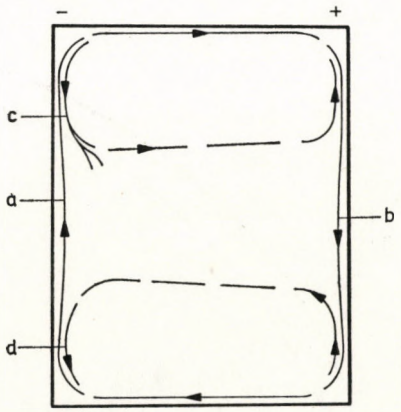

Fig. 3. A schematic diagram of the convection one hour after passing the current. a and b: original flow; c and d: back-flow

Fig. 3 illustrates a schematic diagram of the typical convection one hour after current flow started. $I \simeq 0.91_L$ to show the presence of the back-flow combined with the original flow. Increasing the time of current flow results in increasing the effect of the back-flow and the result is a stratification of the bulk of the cell solution. This explains the results obtained earlier [18] indicating that after a 15 hour duration of electrolysis the concentration in the central region of the bulk was not uniform. Also, the concentration in the lower parts was many times greater than in the higher parts. Recently, VRBA and ROD [19] have made some calculation of mass transfer in a back-flow model.

Since the back-flow at the cathode is primarily a motion of denser solution, so it influences the concentration gradient perpendicular to the cathode. Therefore, in the back-flow region the concentration gradient and consequently the local limiting current become mostly constant along the cathode.

Variation of the back-flow with time is found to depend on the molarity of the electrolyte. However, due to the back-flow, the limiting current is not reached at the same time by the whole surface of the cathode, (Fig. 2,) where the current density remains constant, is not the same for the different concentrations. The width of the plateau, in which the current remains con-

stant with increasing potential, decreases with the increase of molarity. From Fig. 2 it is clear also that the required time to reach the limiting current increases with molarity.

Insertion of the specially designed diaphragm made of a centred glass to separate the cathode compartment from that of the anode is accompanied with an increase in the rate of the back-flow as given in Fig. 4. Moreover, the rate of change of the back-flow increases with the separation of the diaphragm from the cathode towards the anode surface.

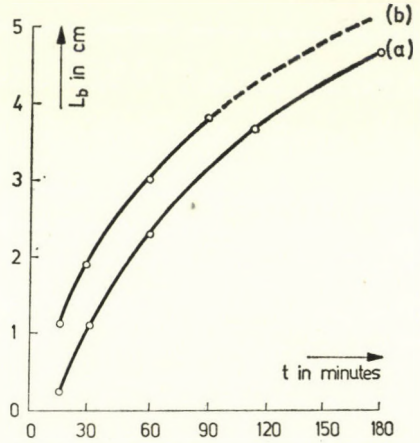

Fig. 4. Rate of change of the back-flow with and without diaphragm.
a: without diaphragm, b: with diaphragm

Variation of the viscosity and diffusion coefficients by the addition of different concentration of glycerol, up to 6.38 M/L, to the acidified copper-sulphate solutions also indicates a constancy in the limiting current measurements along the height of the cathode surface beside presence of the back-flow with the original flow.

Therefore, in conclusion, the back-flow is a physical phenomenon already existing in the fluid motion of the electrolysing cell to grasp the original flow irrespective of viscosity and diffusion coefficients of the electrolyte or of the presence of the diaphragm separating the anode compartment from the cathode compartment.

REFERENCES

1. J. T. Hanratty, D. L. Eckelman and F. Gilead, Turbul. Liquids, Proc. Symp., 140, 1971.
2. J. N. Agar, Discussion Faraday Soc., **1**, 26, 1947.
3. A. Ch. Bairiev, P. M. Brdlik and I. A. Kozhinov, Izv. Akad. Nauk. Turkm. SSR, Ser. Fiz.-Tekh., Khim. Geol. Nauk, **1**, 20, 1973.
4. J. P. Elder and G. Wranglen, Electrochemical Technology, **2**, 34, 1964.
5. J. R. Lloyd, E. M. Sparrow and E. R. G. Eckert, J. Electrochem. Soc., **119**, 702, 1972.

6. W. K. WOLFGANG, AICHE Symp. Ser., **118**, 112, 1972.
7. C. R. WILKE, M. EISENBERG and C. W. TOBIAS, J. Electrochem. Soc., **100**, 513, 1953.
8. C. WANGER, J. Electrochem. Soc., **104**, 129, 1957.
9. C. R. WILKE, C. W. TOBIAS and M. EISENBERG, Chemical Eng. Progress, **49**, 663, 1953.
10. DELAHY and TOBIAS: Advances in Electrochemistry and Electrochemical Engineering, Interscience Book, Vol. 2, 1962.
11. M. EISENBERG, C. W. TOBIAS and C. R. WILKE, J. Electrochem. Soc., **102**, 415, 1955.
12. E. SCHMIDTH, Forsch. Ing.-Wes., **3**, 181, 1932.
13. U. GRIGULL, Int. J. Heat Mass Transfer, **6**, 669, 1963.
14. M. EISENBERG, C. W. TOBIAS and C. R. WILKE, J. Electrochem. Soc., **103**, 413, 1956.
15. E. J. FENECH and C. W. TOBIAS, Electrochem. Acta, **2**, 311, 1960.
16. M. G. FOUND and A. M. AHMED, Electrochem. Acta, **14**, 641, 1969.
17. N. IBL and R. H. MULLER, J. Electrochem. Soc., **105**, 346, 1958.
18. N. IBL, W. RUEGG and C. TRUMPLER, Helv. Phys. Acta, **36**, 1824, 1953 and ibid., 37, 2251, 1854.
19. J. VRBA and V. ROD, Collect. Czech. Chem. Commun., **38**, 2082, 1973.

Acta Physica Academiae Scientiarum Hungaricae, Tomus 41 (4), pp. 241—244 (1976)

A NOTE ON AN INTERIOR SOLUTION FOR A FLUID SPHERE OF CONSTANT GRAVITATIONAL MASS DENSITY IN GENERAL RELATIVITY

By

J. P. SHARMA

DEPARTMENT OF APPLIED SCIENCES, M.M.M. ENGINEERING COLLEGE, GORAKHPUR, INDIA

(Received 12. VIII. 1976)

Solutions of the field equations, for a fluid sphere of constant gravitational mass density, have been obtained in the present note.

I. Introduction

Schwarzschild interior solution of the field equations for a fluid sphere of constant density ϱ is quite well known and is of great importance in general relativity. Recently, in three subsequent papers [1, 2, 3], the author has studied planetary structures in general relativity, in general, and the internal structure of Mars in particular. So far as known to the author, a solution of the field equations for a fluid sphere (which is in hydrostatic equilibrium) of constant gravitational mass density $\varrho c^2 + 3P = H$ (1935) has not been attempted. Gravitational attraction of matter is governed by this expression (rather than ϱ). The physical significance of the parameter $HK/2\delta^2$ has been pointed out.

II. The equations of equilibrium

In the case of spherical symmetry, the time-independent metric in (r, Θ, Φ)-coordinate system is given by (MOLLER [4])

$$a(r)dr^2 + r^2 d\Omega^2 - b(r)c^2 dt^2, \tag{1}$$

where $d\Omega^2 = (\mathrm{d}\Theta^2 + \sin^2\Theta d\Phi^2)$. The gravitational equations, needed for our purpose, reduce to

$$\frac{1}{ar}\left(\frac{1}{b}\frac{db}{dr} + \frac{1}{r}\right) - \frac{1}{r^2} + \lambda = KP, \tag{2}$$

and

$$\frac{1}{ar}\left(\frac{1}{a}\frac{da}{dr} - \frac{1}{r}\right) + \frac{1}{r^2} - \lambda = K\varrho c^2, \tag{3}$$

where symbols have their usual significance. In the general theory, the hydrostatic equilibrium equation becomes

$$\frac{dP}{dr} + (P + \varepsilon)\frac{1}{2b}\frac{db}{dr} = 0, \tag{4}$$

where P is the pressure and $\varepsilon = \varrho c^2$ is the energy density written as an equivalent to mass density ϱ times the square of the speed of light c^2.

III. The desired solutions

For a fluid sphere of constant gravitational mass density, our assumed relation, connecting pressure with the energy density, is

$$\varrho c^2 + 3P = H = \text{constant}. \tag{5}$$

Substituting (5) into (4), we obtain a solution

$$H - 2P = \alpha b, \tag{6}$$

where α is the constant of integration. Adding (2) and (3), we have

$$\frac{1}{b}\frac{db}{dr} + \frac{1}{a}\frac{da}{dr} = K\alpha r(P + \varrho c^2), \tag{7}$$

or, in view of Eqs. (4) and (6), this becomes

$$\frac{d}{dr}(ab) = K\alpha r(ab)^2, \tag{7'}$$

the integration of which yields

$$ab = \frac{2\beta}{2 - K\alpha\beta r^2} = \frac{\beta}{1 - \delta^2 r^2}, \tag{8}$$

where β is another constant of integration and $\delta = (K\alpha\beta/2)^{1/2}$. Making use of Eqs. (6) and (8) in (2), we obtain

$$(1 - \delta^2 r^2)\, r\frac{db}{dr} + b = \beta + \frac{\beta}{2}(KH - 2\lambda)r^2. \tag{9}$$

Solving this linear differential equation, we obtain

$$b(r) = \beta\left\{1 + L - \frac{L}{\delta r}(1 - \delta^2 r^2)^{1/2} \sin^{-1} \delta r\right\} + \frac{M}{r}(1 - \delta^2 r^2)^{1/2}, \tag{10}$$

where
$$L = \frac{1}{2\delta^2}(KH - 2\lambda); \quad M = \text{constant}. \tag{11}$$

Since $b(r)$ remains finite at the centre $r = 0$ of the fluid sphere, M must vanish. Thus Eq. (10) simply reduces to

$$b(r) = \beta\left\{1 + L - \frac{L}{\delta r}(1 - \delta^2 r^2)^{1/2} \sin^{-1} \delta r\right\}. \tag{12}$$

Substituting (12) into (8), we get

$$a(r) = \left\{(1 + L)(1 - \delta^2 r^2) - L(\delta r)^{-1}(1 - \delta^2 r^2)^{3/2} \sin^{-1} \delta r^{-1}\right\}. \tag{13}$$

In view of the above, the product of K and the pressure can be expressed as

$$KP = \lambda - \delta^2 + L\delta \frac{(1 - \delta^2 r^2)^{3/2}}{r} \sin^{-1} \delta r. \tag{14}$$

The central values of KP and $(K\varrho)c^2$ are given by

$$(KP)_{r=0} = \lambda + (L - 1)\delta^2 = 0.5\, KH - \delta^2, \tag{15}$$

and

$$(K\varrho)_{r=0}^{c^2} = 3\delta^2 - 0.5\, KH, \tag{16}$$

respectively. These equations make it clear that KH must satisfy the inequality

$$\delta^2 \leq \frac{KH}{2} \leq 3\delta^2, \tag{17}$$

so that P_0 and ϱ_0 remain positive. One may verify that dP/dr is negative, the physical meaning of which is that as the radius increases, the pressure decreases and attains a zero value at the surface boundary $r = r_1$ of the sphere, where $x_1 = \alpha r_1$ satisfying

$$(\delta^2 - \lambda)x_1 = \frac{1}{2}(KH - 2\lambda)\sqrt{1 - x_1^2} \sin^{-1} x_1, \tag{18}$$

and we find that it lies between 0 and 1. At this point we may replace the interior solution by the Schwarzschild exterior solution for which

$$b(r) = \frac{1}{a(r)} = 1 - \frac{2m}{r} - \frac{1}{3}\lambda r^2. \tag{19}$$

For the exterior solution $a(r)$ and $b(r)$, P and ϱc^2 should be continuous everywhere and $ab = 1$, therefore, from (8) we find that

$$\beta = 1 - \delta^2 r_1^2, \tag{20}$$

Also, from Eqs. (6) and (19), we find

$$\frac{H}{\alpha} = \frac{KH\beta}{2\delta^2} = 1 - \frac{2m}{r_1^2} - \frac{1}{3}\lambda r^2 = \frac{HK}{2\delta^2}(1 - \delta^2 r_1^2). \tag{21}$$

We may note that λ (cosmical constant) has been taken into consideration for the sake of completeness, but in actual situation where the formulae are to be applied we may ignore the same (if not actually zero).

We define the value of the parameter $HK/2\delta^2$, in terms of the central pressure and central density, as follows:

$$\frac{HK}{2\delta^2} = \frac{\varrho_0 c^2 + 3P_0}{\varrho_0 c^2 + P_0}. \tag{22}$$

If we put $\lambda = 0$ in (21), then

$$\frac{2m_1}{r_1} = 1 - \left\{\frac{HK}{2\delta^2}(1 - \delta^2 r_1^2)\right\}. \tag{23}$$

Hence, in order that m remains positive,

$$\frac{HK}{2\delta^2}(1 - \delta^2 r_1^2) < 1, \tag{24}$$

which is a strict inequality so as to satisfy the Schwarzschild exterior solution.

REFERENCES

1. J. P. SHARMA, Pure Appl. Geophys., **97**, 14, 1972.
2. J. P. SHARMA, J. Geophys., **78**, 4821, 1973.
3. J. P. SHARMA, Study of the Internal Structure of a Planet in General Relativity, J. Pure Appl. Maths., accepted 1976.
   J. P. SHARMA, J. Geophys. Res., **78**, 31, 1973.
4. C. MOLLER, The Theory of Relativity, Clarendon Press, Oxford, 1952.

Acta Physica Academiae Scientiarum Hungaricae, Tomus 41 (4), pp. 245—247 (1976)

PLASMA HEATING DUE TO NON-LINEAR INTERACTION IN TWO SPECIAL FOUR-PLASMA-WAVE SYSTEMS

By

JÜRGEN W. WEIL

INSTITUTE FOR THEORETICAL PHYSICS, UNIVERSITY OF INNSBRUCK, INNSBRUCK, AUSTRIA*

(Received 2. IX. 1976)

Two slightly different systems of differential equations for wave-packet-averaged electric-field amplitudes of four interacting waves in a plasma are solved, the solution of the "undamped" system being used as the initial trial function of the "damped" system. The rates of energy transfer from the waves to the plasma are calculated in either case.

In analogy to e.g. TSYTOVICH [1] we start from the following, merely time-dependent system describing non-linear interaction of one longitudinal and three transverse waves in a plasma:

$$\dot{E}_1^l = -i\Delta^l E_2^t E_3^t E_4^t ,$$

$$\dot{E}_2^t = i\Delta_2^t E_1^l E_3^{*t} E_4^{*t}/\gamma_2 , \quad E_4^t = \text{const.}$$

$$\dot{E}_3^t = i\Delta_3^t E_1^l E_2^{*t} E_4^{*t}, \tag{1.a—d}$$

where $E_i^{l,t}$, $i = 1, \ldots 4$, designate wave-packet-averaged electric field amplitudes, $\Delta_i^{l,t}$ are real coupling coefficients, γ_2 is a (large) damping rate, and wave 4 is strong enough to be considered constant during the relevant processes.

Setting $\alpha^l \equiv |E^l|^2/\Delta^l$, $\alpha_3^t \equiv -|E_3^t|^2/\Delta_3^t$, we obtain the conservation law

$$\alpha^l + \alpha_3^t = C = \lambda\big(\equiv \alpha^l(0)\big) + \varkappa\big(\equiv \alpha_3^t(0)\big) \tag{2}$$

with $\varkappa$ and λ as initial values, and the differential equations

$$\dot{\alpha}^l(t) = 2\Delta^l \Delta_2^t \Delta_3^t \alpha^l(t)\,(\alpha^l(t) - C)\,|E_4^t|^2/\gamma_2$$

$$\dot{\alpha}_3(t) = 2\Delta_2^t \Delta^l \Delta_3^t C - \alpha_3^t(t)\big)\alpha_3^t(t)\big)\,|E_4^t|^2/\gamma_2 \tag{3.a,b}$$

solved by

$$\alpha^l(t) = \lambda C e^{2\hat{\gamma}t}/(\varkappa + \lambda e^{2\hat{\gamma}t}) . \tag{4.a}$$

$$\alpha_3^t(t) = \varkappa C e^{-2\hat{\gamma}t}/(\lambda + \varkappa e^{-2\hat{\gamma}t}) . \tag{4.b}$$

with

$$\hat{\gamma} \equiv -C\Delta^l \Delta_2^t \Delta_3^t/\tilde{\gamma}_2, \; \tilde{\gamma}_2 \equiv \frac{\gamma_2}{|E_4^t|^2} .$$

* Present address: IAEA, 1010 Vienna, Kärntner Ring 11, Austria.

The difference in the sums of the energy densities of both waves at times t and $t = 0$ is equal to the change in the internal energy density of the plasma:

$$\frac{3}{2}\varrho k(T(t) - T(0)) = |E^l|^2(0) + \\ + |E_3^t|^2(0) - |E^l|^2(t) - |E_3^t|^2(t) = \frac{\lambda\varkappa\,(\Delta_3^t - \Delta^l)}{\lambda e^{2\hat{\gamma}t} + \varkappa}\,(1 - e^{2\hat{\gamma}t}). \tag{5}$$

Obviously, one of the two waves 1 and 3 "sucks" up the other, the direction of this process given by the sign of $\hat{\gamma}$. The role of the fourth, strong wave consists in controlling the rate of this process, i.e. for positive $\hat{\gamma}$ the amplitude of the longitudinal wave grows the faster the stronger wave 4 (the wave acts as a sort of "pre-stress" in the plasma).

We now include a weak damping in wave 3, i.e. $\dot{E}_3^t + \gamma_3 E_3^t = D_3^t E_4^{*t} E_2^{*t} E_1^l$; the other waves remain as before. In this case (2) is replaced by

$$\dot{\alpha}^l = \dot{\alpha}_3^t + 2\gamma_3\alpha_3^t\,, \tag{2.a}$$

whence

$$\alpha_3^t = -e^{-2\gamma_3 t}\int \dot{\alpha}^l(t)\,e^{2\gamma_3 t}\,\mathrm{d}t \tag{6}$$

and, as the differential equation corresponding to (3.a):

$$\frac{d\ln\alpha^l}{dt} = \frac{2}{\tilde{\gamma}_2}\,\Delta_2^t\,\Delta^l\,\Delta_3^t\,e^{-2\gamma_3 t}\int \dot{\alpha}^l(t)e^{2\gamma_3 t}\,dt\,. \tag{7}$$

An iterative solution of this integro-differential equation now chooses the time derivative of (4.a) as $\dot{\alpha}^l$ on the right-hand side of (7), i.e. the old system is regarded as the limit of the new one for $\gamma_3 = 0$. Taking $2(\hat{\gamma} + \gamma_3) = \mu$, $2\hat{\gamma} \equiv \nu$ we obtain:

$$\frac{d\ln\alpha^l}{dt} = 4\hat{\gamma}^2\varkappa\lambda e^{-2\gamma_3 t}\int \frac{e^{\mu t}}{(\varkappa + \lambda e^{\nu t})^2}\,dt = 2\,\hat{\gamma}\varkappa\lambda\,e^{-2\gamma_3 t}\int \frac{x^{\mu/\nu - 1}}{(\varkappa + \lambda x)^2}\,dx. \tag{8}$$

To have a case with tractable mathematics at hand, we set $\mu/\nu = 2$ which leads to

$$\frac{\alpha^l}{\varkappa + \lambda} = \exp\left\{\frac{\nu\varkappa}{\lambda}\left[\varkappa\int \frac{e^{-\nu t}}{\varkappa + \lambda e^{\nu t}}\,dt + \int e^{-\nu t}\ln(\varkappa + \lambda e^{\nu t})\,dt\right]\right\},$$

i.e.

$$\alpha_{\mathrm{damp}}^l(t) = (\lambda e^{\nu t + 1} + \varkappa e)^{-\varkappa/\lambda}\,e^{-\nu t}(\varkappa + \lambda)\,,$$

$$\alpha_{3\,\mathrm{damp}}^t(t) = e^{-\nu t}\frac{(\varkappa + \lambda)\,\varkappa}{\lambda}\left(\frac{\varkappa}{\varkappa + \lambda e^{\nu t}} + \ln(\varkappa + \lambda e^{\nu t})\right), \tag{9. a, b}$$

where "damp" designates solutions of the second system. Both systems have the property that for $t \to \infty, \hat{\gamma} > 0$, α^l and α^l_{damp} tend to $\varkappa + \lambda$, and α^t_3 and $\alpha^t_{3\text{damp}}$ tend to zero, but the details of energy transfer are different. The change in the internal energy density of the plasma is, for the second system, given by

$$\frac{3}{2}\varrho k\big(T(t) - T(0)\big) = \Delta^l(\varkappa + \lambda)\left[(\varkappa + \lambda)^{-\varkappa/\lambda} e^{-\varkappa/\lambda} - \right.$$

$$- (\lambda e^{\nu t} + \varkappa)^{-(\varkappa/\lambda)e^{-\nu t}} e^{-(\varkappa/\lambda)\, e^{-\nu t}}] +$$

$$+ \Delta^t_3\left[e^{-\nu t}\,\frac{(\varkappa + \lambda)\varkappa}{\lambda}\left(\frac{\varkappa}{\varkappa + \lambda e^{\nu t}} + \right.\right. \tag{10}$$

$$\left.\left. + \ln(\varkappa + \lambda e^{\nu t})\right) - \frac{(\varkappa + \lambda)\varkappa}{\lambda}\left(\frac{\varkappa}{\varkappa + \lambda} - \ln(\varkappa + \lambda)\right)\right] .$$

A fuller account of the work undertaken here will be published soon; in particular, the method of using the solution of one system as the zeroth iterative solution of the next complicated one will be extended to system where the fourth-wave amplitude is no longer constant.

REFERENCE

1. V. N. Tsytovich, Nonlinear Effects in a Plasma, Plenum Press, New York—London, p. 46 ff. 1970.

Acta Physica Academiae Scientiarum Hungaricae, Tomus 41 (4), pp. 249—261 (1976)

SINGULARITIES OF A VARIATIONAL PARTITION FUNCTION

By

W. LUCHT

MARTIN-LUTHER-UNIVERSITÄT, SEKTION MATHEMATIK, HALLE/SAALE, GDR

(Received 7. IX. 1976)

By concrete examples it is shown that a variational approximation to the partition function (VPF) may have singularities of the phase transition types. Sufficient conditions for the existence of such singularities are given. One of these conditions is the presence of a continuous part in the spectrum of the underlying Hamiltonian.

1. Introduction

It was shown [1] that a generalized version of the Lippmann—Schwinger variational principle can be used to calculate (approximately) the partition function of statistical mechanics:

$$\Xi(P) = Tr\left\{e^{-\beta(H+PK)}\right\}, \quad \beta = (k_B T)^{-1}. \tag{1}$$

H and K are the unperturbed and the perturbed parts of a Hamiltonian of a proper physical system, respectively, and P is a variable scalar parameter. k_B and T are, as usual, Boltzmann's constant and the absolute temperature. In this paper we discuss the singularities of the variational approximation to the partition function (called variational partition function, VPF). In order to do this we choose special model Hamiltonians H and K which are assumed to be given in the spectral representation. Furthermore, it is assumed that these Hamiltonians possess a discrete and a continuous spectrum. The presence of the continuous spectrum (typically for the Hamiltonian of a large system) is the essential supposition of this paper. We show then that there is, under some other conditions, a way to derive a VPF which itself is finite and well behaved but which possesses discontinuous derivatives with respect to P of a certain order (at fixed T). This order depends on the properties of the given physical system (e.g. the density of states per energy interval).

First the general theory is reviewed. Then, after a little specialization which makes the procedure tractable, we present the examples.

2. The general theory

Defining the average

$$\langle \ldots \rangle_0 = \frac{1}{\Xi(0)} Tr \{ \ldots e^{-\beta H} \}, \tag{2}$$

one can calculate the partition function in the form [2]

$$\Xi(P) = \Xi(0) \langle U(\beta, 0) \rangle_0, \tag{3}$$

where

$$U(\tau, \tau_1) = 1 - P \int_{\tau_1}^{\tau} d\tau' \, K(\tau') \, U(\tau', \tau_1) \tag{4}$$

$$K(\tau) = e^{\tau H} K e^{-\tau H}. \tag{5}$$

$U(.\,,.)$ is called thermal evolution operator. We introduce the star hermitian conjugation [3] by

$$K(\tau)^* = K^+(-\tau) = K(\tau) \tag{6}$$

and write down the operator valued Lippmann—Schwinger functional [4]

$$F(V^*, V; \tau_2, \tau_1) = 1 - P \int_{\tau_1}^{\tau_2} d\tau \, [V^*(\tau, \tau_2) K(\tau) + K(\tau) V(\tau, \tau_1)] +$$

$$+ P \int_{\tau_1}^{\tau_2} d\tau V^*(\tau, \tau_2) \, K(\tau) \, V(\tau, \tau_1) + P^2 \int_{\tau_1}^{\tau_2} d\tau \int_{\tau_1}^{\tau_2} d\tau' \, V^*(\tau, \tau_2) K(\tau) \cdot \tag{7}$$

$$\cdot \, \Theta(\tau - \tau') \, K(\tau') \, K(\tau') V(\tau', \tau_1) \, ,$$

where

$$\Theta(x) = \begin{cases} 1 \text{ for } x > 0 \\ 0 \text{ for } x < 0. \end{cases} \tag{8}$$

As shown in [1, 4] the following basic theorem is valid:

Theorem: The values of the operators V and V^* for which the functional is stationary, with respect to variations δV and δV^*, are the evolution operators of the Hamiltonian PK. Furthermore, the stationary value of the functional itself reduces to the evolution operator for the interval τ_1 to τ_2.

With the help of the integral equation (4) one can generate the operators

$$U_{n+1}(\tau, \tau_1) = - P \int_{\tau_1}^{\tau} d\tau' \, K(\tau') \, U_n(\tau' \tau_1), \qquad n \geq 0 \tag{9a}$$

$$U^*_{n+1}(\tau, \tau_2) = P \int_{\tau_2}^{\tau} d\tau' U^*_n(\tau', \tau_2) K(\tau') \qquad n \geq 0, \tag{9b}$$

with

$$U_0(\tau, \tau_i) = 1. \tag{9c}$$

At order N we choose $V = U^{(N)}$ and $V^* = U^{(N)*}$ with

$$U^{(N)}(\tau,\tau_1) = \sum_{n=0}^{j} U_n(\tau,\tau_1) + \sum_{n=j+1}^{N-1} U_n(\tau,\tau_1)\mu_n\,, \tag{10a}$$

$$U^{(N)*}(\tau,\tau_2) = \sum_{n=1}^{j} U_n^*(\tau,\tau_2) + \sum_{n=j+1}^{N-1} \lambda_n\, U_n^*(\tau,\tau_2)\,, \tag{10b}$$

where j is an integral number with the restriction

$$-1 \leq j \leq N-2\,. \tag{11}$$

The operators μ_n and λ_n must be determined. After a number of steps [4] one can rewrite the functional (7) in the form

$$F = F_z|_{z=1} \tag{12}$$

$$F_z \equiv F_z(\lambda_{j+1}, \ldots, \lambda_{N-1};\ \mu_{j+1}, \ldots, \mu_{N-1};\ \tau_2, \tau_1) = 1 + zQ_z, \tag{13}$$

$$Q_z = \sum_{n=0}^{2j+1} z^n U_{n+1} + \sum_{N=0}^{N-j-2} z^{2j+2+n}(U_{2j+n+3}\,\mu_{j+n+1} + \lambda_{j+n+1}\,U_{2j+n+3}) - \sum_{n,m+0}^{N-j-2} z^{2j+2+n+m}\,\lambda_{j+n+1}\cdot(U_{2j+3+n+m} - zU_{2j+4+n+m})\,\mu_{j+m+1}\,. \tag{14}$$

Setting the first variations of the functional F, with respect to λ_n and μ_n, equal to zero we obtain the equations which determine the variational operators for $\alpha = j+1,\ j+2,\ \ldots,\ N-1$:

$$\frac{\delta F_z}{\delta\lambda_\alpha} = z^{j+\alpha+2}\left[U_{j+\alpha+2} - \sum_{n=0}^{N-j-2} z^n\,(U_{j+\alpha+n+2} - zU_{j+\alpha+n+3})\cdot\mu_{j+n+1}\right] = 0, \tag{15a}$$

$$\frac{\delta F_z}{\delta\mu_\alpha} = z^{j+\alpha+2}\left[U_{j+\alpha+2} - \sum_{n=0}^{N-j-2} z^n\,\lambda_{j+n+1}\,(U_{j+\alpha+n+2} - z\,U_{j+\alpha+n+3})\right] = 0. \tag{15b}$$

The simplest case (which we shall use in this paper) arises with the choice $j = N-2$. The Eqs. (15) yield the two relations for λ_{N-1} and μ_{N-1}:

$$U_{2N-1}(\tau_2,\tau_1) = [U_{2N-1}(\tau_2,\tau_1) - zU_{2N}(\tau_2,\tau_1)]\mu_{N-1}\,, \tag{16a}$$

$$U_{2N-1}(\tau_2,\tau_1) = \lambda_{N-1}\,[U_{2N-1}(\tau_2,\tau_1) - zU_{2N}(\tau_1,\tau_1)]\,. \tag{16b}$$

Assuming the existence of the inverse operator (this is fulfilled in our models)

$$[U_{2N-1}(\tau_2,\tau_1) - zU_{2N}(\tau_2,\tau_1)]^{-1}$$

we have, according to the above theorem, the following variational approximation to the thermal evolution operator (now $\tau_1 = 0$ and $\tau_2 = \beta$ because of (3))

$$U(\beta, 0) \approx F_{\text{stat}}(\beta, 0) = 1 + \sum_{n=0}^{2N-3} U_{n+1}(\beta, 0) + \\ + U_{2N-1}(\beta, 0)[U_{2N-1}(\beta, 0) - U_{2N}(\beta, 0)]^{-1} U_{2N-1}(\beta, 0). \tag{17}$$

We have used the expressions (12), (13) and (14) with $j = N - 2$ and the solutions of Eq. (16).

Since we are interested in the P-dependence of the VPF we rewrite the representation (17) using the fact that U_n is proportional to P^n (see Eq. (9)). We define

$$U_n(\beta, 0) = P^n w_n(\beta, 0), \tag{18a}$$

where

$$w_n(\beta, 0) = -\int_0^\beta dt \cdot K(t) w_{n-1}(t, 0), \qquad w_0 = 1, \tag{18b}$$

and can then write (for short $w_n = w_n(\beta, 0)$)

$$U(\beta, 0) \approx F_{\text{stat}}(\beta, 0) = 1 + \sum_{n=1}^{2N-2} P^n w_n + P^{2N-1} \cdot \\ \cdot w_{2N-1}[w_{2N-1} - P w_{2N}]^{-1} w_{2N-1} \cdot \tag{19}$$

The VPF is then explicitly given by

$$\Xi_{\text{VPF}}(P) = \Xi(0)\Big[1 + \sum_{n=1}^{2N-2} P^n \langle w_n \rangle_0 + P^{2N-1} \cdot \\ \cdot \langle w_{2N-1}\,[w_{2N-1} - P w_{2N}]^{-1} w_{2N-1} \rangle_0\Big]. \tag{20}$$

3. First model: diagonal perturbation

In order to explain how the theory works we study the simple model

$$H = \sum_\nu E_\nu \mid \nu\rangle\langle\nu \mid + \int_{\mathfrak{C}} d\mathfrak{k} E(\mathfrak{k}) \mid \mathfrak{k}\rangle\langle\mathfrak{k} \mid \tag{21}$$

$$K = \int_{\mathfrak{A}} d\mathfrak{k} W(\mathfrak{k}) |\mathfrak{k}\rangle\langle\mathfrak{k}| + \int_{\mathfrak{B}} d\mathfrak{k} V(\mathfrak{k}) \mid \mathfrak{k}\rangle\langle\mathfrak{k} \mid \tag{22}$$

with the non-overlapping condition

$$\mathfrak{A} \cap \mathfrak{B} = \varnothing \tag{23a}$$

and

$$\mathfrak{A} \subset \mathfrak{C}, \quad \mathfrak{B} \subset \mathfrak{C}, \quad \mathfrak{A} \cup \mathfrak{B} \subseteq \mathfrak{C}. \tag{23b}$$

The fields $|\, \nu\rangle$ and $|\, \mathfrak{k}\rangle$ are supposed to fulfil formally the relations

$$\langle \nu \mid \nu' \rangle = \delta_{\nu\nu'}, \quad \langle \mathfrak{k} \mid \mathfrak{q} \rangle = \delta(\mathfrak{k} - \mathfrak{q}), \quad \langle \nu \mid \mathfrak{k} \rangle = 0. \tag{23c}$$

(The conditions (23a, b) are written in set-theoretic notation, e.g. $\varnothing$ is the empty set.) We consider always parameters P which are not negative,

$$P \geq 0, \tag{24}$$

and assume for reasons of physical stability

$$-\text{const} \leq E_\nu < 0 \quad \text{and} \quad 0 \leq E(\mathfrak{k}) \ , \tag{25}$$

$$W_0 \leq W(\mathfrak{k}) \leq W_1 \text{ with } W_0 < W_1 < 0 \text{ and } 0 \leq V_0 \leq V(\mathfrak{k}). \tag{26}$$

For concreteness we suppose for $V(\mathfrak{k})$ an unbounded function of the type ($\mathfrak{k}_c$ fixed)

$$V(\mathfrak{k}) = v(\mathfrak{k}) \frac{|\, \mathfrak{k}_c \,|^\gamma}{|\mathfrak{k} - \mathfrak{k}_c|^\gamma}, \qquad 0 < \gamma < 1, \tag{27}$$

with $v\,(\mathfrak{k})$ a bounded and positive scalar function. The sum $\sum_\nu$ in (21) represents the discrete part while the integrals in (21) and (22) give the continuous parts of the corresponding operators. The continuous parameter $\mathfrak{k}$ is assumed to be a multidimensional vector of, say, s dimensions ($s \geq 1$)

$$\mathfrak{k} = \{k_1, k_2, \ldots, k_s\} \, . \tag{28a}$$

It is then $\mathrm{d}\mathfrak{k} = \mathrm{d}k_1 \, \mathrm{d}k_2 \ldots \mathrm{d}k_s$ and

$$|\, \mathfrak{k} - \mathfrak{k}_c \,| = \left[\sum_{n=1}^{s} (k_n - k_{cn})^2 \right]^{1/2}. \tag{28b}$$

Later we choose in an explicit example $s = 1$.

Remembering that the subspaces corresponding to the discrete and continuous parts of the spectrum are orthogonal [5] we obtain from (18b) and (19) (because of $HK - KH = 0$)

$$F^{\pm}_{\text{stat}} = 1 + \sum_{n=1}^{2N-2} (-P\beta K)^n/n! + [(-P\beta K)^{2N-1}/(2N-1)!] \frac{x}{x - K \pm i\varepsilon}, \tag{29}$$

where

$$x = -2N/(P\beta) < 0. \tag{30}$$

In (29) we have introduced an infinitesimal positive quantity ε which goes to zero. Using the well-known relation (Pr denotes principal part)

$$\frac{1}{x - K \pm i\varepsilon} = Pr\frac{1}{x - K} \mp i\pi\delta(x - K)$$

and

$$F_{\text{stat}} = (F^{+}_{\text{stat}} + F^{-}_{\text{stat}})/2, \tag{31}$$

we obtain

$$\begin{aligned}\langle F_{\text{stat}}\rangle_0 = 1 + \sum_{n=1}^{2N-2} (-P\beta)^n/n! \cdot \langle K^n\rangle_0 + \\ + \frac{(-P\beta)^{2N-1}}{(2N-1)!} x \left\langle K^{2N-1}\left\{Pr\int_{\mathfrak{A}} d\mathfrak{k}\frac{|\mathfrak{k}\rangle\langle\mathfrak{k}|}{x - W(\mathfrak{k})} + \int_{\mathfrak{B}} d\mathfrak{k}\frac{|\mathfrak{k}\rangle\langle\mathfrak{k}|}{x - V(\mathfrak{k})}\right\}\right\rangle_0.\end{aligned} \tag{32}$$

If this expression shall have a meaning all the averages $\langle K^m\rangle_0$, $1 \leq m \leq 2N-2$, must be finite. This is the criterion which yields the number N. We call it the *truncation criterion*. Since

$$K^m = \int_{\mathfrak{A}} d\mathfrak{k}(W(\mathfrak{k}))^m |\mathfrak{k}\rangle\langle\mathfrak{k}| + \int_{\mathfrak{B}} d\mathfrak{k}(V(\mathfrak{k}))^m |\mathfrak{k}\rangle\langle\mathfrak{k}| \tag{33}$$

and $W(\mathfrak{k})$is finite on $\mathfrak{A}$ we must investigate

$$\left\langle \int_{\mathfrak{B}} d\mathfrak{k}\,(V(\mathfrak{k}))^m |\mathfrak{k}\rangle\langle\mathfrak{k}| \right\rangle_0 = \frac{1}{\Xi(0)}\int_{\mathfrak{B}} d\mathfrak{k} e^{-\beta E(\mathfrak{k})}(V(\mathfrak{k}))^m \varrho(\mathfrak{k}), \tag{34}$$

where $\varrho(\mathfrak{k})$ is a positive function which arises from $Tr\{|\mathfrak{k}\rangle\langle\mathfrak{k}|\}$. (Example: If the given system is enclosed in a three-dimensional volume Ω and $\mathfrak{k}$ is a wave vector, i.e. $s = 3$, then it would be $\varrho(\mathfrak{k}) = \Omega/(2\pi)^3 = \text{const}$).

Now we choose $s = 1$ and employ expression (27). Let the domain of integration, $\mathfrak{B}$, be the finite real interval [a, b], $a < b$. Furthermore, let the function

$$f(k) = e^{-\beta E(k)} \cdot (v(k))^m \varrho(k) \tag{35}$$

fulfil a Lipschitz condition with constant L (e.g. see to this problem [6])

$$|f(k) - f(k')| \leq L|k - k'|.$$

The result is for k_c such that $a < k_c < b$

$$\left\langle \int_{\mathfrak{B}} dk \left(V(k)\right)^m |k\rangle\langle k| \right\rangle_0 = \frac{|k_c|^{m\cdot\gamma}}{\Xi(0)} \cdot \int_a^b dk \frac{e^{-\beta E(k)} \left(v(k)\right)^m \varrho(k)}{|k - k_c|^{m\gamma}} = \tag{36}$$

$$= \begin{cases} \text{finite} & \text{for} \quad m < \left[\frac{1}{\gamma}\right], \\ \infty & \text{for} \quad m > \left[\frac{1}{\gamma}\right]. \end{cases}$$

Here $[x]$ denotes integral part of x (i.e. $x = [x] + \alpha$, $0 \leq \alpha < 1$). Consequently the truncation criterion yields the maximal number for the expansion:

$$N = \left[\frac{1}{2}\left(2 + \left[\frac{1}{\gamma}\right]\right)\right]. \tag{37}$$

For N which are larger than the expression on the right the expansion (32) is meaningless.

After having established this the average (see (32) in connection with (20))

$$I_{2N-1}(x) = \left\langle K^{2N-1} \cdot Pr \int_{\mathfrak{A}} dk \frac{|k\rangle\langle k|}{x - W(k)} \right\rangle_0. \tag{38}$$

can be calculated. Since $x < 0$ and $W(k) < 0$ we must distinguish three cases, namely

$$x < W_0, \quad W_0 < x < W_1 \quad \text{and} \quad W_1 < x. \tag{39}$$

If the principal value integral does exist and is continuous, then, in general, there can be discontinuities in the derivatives of (38) with respect to P along the lines $x = W_0$ and $x = W_1$. Thus the VPF has singularities of a phase transition type. Two explicit examples are given in Appendix A. The integral over $\mathfrak{B}$ in (32) has no singularities because $x < 0$ and $V(k) \geq V_0 \geq 0$. Therefore, we will not discuss it here.

4. Second model: non-diagonal perturbation

The Hamiltonians are defined by

$$H = \sum_\nu E_\nu |\varphi_\nu\rangle \langle\varphi_\nu| + \sum_\alpha \varepsilon_\alpha |\psi_\alpha\rangle\langle\psi_\alpha| + \int_{\mathfrak{C}} d\mathfrak{k} E(\mathfrak{k}) |\varphi(\mathfrak{k})\rangle\langle\varphi(\mathfrak{k})|, \tag{40}$$

$$K = A(W + V) \equiv \sum_{\nu,\mu} A_{\nu\mu} \mid \psi_\nu\rangle\langle\psi_\mu \mid \cdot \Big[\int_{\mathfrak{A}} d\mathfrak{k} W(\mathfrak{k}) \mid \varphi(\mathfrak{k})\rangle\langle\varphi(\mathfrak{k}) \mid + \int_{\mathfrak{B}} d\mathfrak{k}\, V(\mathfrak{k}) \mid \varphi(\mathfrak{k})\rangle\langle\varphi(\mathfrak{k}) \mid \Big], \tag{41}$$

$$-c_1 \leq E_\nu < 0, \quad -c_2 \leq \varepsilon_\alpha < c_3, \quad E(\mathfrak{k}) \geq 0\ . \tag{42a}$$

$$W_0 \leq W(\mathfrak{k}) \leq W_1, \quad W_0 < W_1 < 0, \quad 0 < V_0 \leq V(\mathfrak{k})\,, \tag{42b}$$

$$\mathfrak{A} \subset \mathfrak{C}, \quad \mathfrak{B} \subset \mathfrak{C}, \quad \mathfrak{A} \cup \mathfrak{B} = \mathfrak{C}, \quad \mathfrak{A} \cap \mathfrak{B} = \varnothing. \tag{43}$$

The c_n, $n = 1, 2, 3$, are positive constants. The fields $\mid \varphi\rangle$ and $\mid \psi\rangle$ are assumed to fulfil the relations

$$\left.\begin{aligned} &\langle\varphi_\nu \mid \varphi_{\nu'}\rangle = \delta_{\nu,\nu'}, \quad \langle\psi_\alpha \mid \psi_{\alpha'}\rangle = \delta_{\alpha\alpha'}, \quad \langle\varphi(\mathfrak{k}) \mid \varphi(\mathfrak{q})\rangle = \delta(\mathfrak{k} - \mathfrak{q}), \\ &\langle\varphi_\nu \mid \varphi(\mathfrak{k})\rangle = 0, \ \langle\varphi_\nu \mid \psi_\alpha\rangle = \mid \psi_\alpha\rangle\langle\varphi_\nu \mid, \ \langle\varphi(\mathfrak{k}) \mid \psi_\alpha\rangle = \mid \psi_\alpha\rangle\langle\varphi(\mathfrak{k})\mid . \end{aligned}\right\} \tag{44}$$

Especially we have with product states $\mid z\psi_\alpha\rangle = \mid z\rangle \mid \psi_\alpha\rangle$

$$H \mid z\psi_\alpha\rangle = (E_z + \varepsilon_\alpha) \mid z\psi_\alpha\rangle \quad \text{with} \quad \begin{cases} z \equiv \varphi_\nu \text{ and } E_z \equiv E_\nu\,, \\ z \equiv \varphi(\mathfrak{k}) \text{ and } E_z \equiv E(\mathfrak{k}). \end{cases} \tag{45}$$

These states can be used to calculate the partition function

$$\Xi(0) = Tre^{-\beta H} = \sum_{\nu,\alpha} e^{-\beta(E_\nu + \varepsilon_\alpha)} + \sum_\alpha \int d\mathfrak{k}\varrho(\mathfrak{k}) e^{-\beta(E(\mathfrak{k}) + \varepsilon_\alpha)}\,. \tag{46}$$

$\varrho(\mathfrak{k})$ is given as in Eq. (34).

Let us assume that $V(\mathfrak{k})$ is unbounded (as in Section 3) and such that

$$Tr\left\{e^{-\beta H}(AV)^m\right\} = \sum_\alpha e^{-\beta\varepsilon_\alpha} \langle\psi_\alpha \mid A^m \mid \psi_\alpha\rangle \int_{\mathfrak{B}} d\mathfrak{k} e^{-\beta E(\mathfrak{k})}\, \varrho(\mathfrak{k}) \big(V(\mathfrak{k})\big)^m$$

$$= \infty \quad \text{for} \quad m = 1,$$

i.e. let

$$\int_{\mathfrak{B}} d\mathfrak{k} e^{-\beta E(\mathfrak{k})}\, \varrho(\mathfrak{k})\, V(\mathfrak{k}) = \infty\ . \tag{47}$$

This is our *truncation criterion* again. It follows from Eq. (19)

$$F_{\text{stat}} = 1 + Pw_1(w_1 - Pw_2)^{-1} w_1. \tag{48}$$

The prescription (18) yields with Eqs. (41)—(44)

$$w_1 = (W + V) \cdot \sum_{\nu,\mu} a_{\nu\mu} \mid \psi_\nu\rangle\langle\psi_\mu \mid \tag{49a}$$

and

$$w_1 - Pw_2 = (W + V) \cdot \sum_{\nu,\mu} [a_{\nu\mu} - P(W + V)S_{\nu\mu}] \mid \psi_\nu\rangle\langle\psi_\mu \mid, \tag{49b}$$

where

$$\varepsilon_{\nu\mu} = \varepsilon_\nu - \varepsilon_\mu, \tag{50a}$$

$$a_{\nu\mu} = A_{\nu\mu}(1 - e^{\beta\varepsilon\nu\mu})/\varepsilon_{\nu\mu}\,, \tag{50b}$$

$$S_{\nu\mu} = \sum_{\mu'} A_{\nu\mu'}\, A_{\mu'\mu} \frac{1}{\varepsilon_{\mu'\mu}} \left[\frac{e^{\beta\varepsilon\nu\mu} - 1}{\varepsilon_{\nu\mu'}} - \frac{e^{\beta\varepsilon\nu\mu'} - 1}{\varepsilon_{\mu\nu'}} \right]. \tag{50c}$$

Using the resolution of the identity in the form

$$1 \equiv \int_{\mathfrak{A}\cup\mathfrak{B}} d\mathfrak{k}\, |\, \varphi(\mathfrak{k})\rangle\langle\varphi(\mathfrak{k})\,| \cdot \sum_\nu |\, \psi_\nu\rangle\, \langle\psi_\nu\,| \tag{51}$$

we calculate the inverse of $w_1 - Pw_2$ with the Ansatz

$$(w_1 - Pw_2)^{-1} = \left\{ \int_{\mathfrak{A}} d\mathfrak{k}\, \frac{|\,\varphi(\mathfrak{k})\rangle\,\langle\varphi(\mathfrak{k})\,|}{W(\mathfrak{k})} + \right.$$
$$\left. + \int_{\mathfrak{B}} dk\, \frac{|\,\varphi(\mathfrak{k})\rangle\langle\varphi(\mathfrak{k})\,|}{V(\mathfrak{k})} \right\} \sum_{\nu,\mu} G_{\nu\mu}\, |\psi_\nu\rangle\langle\psi_\mu| \tag{52}$$

$$(w_1 - Pw_2)(w_1 - Pw_2)^{-1} = 1. \tag{53}$$

Inserting (49b) and (52) into this condition we find the identity in the form (51) if we choose the $G_{\nu\mu}$ such that

$$\sum_{\mu'} [a_{\nu\mu'} - P\{W(\mathfrak{k}) + V(\mathfrak{k})\}S_{\nu\mu'}]G_{\mu'\mu} = \delta_{\nu\mu}\,. \tag{54}$$

In matrix form this may be written as

$$[a - P\{W(\mathfrak{k}) + V(\mathfrak{k})\} \cdot S]G = I. \tag{55}$$

I is the unit matrix of a compatible order. Thus we have the representation

$$G = G(\mathfrak{k}) = [a - P\{W(\mathfrak{k}) + V(\mathfrak{k})\}S]^{-1}. \tag{56}$$

The average $\langle F_{\text{stat}}\rangle_0$ can now be written down:

$$\langle F_{\text{stat}}\rangle_0 = 1 + \frac{P}{\Xi(0)}\, Tr\, \{e^{-\beta H} w_1 (w_1 - Pw_2)^{-1} w_1\} = \tag{57}$$

$$= 1 + \frac{P}{\Xi(0)} \sum_{\alpha,\alpha',\alpha''} a_{\alpha\alpha'}\, Pr \left\{ \int_{\mathfrak{A}} d\mathfrak{k} W(\mathfrak{k}) + \int_{\mathfrak{B}} d\mathfrak{k}\, V(\mathfrak{k}) \right\} \cdot \varrho(\mathfrak{k}) e^{-\beta(E(\mathfrak{k})+\varepsilon_\alpha)}\, G_{\alpha'\alpha''}(\mathfrak{k})\, a_{\alpha''\alpha}.$$

We have used the states (45) and the average process indicated in expression (46). The procedure is now, in principle, the same as in Section 3 and Appendix A.

We must calculate the integrals on the right of (57) using eventually principal value integrals if P is such that the determinant

$$\text{Det } [a - P\{W(k) + V(\mathfrak{k})\}S]$$

does vanish on $\mathfrak{A}$ and/or $\mathfrak{B}$ (β is fixed). To discuss this we consider the following specialization:

$$A = \sum_{\nu,\mu=1}^{2} A_{\nu\mu} \mid \psi_\nu\rangle\langle\psi_\mu \mid \qquad \text{with} \qquad A_{12} = A_{21}. \tag{58}$$

The matrices I, G, a and S are then (2,2)-matrices, the elements of the last two are given in Appendix B. G follows then from (56). The determinant of interest may be written

$$\begin{aligned} &\text{Det } [a - P\{W(\mathfrak{k}) + V(\mathfrak{k})\}S] = P^2\{W(\mathfrak{k}) + V(\mathfrak{k})\}^2 \text{ Det } (S) \\ &- P\{W(\mathfrak{k}) + V(\mathfrak{k})\} \cdot [a_{11}S_{11} + a_{22}S_{22} - a_{12}S_{21} - a_{21}S_{12}] + \text{Det}(a). \end{aligned} \tag{59}$$

It is straightforward to compute this expression explicitly and in general. However, for short we consider one special case only.

We choose $A_{11} = A_{22} = 0$ and $A_{12} \neq 0$. Using expression (59) and the matrix elements of Appendix B we obtain ($\varepsilon = \varepsilon_2 - \varepsilon_1$)

$$\begin{aligned} \text{Det } [a - P\{W(\mathfrak{k}) + V(\mathfrak{k})\}S] &= (A_{12}/\varepsilon)^2[P^2\{W(\mathfrak{k}) + V(\mathfrak{k})\}^2 \cdot \\ &\cdot (A_{12}/\varepsilon)^2 f(\beta\varepsilon) + 2 - \exp(\beta\varepsilon) - \exp(-\beta\varepsilon)], \end{aligned} \tag{60}$$

where

$$f(x) = 2 - x^2 + (x - 1)\exp(x) - (x + 1)\exp(-x). \tag{61}$$

It is easy to see from (60) that it is necessary for certain P to do principal value integration in (57) and hence we expect singularities of the VPF. To explain this we derive from (56), (57) and Appendix B the following expression:

$$\begin{aligned} Tr\{e^{-\beta H}w_1(w_1 - Pw_2)^{-1}w_1\} &= (A_{12}/\varepsilon)^4(1 - e^{\beta\varepsilon})(e^{-\beta\varepsilon} - 1)P \cdot \\ \cdot \sum_{n=1}^{2} h_n(\beta)e^{-\beta\varepsilon_n} \cdot Pr &\left\{\int_{\mathfrak{A}} + \int_{\mathfrak{B}}\right\} d\mathfrak{k}\, \frac{\varrho(\mathfrak{k})e^{-\beta E(\mathfrak{k})}\{W(\mathfrak{k}) + V(\mathfrak{k})\}^2}{\text{Det } [a - P\{W(\mathfrak{k}) + V(\mathfrak{k})\}S]}, \end{aligned} \tag{62}$$

where

$$h_1(\beta) = 1 - \beta\varepsilon - e^{-\beta\varepsilon}, \quad h_2(\beta) = 1 + \beta\varepsilon - e^{\beta\varepsilon}$$

and

$$W(\mathfrak{k}) \equiv 0 \text{ on } \mathfrak{B} \text{ and } V(\mathfrak{k}) \equiv 0 \text{ on } \mathfrak{A}.$$

If we now use, for example, the same arguments as in Appendix A we obtain (in the P—T-plane) a continuous VPF which possesses discontinuous derivatives of a certain order (depending on the concrete form of $\varrho(\mathfrak{k})$, $W(\mathfrak{k})$ etc.)

along certain curves. However, these curves are independent of the concrete form of $\varrho(\mathfrak{f})$, $W(\mathfrak{f})$ etc. provided they have no singularities. If this is the case the singular curves of the VPF are the three lines

$$P = \frac{\varepsilon}{|\, xA_{12}\,|}\,[(e^{\beta\varepsilon} + e^{-\beta\varepsilon} - 2)/f(\beta\varepsilon)]^{1/2}, \quad \beta = (k_B\,T)^{-1}\,, \tag{63}$$

for $x = W_0$, W_1 and V_0. It is elementary to discuss the T-dependence of the closed expression on the right. We omit it here.

Since our problem was the existence problem of singularities of the VPF and for the sake of keeping this paper within reasonable length, we will stop here our discussion. The essential conclusion of this model is that the corresponding VPF in fact may have singularities of the phase transition type.

5. Conclusion

The basis of the considerations in this paper is a variational approach to the partition function. We mention that the underlying Hamiltonian $H + PK$ is, e.g., of the form which is used in the theory of pressure induced phase transitions [7]. P represents then the external pressure.

By concrete (transparent, and therefore, simple) examples we have shown that the VPF may possess discontinuities in the derivatives with respect to P, provided certain conditions are fulfilled. The following conditions are shown to be sufficient for a phase transition singularity:

1. The operators H and K possess a continuous spectrum (of the type considered above). This is the case for many systems of statistical mechanics.

2. There is a condition for the truncation of the series which follows from the variational calculation (truncation criterion). The series will break off if the operator K is unbounded in a certain fashion (for details see Eq. (36) or (37)).

3. The density of states $g(W)$ (and, to a little extent, the perturbation K) is of a form such that the principal value integrals of the type indicated in Eq. (32) or (57) do exist.

It is a remarkable result that the singular curves which have been obtained depend on the perturbation K alone. Especially, they are independent of the density of states provided this density is integrable. However, the order of the discontinuous derivative (the derivative of the VPF with respect to P) depends strongly on the density of states. This fact is a general feature of the VPF as can be seen from the explicit expression (20).

Appendix A

In order to be specific let $W(k) = W_0 + E(k)$ on $\mathfrak{A}$. The average (38) can be written (with $m = 2N-1$)

$$I_m(x) = \frac{1}{\Xi(0)} Pr \int_{\mathfrak{A}} dk \frac{(W(k))^m e^{-\beta E(k)} \varrho(k)}{x - W(k)} =$$

$$= \frac{1}{\Xi(0)} Pr \int_{W_*}^{W_1} dW g(W) \tilde{\varrho}(W) \frac{W^m e^{+\beta(W_*-W)}}{x - W},$$

where $g(W)$ is the density of states and $\tilde{\varrho}(W)$ arises from the transformation of $\varrho(\mathfrak{k})$. Let us choose the form

$$g(W) = D[\,|\,W_0 - W\,|\cdot|\,W_1 - W\,|\,]^\eta, \quad \eta \geq 1,$$

D is a constant. For the sake of illustration we consider two simple cases:

First case: $\eta = 1$ and $W^m e^{+\beta(W_*-W)} \tilde{\varrho}(W) \approx C_1 = \text{const}$ on $\mathfrak{A}$. We find

$$I_m(x) = \frac{DC_1}{\Xi(0)} \cdot Pr \int_{W_*}^{W_1} dW \frac{|\,W_0 - W\,|\cdot|\,W_1 - W\,|}{x - W} =$$

$$= \frac{DC_1}{\Xi(0)} \left[(W_0^2 - W_1^2)/2 + x(W_1 - W_0) + (W_0 - x)(W_1 - x) \cdot \right.$$

$$\left. \cdot \begin{cases} \ln\,[(W_1 - x)/(W_0 - x)] & \text{for } x < W_0 \text{ and } x > W_1 \\ \ln\,[(W_1 - x)/(x - W_0)] & \text{for } W_0 < x < W_1 \end{cases} \right].$$

This expression is continuous for all x. However, the first derivative $\frac{\partial}{\partial x}$ is discontinuous at $x = W_0$ and $x = W_1$ (one could call it a transition of first order).

Second case: $\eta = 2$ and $W^m e^{+\beta(W_*-W)} \tilde{\varrho}(W) \approx C_2 = \text{const}$ on $\mathfrak{A}$. In the same way we obtain

$$I_m(x) = \frac{DC_2}{\Xi(0)} \left[[Q_3(x) - [(W_0 - x)(W_1 - x)]^2 \cdot \right.$$

$$\left. \cdot \begin{cases} \ln\,[(W_1 - x)/(W_0 - x)] & \text{for } x < W_0 \text{ and } x > W_1 \\ \ln\,[(W_1 - x)/(x - W_0)] & \text{for } W_0 < x < W_1 \end{cases} \right].$$

$Q_3(x)$ is a polynom of third order in x. As is clear, this expression is continuous with its first derivative $\frac{\partial}{\partial x}$ ... The second derivative $\frac{\partial^2}{\partial x^2}$ ... is discontinuous at $x = W_0$ and $x = W_1$ (one could call it a transition of second order).

In both cases we obtain in the P–T-plane two lines (namely

$$P = 2Nk_B T/|\,W_0\,| \quad \text{and} \quad P = 2Nk_B T/|\,W_1\,|)$$

along which the first resp. the second derivative of the VPF is discontinuous. The VPF itself is continuous in the first quadrant of the $P-T$-plane.

Appendix B

The elements of the (2,2)-matrices a and S are ($\varepsilon \equiv \varepsilon_2 - \varepsilon_1$):

$$a_{nn} = -\beta A_{nn} \quad \text{for} \quad n = 1, 2; \quad a_{12} = A_{12}(e^{-\beta\varepsilon} - 1)/\varepsilon;$$

$$a_{21} = A_{12}(1 - e^{\beta\varepsilon})/\varepsilon;$$

$$S_{11} = (A_{11}\beta)^2/\beta + (A_{12}/\varepsilon)^2(\beta\varepsilon + e^{-\beta\varepsilon} - 1);$$

$$S_{12} = A_{12}[A_{11}(\beta\varepsilon + e^{-\beta\varepsilon} - 1) + A_{22}(1 - (\beta\varepsilon + 1)e^{-\beta\varepsilon})] \cdot \frac{1}{\varepsilon^2};$$

$$S_{21} = A_{12}\,[A_{22}\,(-\beta\varepsilon + e^{\beta\varepsilon} - 1) + A_{11}(1 + (\beta\varepsilon - 1)e^{\beta\varepsilon})] \cdot \frac{1}{\varepsilon^2};$$

$$S_{22} = (A_{22}\beta)^2/2 + (A_{12}/\varepsilon)^2(-\beta\varepsilon + e^{\beta\varepsilon} - 1)\,.$$

REFERENCES

1. W. Lucht, Acta Phys. Hung., **39**, 217, 1975.
2. A. Isihara, Statistical Physics, Academic Press, New York and London, 1971. p. 413.
3. I. Prigogine and P. Mayné, Transport Phenomena, Eds. G. Kirczenow and J. Marro, Springer Verlag, Berlin, 1974.
4. D. Bessis, Padé Approximants, Ed. P. R. Graves-Morris, The Institute of Physics, London Bristol, London, 1973.
5. A. Messiah, Quantum Mechanics, North-Holland Publ. Comp., Amsterdam, 1970, p. 269.
6. W. I. Smirnov, Lehrgang der höheren Mathematik, Teil III/2, Verl. d. Wissenschaften, Berlin, 1964. pp. 80 ff.
7. R. A. Guyer, Selected Topics in Physics, Astrophysics, and Biophysics, Eds. E. Abecassis de Laredo and N. K. Jurisic, D. Reidel Publ. Comp., Dordrecht (Holland)/Boston (USA), 1973. p. 48.

Acta Physica Academiae Scientiarum Hungaricae, Tomus 41 (4), pp. 263—280 (1976)

EFFECT OF BUOYANCY FORCE ON HORIZONTAL FLUCTUATING FLOW

By

P. SINGH

DEPARTMENT OF MATHEMATICS, INDIAN INSTITUTE OF TECHNOLOGY, KHARAGPUR, INDIA

(Received 22. IX. 1976)

The effect of buoyancy force on the flow and heat transfer from a semi-infinite horizontal flat plate, when the free stream oscillates about a non-zero mean, is analysed. Separate solutions valid for low and high frequency ranges are developed. It is found that for low frequencies, the oscillating component of the rate of heat transfer from the plate lags behind the free stream fluctuations by $\pi/2$ and its amplitude decreases with the increase of buoyancy effects. The phase lead in the skin-friction fluctuations increases with buoyancy effects. For very high frequencies, the rate of heat transfer has a phase lead of 135° over the free stream oscillations and the skin-friction has a phase lead of 45°.

Introduction

The paper is devoted to a study of free convection boundary layer flow on a horizontal plate, when the free stream is fluctuating about a non-zero mean. Some aspects of the basic steady flow were considered by GILL and CASAL [1]. SPARROW and MYNKOWYCZ [2] have also considered buoyancy effects on flow past a horizontal plate, employing a series expansion of the stream function which gives the perturbation of a basic forced convection flow. The specific aim of the present study is to gain further insight into the effects of buoyancy force on the oscillating layer from a horizontal plate.

We have reconsidered the basic flow using Kármán—Pohlhausen technique and obtained an approximate solution to be used in the subsequent study of unsteady flow. Two different solutions for low and high frequency ranges are obtained. The method of solving the problem is essentially the same as developed by LIGHTHILL [3] who has investigated the same case in the absence of buoyancy effects. For high frequencies we have adopted a procedure suggested by GLAUERT [4]. It is found that the phase lead in the skin-friction oscillations over the free stream fluctuations increases with the buoyancy effects. The rate of heat transfer, on the other hand, fluctuates with a phase lag of 90° whereas its amplitude decreases with increasing buoyancy effects. It is worthwhile to mention that there is no heat transfer from the plate in the steady case. In the limiting case of very high frequencies, the flow is of the "shear-wave" type unaffected by the mean flow predicting

a phase lead of 45° in the skin-friction oscillations and a phase lead of 135° in the rate of heat transfer fluctuations. In the intermediate frequency range, the velocity and temperature fields are quite complicated due to the interaction of the steady mean flow.

Basic equations

Consider a horizontal surface over which flows a laminar boundary layer with free stream velocity U and free stream temperature T_∞. The surface temperature is T_w. The coordinate x measures the distance along the surface from the leading edge, while y measures the distance normal to the surface (positive vertically-upwards). The boundary layer equations for two-dimensional incompressible unsteady flow are

$$\frac{\partial u}{\partial t} + u\frac{\partial u}{\partial x} + v\frac{\partial u}{\partial y} = g\beta\frac{\partial}{\partial x}\int_y^\infty (T - T_\infty)\,dy + \frac{\partial U}{\partial t} + U\frac{\partial U}{\partial x} + \nu\frac{\partial^2 u}{\partial y^2}, \quad \text{(1a)}$$

$$\frac{\partial u}{\partial x} + \frac{\partial v}{\partial y} = 0, \quad \text{(1b)}$$

$$\frac{\partial T}{\partial t} + u\frac{\partial T}{\partial x} + v\frac{\partial T}{\partial y} = k\frac{\partial^2 T}{\partial y^2}, \quad \text{(1c)}$$

where g is the acceleration due to gravity, u, v are the velocity components in x and y directions and k, β and ν denote the thermal diffusivity, coefficient of thermal expansion and kinematic viscosity, respectively.

In accordance with the usual practice in free convection we restrict the effect of density variations to the formation of a "buoyant force" term, which is the first term appearing in the right hand side of Eq. (1a).

The boundary conditions are

$$y = 0\colon\ T = T_w,\ u = 0,\ v = 0;$$
$$y \to \infty\colon\ T \to T_\infty,\ u \to U(x,t) = U_0(x)(1 + \varepsilon\cos\omega t),\quad \varepsilon \ll 1. \quad \text{(2)}$$

Here $U_0(x)$ is the mean velocity and ω is the frequency of oscillation. Thus the free stream consists of a weak oscillating flow superimposed on a steady non-zero mean flow.

The solution of the above system of differential equations will be obtained in terms of complex functions, the real parts of which will have physical significance. We write U, u, v and T as

$$U = U_0(x) + \varepsilon U_0(x)e^{i\omega t}, \qquad u = u_s + \varepsilon u_1 e^{i\omega t},$$
$$v = v_s + \varepsilon v_1 e^{i\omega t}, \qquad T = T_s + \varepsilon T_1 e^{i\omega t}, \quad \text{(3)}$$

where u_s, v_s, T_s give the steady mean flow and satisfy the equations:

$$u_s \frac{\partial u_s}{\partial x} + v_s \frac{\partial u_s}{\partial y} = g\beta \frac{\partial}{\partial x} \int_y^\infty (T_s - T_\infty)\, dy + U_0 \frac{dU_0}{dx} + \nu \frac{\partial^2 u_s}{\partial y^2}, \quad (4a)$$

$$\frac{\partial u_s}{\partial x} + \frac{\partial v_s}{\partial y} = 0, \quad (4b)$$

$$u_s \frac{\partial T_s}{\partial x} + v_s \frac{\partial T_s}{\partial y} = k \frac{\partial^2 T_s}{\partial y^2}, \quad (4c)$$

with the boundary conditions:

$$\begin{aligned} &y = 0;\ u_s = 0,\ v_s = 0, \quad && T_s = T_w; \\ &y \to \infty:\ u_s \to U_0(x), && T_s \to T_\infty. \end{aligned} \quad (5)$$

Neglecting squares of ε and dividing by $e^{i\omega t}$, we find that u_1, v_1 and T_1 satisfy the following set of differential equations:

$$\begin{aligned} i\omega u_1 + u_1 \frac{\partial u_s}{\partial x} + u_s \frac{\partial u_1}{\partial x} + v_1 \frac{\partial u_s}{\partial y} + v_s \frac{\partial u_1}{\partial y} = \\ = g\beta \frac{\partial}{\partial x} \int_y^\infty T_1\, dy + \frac{d}{dx} U_0^2 + \nu \frac{\partial^2 u_1}{\partial y^2} + i\omega U_0, \end{aligned} \quad (6a)$$

$$\frac{\partial u_1}{\partial x} + \frac{\partial v_1}{\partial y} = 0, \quad (6b)$$

$$i\omega T_1 + u_1 \frac{\partial T_s}{\partial x} + u_s \frac{\partial T_1}{\partial x} + v_1 \frac{\partial T_s}{\partial y} + v_s \frac{\partial T_1}{\partial y} = k \frac{\partial^2 T_1}{\partial y^2}, \quad (6c)$$

with the boundary conditions:

$$\begin{aligned} &y = 0:\ u_1 = 0,\ v_1 = 0,\ T_1 = 0; \\ &y \to \infty:\ u_1 \to U_0(x), \quad T_1 \to 0. \end{aligned} \quad (7)$$

Steady-state solution

Equations (4) and (5) are the boundary layer equations which describe buoyancy effects on steady horizontal boundary layer flow and heat transfer. It is interesting to consider the sign of the buoyancy term. For flow below the plate, the coordinate y would be reversed to measure distances vertically downwards and a negative sign in the buoyancy term will appear. It follows

that a flow above the plate for which $T_w > T_\infty$ or a flow below the plate for which $T_w < T_\infty$, the induced pressure gradient is negative resulting in an accelerated flow. The opposite effect occurs for flow above the plate for $T_w < T_\infty$ and for flow below the plate for $T_w > T_\infty$. It is, therefore, sufficient to consider only one of the four situations. For convenience, we shall discuss flow above the plate for $T_w > T_\infty$.

We shall integrate Eq. (4) with (5) by Kármán—Pohlhausen method since our aim is to get qualitative results. Integrating (4a) and (4c) over the full width of the boundary layer, we obtain

$$\nu\left(\frac{\partial u_s}{\partial y}\right)_{y=0} = g\beta\frac{d}{dx}\int_0^\infty\int_y^\infty (T_s - T_\infty)\, dy\, dy + \frac{d}{dx}\int_0^\infty u_s(U_0 - u_s)dy + \\ + \frac{dU_0}{dx}\int_0^\infty (U_0 - u_s)\, dy\,, \tag{8}$$

$$-k\left(\frac{\partial T_s}{\partial y}\right)_{y=0} = \frac{d}{dx}\int_0^\infty u_s(T_s - T_\infty)dy. \tag{9}$$

The expressions for u_s and T_s may be assumed as

$$\frac{u_s}{U_0} = \frac{1}{3}(5\eta_1 - 5\eta_1^4 + 3\eta_1^5) - \frac{B}{2}(\eta_1 - 2\eta_1^2 + 2\eta_1^4 - \eta_1^5) - \\ - \frac{C}{6}(\eta_1 - 6\eta_1^3 + 8\eta_1^4 - 3\eta_1^5), \tag{10}$$

$$\frac{T_s - T_\infty}{T_w - T_\infty} = \frac{1}{3}(3 - 5\eta_2 + 5\eta_2^4 - 3\eta_2^5) - \frac{A}{6}(\eta_2 - 6\eta_2^3 + 8\eta_2^4 - 3\eta_2^5)\,, \tag{11}$$

where $\eta_1 = y/\delta_1$, $\eta_2 = y/\delta_2$ and A, B, C are given by

$$U_0\frac{dU_0}{dx} + \frac{g\beta}{60}\frac{d}{dx}[\delta_2(T_w - T_\infty)(20 - A)] + \frac{2\nu U_0 B}{\delta_1^2} = 0, \tag{12a}$$

$$6\nu U_0 C = \delta_1^3 g\beta\frac{d}{dx}(T_w - T_\infty), \tag{12b}$$

$$36k\delta_1(T_w - T_\infty)A = U_0\delta_2^3(10 - 3B - C). \tag{12c}$$

and δ_1, δ_2 are the viscous and thermal boundary layer thicknesses, respectively. In general δ_1 and δ_2 are functions of x to be determined from Eq. (8)

and (9). The expressions for U_s and T_s satisfy the boundary conditions:

$$y = 0 \; ; \quad u_s = 0, \; T_s = T_w;$$

$$y \to \infty: \quad u_s \to U_0, \quad \frac{\partial u_s}{\partial y} \to 0, \quad \frac{\partial^2 u_s}{\partial y^2} \to 0,$$

$$T_s \to T_\infty, \quad \frac{\partial T_s}{\partial y} \to 0, \quad \frac{\partial^2 T_s}{\partial y^2} \to 0;$$

$$\nu \left(\frac{\partial^2 u_s}{\partial y^2}\right)_{y=0} + g\beta \frac{d}{dx} \int_0^\infty (T_s - T_\infty) dy + U_0 \frac{dU_0}{dy} = 0,$$

$$\left(\frac{\partial^2 T_s}{\partial y^2}\right)_{y=0} = 0, \tag{13a}$$

$$\nu \left(\frac{\partial^3 u_s}{\partial y^3}\right)_{y=0} = g\beta \frac{d}{dx}(T_w - T_\infty),$$

$$k \left(\frac{\partial^3 T_s}{\partial y^3}\right)_{y=0} = \left(\frac{\partial u_s}{\partial y} \frac{\partial T_s}{\partial x}\right)_{y=0}. \tag{13b}$$

The boundary conditions (13a) are obtained by evaluating equations (4a) and (4c) at $y = 0$, while (13a) are obtained by differentiating (4a) and (4c) with respect to y and then setting $y = 0$.

Substituting (10) and (11) into (8) and (9), we get

$$\frac{\nu U_0}{6\delta_1}(10 - 3B - C) = \frac{g\beta}{315} \frac{d}{dx}[\delta_2^2 (T_w - T_\infty)(25 - 2A)] +$$

$$+ \frac{U_0 \delta_1}{60} \frac{dU_0}{dx}(20 + 2B + C) + \frac{d}{dx}\left[U_0^2 \delta_1 \left(\frac{775}{6237} - \frac{47B^2}{27\,720} - \right.\right.$$

$$\left.\left. - \frac{38C^2}{2835} + \frac{25B}{8316} + \frac{16C}{2079} - \frac{13BC}{27\,720} \right)\right], \tag{14a}$$

$$6k(T_w - T_\infty)(10 + A)\Delta = \delta_1 \frac{d}{dx}[U_0 (T_w - T_\infty)\delta_1 (12h_1(\Delta) - 2Ah_2(\Delta) -$$

$$- 6Bh_3(\Delta) + 3ABh_4(\Delta) - 2Ch_5(\Delta) + ACh_6(\Delta)], \tag{14b}$$

where

$$h_1(\Delta) = \frac{1}{\Delta} - 1 + \frac{25\Delta}{63} - \frac{\Delta^4}{27} + \frac{\Delta^5}{77}, \qquad \Delta \leq 1,$$

$$= \frac{25}{63\Delta^2} - \frac{1}{27\Delta^5} + \frac{1}{77\Delta^6}, \qquad \Delta \geq 1,$$

$$h_2(\Delta) = \frac{3}{10\Delta} - \frac{5\Delta}{21} + \frac{\Delta^3}{4} - \frac{8\Delta^4}{45} + \frac{3\Delta^5}{77} \qquad \Delta \leq 1,$$

$$= \frac{4}{21\Delta^2} - \frac{1}{36\Delta^5} + \frac{4}{375\Delta^6}, \qquad \Delta \geq 1,$$

$$h_3(\Delta) = \frac{1}{5} - \frac{5\Delta}{42} + \frac{\Delta^4}{63} - \frac{9\Delta^5}{1540}, \qquad \Delta \leq 1,$$

$$= \frac{5}{21\Delta^2} - \frac{5}{28\Delta^3} + \frac{2}{45\Delta^5} - \frac{1}{77\Delta^6}, \qquad \Delta \geq 1,$$

$$h_4(\Delta) = \frac{9}{42} - \frac{\Delta^3}{30} + \frac{8\Delta^4}{315} - \frac{9\Delta^5}{1540}, \qquad \Delta \leq 1,$$

$$= \frac{4}{105\Delta^2} - \frac{1}{28\Delta^3} + \frac{1}{90\Delta^5} - \frac{4}{1155\Delta^6}, \qquad \Delta \geq 1,$$

$$h_5(\Delta) = \frac{3}{10} - \frac{4\Delta}{21} + \frac{\Delta^4}{36} - \frac{4\Delta^5}{385}, \qquad \Delta \leq 1,$$

$$= \frac{5}{21\Delta^2} - \frac{1}{4\Delta^4} + \frac{8}{45\Delta^5} - \frac{3}{77\Delta^6}, \qquad \Delta \geq 1,$$

$$h_6(\Delta) = \frac{4\Delta}{105} - \frac{\Delta^3}{42} + \frac{2\Delta^4}{45} - \frac{4\Delta^5}{385}, \qquad \Delta \leq 1,$$

$$= \frac{4}{105\Delta^2} - \frac{2}{35\Delta^4} + \frac{2}{45\Delta^5} - \frac{4}{385\Delta^6}, \qquad \Delta \geq 1;$$

$$\Delta = \delta_1/\delta_2. \tag{15}$$

We shall examine the possibility of obtaining similar solutions of the boundary layer equations. It is natural that we should begin our quest for similar solutions by simultaneously imposing power function variations for both the free stream velocity and wall temperature. Accordingly we consider

$$U_0 = A_0 x^m, \qquad T_w - T_\infty = \alpha x^n,$$

also

$$\delta_1 = \delta_1^* \sqrt{\frac{\nu x}{U_0}}, \qquad \delta_2 = \delta_2^* \sqrt{\frac{kx}{U_0}}. \tag{16}$$

On substituting these values in (14) and requiring that the resulting equations be independent of x, we find

$$m = (2n + 1)/5. \tag{17}$$

The fundamental case of Blasius flow (U_0 constant) past a horizontal flat plate will now be considered in detail. In this case $m = 0$, $n = -1/2$ and

Eqs. (14) and (12) become

$$10 - C = \frac{3N}{7\sigma}\,\delta_1^*\,\delta_2^{*2} + 3\delta_1^{*2}\left(\frac{775}{6237} + \frac{16C}{2079} - \frac{38C^2}{2835}\right),$$

$$12C = -N\delta_1^{*3},\quad A = -10,\quad B = 0\,,$$

$$\sigma\delta_2^{*3}\,(10 - C) = 720\,\delta_1^*\,, \tag{18}$$

where $N = g\beta\alpha\sqrt{\nu}/U_0^{5/2}$ and $\sigma = \nu/k$ is the Prandtl number. Eqs. (18) were solved for various values of N which is a measure of buoyancy effects and for $\sigma = 0.7$.

It is interesting that there is no heat transfer from the plate to the fluid although the plate temperature is nonuniform. GILL and CASAL [5] and NANDA [6] have pointed out similar results. The non-dimensional skin-friction at the wall is

$$\tau_s^* = \frac{\tau_s}{\varrho U_0}\sqrt{\frac{U_0 x}{\nu}} = \frac{10 - C}{6\delta_1^*}\,. \tag{19}$$

The values of the skin-friction along with those of boundary layer thicknesses δ_1^* and δ_2^* are listed in Table I.

Table I

N	δ_1^*	δ_2^*	τ_S^*
0.00	5.179	8.108	0.322
0.025	4.205	7.525	0.402
0.05	3.565	7.117	0.476
0.1	2.786	6.557	0.609
0.5	1.236	5.015	1.359
1.0	0.828	4.394	2.021

The boundary layer thicknesses decrease with N increasing, while the skin-friction at the plate increases with N. Comparing the shear-stress of the present calculation for $N = 0$ with the well-known result of Blasius, the difference is found to be less than 3%. Recently, GILL and CASAL [5] have given an exact numerical solution of Eqs. (4) for $N = 0.0156$ and 0.0312 and for $\sigma = 0.72$. A comparison of the shear-stress at the plate as given by GILL and CASAL with the values obtained by the present method is made in Table II.

It can be seen that the polynomial expressions assumed seem to be fairly good representations of the velocity and temperature fields.

Table II

N	Exact value of τ_s^*	Present values of τ_s^*
0.0156	0.382	0.371
0.0312	0.426	0.419

We now proceed to investigate the nature of the flow and the temperature fields due to fluctuations in the free stream. Two separate solutions will be obtained: one for small frequencies and the other for high frequencies.

Low frequency fluctuations

Equations (6) are considered next. It is convenient to write u_1, v_1 and T_1 as the sum of in-phase and out-of-phase components:

$$u_1 = u_r + iu_2,\ v_1 = v_r + iv_2,\ T_1 = T_r + iT_2. \tag{20}$$

Substituting into (6) and separating real and imaginary parts, we get

$$-\omega u_2 + u_r \frac{\partial u_s}{\partial x} + u_s \frac{\partial u_r}{\partial x} + v_r \frac{\partial u_s}{\partial y} + v_s \frac{\partial u_r}{\partial y} = \\ = g\beta \frac{\partial}{\partial x}\int_y^\infty T_r\, dy + \nu \frac{\partial^2 u_r}{\partial y^2}, \tag{21a}$$

$$\frac{\partial u_r}{\partial x} + \frac{\partial v_r}{\partial y} = 0, \tag{21b}$$

$$-\omega T_2 + u \frac{\partial T_r}{\partial x} + u_r \frac{\partial T_s}{\partial x} + v_s \frac{\partial T_r}{\partial y} + v_r \frac{\partial T_s}{\partial y} = k \frac{\partial^2 T_r}{\partial y^2} \tag{21c}$$

with the boundary conditions

$$y = 0:\quad u_r = 0,\quad v_r = 0,\quad T_r = 0; \\ y \to \infty:\ u_r \to U_0,\ T_r \to 0; \tag{22}$$

and

$$\omega u_r + u_2 \frac{\partial u_s}{\partial x} + u_s \frac{\partial u_2}{\partial x} + v_2 \frac{\partial u_s}{\partial y} + v_s \frac{\partial u_2}{\partial y} = \\ = g\beta \frac{\partial}{\partial x}\int_y^\infty T_2\, dy + \nu \frac{\partial^2 u_2}{\partial y^2} + \omega U_0, \tag{23a}$$

$$\frac{\partial u_2}{\partial x} + \frac{\partial v_2}{\partial y} = 0, \tag{23b}$$

$$\omega T_r + u_2 \frac{\partial T_s}{\partial x} + u_s \frac{\partial T_2}{\partial x} + v_2 \frac{\partial T_2}{\partial y} + v_s \frac{\partial T_2}{\partial y} = k \frac{\partial^2 T_2}{\partial y^2}, \tag{23c}$$

with the conditions

$$\begin{aligned} &y = 0: \quad u_2 = 0, \; v_2 = 0, \quad T_2 = 0; \\ &y \to \infty: \; u_2 \to 0, \; T_2 \to 0. \end{aligned} \tag{24}$$

Thus the difference in phase between the longitudinal component of velocity and the temperature field fluctuations at a point within the boundary layer and the free stream fluctuations is

$$\alpha_2 = \tan^{-1}\left(\frac{u_2}{u_r}\right), \quad \alpha_1 = \tan^{-1}(T_2/T_r).$$

When the frequency is low, it is to be expected that the phase shifts will be small. As such u_2 and T_2 will be small relative to u_r and T_r. Thus when ω is small, the terms $-\omega u_2$ and ωT_2 can be neglected in (21a) and (21c). u_r, v_r and T_r will then be the quasi-steady solution corresponding to $\omega = 0$. This can also be seen from the facts that the same equations are obtained by substituting $u = u_s + \varepsilon u_r$, $v = v_s + \varepsilon v_r$ and $T = T_s + \varepsilon T_r$ in the steady flow boundary layer equations. Following LIGHTHILL [3], u_r, v_r and T_r are obtained as

$$\begin{aligned} u_s &= U_0 \frac{\partial u_s}{\partial U_0} = u_s + \frac{1}{2} y \frac{\partial u_s}{\partial y} - \frac{5}{2} N \frac{\partial u_s}{\partial N}, \\ v_r &= U_0 \frac{\partial v_s}{\partial U_0} = \frac{1}{2}\left(v_s + y \frac{\partial v_s}{\partial y}\right) - \frac{5}{2} N \frac{\partial v_s}{\partial N}, \\ T_r &= U_0 \frac{\partial T_s}{\partial U_0} = \frac{1}{2} y \frac{\partial T_s}{\partial y} - \frac{5}{2} N \frac{\partial T_s}{\partial N}. \end{aligned} \tag{25}$$

That (25) solve equations (21) when $\omega = 0$ can be ascertained by direct substitutions.

It now remains to determine u_2, v_2 and T_2. We shall again employ the Kármán-Pohlhausen technique to solve (23). Consistent with the boundary conditions (24) we assume u_2 and T_2 in the form

$$\begin{aligned} \frac{u_2}{U_0} = {} & A_1(\eta_1 - 4\eta_1^4 + 3\eta_1^5) + A_2(\eta_1^2 - 3\eta_1^4 + 2\eta_1^5) + \\ & + A_3(\eta_1^3 - 2\eta_1^4 + \eta_1^5), \end{aligned} \tag{26}$$

$$\frac{T_2}{T_w - T_\infty} = B_1(\eta_2 - 4\eta_2^4 + 3\eta_2^5) + B_3(\eta_2^3 - 2\eta_2^4 + \eta_2^5), \tag{27}$$

where

$$A_2 = \frac{N}{120}\,\frac{\delta_1^{*3}}{\Delta}\,x\frac{d}{dx}\left(\frac{A_1\delta_2^{*2}}{12\Delta} - 12B_1\right) - \frac{\beta_1\delta_1^{*2}}{2},$$

$$A_3 = \frac{\beta_1\delta_1^{*2}}{72}\left[(10-C)\left(3+\frac{5N}{\delta_1^*}\,\frac{\partial\delta_1^*}{\partial N}\right)+5N\frac{\partial C}{\partial N}\right],$$

$$B_3 = -\frac{A_1\delta_2^{*2}}{12\Delta}, \quad \beta_1 = \frac{\omega x}{U_0}.$$

And A_1, B_1 are functions of x to be determined. These expressions for u_2 and T_2 are chosen to satisfy the additional boundary conditions:

$$y \to \infty: \quad \frac{\partial u_2}{\partial y} \to 0, \quad \frac{\partial T_2}{\partial y} \to 0\,; \tag{28}$$

$$\nu\left(\frac{\partial^2 u_2}{\partial y^2}\right)_{y=0} + g\beta\frac{d}{dx}\int_0^\infty T_2 dy + \omega U_0 = 0, \quad \left(\frac{\partial^2 T_2}{\partial y^2}\right)_{y=0} = 0,$$

$$\nu\left(\frac{\partial^3 u_2}{\partial y^3}\right)_{y=0} = \omega\left(\frac{\partial u_r}{\partial y}\right)_{y=0}, \left(\frac{\partial u_2}{\partial y}\,\frac{\partial T_s}{\partial x}\right)_{y=0} = k\left(\frac{\partial^3 T_2}{\partial y^3}\right)_{y=0}. \tag{29}$$

The last four boundary conditions are obtained by evaluating (23a) and (23c) and their derivatives with respect to y, at $y = 0$.

Integrating (23a) and (23c) from $y = 0$ to $y = \infty$, we obtain the averaging conditions as

$$\omega\int_0^\infty (u_r - U_0)\,dy + 2\frac{\partial}{\partial x}\int_0^\infty u_2\,u_s\,dy - U_0\frac{\partial}{\partial x}\int_0^\infty u_2\,dy = \tag{30}$$

$$= -\nu\left(\frac{\partial u_2}{\partial y}\right)_{y=0} + g\beta\,\frac{\partial}{\partial x}\int_0^\infty\int_y^\infty T_2\,dy\,dy,$$

$$\omega\int_0^\infty T_r\,dy + \frac{\partial}{\partial x}\int_0^\infty [u_s T_2 + u_2(T_s - T_\infty)]dy = -k\left(\frac{\partial T_2}{\partial y}\right)_{y=0}. \tag{31}$$

Substituting for u_r, T_r, U_2 and T_2, we get

$$-\frac{\nu U_0 A_1}{\delta_1} + \frac{g\beta}{105}\,\frac{d}{dx}[\delta_2(T_w - T_\infty)(10B_1 + B_3)] =$$

$$= \frac{\omega U_0\delta_1}{6}\left[\left(1+\frac{C}{20}\right)\left(\frac{5N}{\delta_1^*}\,\frac{\partial\delta_1^*}{\partial N} - 1\right) + \frac{N}{4}\,\frac{\partial C}{\partial N}\right] + \tag{32a}$$

$$+ U_0^2\frac{d}{dx}\left[\delta_1\left(\frac{155A}{2079} + \frac{95A_2}{2772} + \frac{41A_3}{4158} - \frac{13A_1C}{1485} - \frac{5A_2C}{1848} - \frac{13A_3C}{20\,790}\right)\right],$$

$$\frac{kB_1(T_w - T_\infty)}{\delta_2} = \frac{\omega N}{4}(T_w - T_\infty)\left(5\frac{\partial\delta_2}{\partial N} - \frac{\delta_2}{N}\right) -$$

$$- \frac{d}{dx}\left[\delta_2(T_w - T_\infty)U_0\left\{A_1 E(\Delta) + A_2 F(\Delta) + A_3 G(\Delta) + \right.\right. \tag{32b}$$

$$\left.\left. + B_1\left\{H(\Delta) - \frac{C}{6}I(\Delta)\right\} + B_3\left\{J(\Delta) - \frac{C}{6}L(\Delta)\right\}\right\}\right],$$

where

$$E(\Delta) = \frac{1}{5} - \frac{\Delta^2}{3} + \frac{\Delta^4}{3} - \frac{36\Delta^5}{385},$$

$$F(\Delta) = \frac{1}{15} - \frac{5\Delta^2}{36} + \frac{\Delta^4}{7} - \frac{9\Delta^5}{220},$$

$$G(\Delta) = \frac{1}{60} - \frac{5\Delta^2}{126} + \frac{\Delta^4}{24} - \frac{2\Delta^5}{165},$$

$$H(\Delta) = \frac{1}{5\Delta} - \frac{5\Delta}{63} + \frac{4\Delta^4}{135} - \frac{\Delta^5}{77},$$

$$I(\Delta) = \frac{4\Delta}{105} - \frac{\Delta^4}{45} + \frac{4\Delta^5}{385},$$

$$J(\Delta) = \frac{1}{60\Delta} - \frac{\Delta^3}{72} + \frac{2\Delta^4}{135} - \frac{\Delta^5}{231},$$

$$L(\Delta) = \frac{\Delta^3}{105} - \frac{\Delta^4}{90} + \frac{4\Delta^5}{1155};$$

$\partial\delta_1^*/\partial N$, $\partial\delta_2^*/\partial N$ and $\partial C/\partial N$ can be obtained from (18). The solution of equations (32) is easily found to be

$$A_1 = \beta_1\delta_1^{*2}A_1', \qquad B_1 = \beta_1\delta_1^{*2}B_1', \tag{33}$$

where A_1' and B_1' satisfy the relations

$$A_1' = \frac{N\delta_1^{*2}}{105\sqrt{\sigma}}(10B_1' + B_3') - \frac{1}{6}\left[\left(1 + \frac{C}{20}\right)\left(\frac{5N}{\delta_1^*}\frac{\partial\delta_1^*}{\partial N} - 1\right) + \frac{N}{4}\frac{\partial C}{\partial N}\right] -$$

$$- \frac{3}{5}\delta_1^{*2}\left[\frac{155A_1'}{2079} + \frac{95A_2'}{2772} + \frac{43A_3'}{4158} - C\left(\frac{13A_1'}{1485} + \frac{5A_2'}{1848} + \frac{13A_3'}{20790}\right)\right], \tag{34a}$$

$$B_1' = \frac{\delta_2^{*2}}{4\delta_1^{*2}}\left(\frac{5N}{\delta_2^*}\frac{\partial\delta_2^*}{\partial N} + \frac{1}{4}\right) - \delta_2^{*2}\Big[A_1'E(\Delta) + A_2'F(N) + A_3'G(\Delta) + \\ + B_1'\left(H(\Delta) - \frac{C}{6}I(\Delta)\right) + B_3'\left(J(\Delta) - \frac{C}{6}L(\Delta)\right)\Big], \tag{34b}$$

where A_2', A_3' and B_3' are given by

$$A_2 = \beta_1\delta_1^{*2}A_2', \quad A_3 = \beta_1\delta_1^{*2}A_3', \quad B_3 = \beta_1\delta_1^{*2}B_3'.$$

Results: When the frequency of oscillation is small, the temperature and the longitudinal component of velocity at a point within the boundary layer may be written in the form

$$T = T_s + \varepsilon R_1\cos(\omega t + \alpha_1), \\ u = u_s + \varepsilon R_2\cos(\omega t + \alpha_2), \tag{35}$$

where

$$R_1 = (T_r^2 + T_2^2)^{1/2}, \quad R_2 = (u_r^2 + u_2^2)^{1/2},$$

$$\alpha_1 = \tan^{-1}\left(\frac{T_2}{T_r}\right), \quad \alpha_2 = \tan^{-1}\left(\frac{u_2}{u_r}\right).$$

The functions u_r, u_2, T_r and T_2 are shown in Figs. 1 and 2 for various values of N. u_r is positive at all points within the boundary layer. For $N = 0$, the pressure force dominates the inertia force near the plate resulting in phase lead in the oscillating component of velocity, while near the edge of the boundary layer the inertia force dominates the pressure gradient and it produces negative values of u_2. Consequently, the velocity fluctuations near the edge lag behind free stream oscillations. When free convection is taken into consideration, the pressure gradient and buoyancy force together dominate inertia force and phase lag is more than compensated. Near the plate u_2 increases with N for small values of N, but as free convection dominates, u_2 begins to decrease while u_r behaves contrarily indicating the increase in phase advance near the plate with N.

T_r is negative at all points within the boundary layer and T_2 is negative near the edge for all N except for $N = 0$. Hence the temperature fluctuation near the edge has a phase lead but near the plate phase lag results. For $N = 0$, phase lag in temperature oscillations is noted everywhere inside the boundary layer.

The oscillating component of the skin friction at the plate is

$$\tau_1^* = \frac{\tau_1}{\varrho U_0^2}\sqrt{\frac{U_0 x}{\nu}} = \varepsilon R_3\cos(\omega t + \alpha_3),$$

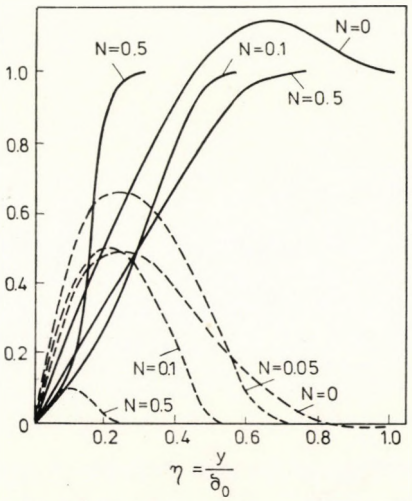

Fig. 1. Flow functions U_r/U_0 and $U_2/\beta_1 U_0$ vs y/δ_0 for various N
δ_0 is the boundary layer thickness when $N = 0$

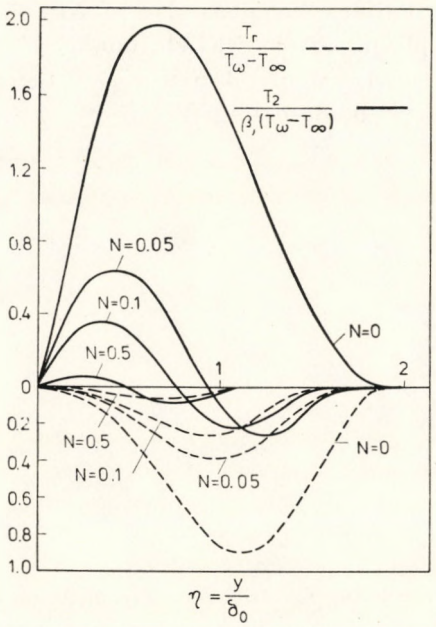

Fig. 2. The functions $T_r/T_w - T_\infty$ and $T_2/\beta_1(T_w - T_\infty)$ vs y/δ_0 for various N

where

$$R_3 = \frac{1}{\delta_1^*}\left[\left\{\left(\frac{5}{3} - \frac{C}{6}\right)\left(\frac{3}{2} + \frac{5N}{2\delta_1^*}\frac{\partial\delta_1^*}{\partial N}\right) + \frac{5N}{12}\frac{\partial C}{\partial N}\right\}^2 + A_1^2\right]^{1/2},$$

$$\tan\alpha_3 = A_1 \Big/ \left[(5/2 - C/6)\left(3/2 + \frac{5N}{2\delta_1^*}\frac{\partial\delta_1^*}{\partial N}\right) + \frac{5N}{12}\frac{\partial C}{\partial N}\right]. \tag{36}$$

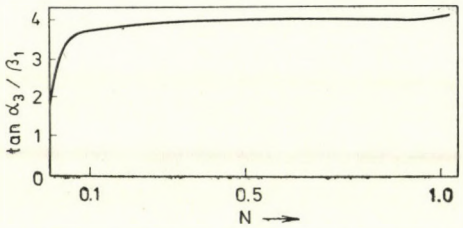

Fig. 3. Phase angle of the oscillating skin friction given by $\tan \alpha_3/\beta_1$ vs N

The oscillating component of the rate of heat transfer in terms of Nusselt number is

$$Nu_1 = \varepsilon \frac{B_1}{\delta_2^*} e^{i(\omega t - \pi/2)}. \tag{37}$$

Variation of phase angle and the amplitude of the skin-friction as functions of N and β_1 are shown in Figs. 3 and 4, respectively. It is remarkable that for low frequency oscillations the phase lag of Nusselt number fluctuations is always 90°. The amplitude of the Nusselt number is exhibited in Fig. 5 and the interesting result noted is that it decreases as N increases. The quasisteady skin friction decreases with increasing N.

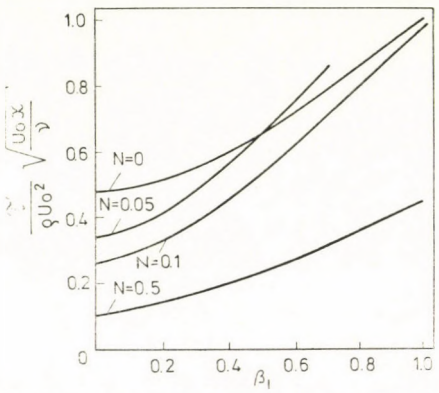

Fig. 4. Amplitude of the oscillating skin friction given by $\tau_1/\varrho U_0 \sqrt{U_0 x/\nu}$ vs β_1 for various N

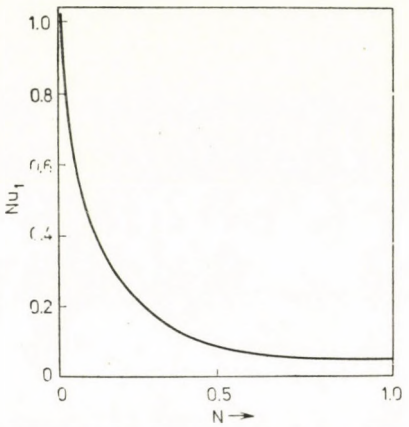

Fig. 5. Amplitude of the Nusselt number Nu_1 vs N

High frequency oscillations

For high frequencies, LIGHTHILL [3] has shown that the oscillating flow is to a close approximation an ordinary "shear wave" unaffected by the mean flow. Thus LIGHTHILL restricts his discussion for large ω to the solution:

$$u_1^{(0)} = U_0\left(1 - e^{-\sqrt{\frac{i\omega}{\nu}}\,y}\right), \tag{38}$$

which is obtained by retaining the terms with the factor ω together with the derivatives of the highest order in (6a). This shows that for high frequencies the thickness of the oscillatory boundary layer is of order $\sqrt{\nu/\omega}$ which is small as compared to the thickness of the steady boundary layer which is of the order of $\sqrt{\nu x/U_0}$. Thus one can visualise the entire oscillatory flow as being contained within the steady boundary layer. In order to solve (6) for large ω, we expand u_1, v_1 and T_1 in inverse powers of $\sqrt{i\omega}$ in the forms:

$$\begin{aligned} u_1 &= \sum_{n=0}^{\infty} (i\omega)^{-n/2}\, u_1^{(n)}(x, \eta), \\ v_1 &= \sum_{n=0}^{\infty} (i\omega)^{-n/2}\, v_1^{(n)}(x, \eta), \\ T_1 &= \sum_{n=0}^{\infty} (i\omega)^{-n/2}\, T_1^{(n)}(x, \eta), \end{aligned} \tag{39}$$

where $\eta = y\sqrt{i\omega/\nu}$. Within the thin layer affected by oscillations, we may approximate u_s, v_s, T_s as

$$\begin{aligned} u_s &= y\left(\frac{\partial u_s}{\partial y}\right)_{y=0} + \frac{y^2}{L^2}\left(\frac{\partial^2 u_s}{\partial y^2}\right)_{y=0} + \frac{y^3}{L^3}\left(\frac{\partial^3 u_s}{\partial y^3}\right)_{y=0} + \ldots, \\ &= A_4(x)y + B_4(x)y^3 + \ldots\ldots, \\ v_s &= y\left(\frac{\partial v_s}{\partial y}\right)_{y=0} + \frac{y^2}{L^2}\left(\frac{\partial^2 v_s}{\partial y^2}\right)_{y=0} + \frac{y^3}{L^3}\left(\frac{\partial^3 v_s}{\partial y^3}\right)_{y=0} + \frac{y^4}{L^4}\left(\frac{\partial^4 v_s}{\partial y^4}\right)_{y=0} + \ldots \\ &= -A_4'(x)\frac{y^2}{2} - B_4'(x)\frac{y^4}{4} + \ldots\ldots, \\ T_s - T_\infty &= y\left(\frac{\partial T_s}{\partial y}\right)_{y=0} + \frac{y^2}{L^2}\left(\frac{\partial^2 T_s}{\partial y^2}\right)_{y=0} + \frac{y^3}{L^3}\left(\frac{\partial^3 T_s}{\partial y^3}\right)_{y=0} + \ldots, \\ &= \lambda(x) + \lambda_1(x)y^3 + \ldots, \end{aligned} \tag{40}$$

where

$$A_4(x) = \frac{U_0}{\delta_1}\left(\frac{5}{3} - C/6\right), \quad B_4(x) = \frac{CU_0}{\delta_1^3},$$

$$\lambda(x) = T_w - T_\infty, \quad \lambda_1(x) = \frac{A}{\delta_2^3}(T_w - T_\infty),$$

and A_4' and B_4' denote the derivatives with respect to x. Substituting in (6a)–(6b) and equating the coefficients of like powers of $\sqrt{i\omega}$ on both sides and solving the resulting differential equations, we get

$$u_1^{(0)} = U_0(1 - e^{-\eta}); \quad u_1^{(1)} = 0, \quad u_1^{(2)} = 0,$$

$$u_1^{(3)} = U_0 \sqrt{\nu}\, A_4'(x)\left[\left(\frac{3}{8}\eta + \frac{3}{8}\eta^2 + \frac{\eta^3}{12}\right)e^{-\eta} - \eta\right], \quad u_1^{(4)} = 0,$$

$$u_1^{(5)} = U_0 B_4'(x)\nu^{3/2}\left[\left(\frac{9}{32} + \frac{9}{16}\eta + \frac{9}{16}\eta^2 + \frac{9}{16}\eta^3 + \frac{9}{16}\eta^4 + \frac{1}{40}\eta^5\right)e^{-\eta} - \right.$$

$$\left. - \left(\frac{9}{32} + 6\eta + \eta^3\right)\right] + \sigma g\beta U_0 \lambda''(x)\sqrt{\nu}\left[\frac{e^{-\eta\sqrt{\sigma}}}{\sigma^{3/2}(1-\sigma)^2} - \frac{1+\eta}{2(1-\sigma)}e^{-\eta} + \right.$$

$$\left. + \frac{\sigma^{3/2} - \sigma^{5/2} - 2}{2\sigma^{3/2}(1-\sigma)} + \frac{1}{\sigma}\eta\right] + DU_0(1 - e^{-\eta}); \tag{41}$$

$$T_1^{(0)} = 0, \; T_1^{(1)} = 0, \; T_1^{(2)} = -U_0\lambda'(x)\left[1 + \frac{\sigma e^{-\eta}}{1-\sigma} - \frac{e^{-\eta\sqrt{\sigma}}}{1-\sigma}\right],$$

$$T_1^{(3)} = 0, \quad T_1^{(4)} = 0,$$

$$T_1^{(5)} = \sigma U_0\sqrt{\nu}\left\{A_4\lambda''(x)\left[\frac{1}{\sigma}\eta - \frac{\sigma}{(1-\sigma)^2}\left(\eta + \frac{2}{1-\sigma}\right)e^{-\eta} - \right.\right.$$

$$\left. - \frac{1}{2\sqrt{\sigma}(1-\sigma)}\left(\frac{1}{2}\eta^2 + \frac{1}{2\sqrt{\sigma}}\eta - \frac{4\sigma^{3/2}}{(1-\sigma)^2}\right)e^{-\sqrt{\sigma}\eta}\right] +$$

$$+ A_4'\lambda'\left[\frac{1}{\sigma}\eta + \frac{1}{1-\sigma}\left(\frac{1}{12}\eta^3 + \frac{7}{8}\eta^2 + \frac{3(9-\sigma)}{8(1-\sigma)}\eta + \frac{5+\sigma}{(1-\sigma)^2}\right)e^{-\eta} - \right.$$

$$- \frac{1}{4\sqrt{\sigma}(1-\sigma)}\left(\frac{1}{3}\eta^3 + \frac{1}{2\sqrt{\sigma}}\eta^2 + \frac{1}{2\sigma}\eta + \frac{4\sqrt{\sigma}(5+\sigma)}{(1-\sigma)^2}e^{-\sqrt{\sigma}\eta}\right] -$$

$$- \nu\lambda_1'\left[\frac{3}{\sigma^2}\eta^2 + \frac{1}{\sigma}\eta^3 + \frac{1}{1-\sigma}\left(\eta^3 + \frac{6}{1-\sigma}\eta^2 + \frac{6(3+\sigma)}{(1-\sigma)^2}\eta + \right.\right.$$

$$\left.\left. + \frac{24(1+\sigma)}{(1-\sigma)^3}\right)e^{-\eta} - \frac{24(1+\sigma)}{(1-\sigma)^4}e^{-\sqrt{\sigma}\eta}\right], \tag{42}$$

where D is a constant yet to be determined. Away from the wall, Eq. (6c) can be written as

$$T_1 = -\frac{u_1}{i\omega}\left(\frac{\partial T_s}{\partial x}\right), \tag{43}$$

since $\partial^2 T_1/\partial y^2$ is negligible away from the wall. From (43), we get

$$T_1^{(2)} = -U_0\frac{\partial T_s}{\partial x}(1 - e^{-\eta}). \tag{44}$$

Solutions (42) and (44) for $T_1^{(2)}$ fit smoothly (at $y = \delta_0 \approx \sqrt{\nu/\omega}$) as exponentials become negligible. The constant D in (41) is now determined from the condition at the plate, i.e.

$$i\omega U_0 + i\omega \frac{\partial^2 u_1}{\partial \eta^2} + \sqrt{\frac{\nu}{i\omega}}\, g\beta \frac{\partial}{\partial x} \int_0^\infty T_1 d\eta = 0 \quad \text{at } \eta = 0,$$

as

$$D = \frac{9}{32} B_4' \nu^{3/2} + \frac{2 - \sigma^{3/2} + \sigma^{5/2}}{2\sqrt{\sigma}(1-\sigma)^2} g\beta\lambda''\sqrt{\nu} + 0(\delta_0^4). \tag{45}$$

We notice from (41) and (42) that the boundary conditions $u_1^{(3)}(\infty) = 0$, $u_1^{(5)}(\infty) = 0$, $T_1^{(2)}(\infty) = 0$ and $T_1^{(5)}(\infty) = 0$ are not fulfilled. This is due to the fact that the method of solution involves expansions for small y. In (41) and (42), the part multiplied by $e^{-\eta}$ corresponds to flow noticeable only within a layer of thickness $\delta_\delta \sim \sqrt{\nu/\omega}$. The polynomial part, not multiplied by $e^{-\eta}$, protrudes into the outer layer. The non-decaying part of the solution can be interpreted as the high frequency influence on the outer layer. The outer solution joins the free stream conditions and can be obtained as expansion starting from interface between the two layers at about $\delta_1 - \delta_0$ distance which is still near the wall. Solution (45) for T_1 is such a solution. In the polynomial part, we come across the existence of a high frequency boundary layer flow affecting the whole domain of the basic boundary layer. But, unlike the buoyancy free case [7], the process is twofold in this case. Here we find that the outer unsteady flow also influences the flow inside the oscillating boundary layer. This is due to free convection effects (though small) which manifest themselves through the integral in (45). But in the particular case of Blasius flow these effects are negligibly small as we have already seen. For an arbitrary basic steady horizontal flow with free convection, the influence of the outer unsteady flow on the oscillatory flow near the wall may be considerable.

Using the high frequency expansion terms up to $u_1^{(5)}$ and $T_1^{(5)}$ the oscillating components of skin friction and the rate of heat transfer are obtained as

$$\tau_{1h}^* = \frac{\tau_1}{\varrho U_0^2} \sqrt{\frac{U_0 x}{\nu}} = \varepsilon R_5 \cos(\omega t + \Phi_1), \tag{46}$$

$$Nu_{1h} = \frac{q_1 \delta_1}{k(T_w - T_\infty)} = \varepsilon R_6 \cos(\omega t + \Phi_2), \tag{47}$$

where

$$R_5 = (P_1^2 + Q_1^2)^{1/2}, \quad \Phi_1 = \tan^{-1}\left(\frac{P_1}{Q_1}\right),$$

$$R_6 = (P_2^2 + Q_2^2)^{1/2}, \quad \Phi_2 = \tan^{-1}\left(\frac{P_2}{Q_2}\right)$$

and P_1, Q_1, P_2, Q_2 are given by

$$P_1 = \sqrt{\frac{1}{2}\beta_1} - \frac{1}{\beta_1}\frac{5(10-C)}{96\delta_1^*},$$

$$Q_1 = \sqrt{\frac{1}{2}\beta_1} - \frac{1}{\beta_1^2}\left[\frac{261C}{32\delta_1^{*3}} + \frac{3N}{4}\frac{2+2\sqrt{\sigma}+4\sigma+3\sigma^{3/2}}{2\sqrt{\sigma}(1+\sqrt{\sigma})^2}\right],$$

$$P_2 = \sqrt{\frac{1}{2}\beta_1}\frac{\sqrt{\sigma}\,\delta_1^*}{2(1+\sqrt{\sigma})},$$

$$Q_2 = -\sqrt{\frac{1}{2}\frac{1}{\beta_1}}\frac{\sqrt{\sigma}\,\sigma_1^*}{2(1+\sqrt{\sigma})} + \frac{1}{\beta_1^2}\left[\frac{120\sigma^{5/2}\,\delta_1^*}{(1+\sqrt{\sigma})^4\,\delta_2^{*3}} + \right.$$

$$\left. + \frac{10-C}{12}\frac{5\sigma^{3/2}+50\sigma+24\sqrt{\sigma}-1}{16\sqrt{\sigma}\,(1+\sqrt{\sigma})^2}\right].$$

As $\omega \to \infty$, we find that $\Phi_1 \to 45°$ and $\Phi_2 \to 135°$. It may be mentioned that in the absence of free convection effects, LIGHTHILL found that $\Phi_2 \to -90°$.

Acknowledgement

My thanks are due to Prof. R. S. NANDA and Dr. S. S. CHAWLA for many useful suggestions in the preparation of this paper.

REFERENCES

1. W. B. GILL and R. D. CASAL, A. I. Ch. E. Journal, **8**, 512, 1962.
2. E. M. SPARROW and W. J. MINKOWYCZ, Int. J. Heat Mass Transfer, **5**, 505, 1961.
3. M. J. LIGHTHILL, Proc. Roy. Soc., A **224**, 1, 1954.
4. M. B. GLAUERT, J. Fluid Mech., **1**, 97, 1956.
5. W. N. GILL and R. D. CASAL, A.I.Ch.E. Journal, **8**, 473, 1962.
6. R. S. NANDA, Proc. Summer Seminar in MHD, Bangalore, India, 167, 1965.
7. N. ROTT and ROSENZWEIG, Int. J. Heat Mass Transfer, **5**, 505, 1961.

Acta Physica Academiae Scientiarum Hungaricae, Tomus 41 (4), pp. 281—288 (1976)

INVESTIGATION OF D-REGION PLASMA BY MODULATION TECHNIQUES

By

F. M. RAGAB

DEPARTMENT OF PHYSICS, TRIPOLI UNIVERSITY, TRIPOLI
THE LIBYAN ARAB REPUBLIC

(Received in revised form 28. IX. 1976)

Ionospheric electrons of the D-region were investigated by means of cylindrical Langmuir probes. It was found that the energy distribution and the density of the electrons are affected by the presence of negative ions of ionospheric origin and by the high energetic protons which cause an auroral activity at arctic latitudes. A measurable difference is detected between the electron temperature and the neutral gas temperature at D-region altitudes. The fast protons of the aurora are believed to be the origin of the partial heating.

Introduction

The density and energy of ionospheric thermal electrons have been studied by different experimental techniques, such as among them R. F. probes, Gerdien condensers at subsonic and supersonic speeds, and by radio waves propagated from the ground. The results obtained about the thermal electrons are not interpreted to a high degree of accuracy due to many factors, such as interference perturbations caused by interaction between the ionospheric medium and the radio waves, the effect of the geomagnetic field in the ionospheric charged particles and the influence of collisions between particles on the outputs of the measuring devices.

To have reliable measurements about the physical parameters which govern the different ionospheric layers one should resort to "in situ" measurements by application of Langmuir probes since they are a good tool in diagnosing the plasma characteristics both in the ionosphere and in the laboratory.

The method used successfully to study the electron density and energy distribution of thermal electrons under different conditions such as P.C.A., auroral activity, sporadic E nocturnal and daytime conditions, presence of sun spots, eclipse and the conditions in the magnetosphere is discussed as follows:

1. It makes use of the double differentiation techniques of two signals in the audio-frequency range together with a sweep potential applied to a Langmuir probe of cylindrical shape, which sweeps through the ionosphere by means of a spin stabilized spacecraft [1]. This electronic method has proved

its validity as a successful technique in studying the energy distribution function of a plasma experimentally [2].

2. The conditions required for the application of this method are: a. Maxwellian velocity distribution of the charged particles. b. Few collisions inside the plasma surrounding the probe.

The experiment

The experiment makes use of the probe technique developed successfully by IRVING LANGMUIR as early as 1924 in the field of plasma diagnostics in the laboratory. The same method can be applied in the ionosphere to measure the thermal electron temperature and density. In its simplest form a Langmuir probe is merely a small metallic electrode, usually a plane disc, a sphere or a cylindrical wire which is inserted in the plasma. The probe is attached to a power supply capable of biasing it at different voltage positive and negative with respect to a certain reference level which is taken as the space potential of the plasma; the current collected by the probe then provides information about the conditions of the ionospheric plasma.

The disturbances caused by the presence of the probe are localized and the probe can act truly as a probe in the sense that its very presence has no effect on the measurements. This is attained by choosing a probe to satisfy certain mechanical and physical requirements depending on the regions of the ionosphere through which it is to be flown.

On applying the sweep voltage to the probe which passes through space potential a current-voltage characteristic curve is obtained for the probe. When the probe is at space potential the sheath thickness drops to zero. The ionospheric charged particles move freely and diffuse to the probe. The current collected by the probe is predominantly electron current (ions have small mobility). If the probe is made positive electrons and negative ions will be accelerated towards the probe. Moreover, the positive ions are repelled and what little ion current was present at space potential vanishes.

If the probe potential is made negative the probe starts to repel electrons and negative ions and accelerate positive ions. If the electron velocity distribution function is Maxwellian the characteristic curve due to electron collection will be exponential in shape.

The current per unit area collected i_0 due to electrons by the probe at space potential is

$$i_0 = \frac{1}{4} en\bar{c} \,, \tag{1}$$

where $\bar{c}$ is the mean electron velocity ($\bar{c} = \sqrt{8KT/\pi m_e}$, n = density of electrons, e = electronic charge.

By using Boltzmann's equation and applying a retarding potential V to the probe, the electron collected current becomes

$$i_P = Ai_0 \exp\left(\frac{-eV}{KT}\right), \tag{2}$$

A = the area of the probe surface, K = Boltzmann's constant, T = electron temperature in °K.

Differentiating Eq. (2) once we obtain a mathematical expression for the first derivative of the probe characteristics. Differentiating Eq. (2) twice we obtain a mathematical expression for the probe characteristics which is related to the energy distribution function $f(V)$ of the electrons in the form

$$f(V) = \frac{2}{A_e}\left(\frac{2M}{e}\right)^{1/2} v^{1/2}\,\frac{d^2 i}{dV^2}\,. \tag{3}$$

Dividing the second derivative by the first derivative we obtain the modulation depth m expression for electrons in the form

$$m = \left(\frac{e}{KT_e}\right). \tag{4}$$

RAGAB [3] proved that the relationship between the modulation depth m and β which is the amplitude of the modulating signal divided by the mean electron energy is as follows:

$$m = \frac{I_1(\beta)}{I_0(\beta)}, \tag{5}$$

where $I_0(\beta)$ and $I_1(\beta)$ are the modified Bessel functions of the first kind and of order zero and one, respectively. From Eqs. (4) and (5) the electron temperature T depth could be obtained through meaning the modulation.

From the carrier current at its maximum level, electron density can be calculated from

$$i(V_{\text{carr}})_{\max} = V_{3\cdot 2Kc/s}\left(\frac{d^i p}{dV_p}\right), \quad V_p = 0\,, \tag{6}$$

where $V_{3.2Kc/s}$ is the amplitude of the 3.2 Kc/s carrier wave and

$$\left(\frac{di_p}{dV_p}\right)_{V_p=0} = \frac{e^2 nA}{(2\pi MKT)^{1/2}}\,. \tag{7}$$

A is the area of the probe applied and M is the electronic mass.

Particulars about the mechanical and electronic design of the experiment

The probes used to study thermal electrons were in the form of 30 cylindrical wires of circular cross-section. The wires were rhodium plated to provide a good conducting surface for the charged particles collected by the probes. In the case of daytime launching, it can also prevent photo emission of electrons from the probe array surface or decrease it according to the work functions of the material used in plating. It is also important to note here that one of the advantages of the use of Langmuir probes is that they are not sensitive to photo-emission as long as the potential applied is negative with respect to space potential. The rate of change of photo-current varies very slowly with the applied potential and hence its contribution to the modulation depth and the carrier frequency signal output is negligibly small. Photo-emission effect, though, is significant if the charged particle parameteres are evaluated from the collected current only, rather than from the probe characteristics as in the case under discussion.

The wires are manufactured from steel, each of them is 50 cm long and has a radius of 1 mm. Each probe is surrounded by a guard ring of the same material as the probe and of circular shape. The probes and the guard rings are separated from the body of the rocket by an electrical insulator. The 30 probes are connected so that they act as one probe. The probes are situated on the payload in a waisted portion near the nose cone.

On deployment, under the effect of spin, the wires rise to a position perpendicular to the rocket body.

The probes are connected to the components of an a.c. bridge network.

Both the probe-to-rocket and rocket-to-guard ring capacitances are neutralized by means of capacitors of equal values inserted with the head unit components so that the capacitative a.c. currents could be minimized.

The complete probe assembly is connected to the electronics via two co-axial leads. The electronics contained a probe voltage wave form generator and an a.c. current detector and analyser circuits. The composite wave form to the probe consisted of three components.

i) Sawtooth sweep of 0.7 to 2.3 volts of 2 second period.
ii) Sine wave of amplitude 28 millivolt and frequency 3.2 Kc/s as the carrier wave.
iii) Sine wave of amplitude 28 millivolt and frequency 0.5 Kc/s.

The probe current analyser produced two telemetry output voltages. The first output was calibrated against the r.m.s. carrier current and required a band width of 40 c/s, while the second output was calibrated against the modulation depth of the carrier at 0.5 Kc/s with the carrier current as a parameter. The telemetry bandwidth required for this was 80 c/s. The power supply to the experiment was 13.4 volt.

The experiment was launched from Andoya rocket range in Norway during 1970 and the temperature monitor showed that the temperature inside the payload during flight varied between 19 °C and 27 °C. Calibration curves of the electronics at 20 °C were chosen in the data analysis. Fig. 1 shows the

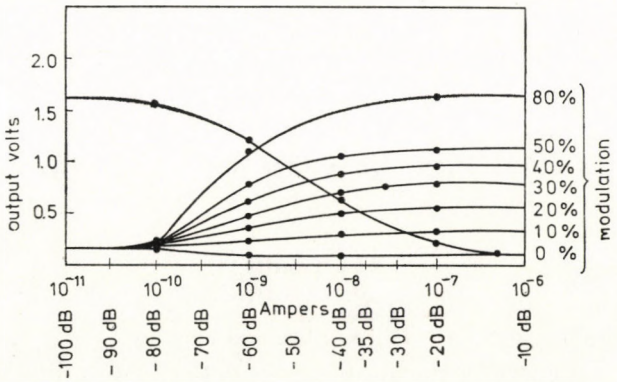

Fig. 1. C 13 rocket 115. Pye calibration curves 20 °C

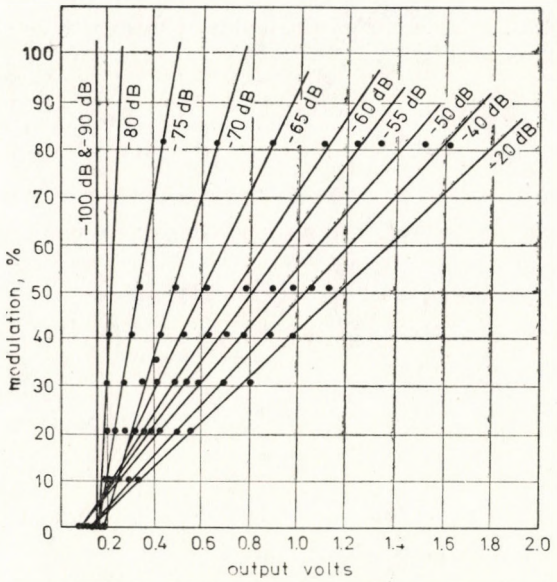

Fig. 2. Modulation depth calibration curves

outputs in volts which are proportional to the first derivative and the modulation depth. The curves are plotted on a semi-logarithmic scale with first derivative output calibration curve at the value 1.55 volt when the capacitance

bridge in the head unit is well neutralized with the difference of currents flowing in the two arms of the bridge being 10^{-11} or 10^{-10} A. When the difference is greater (10^{-9} — 10^{-6} A) the output drops as shown.

The modulation curves were carried at 0%, 20%, 50% and 80% modulation at Pye's electronics and the values 10%, 30% and 40% were calculated by interpolation. The percent modulation curves are plotted against the output in volts at constant current (10^{-7} A, 10^{-8} A) and so on, or against power in dB (—20 dB, —40 dB) with 10^{-6} A taken as reference current. The plotting of the modulation depth as function of output voltage at constant current is shown in Fig. 2. These calibration curves are used to find out the modulation depth and the first derivation due to thermal electron collection.

The results

The results of applying the calibration curves to the data are shown in Fig. 3. Fig. 3 is a semi-logarithmic plot for the first derivative against the applied sweep voltage when the electrons are retarded. From Eq. (2) the relation $\log \mathrm{d}I/\mathrm{d}V$ and V is linear. This is shown up till the current is 10^{-8} A and then the slope changes abruptly due to the influence of space potential. The thermal electron temperature is calculated from the slope under retardation as follows:

$$\text{slope} = d\frac{(\log I)}{dV} = \frac{\mathrm{d}(\log I')}{dV} = \frac{d(\log I'')}{dV} = \frac{1}{V}. \tag{8}$$

Also, from the same plot, the electron density n could be calculated by using the relation

$$\left(\frac{dI}{dV}\right)_{V = \text{ space potential}} = \frac{1}{4}\frac{neA\bar{c}}{\bar{V}},$$

where $A = (30)\,(2\pi rl)$, r is the radius of the probe and l its length.

$$\bar{c} = \sqrt{\frac{8kT}{\pi m}} = 6.19 \times 10^5 \times T \text{ cm/sec}.$$

Fig. 3 also shows the change in the slope due to negative ion collection. The space potential corresponds to 0.95 volt, the electrons temperature is 300 °K and the density is 5×10^2 electrons/cc. All measurements were taken at 78 km altitude. More results of the same kind were discussed earlier [3].

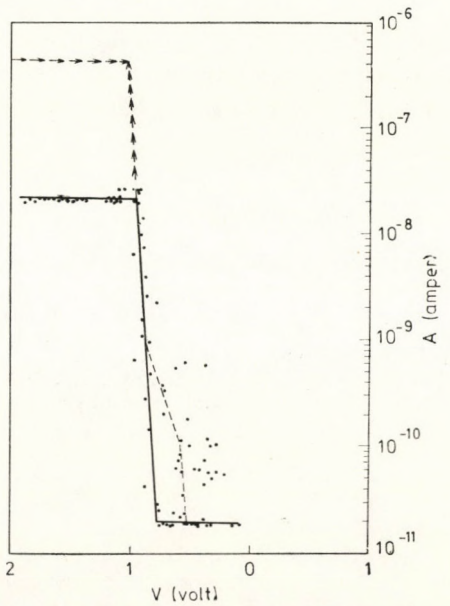

Fig. 3. First derivative of 1-V character (electrons and negative ions) $Z = 78$ km

Conclusion

The electron temperature in the lower ionosphere is found to be affected by the presence of negative ions, flux of high energy charged particles and by different kinds of collisions. The results indicate a difference between the neutral gas temperature and the ionospheric thermal electron temperature. The electron density is a factor of 2 less than that calculated from a radio-wave propagation experiment [4] on the same payload. This is believed to be due to the current damping problem discussed earlier by BODY [5]. Care should be taken about factors affecting the experiment and their effect should be eliminated. The probes should not be placed in the wake of the rocket otherwise there will be a measurable decrease in their density. Among factors affecting the experiment are:

i) Ionization by R.F. excitation, resulting in the increase of electron density content.
ii) Absorption of R.F. energy increases the electron temperature.
iii) Rectification at the antenna changes the vehicle potential.
iv) Escaping gas and outgassing tend to dilute the plasma.
v) Vehicle motion modifies the spatial distribution of density.
vi) Shock-wave ionization increases the electron density.
vii) The geomagnetic field modifies the probe current.

It should be pointed out that no comprehensive theoretical treatment of Langmuir probe theory exists in the presence of magnetic field. Plasma

diagnostic research makes it necessary to call for such a treatment, especially when a complete study of the geomagnetic field effect on electron density and temperature in the ionosphere is required.

REFERENCES

1. P. J. Bowen, R. L. F. Body, C. L. Henderson and A. P. Willmore, Proc. Roy. Soc. A. V 281, 1946.
2. R. L. F. Body, in Plasma Diagnostics, ed. by W. Lochte — Holtgreven, Pergamon Press, 1967.
3. F. M. Ragab, Libyan Journal of Science, Vol. II. 1972.
4. M. Jesperson et al., Journal of Atm. and Terr. Phys. IX, 1970.
5. R. L. F. Body, Advances in Atomic and Molecular Physics, 1968.

Acta Physica Academiae Scientiarum Hungaricae, Tomus 41 (4), pp. 289—297 (1976)

ONE-DIMENSIONAL SPIN MODEL WITH ARBITRARY HIGH POWER TERMS

By

G. I. GEORGIEV

"P. HILENDARSKII" UNIVERSITY, PLOVDIV, BULGARIA

(Received 28. IX. 1976)

Basic spectral and thermodynamical properties of a spin chain ($S = 1/2$) with a longitudinal — transverse anisotropy and nearest-neighbour interaction are considered, assuming the Hamiltonian to be a sum of arbitrary high power terms. After the renormalization of the spectrum, the rigorous solutions of the bilinear X-Y-model turn out to be stable with respect to the arbitrary high power terms. As to the low-excited and magnon-bound states in the spectrum of the system considered, they can be readily obtained from the known results for a "usual" bilinear anisotropic Heisenberg chain.

1. Introduction

As was shown by SCHRÖDINGER [1], in describing the properties of the localized spin systems it is necessary to take into account not only the bilinear term in the Hamiltonian, but the biquadratic and the higher power terms as well (including $(\vec{S_n} \cdot \vec{S_m})^{2S}$). The biquadratic term having an effect on the spectral and thermodynamical characteristics of spin models reflects successfully the properties of many real systems [2—12]. In the case of the isotropic spin system at $S = 1/2$ the addition of the biquadratic term is reduced to a renormalization of the bilinear exchange integral [2]. On the other hand, as has been shown by us [11, 12], the inclusion of the anisotropic biquadratic exchange interaction in the one-dimensional spin system (chain) with $S = 1/2$ and a bilinear transverse interaction between the nearest neighbours (X—Y-model) yields some interesting results, e.g. the displacement of the point of the second kind phase transition about the magnetic field (at $T = 0$) and the emergence of two-magnon complexes being most important for our work.

This paper is devoted to the basic spectral and thermodynamical properties of spin chains with a longitudinal — transverse anisotropy and nearest neighbour interaction, when the Hamiltonian contains arbitrary high power terms

$$\mathcal{H} = -I \sum_{l=1}^{P} \varepsilon_l \sum_{n=1}^{N} [\sigma(S_n^x S_{n+1}^x + S_n^y S_{n+1}^y) + \gamma S_n^z S_{n+1}^z]^l - H \sum_{n=1}^{N} S_n^z . \qquad (1)$$

In this formula $\vec{S}_n$ is the spin operator for the n-th site ($n = 1, 2, \ldots, N$), $\varepsilon_l I$ is the exchange interaction constant of the l-power term, σ and γ are the parameters of anisotropy, H is the strength of the external constant magnetic field. Here we shall follow the methods given in [13].

2. Effect of biquadratic and higher power terms on the ground state and the phase transition of the X-Y-model

At first we write the Hamiltonian (1) as

$$\mathcal{H} = \mathcal{H}_0 + V, \tag{2}$$

where

$$\mathcal{H}_0 = -\sigma I \sum_n (S_n^x S_{n+1}^x + S_n^y S_{n+1}^y) - H \sum_n S_n^z (\varepsilon_1 = 1). \tag{3}$$

After the transition from the spin operators to the Fermi ones by the formulae [14]

$$S_n^+ = \prod_{m<n} \sigma_m a_n;\ S_n^- = \prod_{m<n} \sigma_m a_n^+;\ S_n^\pm = S_n^x \pm S_n^y;\ \sigma_m \equiv 2S_n^z = 1 - 2a_m^+ a_m \tag{4}$$

we obtain

$$\mathcal{H}_0 = -\frac{NH}{2} + H \sum_n a_n^+ a_n - \frac{\sigma I}{2} \sum_n (a_n^+ a_{n+1} + a_{n+1}^+ a_n), \tag{5}$$

and

$$V = -NI_0 - \frac{I_1}{2} \sum_n (a_n^+ a_n + a_{n+1}^+ a_{n+1}) - \frac{I_2'}{2} \sum_n (a_n^+ a_{n+1} + a_{n+1}^+ a_n) + \\ + I_1 \sum_n a_n^+ a_n a_{n+1}^+ a_{n+1}. \tag{6}$$

Here, as well as in the following

$$I_1 \equiv 2(I_1^{xy} - I_1^z + I_1^{\sigma\gamma});\ I_1^{xy} \equiv I \sum_{l=1}^{P} \frac{\varepsilon_{2l} \sigma^{2l}}{2^{2l}};\ I_1^z \equiv I \sum_{l=1}^{P} \frac{\varepsilon_{2l-1} \gamma^{2l-1}}{2^{4l-3}};$$

$$I_0 \equiv I \sum_{l=1}^{P} \frac{\varepsilon_l \gamma^l}{2^{2l}};\ I_2 \equiv 2(I_2^{xy} + I_2^{\sigma\gamma});\ I_2^{xy} \equiv I \sum_{l=1}^{P} \frac{\varepsilon_{2l-1} \sigma^{2l-1}}{2^{2l-1}};$$

$$I_1' \equiv 2(I_2^{xy} - I_1'^z + I_1^{\sigma\gamma});\ I_2' \equiv 2(I_1'^{xy} + I_2^{\sigma\gamma}),$$

the only difference of $I_2'^{xy}$ ($I_1'^z$) from $I_2^{xy}(I_1^z)$ is that the summing starts from $l = 2$; $I_1^{\sigma\gamma}$ and $I_2^{\sigma\gamma}$ are sums of the products of σ and γ parameters, i.e. coefficients of the multiple products of X—Y and Ising parts in the bilinear term.

As is well known [14, 15], the Hamiltonian $\mathcal{H}_0$ can be diagonalized with the help of the Fourier components of the operators a_n^+ and a_n:

$$a_n = N^{-1/2} \sum_k e^{ikn} a_k, \; a_n^+ = N^{-1/2} \sum_k e^{-ikn} a_k^+ . \tag{7}$$

Thus, the system (3) is reduced to an ideal gas of Fermi magnons

$$\mathcal{H}_0 = \sum_k \left(a_k^+ a_k - \frac{1}{2} \right) \varepsilon_k, \; \varepsilon_k = H - \sigma I \cos k . \tag{8}$$

At $H > H_0 \equiv \sigma I_1 \varepsilon_k > 0$ for all k, a_k^+ is a creation operator, and there is an energy gap $H - \sigma I$ in the spectrum. At $H < H_0$, $\varepsilon_k > 0$ only for $| k | > k_{cr}$,

$$\varepsilon_{k_{cr}} = 0, \; k_{cr}(H) = \arccos \frac{H}{H_0}, \; k_{cr}(H_0) = 0; \tag{9}$$

the energy gap in the spectrum is absent. By the use of the canonical transformation

$$\begin{matrix} a_k = c_k & (| k | > k_{cr}) \\ a_k = c_k^+ & (| k | < k_{cr}) \end{matrix} , \quad c_k | 0 \rangle = 0 , \tag{10}$$

the Hamiltonian of the X—Y-model is written as

$$\mathcal{H}_0 = \sum_k \left(c_k^+ c_k - \frac{1}{2} \right) | \varepsilon_k | . \tag{11}$$

In the formulae (10) by $| 0 \rangle$ we denote the ground-state wave function. At $T = 0$ the susceptibility of the system has a root type singularity about the field at $H \to H_0$.

When $| I_1 | \ll \sigma I$ and $| I_2' | \ll \sigma I$, the operator V is regarded to be a small perturbation. The average in the ground state of the system (3), $\langle 0 | V | 0 \rangle \equiv \langle V \rangle$, can be obtained directly with the help of the formulae ($N \to \infty$)

$$\langle a_n^+ a_n \rangle = \frac{k_{cr}}{\pi} ; \; \langle a_n^+ a_{n+1} \rangle = \frac{\sin k_{cr}}{\pi} ; \; \langle a_n^+ a_n a_{n+1}^+ a_{n+1} \rangle = \frac{k_{cr} - \sin^2 k_{cr}}{\pi^2} . \tag{12}$$

Now, we find the first-order correction to the energy of the ground state

$$\delta E^{(1)} = \langle V \rangle = -NI_0 - \frac{2N}{\pi} I_1 (k_{cr} + \frac{I_2'}{I_1} \sin k_{cr} - \frac{k_{cr}^2 - \sin^2 k_{cr}}{\pi} . \tag{13}$$

The corresponding correction to the magnetic moment is

$$\delta M^{(1)} = -\frac{2NH}{\pi^2 H_0^2} I_1 - \frac{2N}{\pi} I_1 \frac{1+I_2' H/I_1 H_0}{\sqrt{H_0^2 - H^2}} + \frac{2N}{\pi^2} I_1 \frac{\arccos H/H_0}{\sqrt{H_0^2 - H^2}}. \quad (14)$$

In the isotropic case ($\sigma = \gamma$) the application of the perturbation theory is permissible only if we neglect the Ising bilinear term, i.e. after changing $I_1 \to I_1'$. Then for the terms $l = 1, 2, \ldots, 5$ in $\mathcal{H}$ we can verify that $I_2' = -I_1'$, there is no singularity in $\delta M^{(1)}$, and in the correction to the susceptibility $\delta x^{(1)}$ the typical square root type singularity emerges at $H \to H_0$, $\delta x^{(1)} \sim NI_1'/\pi\sqrt{H_0^2 - H^2}$. In the anisotropic case, however, $I_2' \neq -I_1$, $\delta M^{(1)}$ has a square root type singularity at $H \to H_0$, which is a physically meaningless result. Similarly to [13], this obstacle can be eliminated by transferring the quadratic terms from V into $\mathcal{H}_0$. Let us write then

$$\tilde{\mathcal{H}}_0 \equiv -\frac{NH}{2} - NI_0 + H\sum_n a_n^+ a_n - \frac{I_1}{2}\sum_n (a_n^+ a_n + a_{n+1}^+ a_{n+1}) - \\ - \frac{I_2}{2}\sum_n (a_n^+ a_{n+1} + a_{n+1}^+ a_{n+1}) . \quad (15)$$

and

$$\tilde{V} \equiv I_1 \sum_n (a_n^+ a_n a_{n+1}^+ a_{n+1}) . \quad (16)$$

Now, $\tilde{\mathcal{H}}_0$ can be diagonalized by (7) with a new dispersion function $\tilde{\varepsilon}_k$:

$$\tilde{\mathcal{H}}_0 + N\left(I_0 + \frac{I_1}{2}\right) = \sum_k \left(a_k^+ a_k - \frac{1}{2}\right)\tilde{\varepsilon}_k, \ \tilde{\varepsilon}_k = \tilde{H} - I_2 \cos k ,$$

$$\tilde{H} = H - I_1, \ k_{cr} = \arccos\frac{\tilde{H}}{\tilde{H}_0}, \ \tilde{H}_0 = I_2 . \quad (17)$$

Therefore, the influence of the quadratic term from V on the unperturbed, rigorously solvable model with a Hamiltonian $\mathcal{H}_0$ is expressed in:

— a displacement of the energy of the ground state without changing its character;

— an effective displacement about the field $H \to \tilde{H}$, originating from the even powers of the X — Y-part, the odd powers of the Ising part, and from $I_1^{\sigma\gamma}$;

— a renormalization of the exchange constant due to the odd powers of the X—Y-part and to $I_2^{\sigma\gamma}$. All the characteristics of the system (15) can be directly obtained (see for example [15]).

In the first order from the perturbation $\tilde{V}$ we obtain

$$\delta\tilde{E}^{(1)} = \langle\tilde{V}\rangle = \frac{NI_1}{\pi^2}(\tilde{k}_{cr}^2 - \sin^2\tilde{k}_{cr}) . \quad (18)$$

In the correction to the magnetic moment the singularity on the band edge is absent, $\delta M^{(1)} \to 0$ at $H \to H_0$. The singularity is absent in the correction to the susceptibility too,

$$\lim \delta \widetilde{X}^{(1)} = -\frac{8N}{3\pi^2}\frac{I_1}{I_2} \quad \text{at} \quad \widetilde{H} \to \widetilde{H}_0 . \tag{19}$$

Therefore, the perturbation (6) causes a transference of the point of the second kind phase transition. After the renormalization of the spectrum, the rigorous solutions of the unperturbed system are stable with respect to the arbitrary high power terms in the Hamiltonian.

3. Magnon bound states

Let us write the Hamiltonian (1) as follows:

$$H = -\frac{NH}{2} - NI_0 + H\sum_n S_n^- S_n^+ - \\ -\frac{I_1}{2}\sum_n (S_n^- S_n^+ + S_{n+1}^- S_{n+1}^+ - 2\, S_n^- S_{n+1}^- S_n^+ S_{n+1}^+) - \frac{I_2}{2}\sum_n (S_n^- S_{n+1}^+ + S_{n+1}^- S_n^+). \tag{20}$$

Evidently, from the bilinear term ($l = 1$, $\varepsilon_1 = 1$) we obtain the Hamiltonian (20) by the changes

$$\sigma I \to I_2 \quad \text{and} \quad \gamma I \to -I_1 . \tag{21}$$

Therefore, all the characteristics of the system (20) can be obtained directly from the corresponding ones for the well known anisotropic Heisenberg chain.

The ground state of the system (20) at $-I_1 > I_2 > 0$ is the ferromagnetic one at arbitrary H. In this case multimagnon bound states and low-excited states of the spectrum can readily be obtained from the results given in [16], by the change $g \to -I_1/I_2, I \to -I_1$. However for $0 < -I_1 < I_2$ the ground state is the ferromagnetic one only at

$$H \geq I_1 + I_2. \tag{22}$$

In this case the spectral and thermodynamical characteristics can be obtained from the corresponding ones in [17] through the replacements $\gamma \to -I_1/I_2$, $I \to I_2$. Here we confine our consideration to the two-magnon problem as an example.

Let us denote by $|\uparrow\rangle$ the wave function of the ferromagnetic state of the chain, such that $S_n^+|\uparrow\rangle = 0$ for all n, and by E_f — the energy of this state. Evidently $E_f \equiv -NH/2 - NI_0$. As usual, we present the wave functions

of the stationary states with one reversed spin in the form

$$|1\rangle = \sum_n e^{ikm} S_m^- |\uparrow\rangle, \tag{23}$$

the one-magnon spectrum is expressed by the formula

$$E_k = H - I_1 - I_2 \cos k\,. \tag{24}$$

The wave functions of the stationary states with two reversed spins can be expressed as a linear combination

$$|2\rangle = \sum_{l \neq m} A_{lm} S_l^- S_m^- |\uparrow\rangle, \quad A_{lm} = A_{ml}\,. \tag{25}$$

Bearing in mind the translational invariance of the system considered, the solution can be expressed in the form

$$A_{lm} \sim \exp\left(ik \frac{l+m}{2}\right) b(q),\ q \equiv m - l = \pm 1, \pm 2, \ldots,\ b(q) = b(-q), \tag{26}$$

separating in this way the motion of "the centre of attraction" of the system of two reversed spins with quasi-momentum $k \in [-\pi, \pi]$, and its relative motion. From the Schrödinger equation in this invariant subspace $\mathcal{H}|2\rangle = (E_f - E)|2\rangle$ we obtain the following difference equation for the function $b(q) \equiv b_q$:

$$\begin{aligned}[E - 2H + 2I_1 - I_1(\delta_{q,1} + \delta_{q,-1})]\, b_q + \\ + I_2 \cos\frac{k}{2}\,[b_{q+1}(1 - \delta_{q,-1}) + b_{q-1}(1 - \delta_{q,-1})] = 0,\end{aligned} \tag{27}$$

i.e.

$$[E - 2(H - I_1)]b_q + I_2 \cos\frac{k}{2}\,(b_{q+1} - b_{q-1}) = 0, \quad q > 1, \tag{27a}$$

$$(E - 2H + I_1)b_1 + I_2 \cos\frac{k}{2}\, b_2 = 0\,. \tag{27b}$$

Let us find a partial solution in the form:

$$b_q = r^q. \tag{28}$$

Denoting $a \equiv [E - 2(H - I_1)]/I_2 \cos k/2$, $k \neq \pm\pi$, from (27a) we obtain the following characteristic equation for the parameter r:

$$r^2 + 2ar + 1 = 0,\ r_{1,2} = -a \pm \sqrt{a_2 - 1},\ r_1 r_2 = 1,\ r_1 + r_2 = -2a. \tag{29}$$

Three cases are possible, namely:

A. $|a| < 1$, $r_1 = r_2^* = e^{iR}$, where R is real. Here

$$E_k(R) = 2H - 2I_1 - 2I_2 \cos\frac{k}{2} \cos R, \quad -\pi < R < \pi \tag{30}$$

expresses the energy of two free scattered magnons with a total quasi-momentum k and a relative one $-R$, i.e. this is the two-magnon continuum. The general solution of Eq. (27a) is

$$b(q) = c_1 e^{iRq} + c_2 e^{-iRq}, \tag{31}$$

where from the "boundary condition" (27b) we obtain the relation

$$c_2 = -\frac{E - 2H + I_1 + I_2 \cos\frac{k}{2} e^{iR}}{E - 2H + I_1 + I_2 \cos\frac{k}{2} e^{-iR}} e^{2iR} c_1.$$

B. $a = \mp 1$, $r_1 = r_2 = \pm 1$. In this case, at $I_2 > 0$ the expression

$$E = 2H - 2I_1 \mp 2I_2 \cos\frac{k}{2} = E_k^{\text{extr}} \tag{32}$$

coincides with the lower and upper continuum boundaries, respectively (if $I_2 < 0$, the opposite is true). Analogous results can be obtained from (30) for $R = 0$ and $R = \pm\pi$.

C. $|a| > 1$, $r_1 = r_2^{-1} = r$, let us suppose that

$$|r| < 1. \tag{33}$$

The bounded solution at $q \to +\infty$ is expressed by (28), where

$$r = -\frac{I_2}{I_1} \cos\frac{k}{2}. \tag{34}$$

From (34) we obtain the existence condition for the solution (33) (i.e. for the two-magnon complex or bound state), in the k-space:

$$k > 2 \arccos\left|\frac{I_1}{I_2}\right|. \tag{35}$$

Thus, in the model considered only one kind of bound states can exist, namely a short-wavelength one, possessing a probability maximum at $q = 1$. From (29) and (33) we obtain the energy of the complex

$$E_{sp.c.} = 2H + I_1\left(\frac{I_2^2}{I_1^2}\cos^2\frac{k}{2} - 1\right), \tag{36}$$

at $H = 0$, sign $E_{sp.c.} = -$sign I_1.

Comparing the bound-state energy with the extrema of the continuum at the same total quasi-momentum k, by the use of (32) and (36) we obtain

$$E_{sp.c.} - E_k^{\text{extr}} = \frac{1}{I_1}\left(I_1 \pm I_2\cos\frac{k}{2}\right)^2. \tag{37}$$

It is obvious that the relative arrangement of the continuum boundaries and bound-state energy is independent of sign I_2, but

$$\text{sign}\,(E_{sp.c.} - E_k^{\text{extr}}) = \text{sign}\, I_1. \tag{38}$$

Further we shall consider the case $I_1 < 0$, when $E_{sp.c} < E_k^{\min}$ and the complex formation leads to an energy gain.

There are no complexes at $I_1 = 0$. At small I_1 near the boundaries of the Brillouin zone a branch is detached from the continuum, due to the two-magnon complex. From formulae (34) — (38) it is seen that, when $|I_1|$ is increased, the detaching of the branch takes place at the gradually decreasing values of $|k|$, the width of the zone increases and both of the reversed spins are bound more and more closely together. When increasing $|I_1|$, at a fixed k, $E_{sp.c}$ and $E_k^{\min} - E_{sp.c}$ increase. At $-I_1 = I_2$ we obtain the well-known results for the isotropic Heisenberg chain [18]. At $-I_1 > I_2$ the complex exists for all k [16].

Let us examine now the relative arrangement of the one-magnon spectrum and the energy of the complex at the same values of k. From (24) and (37) we obtain:

$$E_k - E_{sp.c.} = -H - \frac{I_2^2}{2I_1}\left[1 + \left(1 + \frac{2I_1}{I_2}\right)\cos k\right]. \tag{39}$$

Let us elucidate the case a) $-I_1/I_2 < 1/2$. At $H < -I_2/I_1(I_1 + I_2)$ an interval exists for k, namely

$$\cos k > -\frac{1 + 2HI_1/I_2^2}{1 + 2I_1/I_2}, \tag{40}$$

where $E_k > E_{sp.c}$. Bearing in mind the condition (35) of the existence of the

complex (35) we obtain a stronger unequality for the magnetic field, $H < I_2 - I_1(1 + 2I_1/I_2)$, as the region of values of k is given by

$$2\left(\frac{I_1}{I_2}\right)^2 - 1 > \cos k > -\frac{1 + 2HI_1/I_2^2}{1 + 2I_1/I_2}. \tag{41}$$

For sufficiently small values of $|I_1|$ we can get the interval for H, where at a ferromagnetic ground state the energy of the complex is lower than that of the one-magnon, for all k from (41):

$$I_1 + I_2 \leq H < I_2 - I_1\left(1 + \frac{2I_1}{I_2}\right). \tag{42}$$

The case b) $-I_1/I_2 > 1/2$ can be analyzed in a similar way.

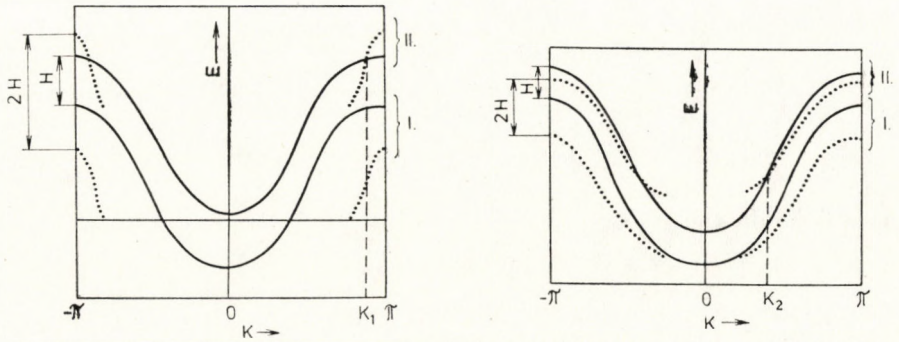

Fig. 1. Relative (qualitative) arrangement of the one-magnon spectrum and two-magnon bound state energy (dotted line): a) $-I_1/I_2 < 1/2$; I) $H = 0$, and II) for int. (42); b) $-I_1/I_2 > 1/2$; I) for int. (42), and II) $H > I_2 - I_1(1 + 2I_1/I_2)$; $\cos k_{1,2} = -(1 + 2HI_1/I_2^2)/(1 + 2I_1/I_2)$

Fig. 1 shows qualitatively the arrangement of E_k and $E_{sp.c.}$ in cases a) and b).

All the results in part 3, after the replacement (21) coincide with the corresponding ones for the bilinear Hamiltonian (at $l = 1$ only) [13, 16, 17, 18]. Thus, the problem for the determination of the low-excited states of the system with Hamiltonian (1) is solved.

In conclusion, investigating the spin Hamiltonians, $S > 1/2$, containing the scalar products of the spin operators of the nearest and following neighbours, of power $l > 2$, some new, interesting physical effects may be expected.

Appendix

The term with an arbitrary power in the sum $l = 1, 2, \ldots, P(1)$, i.e. the arbitrary power of the bilinear Heisenberg anisotropic Hamiltonian

($S = 1/2$) can be obtained in the following way. Let $\mathcal{H}_i$ and $\mathcal{H}_j$ be the terms of the i-th and the j-th power, respectively

$$\mathcal{H}_{i,j} = -\varepsilon_{i,j} I \sum_{i,n} [\sigma (S_n^x S_{n+1}^x + S_n^y S_{n+1}^y) + \gamma S_n^z S_{n+1}^z]^{i,j} .$$

Let us introduce conventional signs for the coefficients of the different operator terms:

$$\mathcal{H}_i = -\varepsilon_i I \sum_n \left\{ ① + ⑪ (a_n^+ a_n + a_{n+1}^+ a_{n+1}) + ⑪ (a_n^+ a_{n+1} + a_{n+1}^+ a_n) + ⑪ a_n^+ a_n a_{n+1}^+ a_{n+1} \right\}$$

$$\mathcal{H}_j = -\varepsilon_j I \sum_n \left\{ ⊖ + ⊜ (a_n^+ a_n + a_{n+1}^+ a_{n+1}) + ⊜ (a_n^+ a_{n+1} + a_{n+1}^+ a_n) + ⊜ a_n^+ a_n a_{n+1}^+ a_{n+1} \right\}$$

The product can be expressed in a conventional form:

$$\mathcal{H}_{i+j} = -\varepsilon_{i+j} I \sum_n \left\{ ①×⊖ + \left(① × ⊜ + ⊖ × ⑪ + ⊜ × ⑪ + ⑪ × ⊜\right) \left(a_n^+ a_n + a_{n+1}^+ a_{n+1}\right) + \right.$$

$$+ \left(① × ⊜ + ⊖ × ⑪ + ⑪ × ⊜ + ⊖ × ⑪\right) \left(a_n^+ a_{n+1} + a_{n+1}^+ a_n\right) +$$

$$\left. + \left(① × ⊜ + ⊖ × ⑪ + 2⑪ × ⊖ - 2⑪ × ⊜ + ⑪ × ⊜ + 2⑪ × ⊜ + 2⊖ × ⑪\right) a_n^+ a_n a_{n+1}^+ a_{n+1} \right\}$$

In this formula the $\times$ sign means the usual product.

REFERENCES

1. E. Schrödinger, Proc. Roy. Irish Acad., **A48,** 39, 1941.
2. H. Brown, Phys. Rev., **B4,** 115, 1971.
3. H. Chen and P. Levy, Phys. Rev. Lett., **27,** 1383, 1971.
4. M. Nauciel-Bloch, G. Sarma and A. Castets, Phys. Rev., **B5,** 4603, 1972.
5. V. Matveev, Zh. eksper. teor. fiz., **65,** 1626, 1973.
6. K. Chakraborty, Zs. Phys., **268,** 179, 1974, and **B20,** 412, 1975.
7. J. Buchbinder and B. Westwanski, Preprint P-4-7766, Joint Institute for Nuclear Research, Dubna, 1974.
8. R. Micnas, Phys. Stat Sol. (b), **66,** K25, 1974.
9. D. Pink and R. Ballard, Can. J. Phys., **52,** 33, 1974;
   D. Pink and V. Sachdeva, Can. J. Phys., **53,** 637, 1975.
10. V. Barjahtar, V. Gann and D. Jablonskij, Fiz. Tverdogo Tela, **17,** 1744, 1975.
11. G. Georgiev and S. Kuzmanova, Phys. Stat. Sol. (b), **74,** K173, 1976.
12. G. Georgiev, Fiz. Tverdogo Tela, **18,** 1812, 1976.
13. G. Georgiev, V. Kontorovich and V. Zukernik, Fiz. Met. Met., **38,** 928, 1974.
14. E. Lieb, T. Schultz and D. Mattis, Ann. Phys. (USA), **16,** 407, 1961;
    S. Katsura, Phys. Rev., **127,** 1508, 1962; **129,** 2835, 1963.
15. S. Pikin and V. Zukernik, Zh. eksper. teor. fiz., **50,** 1377, 1966.
16. I. G. Gochev, Zh. eksper. teor. fiz., **61,** 1674, 1971.
17. G. Georgiev and V. Zukernik, to be published.
18. H. Bethe, Zs. Phys., **71,** 205, 1931.

Acta Physica Academiae Scientiarum Hungaricae, Tomus 41 (4), pp. 299—303 (1976)

THE INVESTIGATION OF AGGREGATION PROCESSES IN QUENCHED NaCl : $CaCl_2$ CRYSTALS BY DIELECTRIC LOSS MEASUREMENTS

By

J. SÁRKÖZI and CS. KUTI

INSTITUTE OF PHYSICS, DEPARTMENT OF EXPERIMENTAL PHYSICS
TECHNICAL UNIVERSITY, BUDAPEST

(Received in revised form 27. X. 1976)

The aggregation processes of the Ca^{2+} ion-vacancy dipoles of NaCl single crystals strongly doped with Ca^{2+} were investigated by means of electrical conductivity and dielectric loss measurements. From the kinetical curves obtained taking into consideration also the electrical conductivity curves the binding energy of the dipoles in the aggregates were determined.

1. Introduction

It is a well known fact that bivalent cation impurities connected with cation vacancies form dipoles in alkali halides. This dipole formation results in dielectric losses. By ageing the crystals at elevated temperatures the dielectric loss values decrease because of the production of dipole aggregates. Since the physical properties of the crystals are much influenced by the changes of the impurity distribution investigations concerning the aggregation processes have recently gained in importance [1, 2, 3]. The general characteristics of the disappearance (aggregation) of dipoles in crystals containing small amounts of impurities appear to be identical for every system. According to the literature [1] three single dipoles form one aggregate (one trimer). If, however, the concentration of divalent cation impurities is large enough, aggregates already exist in the crystal practically at any heat treatment, consequently the dipole decay which may be expected will be different from the trimer case. The impurity content of the NaCl:$CaCl_2$ crystals used in the experiments to be described was large enough (1.6×10^{-2} mol%) to enable the investigation of this case. Specially grown crystals were used free of any anion or OH^- content whose eventual presence may create difficulties in the interpretation of the results [4].

2. Experimental details

Two types of samples were used; one group consisted of crystals whose impurity content was at normal temperature in a thermodynamically stable i.e. in a precipitated state (aged crystals), whereas the samples of the second

group were quenched, consequently their impurity content became precipitated only to a small degree, which corresponds to a thermodynamically unstable state. This crystal type is suitable for ageing experiments.

The dielectric loss in alkali halides consists of two parts: conductivity loss, which is connected with free vacancies, and of losses due to dipole reorientation. These two loss components can be separated, since their temperature dependence is different. If the conductivity loss is subtracted from the total loss the dielectric loss obtained is proportional to the number of dipoles. In our tg δ versus T(= dielectric loss temperature) curves one maximum was observed at approximately 500 °C for the fixed frequency $\omega = 10^4$ Hz. Subtracting the conductivity loss from this maximal value the tg δ value proportional to the number of dipoles has been obtained. Object of our investigation was the determination of the dependence of the number of dipoles on the quenching temperature and the time of heat treatment at this temperature. The quenching was carried out in a low heat capacity furnace in an inert gas atmosphere at a cooling rate of 100 °C/min from T_q to room temperature. The dimension of the samples was $10 \times 10 \times 1$ mm^3, the quenching did not change the dislocation density of the crystals.

3. Results and discussion

Fig. 1 depicts the change of the tg $\delta \equiv \varepsilon''$ values, which is proportional to the number of dipoles, for both sample types. The tg δ value of the aged samples increases nearly exponentially up to 150 °C to become stable above this temprature (curve 1, Fig. 1). The time of heat treatment at the quenching temperature was 10 hours. Repeated quenching (ageing) of already quenched

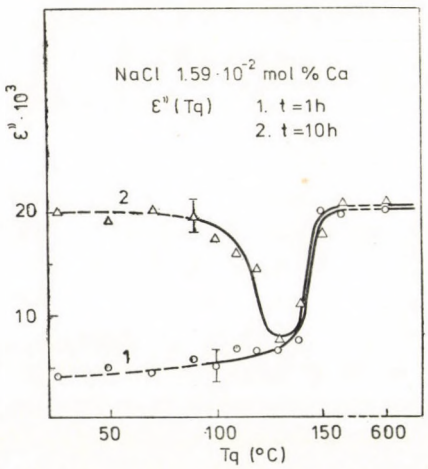

Fig. 1. Quenching temperature dependence of tg δ.
Curve 1: "aged" sample, Curve 2: "prequenched" sample

samples resulted in a minimum (curve 2, Fig. 1). In these experiments the time of heat treatment at the quenching temperature was 10 hours. While the first case seems to be an evidence of the dissolution of the precipitates, the second may be explained by a local precipitation at the $T_q = 150$ °C quenching temperature.

The dielectric loss dependence on the time of heat treatment at various temperatures is depicted in Figs. 2. and 3. The dielectric loss presents an exponential function of the time of heat treatment for the aged crystals as well as for the pre-quenched samples, for this latter case it takes for example the form (Fig. 3):

$$\varepsilon''(t) = \varepsilon''_{\min} + (\varepsilon''_{\max} - \varepsilon''_{\min})\, e^{-t/\tau}, \tag{1}$$

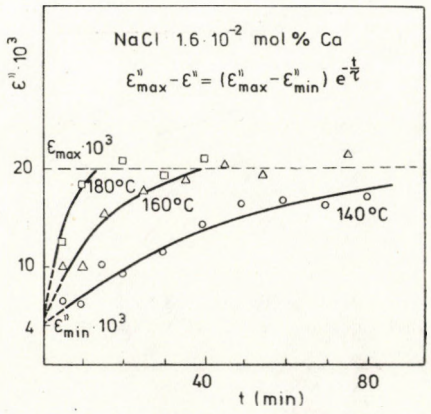

Fig. 2. Time of heat treatment dependence of tg δ of "aged crystals" at various heat treatment temperatures

where $\varepsilon''_{\max} \equiv \varepsilon''(0)$, $\varepsilon''_{\min} \equiv \varepsilon''(\infty)$ and τ is the relaxation time characterizing the decay of the dielectric loss. The fact that for both sample types the time dependence of the loss values is represented by an exponential function leads to the conclusion that the impurity dissolution (aged samples Fig. 2) as well as the precipitation (pre-quenched samples Fig. 3) can be accounted for by the same mechanism. In order to obtain the activation energy of the process responsible for the measured decay the logarithm of the τ values was plotted against the reciprocal temperature. The activation energies as calculated from the slopes of the straight lines obtained in this way were 0.98 ± 0.05 eV and 0.86 ± 0.05 eV for aged samples and for pre-quenched crystals, respectively.

Accordingly, the number of dipoles proportional to the dielectric loss value increases or else decreases by diffusing away from a fixed number of sources or diffusing to a fixed number of sinks. The sinks or sources consist most probably of aggregates of more than three dipoles. The actual existence of such aggregates in the aged as well as in the pre-quenched samples is also

indicated by the conductivity ($\log \sigma T$ versus $1/T$) curves of the same samples. The curves contain in every case a precipitation stage as can be seen in Fig. 4. Curve 1 refers to the change of conductivity of the "aged", whereas Curve 2 depicts this change for pre-quenched crystals. As can be seen from Curve 2 the pre-quenching does not cancel the precipitation state in Stage IV.

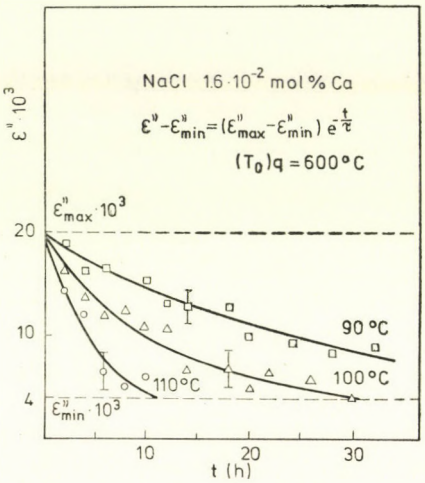

Fig. 3. Time of heat treatment dependence of tg δ of "pre-quenched" crystals at various heat treatment temperatures

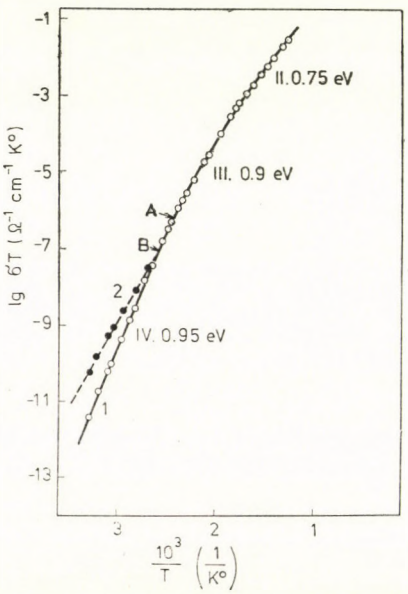

Fig. 4. Electrical conductivity curves of NaCl.Ca single crystals. Curve 1: "aged" sample, Curve 2: "pre-quenched" sample. The letter A denotes the end of the precipitation range, and B indicates that the "pre-quenching" does not discontinue the precipitation state

The activation energy corresponding to the values 0.86 eV and 0.98 eV may be explained in the following way. From the slope of Stage IV (precipitation) one obtains 0.95 eV, the slope of the association Stage (Section III) yields 0.9 eV and the slope of the dissociation stage corresponds to 0.75 eV. It seems to be generally accepted that the energy of migration of the cation vacancies $E_m = 0.75$ eV. The value 0.9 eV can be resolved into the form $E_m + E_s/2$, where E_s is the binding energy of a dipole. Furthermore the value 0.95 eV can be resolved into the form $E_m + E_a/2$ where E_a, the energy of dissolution of an impurity atom, is according to the literature [5] $E_s = E_{s_1} + E_a$, here E_{s_1} represents the energy necessary to tear away one dipole from the aggregate. From these values one obtains $E_a = 0.3$ eV and $E_s = 0.38$ eV, respectively. Taking into consideration equation $E_s = E_{s_1} + E_a$ we obtain for the more interesting term of our investigation E_{s_1} the value 0.08 eV. Hence this energy (0.08) should be invested to tear off one dipole from the aggregate or else this energy becomes free when a dipole becomes attached to the aggregate. However, these dipoles do not remain in the surroundings of the aggregates but diffuse away in the crystal with an energy of diffusion of 0.92 eV($=E_{ma}$) [6]. The sum of these two energies $E_{s_1} + E_{m_a} = 1$ eV appears to be within experimental error in good agreement with the energy of activation obtained from the kinetical curves, hence the described mechanism should also be in agreement with the experimental results. The kinetical curves obtained with pre-quenched samples (Fig. 3) yielded an activation energy of 0.86 eV. The sum $-E_{s_1} + E_{m_a}$ ($= 0.84$ eV) is in good agreement with this result, i.e. any aggregation of the dipole takes up the energy of diffusion $E_{m_a} = 0.92$ eV whereas by joining the aggregate an $E_{s_1} = 0.08$ eV energy is released. Summarizing for the discussed dissolution and precipitation processes the equation

$$E = E_{m_a} \pm E_{s_1}$$

may be applied, where E_{s_1} corresponds to the binding energy characterizing the attachement of a dipole to an aggregate, whereas E_{m_a} represents the energy of diffusion of a dipole.

The authors wish to thank Mr. A. TÓTH for valuable discussions.

*

REFERENCES

1. M. HARTMANOVA, phys. stat. sol. (a) **7**, 203, 1971.
2. G. P. WILLIAMS, Ir and I. W. MORTON, phys. stat. sol., (a) **17**, 305, 1973.
3. F. FRÖHLICH and G. HENSEL, phys. stat. sol., **24**, 535, 1967.
4. R. VOSZKA, Fizikai Szemle, *XX*, 6, 1, 1970.
5. R. CAPPELLETTI and R. FIESCHI, Crystal Lattice Defects, **1**, 69, 1969.
6. P. SÜPTITZ and I. TELTOW, phys. stat. sol., **23**, 9, 1967.

Acta Physica Academiae Scientiarum Hungaricae, Tomus 41 (4), pp. 305—308 (1976)

AGAIN THE KENNEDY—THORNDIKE EXPERIMENT

By

L. JÁNOSSY

CENTRAL RESEARCH INSTITUTE OF PHYSICS, BUDAPEST

(Received 28. X. 1976)

Answering valuable criticism of our former article on the interpretation of the Kennedy-Thorndike experiment we analyse the relevance of a number of experiments in proving the validity of various aspects of the Lorentz transformation.

The interesting article of Ø. GRØN [1] following hereafter criticising my paper [2] gives me the opportunity to return to the problem of the significance of the KENNEDY—THORNDIKE experiment (K.T.E) once more. In my former paper I have indeed oversimplified the discussion of the experiment and thus the discussion has to be modified in the following manner.

Consider one system of reference K in the measures of which light is propagated isotropically. Such a system was considered by MICHELSON interpreting the Michelson—Morley experiment (M.M.E.) and also by KENNEDY and THORNDIKE.

In the measures of K, points A and B moving with constant velocity $\mathbf{v}$ relative to K, have coordinate vectors

$$\mathbf{r}_A(t) = \mathbf{v}t, \quad \mathbf{r}_B(t) = \mathbf{a} + \mathbf{v}t. \tag{1}$$

The time of to and fro flight of a light signal between A and B is found in the usual way

$$T_{AB} = \frac{2a}{c} \frac{\sqrt{1 - v^2/c^2 \sin^2 \vartheta}}{1 - v^2/c^2}, \tag{2}$$

where ϑ is the angle between $\mathbf{a}$ and $\mathbf{v}$. The interferometer used in the M.M.E. can be schematized as consisting of two rods AB and AC. The fact that no fringe shift is observed when the interferometer is turned round can be expressed by supposing

$$(T_{AB} - T_{AC})\, \nu \quad = \text{independent of } \vartheta, \tag{3}$$

where ν is the frequency of the light source, T_{AB}, T_{AC} are the times of to and return flights between AB, respectively AC.

It is natural to suppose that (3) is valid because v independent of ϑ

$$v \text{ independent of } \vartheta \tag{4}$$

and both

$$T_{AB},\ T_{BC} = \text{independent of } \vartheta. \tag{5}$$

Accepting (4) and (5) we have to suppose in accord with (2) that the length a of a rod changes when it is turned round; denoting with $a(\vartheta, \mathbf{v})$ the length of a rod it attains when moving with the velocity $\mathbf{v}$ and being orientated at an angle ϑ to $\mathbf{v}$ we find with the help of (2)

$$a(\vartheta, \mathbf{v}) = \frac{af(v)}{\sqrt{1 - v^2/c^2 \sin^2 \vartheta}}, \tag{6}$$

where $f(v)$ is an arbitrary function of v.

The K.T.E. investigates the possible change of interference pattern while $\mathbf{v}$, the velocity of the interferometer, changes relative to K. The very careful invnstigation shows that the interference pattern does not change with v.

The negative result of the experiment proves that

$$(T_{AB} - T_{AC})v \quad = \text{independent of } v. \tag{7}$$

We may interpret (7) supposing that

$$v = \text{independent of } \mathbf{v}, \tag{8.a}$$

$$T_{AB},\ T_{AC} = \text{independent of } \mathbf{v}. \tag{8.b}$$

With the help of (2) we can thus account for the negative result of the K.T.E. supposing deformations in accord with

$$a(\vartheta, \mathbf{v}) = \frac{(1 - v^2/c^2)a}{\sqrt{1 - v^2/c^2 \sin^2 \vartheta}}. \tag{9}$$

Since (9) is a particular case of (6) we see that the deformation (9) is suitable to account for both negative result of the M.M.E. and the K.T.E.

The type of "LORENTZ contraction" described by (9) is not the one which was suggested by LORENTZ. It gives a contraction proportional to $1 - v^2/c^2$ in the longitudinal and one proportional to $\sqrt{1 - v^2/c^2}$ in the transverse direction; nevertheless if we wish to interpret only the M.M.E. and K.T.E. this can be done supposing (9) to be true.

We note that the assumption (8.a) is not essential for the interpretation of the experiments. Indeed, if we suppose that the frequency of the source

changes with $\mathbf{v}$, say so that

$$v(\mathbf{v}) = v_0 g(\mathbf{v}),$$

then we may replace (9) by

$$a(\vartheta, \mathbf{v}) = \frac{(1 - v^2/c^2)a/g(\mathbf{v})}{\sqrt{1 - v^2/c^2 \sin^2 \vartheta}} \tag{10}$$

and the contraction of the type (10) accounts for both the M.M.E. and the K.T.E. — no matter of how we chose $g(\mathbf{v})$.

So as to obtain information about the rate of clocks some third experiment is needed. Considering e.g. the experiments concerning the perpendicular DOPPLER effect [3] (P.D.E.) one finds (see e.g. [4])

$$g(v) = \frac{1}{\sqrt{1 - v^2/c^2}} . \tag{11}$$

and thus as a result of M.M.E., K.T.E. and P.D.E. we find

$$a(\vartheta) = \frac{\sqrt{1 - v^2/c^2}}{\sqrt{1 - v^2/c^2 \sin^2 \vartheta}} \tag{12}$$

This is the expression arrived at by LORENTZ and by FITZ-GERALD. However, even the above three experiments are insufficient to prove all the terms of the LORENTZ transformation.

Indeed from the LORENTZ transformation it follows that a system consisting of two physically connected clocks when accelerated adiabatically suffers three types of deformation:

1. Lorentz contraction in accord with (12),
2. Slowing down of the rates of clocks in accord with (11).
3. A phase shift is caused between the clocks to the amount

$$\Delta T = \frac{\mathbf{av}}{c^2 - v^2} .$$

$\mathbf{a}$ is the vector connecting the clocks. The third effect can be proved only by some additional experiment.

Summarizing the argument we find that the M.M.E. and K.T.E. can be interpreted both by a suitable type of deformation hypothesis; the type of deformation which has thus to be postulated contains as particular case the LORENTZ deformation (12). That the deformations supposed to be suffered by a closed system are indeed of the form (12) can be established by making use of a third experiment, e.g. P.D.E.

All the terms of the LORENTZ transformation can be supported experimentally only by adding at least one fourth experiment to the other three considered above, the TROUTON—NOBLE experiment seems to give some indirect evidence for the third effect.

REFERENCES

1. Ø. GRØN, Acta Phys. Hung., **41,** 309, 1976.
2. L. JÁNOSSY, Remark to the Interpretation of the Kennedy-Thorndike Experiment, Acta Phys. Hung., **25,** 275, 1968.
3. H. E. IVES and G. R. STILLWELL, J. Opt. Soc., **28,** 215, 1938, G. OTTING, Phys. Zs., **40,** 681, 1939.
4. L. JÁNOSSY, Theory of Relativity based on Physical Reality, Akad. Kiadó, Budapest (in English) p. 38—41.

Acta Physica Academiae Scientiarum Hungaricae, Tomus 41 (4), pp. 309—310 (1976)

COMMUNICATIONES BREVES

ON JÁNOSSY'S INTERPRETATION OF THE KENNEDY—THORNDIKE EXPERIMENT

By

Ø. GRØN

ST. GEORGS VEI 6, OSLO 2, NORWAY

(Received 9. VIII. 1976)

In the words of KENNEDY and THORNDIKE [1] their experiment "was devised to test directly whether time satisfies the requirements of relativity". The experiment is a modification of the Michelson—Morley experiment. Here, however, an interferometer with arms of different lengths was used. As in the Michelson—Morley experiment they did not observe the effect predicted for the experiment by an "ether"-theory based on the validity of the Lorentz-FitzGerald contraction and the concept of absolute time. From this null result and that of the Michelson—Morley experiment KENNEDY and THORNDIKE derive the Lorentz—Einstein transformations.

Now JÁNOSSY [2—4] states that "contrary to the general belief the negative outcome of the KENNEDY—THORNDIKE experiment can be fully accounted for in terms of the Lorentz—FitzGerald contraction of the arms of the interferometer". In order to show this JÁNOSSY calculates the change of length of a moving rod when it is turned round, and proves that turning round the interferometer produces no shift of fringes in the interference pattern, even when the arms have different lengths.

This fact is however of no relevance as to the experiment of KENNEDY and THORNDIKE. They did not turn the interferometer round. KENNEDY and THORNDIKE write: "The present experiment was devised to test directly whether time satisfies the requirements of relativity. It depends on the fact that if a pencil of homogeneous light is split into two components which are made to interfere after traversing paths of different lengths, their relative phases will depend on the translational velocity of the optical system unless the Lorentz—Einstein transformation equations are valid. Hence, such a system at a point on the earth should give rise to an interference pattern which varies periodically as the velocity of the point changes in consequence of the rotation and revolution of the earth."

The difference in travel time for light signals moving along two arms, with a length difference Δl, is calculated by KENNEDY and THORNDIKE, and

is equal to $2\gamma\Delta l/c$, where $\gamma = (1 - v^2/c^2)^{-1/2}$. This is in accordance with the result of JÁNOSSY's calculation [2], showing that the travel time for a light signal from one end of a rod with rest length l_0 and back is independent of the direction and given by $2\gamma l_0/c$, where v is the velocity of the rod.

KENNEDY and THORNDIKE were obviously aware of the fact that the above result implies that no fringe shift occurs when the arrangement is turned round. They write: The interference pattern is seen to be independent of orientations, lengths and dispositions of paths, but depend upon difference of path lengths and the velocity. Further: "Although the rotation of the apparatus with the earth involves a slight effect on the time difference computed above (whether regarded from the standpoint of relativity or classical theory), it turns out to be altogether negligible in amount. This effect is a function of rotational velocity, not of orientation of apparatus." KENNEDY and THORNDIKE conclude that the hypothesis that time satisfies the requirements of relativity can be tested by determining whether the interference pattern is unchanged as v changes in consequence of the motions of rotation and revolution of the earth. The result of the experiment is summarized with the words: "We have shown that there is no effect corresponding to absolute time unless the velocity of the solar system in space is no more than about half that of the earth in its orbit."

One must conclude that the Lorentz—FitzGerald contraction alone cannot explain the results of the KENNEDY—THORNDIKE experiment, and that the interpretation of their experiment given by KENNEDY and THORNDIKE is correct.

REFERENCES

1. R. J. KENNEDY and E. M. THORNDIKE, Phys. Rev., **42**, 400, 1932.
2. L. JÁNOSSY, Acta Phys. Hung., **25**, 275, 1968.
3. L. JÁNOSSY, Found. Phys., **1**, 111, 1970.
4. L. JÁNOSSY, Theory of Relativity Based on Physical Reality, Akadémiai Kiadó, Budapest, 1971, p. 60—64.

Acta Physica Academiae Scientiarum Hungaricae, Tomus 41 (4), pp. 311—315 (1976)

THE EFFECT OF THE CHANGE OF THE STATE OF IMPURITIES RESULTING FROM HEAT TREATMENT ON THE MICROHARDNESS OF NaCl CRYSTALS

By

J. SÁRKÖZI and Z. MORLIN*

INSTITUTE OF PHYSICS, DEPARTMENT OF EXPERIMENTAL PHYSICS
TECHNICAL, UNIVERSITY, BUDAPEST

(Received in revised form 4. XI. 1976)

The interaction among dislocations in alkali halides is according to experience much weaker than the interaction between dislocations and point or point like defects, or interactions between dislocations and some other defects of various type. Consequently, the strength and plastical properties of these crystals are mainly determined by the latter interactions. [1]. Point-like defects exist also in "pure" crystals (e.g. vacancy clusters) though their effect on hardness and plastical properties is considerably smaller than the effects due to impurities in doped crystals. It is a well known fact that impurities, especially divalent cations, introduced into sodium chloride type crystals result in considerable hardening, which depends upon the type of impurity, its concentration and the way of impurity arrangement in the crystal [1, 2, 3].

In the experiments to be discussed the various impurity states of pure and doped NaCl crystals were realized by heat treatment, the resulting effect was investigated by measuring the microhardness of the quenched crystals. In order to avoid any contamination due to various contaminants diffusing at high temperature from the air into the crystals the quenching has been carried out in dry nitrogen atmosphere. Because of the requirement of fast heating and cooling a furnace of low heat capacity was used. The mechanical stresses and plastic deformation formed during the quenching process were investigated by a polarization microscope. In the experiments the heating time up to T_q as well as the cooling time from T_q was negligibly small compared to the time of heat treatment at T_q. With NaCl · Ca^{2+} crystals as well as with NaCl · K^+ crystals two types of samples were quenched: aged crystals in which at room temperature the contaminant was thermodynamically stable and pre-quenched crystals, in which it was in a thermodynamically unstable state. The OH^- free pure crystals and samples doped with Ca^{2+} or K^+ impurities were grown by the Research Group for Crystal Physics of the Hunga-

* Present address: Research Laboratory for Crystal Physics of the Hungarian Academy of Sciences, Budapest

rian Academy of Sciences [4]. Since considerable research work has been done with pro analysi sodium chloride crystals the present work describes also changes of hardening due to heat treatment obtained with crystals of analytical purity.

1) The quenching rate dependence of the microhardness was investigated on NaCl · Ca^{2+} systems of both (aged, and pre-quenched) types. The aged samples were heated at a rate of 100 °C/min to 100 °C and kept at this temperature for one hour, after which they were quenched to room temperature at various cooling rates and their microhardness measured; the same procedure was applied for 130 °C.

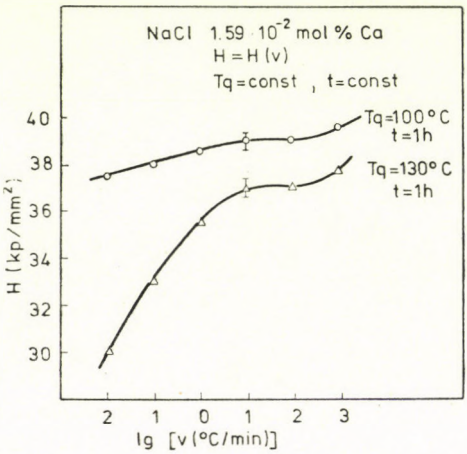

Fig. 1. Quenching rate dependence of the microhardness of NaCl.Ca samples aged at various quenching temperatures

According to microscopic investigations in polarized light between crossed Nickols plastic deformation and stresses could be detected only with cooling rates above 150 °C/min. The microhardness dependence on the quenching rate for NaCl · Ca^{2+} is depicted in Fig. 1. With lower cooling rate the softening of the crystal increases, a process which is very manifest at quenching from 130 °C. This is understandable since because of the slow cooling the sample remains for a relatively long time at high temperature, and the impurity structure of the crystal may change. In accordance with this result electrical conductivity measurements to be published elsewhere on the same samples show that the solubility of the impurities increases with decreasing quenching rate which means that the impurities pass over from a dissolved into a precipitated state. Finally, if no considerable change of the defect structure formed at temperature T_q during some given time t is desired one should select (for samples of the dimensions of $8 \times 8 \times 2$ mm^3) quenching rates belonging to the plateau in Fig. 1 which is e.g. for NaCl · $1{,}6 \times 10^{-4}$ mol/mol Ca^{2+} 100 °C/min.

2) The dependence of the microhardness on the heat treatment shows a varying picture for aged and pre-quenched NaCl · Ca^{2+}, NaCl · K^+, and pro analysi NaCl crystals, respectively. The microhardness of aged NaCl · Ca^{2+} crystals ($t = 60$ minutes, $v = 100$ °C/min) measured at room temperature practically do not change if the temperature of heat treatment is changed up to 150 °C, after a rapid decrease, however, at a treatment above this temperature it approaches a stable value (curve 2, Fig. 2). A "pre-quenched" sample of this same material quenched again ($t = 10$ hours, $v = 100$ °C/min) gives a low initial microhardness value after which it increases up to approximately $T_q = 140$ °C and then decreases. This gives a maximum at 140 °C. The electrical

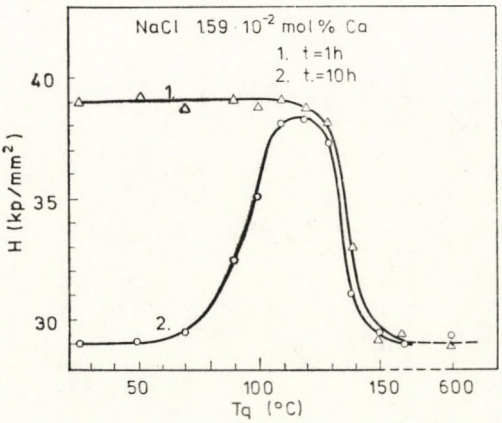

Fig. 2. The quenching temperature dependence of the microhardness of NaCl.Ca systems Curve 1: "pre-quenched" sample, Curve 2: "aged sample"

conductivity of the same "pre-quenched" samples shows a minimum at $T_q = 140$ °C, which means that the maximum of the hardness value at this temperature can be interpreted as a precipitation process, while the softening observable in curve 2 of Fig. 2 accompanied by an increase of the electrical conductivity of the respective samples may be explained by the dissolution of the impurities.

The quenched samples of the "aged" NaCl · 10^{-2} mol/mol K^+ system ($t = 60$ minutes, $v = 100$ °C/min) show a decrease of the microhardness value at a high quenching temperature (450 °C) after which it decreases and becomes unchanged from 550 °C (curve 2., Fig. 3).

A repeated quenching of the "pre-quenched" samples ($t = 7$ hours, $v = 100$ °C/min) results in a microhardness maximum at $T_q = 450$ °C (curve 1, Fig. 3). By means of a vacuum decorating method it could be shown electron-microscopically [5] that the quenching of aged samples is connected with the dissolution of impurities, whereas the quenching from 450 °C of pre-quenched samples results in impurity precipitation. Consequently, the decrease of the

microhardness of the aged samples at 450 °C may be explained by the disintegration of the precipitations checking the movement of dislocations, whereas the hardening of the "pre-quenched" samples in the neighbourhood of this temperature can be accounted for by impurity precipitation.

It appears to be instructive to compare the change of microhardness of nominally pure NaCl crystals with extremely pure crystals. The divalent impurity of the NaCl crystals used in these experiments was mainly Ca^{2+}, whereas the monovalent impurity was K^+. The experiments were also in this case carried out with "aged" and "pre-quenched" crystals, respectively. The time of heat treatment was in the first case 1,0 hour, in the second case

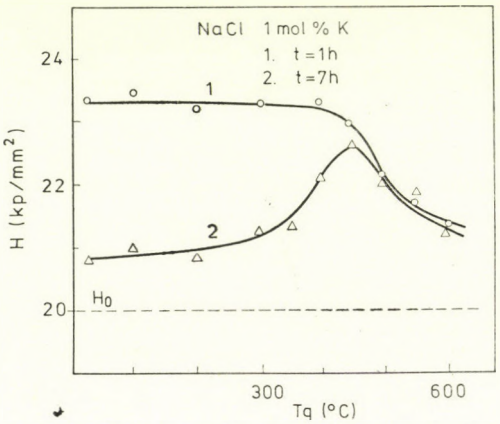

Fig. 3. The quenching temperature dependence of the microhardness of NaCl.K systems. Curve 1: "pre-quenched" sample, Curve 2: "aged sample"

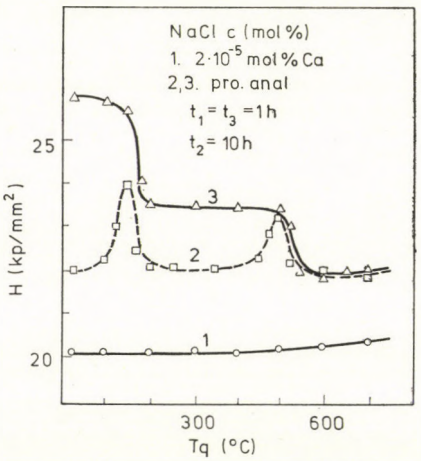

Fig. 4. The quenching temperature dependence of pure and pro analysi NaCl single crystals. Curve 1: pure NaCl, Curve 2: "pre-quenched" pro analysi NaCl, Curve 3: "aged" pro analysi NaCl

10 hours with a quenching rate of 100 °C/min for both. The hardness of the aged samples softened in two steps (curve 3, Fig. 4), the first softening phase (period) could be observed at 150 °C $< T_q <$ 200 °C, whereas the second at 500 °C $< T_q <$ 600 °C. A repeated quenching of "pre-quenched" crystals resulted in two maxima in the $H - T_q$ curve, at $T_q = 140$ °C and $T_q = 500$ °C, respectively (curve 2, Fig. 4).

Since the divalent impurity of nominally pure NaCl crystals consists mainly of Ca^{2+}, and the monovalent impurity of K^+ cations the interpretation of the experimental results may be the same as the interpretation of the results obtained with NaCl · Ca^{2+} and NaCl · K^+ systems, respectively. It follows that the two step-softening as presented in curve 3 of Fig. 4 may be explained by the dissolution of Ca and K impurities, whereas the maxima of curve 2 may be accounted for by the precipitation of these impurities. Quenching practically does not change the hardness of very pure NaCl crystals (curve 1, Fig. 4). This fact seems rather convincingly to support the interpretation of our experimental results according to which the various changes of the microhardness values of the heat treated crystals are due to the changes of the state of their impurity structure. This change of state consists in our case of dissolution or precipitation of impurities at high temperatures of aged and pre-treated crystals, respectively. The precipitation of impurities at 140 °C in CaCl · Ca systems, and a full dissolution of these impurities into the lattice may be easily understood by electrical conductivity measurements. The association domain appears above 140 °C, whereas the precipitation takes place below this temperature. Consequently at quenching temperatures above 140 °C the impurity is in an already dissolved state. However, the dissolution of potassium at 450 °C is up to now not clearly understood. This problem needs further investigations.

REFERENCES

1. A. A. Vorobjev, Mehanicseszkie i tyeplovüe szvojsztva selocsnogaloidnüh monokrisztallow Izd: "Vüszsaja Skola".
2. Z. Morlin, Magyar Fizikai Folyóirat, **10**, 169, 1962.
3. Z. Morlin, phys. stat. sol., **8**, K 77, 1965.
4. R. Voszka, I. Tarján, L. Berkes and I. Krajsovszky, Kristall und Technik, **1**, 423, 1966.
5. A. Tóth and J. Sárközi, phys. stat. sol., (a) **28**, K 93, 1975.

RECENSIONES

P. GOMBÁS and D. KISDI: Wave Mechanics and its Applications

International Series of Monographs in Natural Philosophy, Volume 58, pp. XII + 238
Pergamon Press, Oxford, New York, Toronto, Sydney, Braunschweig, 1973.

After the Hungarian edition issued in 1967 the Publishing House of the Hungarian Academy of Sciences published the book also in German and English. These new editions mark the very favourable reception of the book by wide circles of physicists.

The English edition was taken over by Pergamon Press as Volume 58 in the "International Series of Monographs in Natural Philosophy."

To be included in a well-known series like this will certainly bring the work further success and promote its wider use in and outside the English-speaking countries.

As the earlier editions — including the English edition published by the Publishing House of the Hungarian Academy of Sciences — were recently reviewed in Acta Physica Hungarica, it seems unnecessary to give here full details. The contents of the book can be briefly summarized as follows: Starting from the fundamental experimental facts through classical physical analogies, after a short discussion of the Bohr-Sommerfeld theory one arrives at the Schrödinger equation. This is followed by examples, which can be treated as exactly solvable cases of the equation. Then follow the scattering theory and finally, the perturbational and variational methods with several physically important applications.

The clear treatment and consequent construction qualify the book an easily readable, pedagogically good text-book. We recommend it warmly for students in the upper grades in physics and chemistry and for young researchers.

A. KÓNYA

A. P. JUCYS, and A. J. SAVUKYNAS:

Mathematical Foundations of the Atomic Theory

(In Russian) "Mintis" Publishers, Vilnius, 1972.

This monograph seeks to provide a theoretical background for physicists engaged, or about to engage, in the quantum theory of atoms, atomic spectroscopy and related fields of physical science.

Primary emphasis is given to the methods of constructing the antisymmetrical wave functions of many electron configurations with the help of one electron wave functions (spin orbitals) and of expressing the matrix elements of atomic quantity operators in terms of radial integrals. For the shells of equivalent electrons the fractional parentage coefficients are used. The wave function of the whole configuration is expressed in the form of antisymmetrized product of antisymmetric functions of individual shells. For the operators the mathematical apparatus of irreducible tensor operators are used throughout.

The extensive tables given at the end of the book enable to construct the expressions for the matrix elements of operators in a quite easy way at least for the configurations having one or two open shells outside any number of closed shells of equivalent electrons.

The well written book may be very useful for scientists working on the theory of nuclei, atoms and molecules.

R. GÁSPÁR

J. M. ZIMAN: Prinzipien der Festkörpertheorie

Akademie-Verlag, Berlin, 1974, pp 443

Nowadays ZIMAN's Principles of the Theory of Solids is considered as one of the gems of the literature on solid state physics. It was first published in 1964 and two reprints were issued shortly afterwards. The second edition came out in 1972 as an enlarged version of the first one in the sense that several sections covering subjects which have come into the focus of interest in the period between the two editions, like type-II superconductivity, have been added. The German translation has been prepared from this second edition, by P. RENNER.

The structure and content of the book is truly reflected by its title: the main emphasis is on the discussion of the principles governing solid state physics. While the most modern physical approach is applied, the formalism is kept on a relatively simple level. Thus use of sophisticated modern mathematical tools like Green function technique is avoided. ZIMAN is able to extract the essence of a physical problem from the multiplicity of facts and give insight into the physical meaning of abstract formulas. This book is a basic textbook, to be consulted by all solid state physicists who want to be informed about the ideas underlying phenomena.

ZIMAN's Principles has been translated into Russian, Japanese and Spanish. The present German translation bears further evidence of the ceaseless interest towards this excellent textbook. Besides its high quality get-up this edition has the following remarkable features. The even originally comprehensive bibliography has been completed by pertinent literature in German and Russian. Moreover, a tri-lingual (German—English—Russian) version of the detailed index helps the reader to find passages of interest easily.

P. SZÉPFALUSY

A kiadásért felel az Akadémiai Kiadó igazgatója Műszaki szerkesztő: Botyánszky Pál
A kézirat nyomdába érkezett: 1976. XII. 16. – Terjedelem: 8 (A/5) ív, 22 ábra

77.3948 Akadémiai Nyomda, Budapest – Felelős vezető: Bernát György

Simul — Ein Programm für die mathematische Simulation von verfahrenstechnischen Systemen

Herausgegeben von P. Benedek

Autorenkollektiv: G. Almásy, P. Benedek, M. Farkas,
I. Pallai, F. Simon, P. Szepesváry,
T. Sztanó

Das Buch gibt dem Leser eine Vorstellung über die Möglichkeiten, die für die chemische Technologie durch den Einsatz von Digitalrechnern geboten werden. Es vermittelt die von den Autoren angewendeten Methoden zur Errechnung physikalish-chemischer Größen, beschreibt die zur Simulation der einzelnen Operationen ausgearbeiteten Modelle, und führt vor Augen, wie immer ein kompletter chemisch-technologischer Verfahrenszug in seinem stationären Ablauf von dem SIMUL-System simuliert werden kann. Die mit speziellen Problemen einhergehenden Regelungs-, Rezirkulations- und Optimalisierungsfälle werden auch im besonderen auseinandergesetzt. Das letzte Kapitel demonstriert am Beispiel einer Anlage für Essigsäureanhydriderzeugung die Anwendung des SIMUL-Systems.

In deutscher Sprache · Etwa 320 Seiten · Ganzleinen
ISBN 963 05 1111 8

AKADÉMIAI KIADÓ
Verlag der Ungarischen Akademie der Wissenschaften
Budapest

Atom and Ion Sources

by L. Vályi

Atom and ion beams are becoming more and more extensively used both in science and technology. The broad field of applications gives grounds for the publication of this book, rendering it most timely. In this monography both the theoretical and practical problems concerning the use of particle sources are discussed in detail. All the available knowledge in this field is reviewed and further developed. The large number of illustrations is of great help in the understanding and utilization of the discussed material.

In English · Approx. 380 pages · Cloth

A co-edition — distributed in the socialist countries by KULTURA, Budapest; in all other countries by JOHN WILEY AND SONS LTD., Chichester

ISBN 963 05 1113 4

AKADÉMIAI KIADÓ
Budapest

JOHN WILEY AND SONS LTD.
Chichester

NOTES TO CONTRIBUTORS

I. PAPERS will be considered for publication in Acta Physica Hungarica only if they have not previously been published or submitted for publication elsewhere. They may be written in English, French, German or Russian.

Papers should be submitted to

Prof. I. Kovács, Editor
Department of Atomic Physics, Polytechnical University
1521 Budapest, Budafoki út 8, Hungary

Papers may be either articles with abstracts or short communications. Both should be as concise as possible, articles in general not exceeding 25 typed pages, short communications 8 typed pages.

II. MANUSCRIPTS

1. Papers should be submitted in five copies.

2. The text of papers must be of high stylistic standard, requiring minor corrections only.

3. Manuscripts should be typed in double spacing on good quality paper, with generous margins.

4. The name of the author(s) and of the institutes where the work was carried out should appear on the first page of the manuscript.

5. Particular care should be taken with mathematical expressions. The following should be clearly distinguished, e.g. by underlining in different colours: special founts (italics, script, bold type, Greek, Gothic, etc); capital and small letters; subscripts and superscripts, e.g. x^3, x_3; small *l* and 1; zero and capital O; in expressions written by hand: *e* and *l*, *n* and *u*, *v* and *v*, etc.

6. References should be numbered serially and listed at the end of the paper in the following form: J. Ise and W. D. Fretter, Phys. Rev., *76*, 933, 1949.

For books, please give the initials and family name of the author(s), title, name of publisher, place and year of publication, e.g.: J. C. Slater, Quantum Theory of Atomic Structures, I. McGraw-Hill Book Company Inc., New York, 1960.

References shold be given in the text in the following forms: Heisenberg [5] or [5]

7. Captions to illustrations should be listed on a separate sheet, not inserted in the text.

III. ILLUSTRATIONS AND TABLES

1. Each paper should be accompanied by five sets of illustrations, one of which must be ready for the blockmaker. The other sets attached to the copies of the manuscript may be rough drawings in pencil or photocopies.

2. Illustrations must not be inserted in the text.

3. All illustrations should be identified in blue pencil by the author's name, abbreviated title of the paper and figure number.

4. Tables should be typed on separate pages and have captions describing their content. Clear wording of column heads is advisable. Tables should be numbered in Roman numerals (I, II, III, etc.).

IV. MANUSCRIPTS not in conformity with the above Notes will immediately be returned to authors for revision. The date of receipt to be shown on the paper will in such cases be that of the receipt of the revised manuscript.

Reviews of the Hungarian Academy of Sciences are obtainable at the following addresses:

AUSTRALIA

C. B. D. Library and Subscription Service
Box 4886, G. P. O.
Sydney N. S. W. 2001

Cosmos Bookshop
145 Acland St.
St. Kilda 3182

AUSTRIA

Globus
Höchstädtplatz 3
A—1200 Wien XX

BELGIUM

Office International de Librairie
30 Avenue Marnix
1050-Bruxelles

Du Monde Entier
162 Rue du Midi
1000—Bruxelles

BULGARIA

Hemus
Bulvar Ruszki 6
Sofia

CANADA

Pannonia Books
P. O. Box 1017
Postal Station "B"
Toronto, Ont. M5T 2T8

CHINA

C N P I C O R
Periodical Department
P. O. Box 50
Peking

CZECHOSLOVAKIA

Mad'arská Kultura
Národní třida 22
115 66 Praha

PNS Dovoz tisku
Vinohradská 46
Praha 2

PNS Dovoz tlače
Bratislava 2

DENMARK

Ejnar Munksgaard
Nörregade 6
DK—1165 Copenhagen K

FINLAND

Akateeminen Kirjakauppa
P. O. Box 128
SF—00101 Helsinki 10

FRANCE

Office International de Documentation et Librairie
48, Rue Gay-Lussac
Paris 5

Librairie Lavoisier
11 Rue Lavoisier
Paris 8

Europeriodiques S. A.
31 Avenue de Versailles
78170 La Celle St.-Cloud

GERMAN DEMOCRATIC REPUBLIC

Haus der Ungarischen Kultur
Karl-Liebknecht-Strasse 9
DDR—102 Berlin

Deutsche Post
Zeitungsvertriebsamt
Strasse der Pariser Kommüne 3—4
DDR—104 Berlin

GERMAN FEDERAL REPUBLIC

Kunst und Wissen
Erich Bieber
Postfach 46
7 Stuttgart S

GREAT BRITAIN

Blackwell's Periodicals
P. O. Box 40
Hythe Bridge Street
Oxford OX1 2EU

Collet's Holdings Ltd.
Denington Estate
London Road
Wellingborough Northants NN8 2QT

Bumpus Haldane and Maxwell Ltd.
5 Fitzroy Square
London W1P 5AH

Dawson and Sons Ltd.
Cannon House
Park Farm Road
Folkestone, Kent

HOLLAND

Swets and Zeitlinger
Heereweg 347b
Lisse

Martinus Nijhoff
Lange Voorhout 9
The Hague

INDIA

Hind Book House
66 Babar Road
New Delhi 1

India Book House
Subscription Agency
249 Dr. D. N. Road
Bombay 1

ITALY

Santo Vanasia
Via M. Macchi 71
20124 Milano

Libreria Commissionaria Sansoni
Via Lamarmora 45
50121 Firenze

JAPAN

Kinokuniya Book-Store Co. Ltd.
826 Tsunohazu 1-chome
Shinjuku-ku
Tokyo 160—91

Maruzen and Co. Ltd.
P. O. Box 5050
Tokyo International 100—31

Nauka Ltd—Export Department
2—2 Kanda
Jinbocho
Chiyoda-ku
Tokyo 101

KOREA

Chulpanmul
Phenjan

NORWAY

Tanum-Cammermeyer
Karl Johansgatan 41—43
Oslo 1

POLAND

Węgierski Instytut Kultury
Marszalkowska 80
Warszawa

CKP I W
ul. Towarowa 28
00—958 Warsaw

ROUMANIA

D. E. P.
Bucureşti

Romlibri
Str. Biserica Amzei 7
Bucureşti

SOVIET UNION

Sojuzpechatj — Import
Moscow
and the post offices in each town
Mezhdunarodnaya Kniga
Moscow G—200

SWEDEN

Almqvist and Wiksell
Gamla Brogatan 26
S—101 20 Stockholm

A. B. Nordiska Bokhandeln
Kunstgatan 4
101 10 Stockholm 1 Fack

SWITZERLAND

Karger Libri AG.
Arnold-Böcklin-Str. 25
4000 Basel 11

USA

F. W. Faxon Co. Inc.
15 Southwest Park
Westwood, Mass. 02090

Stechert-Hafner Inc.
Serials Fulfillment
P. O. Box 900
Riverside N. J. 08075

Fam Book Service
69 Fifth Avenue
New York N. Y. 10003

Maxwell Scientific International Inc.
Fairview Park
Elmsford N. Y. 10523

Read More Publications Inc.
140 Cedar Street
New York N. Y. 10006

VIETNAM

Xunhasaba
32, Hai Ba Trung
Hanoi

YUGOSLAVIA

Jugoslovenska Knjiga
Terazije 27
Beograd

Forum
Vojvode Mišića 1
21000 Novi Sad